Stony Brook University

Spatial, temporal and reversible regulation of endogenous genes *in vivo* using RNA interference

A Dissertation Presented

by

Prem K. Premsrirut

to

The Graduate School

in Partial Fulfillment of the

Requirements

for the Degree of

Doctor of Philosophy

in

Genetics

Stony Brook University

May 2010

Stony Brook University

The Graduate School

Prem K. Premsrirut

We, the dissertation committee for the above candidate for the Doctor of Philosophy degree, hereby recommend the acceptance of this dissertation.

Dr. Scott Lowe, Thesis Advisor
Professor, Cold Spring Harbor Laboratory

Dr. Senthil Muthuswamy, Chair of Defense
Professor, Cold Spring Harbor Laboratory

Dr. Gregory Hannon, Committee Member
Professor, Cold Spring Harbor Laboratory

Dr. Howard Crawford, Committee Member
Associate Professor, SUNY Stony Brook

Dr. Raffaella Sordella, Committee Member
Assistant Professor, Cold Spring Harbor Laboratory

Dr. Cijiang He, Outside Member
Associate Professor, Mount Sinai School of Medicine

This dissertation is accepted by the Graduate School

Lawrence Martin
Dean of the Graduate School

Abstract of the Dissertation

Spatial, temporal and reversible regulation of endogenous genes *in vivo* using RNA interference

by

Prem K. Premsrirut

Doctor of Philosophy

in

Genetics

Stony Brook University

2010

RNA interference is a powerful tool for controlling gene expression in mammalian systems; as such, it has become an effective alternative to conventional knockout approaches. RNAi has proven to be an efficient method to inhibit tumor suppressor gene function and yield insight into the important players in cancer biology. Still, the promise of regulatable RNAi transgenic mice has yet to be realized because the reproducible generation of these animals remains a significant technical limitation. By combining optimized fluorescence-coupled mir30-based shRNA technology with high efficiency ES cell targeting, I developed a flexible and scalable pipeline for the rapid and reliable production of doxycycline-regulated shRNA transgenic mice. These RNAi mice contain single copy DOX-regulatable shRNAs downstream of the endogenous *Collagen Type 1* locus, allowing for spatial, temporal and reversible gene expression in mice. Using this platform, I generated novel DOX-regulated shRNA transgenic lines targeting the bioluminescence reporter *Luciferase* and endogenous tumor suppressor genes, including *Trp53*, *INK4a* and *ARF*, each showing strong

doxycycline-dependent knockdown of its target protein, without disrupting processing of endogenous miRNAs. To study the role of these TSGs in the maintenance of *Kras*^{G12D} driven lung adenocarcinomas, I crossed these to produce mice bearing an shRNA, CCSP-rtTA (clara cell specific promoter - reverse tet-transactivator), *LSL-Kras*^{G12D} and *LSL-Luciferase* alleles. However, owing to the slow rate and high expense of producing quadruple transgenic mice, I later devised a strategy for "speedy" mouse model production. This approach entailed re-derivation of embryonic stem cells harboring the relevant alleles and subsequent generation of "mosaic" models produced by blastocyst injection. Using these RNAi mouse models, I show that *INK4a*/*ARF* or *Trp53* downregulation by RNAi cooperates with *Kras*^{G12D} to accelerate lung tumorigenesis and recapitulate the phenotypes of knockout models. Additionally, I investigate whether *INK4a*/*ARF* or *Trp53* knockdown is required for tumor maintenance. Together, this work built a platform that greatly accelerates the rate at which one can study genetic interactions and tumor maintenance genes and also identify and validate new drug targets *in vivo.* This approach can be applied to build many other complex cancer models and thus may have significant implications for guiding future therapies.

Table of Contents

Abbreviations

BACs – bacterial artifical chromosomes
CC10 – Clara cell secretory protein (or CCSP)
CCSP – Clara cell secretory protein (or CC10)
CMV – cytomegalovirus (promoter)
DOX - doxycycline
ES – embryonic stem
GEM – genetically engineered mice
GFP – green fluorescence protein
KO – knockout
LSL – Lox-STOP-Lox
MEFs – mouse embryonic fibroblasts
miRNA – microRNA
MOI – multiplicity of infection
rCCSP – rat CCSP promoter
RIP – rat insulin promoter
RIR1 – rat insulin promoter reverse
RISC – RNA-induced silencing complex
RMCE – recombinase-mediated cassette exchange
RNAi – RNA interference
rtTA – reverse tetracycline-transactivator
shRNA – short hairpin RNA
shRNA-mir – miRNA-based shRNA
siRNA – small interfering RNA
T-Ag – SV40 T antigen
TGM – TRE-GFP-miR30
TGMP – TRE-GFP-miR30-PGK-Puro
TMP – TRE-miR30-PGK-Puro
TRE – tetracycline response element
TSG – tumor suppressor gene
tTA – tetracycline transactivator

Acknowledgements

I would like to thank Scott Lowe and all members of the Lowe lab for their continual support, advice and mentorship. Special thanks to my mentors: Masahi Narita, Ross Dickins, Lars Zender, Jack Zilfou, Johannes Zuber, Mona Spector, Luke Dow, Cornelius Miething and Agustin Chicas. To my friends and colleagues who helped guide me through these many years: Zhen Zhao, Claudio Scuoppo, Yuchen Chien, Mila McCurrach and Young Park. To others who have been instrumental in the preparation of this thesis: Shirley Guo, Jessica Bolden, Felix Muerdter, Thomas Kitzing, Myra Shankin and Puoy Premsrirut. To experimental collaborators: Sang Yong Kim, Colin Malone, Matthew Camiolo, Jacob Hooker (of Brookhaven National Laboratory), Claudio Scuoppo and Luke Dow. For outstanding technical assistance: Janelle Simon, Danielle Grace and Jacqueline Cappellani.

I thank Caroline Beard and Rudolph Jaenisch (Whitehead Institute) for pBS31 flp-in and pCAGGs-FLPe-Puro vectors, ColA1 3' probe and KH2 ES cells; Dr. Jeff Whitsett (Children's Hospital, Cincinnati, Ohio) for the CCSP-rtTA mouse strain; Luke Dow and Cornelius Miething for the CAGs-rtTA3 strain. Many thanks to Lisa Bianco, Jodi Coblentz, Eileen Earl and the Cold Spring Harbor Laboratory animal house staff. This study was supported by a Mouse Models of Human Cancer Consortium grant, a program project grant from the National Cancer Institute, and the Medical Scientist Training Program of SUNY Stony Brook University and Medical School.

I would like to thank my friends: Kelly Shen, Janice Lai, Killian Rieder, Shireen Khoo, Brandi Bowers, Jessica Palomino, Courtney Vergillis, Philipp Lederer, Bhavik and Krisha Katira and Maria Pineda; and my family for their never-ending support: Mom, Dad, Kay, Puoy and Rutt.

Chapter 1

Introduction

1.1 Mouse models of cancer

Genetically engineered mice (GEM) have become the premier mammalian model system for cancer research. These invaluable tools have enabled researchers to explore questions about human disease in an intact experimental system. They have also provided an opportunity to observe and analyze complex pathological processes in cancer in a manner impossible to perform in patients. In addition to their ability to be genetically modified, their small size, rapid life cycle and similar genetic makeup to humans, has rendered them as a vital and economically feasible resource that has already provided enormous insight and led to a better understanding and treatment of human cancers (Frese and Tuveson, 2007; Rangarajan and Weinberg, 2003; Tuveson and Jacks, 1999, 2002; Van Dyke and Jacks, 2002).

Since 1971 when Richard Nixon declared a “War on Cancer”, billions of dollars have been funneled into basic and clinical cancer research and in turn, have led to the development of a tremendous number of mouse models of cancer that captured elements of the human disease (http://mouse.ncifcrf.gov/). However, the fight against cancer has only begun. Even with our expanding wealth of knowledge, cancer still represents an increasing cause of morbidity and mortality throughout the world, therefore creating a continuous need for mouse models that more accurately recapitulate human cancer pathology. With recent advancements in mouse engineering technology, we are now able to develop even more elegant and powerful models that faithfully mimic the human disease.

We must fully utilize these advancements and continue to expand upon our collection of GEMs that will become increasingly important not only for cancer gene identification and validation, but also for the development of a new generation of targeted therapies to combat this disease.

Early mouse models

Much of our early conceptualization of how tumorigenesis occurs in humans is owed to studies performed in mice. Prior to GEMs, inbred strains of mice that developed tumors either spontaneously or following exposure to various environmental agents including radiation, chemicals and pathogens have been useful for the identification of oncogenes and tumor suppressor genes (TSGs), the mapping of tumor susceptibility traits (Balmain, 2002) and the assessment of the carcinogenic or chemopreventative effects of various compounds (Frese and Tuveson, 2007). However, these mouse models were prone to only a small subset of tumor types with varying aggressiveness, latency and penetrance, forcing researchers to develop new technologies that would allow for more systematic investigation of tumorigenesis.

Oncomice

It was not long before DNA transfer by direct microinjection into the pronuclei of fertilized zygotes (Capecchi, 1980; Gordon et al., 1980) made it feasible to generate the first transgenic mice carrying dominant oncogenes later termed “oncomice” (Table 1.1). These mice collectively substantiated the

hypothesis that expression of oncogenes in normal cells of a mammalian organism could predispose them to cancer. For example, transgenic expression of the *SV40 T antigen (T-Ag)* in brain epithelium or *c-myc* expression in mammary epithelium led to brain cancer (Brinster et al., 1984) and mammary adenocarcinomas in mice, respectively (Leder et al., 1986). Additional examples followed that demonstrated *c-fos* expression induced osteosarcomas (Ruther et

Table 1.1 | Oncomice. Several early transgenic animal models overexpressing oncogenes.

Gene	Transgene	Types of neoplasms	References
Myc	MMTV-*myc*	Adenocarcinoma of the breast, testicular neoplasms, mast cell neoplasms, lymphomas	(Leder et al., 1986; Stewart et al., 1984)
	Heavy chain[Ig] enhancer-*c-myc* or Eμ-*myc*	Pre-B cell lymphomas	(Adams et al., 1985; Schmidt et al., 1988)
Ras	MMTV-*Ha-ras*	Adenosquamoid carcinomas of the breast (males and females), salivary gland neoplasms, lymphoma	(Sinn et al., 1987)
	Elastase promoter-*Hras1*	Pancreatic tumors	(Quaife et al., 1987)
ErbB2, neu	MMTV-*erb-B2/neu*	Synchronous development of breast carcinomas (males and females)	(Muller et al., 1988)
SV40 T antigen	*SV40 T-MK* (metallothionein-thymidine kinase)	Brain tumors within the choroid plexus	(Brinster et al., 1984)
	RIR-*T-Ag* and RIP1-*T-Ag* (rat insulin promoter)	Pancreatic islet tumors	(Hanahan, 1985)
Fos	LTR-*c-fos*	Osteosarcomas and chondrosarcomas	(Ruther et al., 1989)
PymT	MMTV-*PymT*	Hemangiomas	(Bautch et al., 1987; Williams et al., 1988)

al., 1989) and transgenic mice harboring RIP-*T-Ag* or *RIR-T-Ag* (rat insulin promoter fused to SV40 *T-Ag*) developed pancreatic islet tumors (Hanahan, 1985). Together, these early models provided groundbreaking results that have shaped much of our initial understanding and appreciation for the complexity of cancer. They also uprooted an explosion in the field and set the stage for the development of increasingly refined technologies that have enabled manipulation of gene expression and mutations in the mouse.

Knockout and knock-in mutants

The next wave of GEMs that further enhanced our understanding of cancer genes and their mechanisms came shortly after the discovery of homologous recombination and its application in pluripotent embryonic stem (ES) cells (Thomas and Capecchi, 1987; Thomas et al., 1986). By utilizing the endogenous homologous recombination machinery, new gene targeting approaches in ES cells were developed that enabled gene deletion and the production of knockout (KO) models. This technology permitted deletion of either one or both copies of tumor suppressor genes (TSGs) to give rise to a new class of cancer-prone mouse strains. In addition, this same approach was used to develop knock-in mouse models, in which mutant alleles (e.g. $Kras^{G12D}$ or $Trp53^{R172H}$) were targeted to replace the endogenous allele. Several of the most commonly used knockout/knock-in models are listed in Table 1.2.

Table 1.2 | Germline mouse cancer model. Much of the information is adapted from Zender L, Zuber J, Lowe SW. Snapshot: genetic mouse models of cancer. Cell. 2007 May 18;129(4):838.

Gene	Genetic Approach	Primary Tumor Types	Cooperativity Models
Trp53	*Trp53*$^{-/-}$	*Trp53*$^{-/-}$ 100% tumor penetrance at ~4.5 months (T cell lymphoma, soft tissue sarcoma, osteosarcoma, etc). *Trp53*$^{+/-}$: 50% tumor penetrance at 17 months	*Rb*$^{-/-}$ or Eμ-*myc*. Genotoxic agents or irradiation induced carcinogenesis
	Trp53^{R172H} or *Trp*^{R270H}	Tumor spectra differ from germline *Trp53* knockout mice with more carcinomas, B cell lymphomas, endothelial tumors	*Trp53*^{R172H} and *Kras*^{G12D} cooperate to promote metastatic pancreatic adenocarcinoma
	Trp53$^{loxP/loxP}$	The same tumor spectrum (+Cre) as *Trp53* germline knockout	Breast cancer with *Brca2* conditional knockout and *K14-Cre*. Small-cell lung cancer with *Rb1 loxP/loxP* and Adeno-Cre
	p53-ER^{TAM}	Endogenous *Trp53* gene is replaced with the *Trp53-ER*^{TAM} fusion gene. 4-OHT treatment allows p53-ER enter the nucleus	
	LSL-p53	*Trp53* knock-in with Lox-STOP-Lox cosset between exon 1 and 2. Cre excises *LSL* and activates p53	
p16$^{INK4a/}$ *p19*^{ARF}	*p16*$^{INK4a/}$ *p19*$^{ARF-/-}$	Homozygous mice develop sarcomas (50%) and B cell lymphomas (50%) by ~32 weeks. Tumors with lower penetrance and longer latency in heterozygous animals	tyrosinase-*Ras* (melanomas) and Eμ-*Myc* (B cell lymphomas)
	ARF $^{-/-}$	80% of homozygous mice (sarcomas, T cell lymphomas, carcinomas, etc) by ~38 weeks. Tumors in heterozygous mice are less frequent	mitogenic oncogenes
	INK4a$^{-/-}$	~25% of the homozygous (sarcomas and lymphomas) by ~44 weeks	chemically induced carcinogenesis
Pten	*Pten*$^{-/-}$	*Pten*$^{-/-}$ results in embryonic lethality (E9.5). *Pten*$^{+/-}$ mice develop multiple tumor types (breast, thyroid, endometrium, prostate, breast and T cell lymphoma)	*Pten*$^{+/-}$ with *MMTV-Wnt1 (breast cancer)* or *Cdkn1b*$^{-/-}$ (prostate carcinomas)

	Pten$^{flox/flox}$	Prostate-specific knockout of *Pten* by *probasin-Cre* (*PB-Cre*) leads to senescence	Senescence is bypassed by loss of *Trp53*
Nf1	*Nf1(n31)*$^{-/-}$	*NF1*$^{-/-}$ are embryonic lethal, het are susceptibility to pheochomocytoma and myeloid leukemia at 10 month, LOH	Nf1$^{-/-}$; *Trp53*$^{-/-}$ sarcomas between 3 and 7 months of age
Nf2	*Nf2*$^{-/-}$	*Nf2*$^{-/-}$ die at E7*. Het* develop cancer at advanced age, osteosarcomas at a high frequency and fibrosarcoma and HCC	
	Nf2^{flox2}	*Nf2*$^{flox2/flox2}$;P0*cre mice (*Schwann cell specific*)* develop schwannomas	With *Trp53*$^{+/-}$
Brca1	*Brca1*$^{-/-}$	$^{-/-}$ embryonic lethal E5.5-E13.5	
	Brca1^{loxP}	*Brca1*^{loxP}; MMTV-Cre develop mammary tumors at 10 months	
Brca2	*Brca2*$^{-/-}$	$^{-/-}$ embryonic lethal E8.5; hypomorphic mutant develop thymic lymphomas	
	Brca2^{loxP}	*Brca1*^{loxP}; Wap-Cre develop mammary tumors at 1.4 year (77%)	
Apc	*Apc*$^{-/-}$	$^{-/-}$ embryonic lethal at E8	
	Apc^{min}	*Apc*$^{min/+}$ intestinal tumors at an early age, die before d120	
Myc	*Conditional tet-o-Myc*	Liver carcinoma (*LAP-tTA* mice); T cell lymphoma (*E*μ-*SR-tTA*); breast adenocarcinoma (*MMTV-rtTA*)	*Myc* withdrawal leads *to* tumor regression by apoptosis or senescence
Kras	*LSL-Kras*^{G12D}	Non-small-cell lung adenocarcinoma by intranasal Adeno-Cre	*Trp53* loss or mutation
		Pancreatic cancer produced by crossing with *Pdx-1-Cre* transgenic mice	p16$^{INK4a/}$p19^{ARF} deficiency (metastatic pancreatic adenocarcinoma)
		Myeloproliferative Disease (MPD) by crossing with *Mx1-Cre* mice and pI-pC treatment	

The accumulation of gene knockout/-in models has led to more precise functional analysis of numerous TSGs *in vivo.* For instance, one of the most frequently mutated or deleted genes seen across all human tumors is *Trp53*,

which encodes for the p53 tumor suppressor protein. Early examples of mice lacking both copies of *Trp53* supported its role as a crucial TSG, functioning as a negative regulator of cell division and growth. These mice were highly susceptible to tumor development and often developed lymphomas and sarcomas at high penetrance and a short latency of ~4.5 month (Donehower et al., 1992). In contrast, haploinsufficient mice lacking one *Trp53* allele developed tumors at a 50% penetrance and a latency of ~17 months. However, unlike these germline deletion models, patients often have *Trp53* point mutations, as seen in Li-Fraumeni syndrome. To develop a more accurate model of this syndrome, knock-in mice with defined p53 mutations (e.g. $p53^{R172H}$ and $p53^{R270H}$) were generated and shown to succumb to a wider range of tumors commonly seen in humans, including carcinomas, B cell lymphomas and endothelial tumors (Olive et al., 2004).

Germline mutations that can be propagated to progeny have prompted the development of compound mutants. By breeding transgenic and knockout/-in strains to one another, typically ones that harbor activated oncogenes and deletion of TSGs, many cancer models comprised of multiple genetic lesions were generated. These models have served to support the idea that cancer is a multi-step process that requires the acquisition of several lesions to progress from hyperplasia to a benign lesion and even further alterations to progress to invasive and metastatic carcinomas. For example, Eμ-*myc* transgenic mice were prone to develop pre-B or B cell lymphoma and had a median survival of 6 months (Adams et al., 1985). This lymphomagenesis was markedly accelerated

in bitransgenic mice containing both Eμ-*myc* mice and *Trp53* deficiency (Schmidt et al., 1988).

Conditional mouse models

For cancer susceptibility, most models require homozygous deletion of TSGs; however, the majority of homozygous mutants suffer from embryonic lethality. Therefore, it was necessary to create a conditional deletion strategy that would allow for deletion in mice during adulthood and preferentially in a specific tissue, since the majority of cancers in humans arise from somatic mutations. This was accomplished using exogenous DNA recombinases: Cre recombinase of bacteriophage P1 (Sauer and Henderson, 1989), which mediates recombination of lox sites, and Flp recombinase of yeast (O'Gorman et al., 1991), which recognizes FRT sites. Cre excises stretches of DNA that are flanked (or "floxed") by unidirectional lox sequences or inverts DNA if flanked by opposing sites. Flp acts analogously on DNA fragments flanked by FRT sites. This recombinase-mediated deletion strategy was also applied to generate conditional mutants, by placing a floxed polyadenylation signal (*Lox-STOP-Lox* or *LSL* cassette) after the transgenic open reading frame (ORF); this configuration terminates transcription until Cre-recombinase mediates excision of the *LSL* cassette. In order to control Cre recombination spatially, hundreds of transgenic tissue-specific Cre mouse strains were developed and are listed at http://www.informatics.jax.org/recombinase.shtml. Tissue-specific Cre mice were

combined with floxed mutant mice to generate binary transgenics that contained the desired mutation in the tissue of interest.

Tetracycline inducible systems are also powerful tools for gene regulated expression (Gossen and Bujard, 1992). They were initially developed for use in cultured cells, but were also found to be effective in transgenic mice (Furth et al., 1994). Regulated transcription from the tet-responsive (TRE) promoter relies on activity of a tet-transactivator (tTA) protein, which can be either activated ('tet-on') or repressed ('tet-off') by tetracycline or its analog doxycycline (DOX). Expression of tet-transactivators from tissue-specific promoters allows spatial and temporal control of gene overexpression, a strategy widely used to study mouse embryonic and postnatal development (Kistner et al., 1996). Hence, many mouse lines have been developed that express the tTA (tet-off) or rtTA (tet-on) transactivators in different cell types. For a complete list, see http://www.zmg.uni-mainz.de/tetmouse/index.htm.

Inducible systems made it possible to control transgene expression temporally and spatially in mice – to turn transgenes on and off by administration and/or withdrawal of DOX treatment. This technology was quickly applied to develop transgenic mouse models in which oncogenes were expressed to promote tumor development and then turned off once tumors were formed. Studies using inducible models have transformed our knowledge of the roles of oncogenes and demonstrated that oncogenes not only play a role in tumor inhibition but also in tumor maintenance. These models provided further evidence that supports the hypothesis of "oncogene dependence" put forth in

2002 by I.B. Weinstein, which will be later discussed in more detail. In short, to describe the ongoing clinical success with targeted therapies, Weinstein hypothesized that some cells harnessed vulnerabilities to disruption of dominant oncogenic pathways (Weinstein, 2002). Inducible oncogene expressing mouse models of melanoma (Chin et al., 1999), leukemia (Felsher and Bishop, 1999), breast cancer (Moody et al., 2002) and lung cancer (Fisher et al., 2001) have provided much evidence to support this hypothesis. In all cases, tumors were susceptible to loss of the initiating oncogene and once removed, they failed to sustain tumor development and growth even in the presence of additional genetic lesions.

In summary, the technologies described have been used to generate a number of sophisticated mouse models with compound and binary transgenic alleles that express cancer predisposing mutations, many of which were isolated to specific organs at selected developmental times (Table 1.2; 1.3). For example, *Trp53*$^{flox/flox}$ mice crossed to *Brca2*$^{flox/+}$ and K14-Cre (keratin promoter) mice produced progeny that develop breast cancer (Jonkers et al., 2001). Mice with TRE-*Kras*^{G12D}, CCSP-rtTA and homozygous deletion of *Trp53* (p53$^{-/-}$) developed aggressive lung adenocarinomas following one month of exposure to doxycycline (Fisher et al., 2001). Furthermore, conditional *LSL-Kras*^{G12D} mice that express an activated mutant *Kras* allele from the endogenous promoter were predisposed to a number of cancers following Cre-mediated excision of a STOP cassette (Jackson et al., 2001). From this single conditional mouse model, multiple cancer types were developed: lung adenocarcinoma was produced by intranasal

administration of Adeno-Cre or lentiviral-Cre to the lung (Jackson et al., 2005); and pancreatic cancer was produced by crossing *LSL-Kras*^{G12D} mice to pancreas-specific *Pdx-1-Cre* transgenic mice (Hingorani et al., 2003). Mergence of the expanding transgenic and gene targeting technologies enabled production of tailored mouse models that resulted in cancers that more faithfully represented the human disease.

Mouse versus humans

There is no question that mouse models play important roles for the study of human cancer; however, we must also address the fact that a mouse will never equate to a human and therefore, there will never be a perfect system. Clearly, there are many discrepancies between humans and mice, but the overwhelming overlap of the genome surprisingly translates between the two organisms. Humans have a much longer lifespan and therefore a greater turnover of cells. It is estimated that humans undergo 10^5 more cells divisions in a lifetime (Rangarajan and Weinberg, 2003). Because of this, we would expect humans to experience a greater cancer incidence, but on the contrary, both species have a cancer susceptibility rate of ~30%. The high rate of cancer in mice may be attributable to metabolic rate, which is seven times higher than humans and is responsible for the generation of reactive oxygen species (ROS) that are known to cause DNA damage.

Several notable molecular differences between mice and humans do exist and may explain dissimilar pathologies that occasionally arise. For instance, lab

mice tend to develop cancer in mesenchymal tissues, such as lymphomas and sarcomas. Humans, on the other hand, predominantly develop carcinomas that arise from epithelial cells (DePinho, 2000). Most epithelial carcinomas of humans contain highly abnormal karyotypic profiles characterized by changes in chromosome number and numerous non-reciprocal translocations (NRTs) – features that are uncommon in murine tumours. Some mutations do not precisely translate, such as mice deficient in the adenomatosis polyposis coli gene (*APC*); $APC^{min/+}$ acquire polyps in the small intestine but humans with *APC* mutations get polyps in the colon (Heyer et al., 1999). Fortunately, many gene mutations do accurately reflect human disease, such as p53 mutant mice, which develop carcinomas that resemble human epithelial cancers.

From cell culture experiments, it is clear that notable differences between signaling pathways also exist, including signals that induce senescence and apoptosis (Rangarajan and Weinberg, 2003). For instance, the p53 pathway plays a predominant role in the senescence response in murine cells. In humans, Rb is the principle player. Mouse embryonic fibroblasts also require less genetic aberrations to undergo transformation; oncogenic *Ras* and loss of p53 or ARF is sufficient to initiate this process (Rangarajan et al., 2004). That is not the case in human fibroblasts, which must not only overcome replicative senescence but also a crisis stage in order to become immortalized. These differences may be attributable to the fact that mice have longer telomeres than humans. Another key difference is that human tumors generally have “noisy” genomes harboring numerous DNA copy number losses and gains; mouse tumors usually have far

fewer genomic deletions than humans. Lastly, as mice and humans do not have the exact genomes, they may have distinct metabolic differences that may affect their response to therapy. Nevertheless, mouse models are the gold standard to study human cancer that enable cross species comparisons to integrate information obtained in both human and mouse tumors. They provide the means to dissect the intricate networks involved in cancer pathogenesis. Without them, we would be at a loss in our fight against cancer.

Table 1.3 | Examples of genetically engineered mouse models that recapitulate human solid cancers. Adapted from Frese, K.K. and Tuveson, D.A. *Nat Rev Cancer.* Maximizing mouse cancer models. 7(9):645-58 (2007).

Organ	Histopathology	Genetics
Lung	Adenocarcinoma	*Kras* (Jackson et al., 2001)
	Squamous cell carcinoma	NA
	Large cell carcinoma	NA
	Small cell carcinoma	*Rb1;Trp53* (Meuwissen et al., 2001)
Colon	Polyploid adenocarcinoma	*Kras;Apc* (Sansom et al., 2006)
	Hereditary non-polyposis carcinoma	*Msh6* (Edelmann et al., 1997)
Breast	Ductal carcinoma	*Brca2;Trp53* (Jonkers et al., 2001)
	Lobular carcinoma	*Cdh1;Trp53 (*Derksen et al., 2006)
Pancreas	Ductal adenocarcinoma	*Kras;Cdkn2a* (Aguirre et al., 2003), *Kras;Trp53* (Hingorani et al., 2005)
	Mucinous cystic neoplasm	*Kras;Dpc4* (Izeradjene et al., 2007)
	Intraductal papillary mucinous neoplasia	NA
Prostate	Prostate carcinoma	*Pten* (Wang et al., 2003)*, Pten;Nkx.1* (Kim et al., 2002)*, Rb1; Trp53* (Zhou et al., 2006)
Liver	Hepatocellular carcinoma	*Apc* (Colnot et al., 2004)*, Myc;Trp53* (Zender et al., 2006) *Myc;TGFA* (Santoni-Rugiu et al., 1996)
Ovary	Endometroid carcinoma	*Kras;Pten* (Dinulescu et al., 2005)*, Apc;Pten* (Wu et al., 2007b)
	Serous carcinoma	NA
	Mucinous carcinoma	NA
Oesophagus	Squamous cell carcinoma	*Pten;Dpc4* (Teng et al., 2006)*, Ccnd1;Trp53* (Opitz et al., 2002)
	Adenocarincoma	NA
Bladder	Transitional cell carcinoma	*Hras* (Mo et al., 2007)
Kidney	Renal cell carcinoma	*Apc;Trp53* (Sansom et al., 2005)
Brain	Astryocytoma	*Pten;Rb1* (Xiao et al., 2005)
	Glioblastoma	*Nf1;Trp53* (Reilly et al., 2000)
Stomach	Gastric carcinoma	*Wnt;Ptgs;Ptges* (Oshima et al., 2006)
Skin	Melanoma	*Hras;INK4a* (Chin et al., 1999)
	Squamous cell carcinoma	*Xpd* (Andressoo et al., 2006)

1.2 Mouse engineering strategies

Classical transgenesis

The birth of genetically modified animals began with the ability to microinject DNA into the pronuclei of fertilized zygotes (Capecchi, 1980) (Fig. 1.1). This procedure is commonly known as classical or standard transgenesis. One of the major advantages of this method and why it is still widely used today is that it is a fast and simple procedure and the technology imposes virtually no limits on transgene size. For example, fragments as large as 2Mb encompassing the chromosomal region 21q22.2 have been integrated into the mouse genome in order to model the complex traits of Down syndrome (Smith et al., 1997). On the other hand, due to the inability to control the site of integration and copy number, pronuclear injection imposes several drawbacks. To begin with, transgene integration is stochastic, such that most transgenes are integrated into the genome at high copy number and insert in a head-to-tail manner. Additionally, depending on the site of integration, transgene expression may be affected by neighboring chromosomal elements that can modulate promoters to a high extent – this is known as position-effect variegation (West and Fraser, 2005). Nearby or close promoter elements may also interact with incoming promoters, creating promoter crosstalk, which can result in downregulation or potentiation, also known as promoter occlusion. In many cases, the transgene lands in a heterochromatically silenced region and is therefore not expressed. Another major caveat due to random transgene insertion is that each transgenic

founder will be unique and therefore the expression between each founder will be variable. Thus to control for phenotypic distortions, it is necessary to breed and characterize multiple transgenic lines for each construct independently. Finally, not all founders will have transgenic insertions in the germline and so it will also be essential to screen for transmission to progeny (Wilson et al., 1990). Ultimately, these limitations necessitate laborious and costly screening protocols to identify functional founders.

An alternative and less invasive procedure to classical transgenesis is the use of lenti- or retroviral systems for transgene delivery into ES cells or embryos, which often result in higher survival rates (Lois et al., 2002). Infected cells reverse transcribe the viral RNA into DNA and then insert it into the genome as single copies, but potentially at multiple sites and on different chromosomes, creating a high multiplicity of infection (MOI). Although proviruses tend to preferentially integrate into actively transcribed loci and are prone to less epigenetic silencing (Imren et al., 2004), the random integration creates many of the same drawbacks discussed for pronuclear injection.

To overcome these caveats and produce founder mice with less variable and more reliable transgene expression, several researchers have turned to incorporating insulator sequences to flank transgenes. These sequences are believed to shield transgenes from position effects by blocking promoter interference and/or recruiting demethylation complexes and preventing heterochromatic silencing (Bell and Felsenfeld, 2000). Specifically, the use of chicken β-globin 5'HS4 elements to flank transgenes have yielded positive

results by improving efficiency and reducing the variation between founder animals, as illustrated in Fig. 1.2 (Hsiao et al., 2004; Potts et al., 2000).

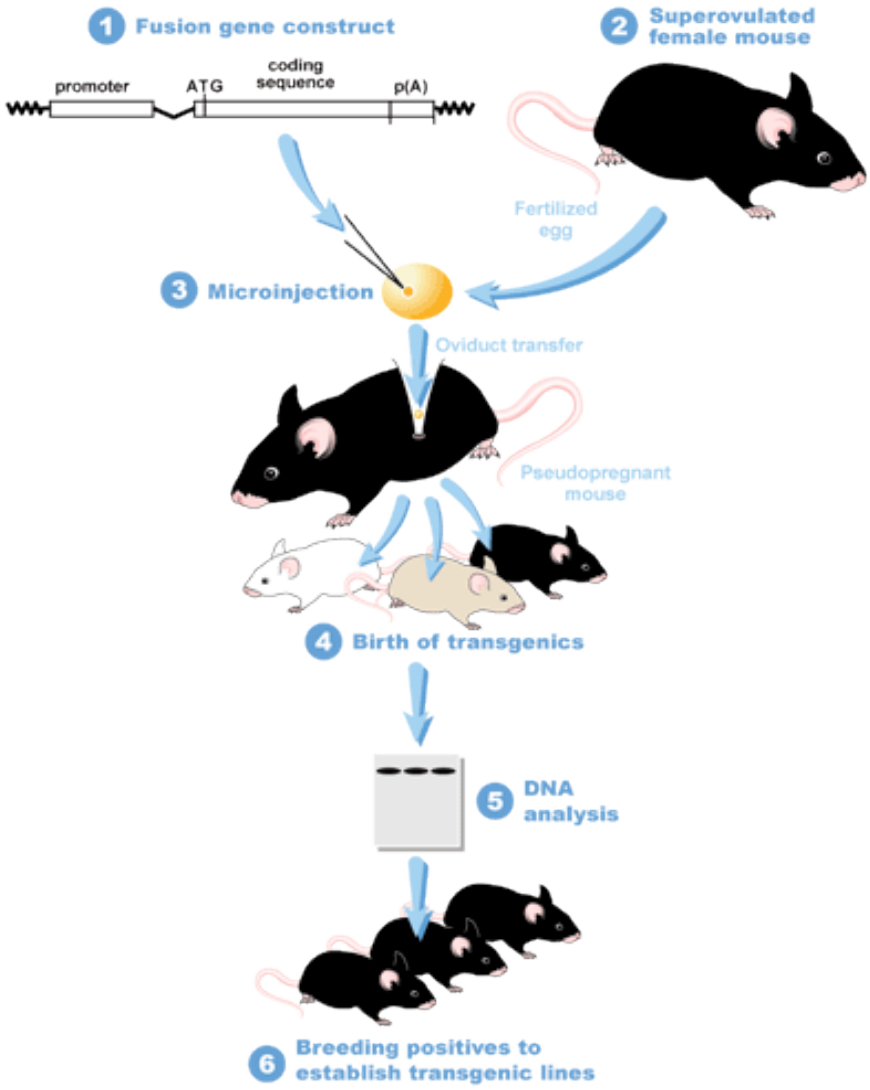

Figure 1.1 | Classical transgenesis by pronuclear injection to generate founder lines. Transgenes are directly injected into the pronucleus of fertilized zygotes harvested from superovulated females. Following microinjection, embryos are transplanted into surrogates. DNA analysis and F_1 generations are necessary to determine germline transmission. Taken from http://cancer.ucsd.edu/tgm/pronuclear.asp.

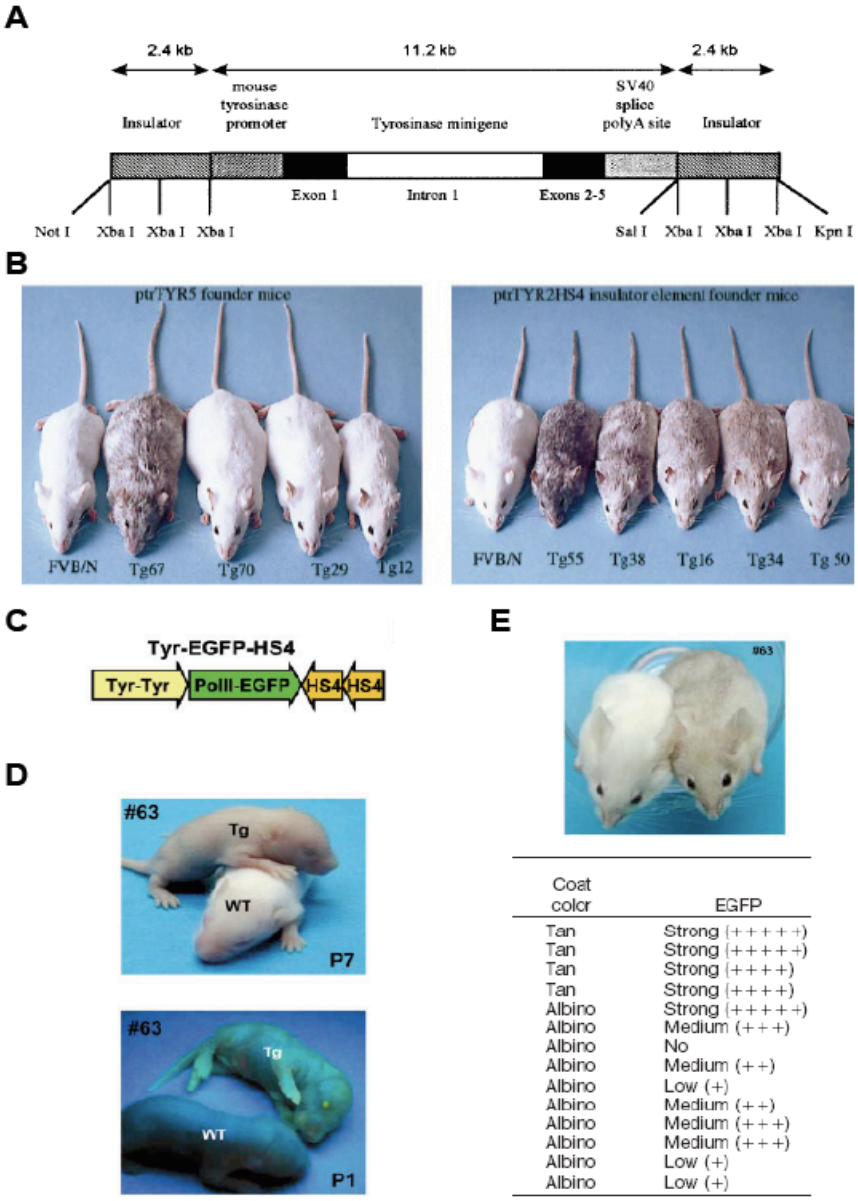

Coat color	EGFP
Tan	Strong (+++++)
Tan	Strong (+++++)
Tan	Strong (++++)
Tan	Strong (++++)
Albino	Strong (+++++)
Albino	Medium (+++)
Albino	No
Albino	Medium (++)
Albino	Low (+)
Albino	Medium (++)
Albino	Medium (+++)
Albino	Medium (+++)
Albino	Low (+)
Albino	Low (+)

Figure 1.2 | Insulators increase the efficiency and decrease the variability of transgene expression in founder mice. *A*, A transgene carrying the tyrosinase gene with and without flanking HS4 insulator sequences was used for generating transgenic mice. *B*, Photograph of pigmented and control FVB/N mice generated with (*right*) and without (*left*) HS4 insulators. Those with insulators have more tyrosinase expression as seen in their coat color. *C*, Schematic representation of the transgenic construct with eGFP and tyrosinase and 3' HS4 sequences. *D-E*, Visualization of tyrosinase and GFP in transgenic mice. A-B, Adapted from Potts, W. et al. Biochem Biophys Res Commun. 2000; 273(3):1015-8. C-E, Adapted from Hsiao, Y. et al. Genesis. 2004; 39(2): 122-9.

Gene targeting by homologous recombination

For introducing specific gene modifications (i.e. deletion or knock-in mutants) in mice, homologous recombination in ES cells has become the accepted standard (Capecchi, 1989). Homologous recombination is preferred because it overcomes the limitations imposed by standard transgenesis by directing insertion cassettes to a specific locus at single copy integration. To begin, it requires construction of a targeting vector containing three essential components: two homology arms (a 5' and 3' arm) that contain stretches of identical mouse genomic DNA and a mini-transgene that serves as a positive selection marker (i.e. antibiotic resistance genes). Following introduction of the targeting cassette, generally done by electroporation, ES cells are selected, propagated and analyzed by southern blot for correct integration (Fig. 1.3A). Once integration has been verified, targeted ES cells are injected into blastocysts to produce chimeric mice (Schuster-Gossler et al., 2001), which must be further screened to test for germline transmission (Fig. 1.3B). An alternative approach to chimeric generation is the production of fully ES cell-derived mice by tetraploid embryo complementation (Eggan et al., 2001). This procedure, illustrated in Fig. 1.4 (Cross, 2001), makes use of 4N host blastocysts that cannot contribute to the developing fetus and therefore results in founder mice at a near 100% efficiency that are fully derived from the targeted ES cells.

Homologous recombination may be the preferred method for specific gene targeting, however it relies on the endogenous enzymatic machinery for its completion and generally occurs at a low frequency, roughly one event per 10^{5-}

10^7 targeted cells (Vasquez et al., 2001). It also requires detailed cloning strategies using bacterial artificial chromosomes (BACs) that contain large homology regions surrounding the gene of interest, generally between 6-8 kb in length combined for both 5' and 3' arms (Thomas and Capecchi, 1987). Additionally, the low frequency of targeted recombination is greatly surpassed by the number of random integrations, estimated to be ~1000 fold higher (Vasquez et al., 2001). To rule out non-homologous recombination, targeting vectors will often incorporate negative selection markers as well (i.e. HSV-tk or DTA genes), but even with positive and negative selection, robust and costly genetic screens of several hundred clones are still necessary to identify correctly targeted clones. For these reasons, homologous recombination is also not a suitable method for directing site-specific integration for a large number of different transgenes.

Recombinase-mediated cassette exchange

Targeted gene knock-in technology using recombinase-mediated cassette exchange (RMCE) provides an attractive alternative to both pronuclear/viral transgenesis and homologous recombination approaches (Baer and Bode, 2001). This approach increases the rate of recombination by relying on the enzymatic activity of foreign recombinases, such as Cre and Flp, as previously described. There are many unique RMCE strategies, and depending on the design, many of these systems can yield high efficiency targeting rates and dramatically decrease the number of ES cell clones that must be screened. However, before these recombinases can be used for high efficiency

recombination, site-specific chromosomal integration by homologous recombination is first required to incorporate a “homing” cassette that contains either lox, FRT or attA/B recognition sequences flanking an mini-transgene selection cassette. These sequences serve as recognition sites that promote a second retargeting event – intra- and interchromosomal recombination between the “homing” cassette and a targeting vector containing the desired transgene. The details of several RMCE strategies are depicted in Fig. 1.5.

For this method, two mouse genes have been extensively used as host loci for targeted transgene insertion, *Hprt1* and *Gt(Rosa)26* (or commonly referred to *Rosa26*). The *Rosa26* locus has been more widely used than the X-linked genomic targeting *HPRT* site, however recent studies caution against the insertion of exogenous promoters into this locus due to promoter interference (Nyabi et al., 2009). Another alternative that we have used extensively in our lab makes use of the transcriptionally accessible *ColA1* locus, in which an FRT “homing” cassette has been inserted downstream of the Collagen Type I gene (Beard et al., 2006). For our purposes, RMCE remains a significant improvement over conventional homologous recombination schemes in that it allows for rapid and efficient production of genetically modified mice without the need for elaborate and custom gene targeting vectors.

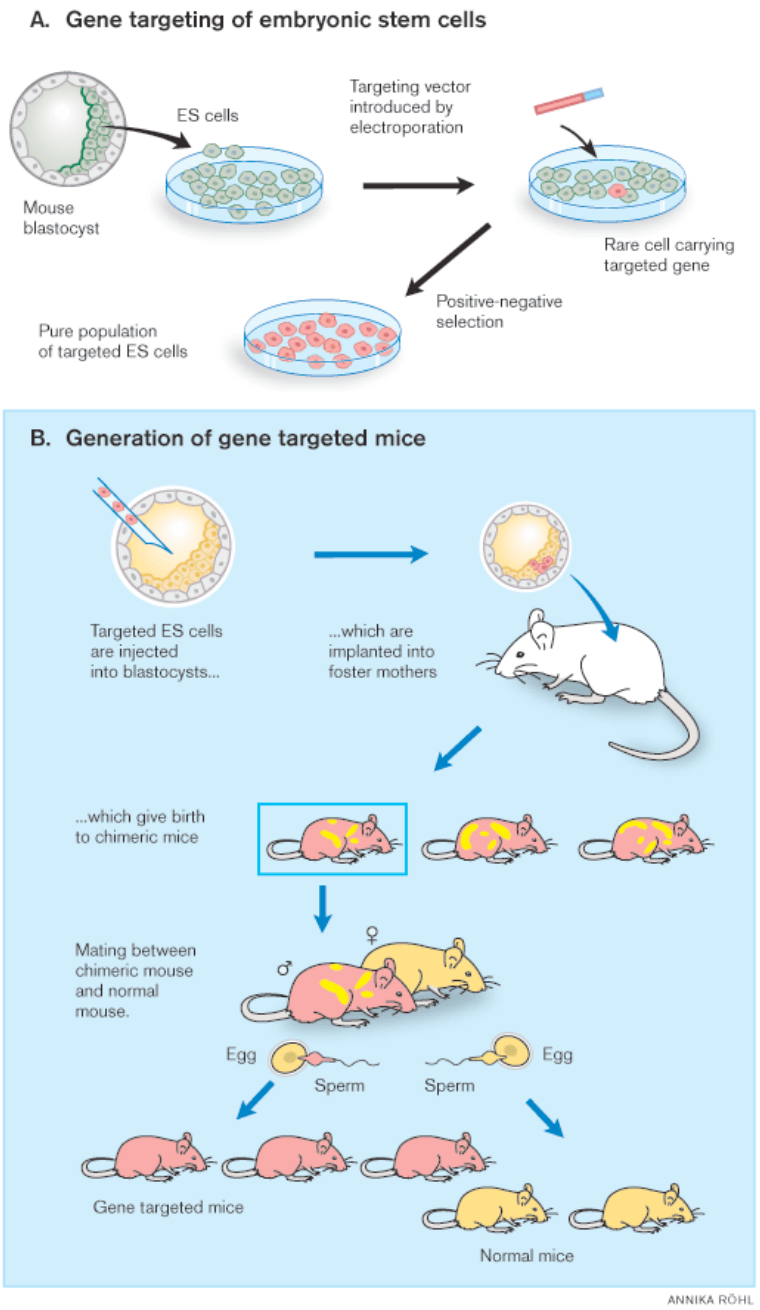

Figure 1.3 | General strategy for gene targeting in mice. *A,* Gene targeting of embryonic stem (ES) cells in culture, followed by positive-negative selection to enrich for ES cells containing the modified genes. *B,* Targeted ES cells are injected into blastocysts, which are injected into foster mothers to generate chimeric mice able to transmit the mutant gene to their progeny. To facilitate isolation of the desired progeny, the ES cells and recipient blastocysts are derived from mice with different coat color alleles (red – targeted ES cells; yellow – host blastocysts). Adapted from http://nobelprize.org/nobel_prizes/medicine/laureates/2007/adv.html

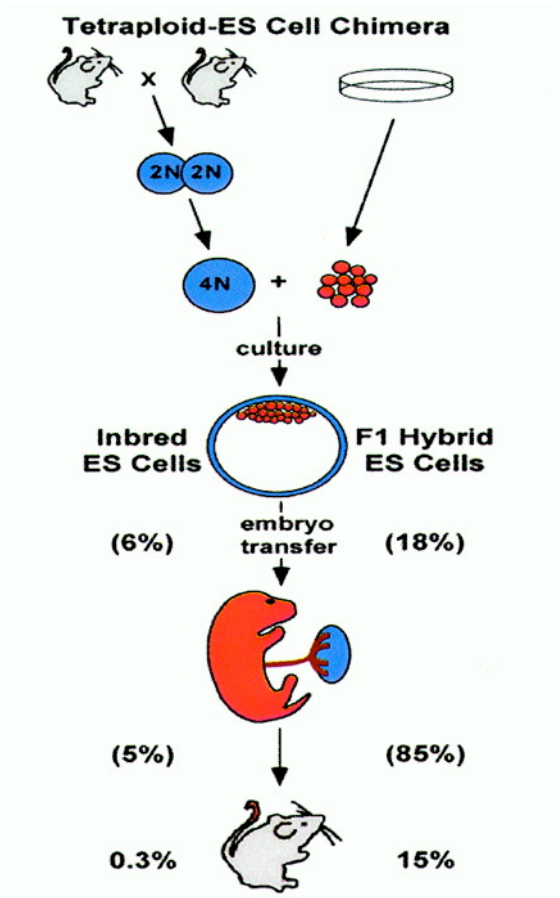

Figure 1.4 | General strategy for generation of ES cell-derived mice. Two cell-staged host blastocysts *(blue)* are given an electropulse for cell fusion to generate 4N blastocysts. Targeted ES cells *(red)* are injected by into the 4N blastocysts and blastocysts are transferred to surrogates. Fetuses are comprised of targeted ES cells while the host cells contribute to only the extraembryonic tissue. F_1-hybrid contain hybrid vigor and more successfully generate ES cell-derived mice. Adapted from Cross, J.C. *PNAS*. Factors affecting the developmental potential of cloned mammalian embryos. 98(11):5949-51 (2001).

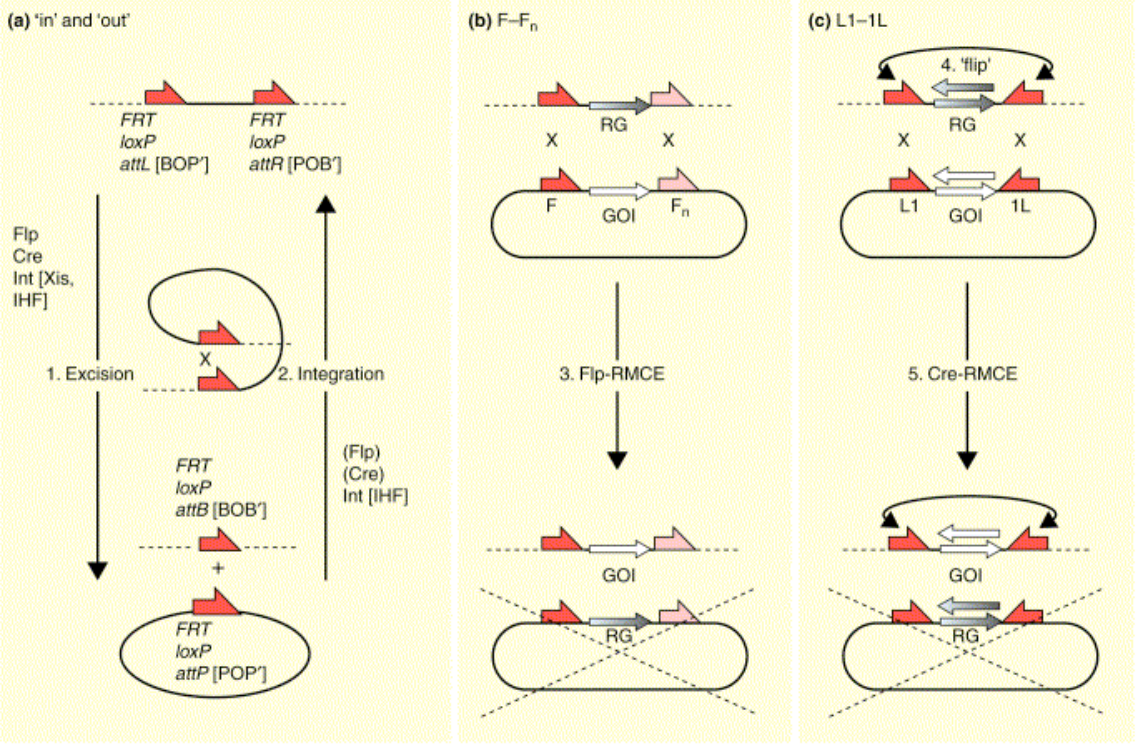

Figure 1.5 | Recombinase-mediated exchange strategies. *A,* Excision 'in' and 'out' (reaction 1) between two equally oriented target sites and its formal reversal, integration (reaction 2) by the 'addition' of a complete vector sequence. *B,* Recombinase-mediated cassette exchange (RCME, reaction 3) between established sets of heterospecific *FRT* sites (F and F_n). *C,* RMCE between two inversely oriented identical target sites (in this case *loxP,* L1 and 1L). The exchange yields both possible gene orientations due to the 'flip-principle'. Adapted from Baer, A. and Bode, J. *Curr Opin Biotechnol*. Coping with kinetic and thermodynamic barriers: RMCE, an efficient strategy for the targeted integration of transgenes. 12(5):473-80 (2001).

1.3 *In vivo* RNAi

The emergence of RNA interference (RNAi) has tremendously expanded the possibilities in cancer research. Historically, RNAi was known as post-transcriptional gene silencing (PTGS) and was first described in plants (Voinnet et al., 1998); only later was the phenomenon more clearly characterized in *C.*

elegans by Andrew Fire and Craig C. Mellos, who shared the Nobel Prize in 2005 for this discovery (Fire et al., 1998). Shortly after their initial description in *C. elegans*, RNAi was shown to be a conserved mechanism across species including mammalian organisms. Briefly, RNAi is initiated when double-stranded RNA (dsRNA) molecules are recognized and cleaved by the ribonuclease enzyme Dicer to produce small interfering RNAs (siRNAs) 21-25 bp in length with a few unpaired overhang bases on each end (Zamore et al., 2000). These siRNAs are incorporated into the RNA-induced silencing complex (also known as RISC) where they are paired to their target mRNA and induce cleavage of the mRNA, therefore preventing expression of the specific gene target.

Following this discovery, a new class of small, non-coding RNAs called microRNAs was characterized and shown to behave similar to siRNAs. Distinct from exogenous dsRNAs, miRNAs exist within the genome and are transcribed as pri-miRNAs. Following transcription, they are processed by the ribonuclease enzyme Drosha, to yield ~70nt precursors (pre-miRNAs) with stem-loop structures that are then exported to the cytoplasm where they undergo Dicer cleavage in a similar manner as dsRNAs (He and Hannon, 2004) (Fig. 1.6). Usually, one strand from the miRNA duplex is incorporated into RISC, which recognizes specific target mRNAs through imperfect base-pairing, often but not solely located in the 3' untranslated region (UTR), and downregulates their expression by preventing translation or possibly inducing mRNA cleavage. The eight nucleotides at the 5' end of a mature miRNA are designated as the "seed" sequence, which is complementary to the target mRNA.

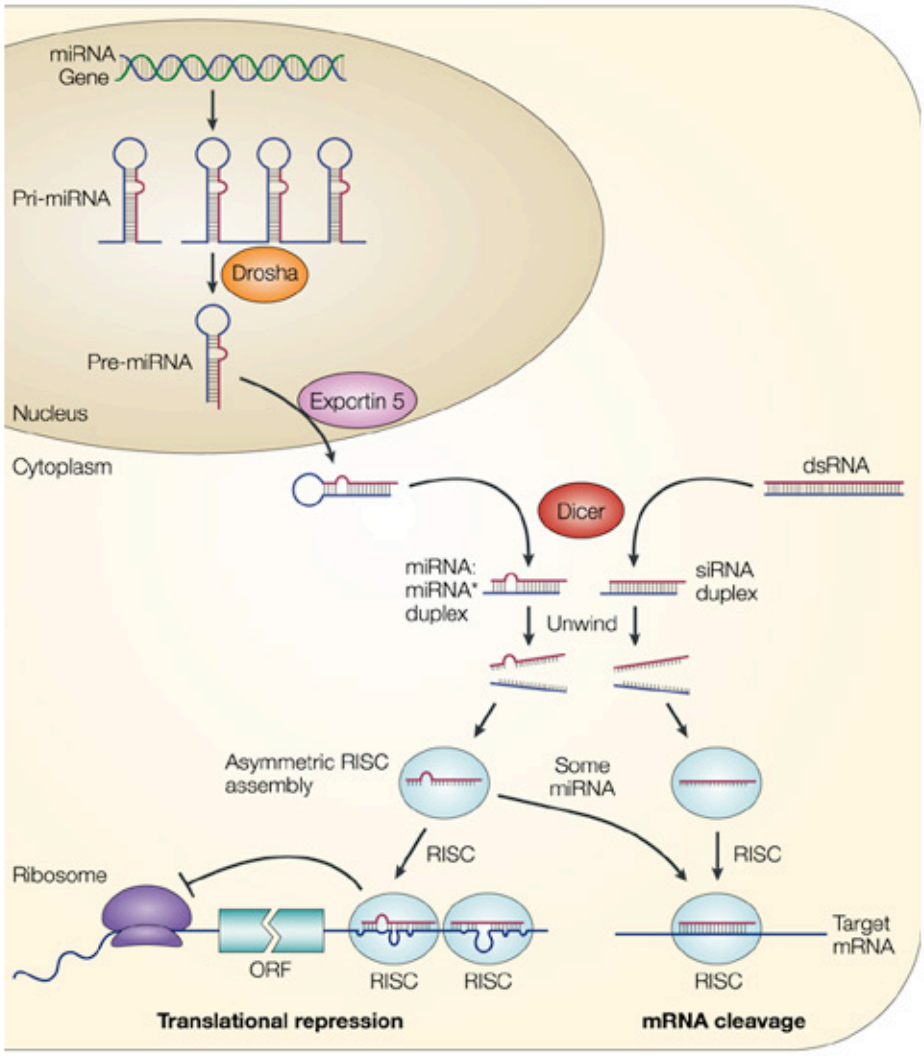

Figure 1.6 | The current model for the biogenesis and post-transcriptional suppression of microRNAs and small interfering RNAs. Adapted from He L, Hannon G.J. *Nat Rev Genet.* MicroRNAs: small RNAs with a big role in gene regulation. Nat Rev Genet. 5(7):522-31 (2004).

Undoubtedly, RNAi has revolutionized the study of biological processes, not only in cell-based systems, but also *in vivo*. It was not long after its initial characterization that its potential as a powerful tool was realized. By using synthetic short hairpin RNAs (shRNAs) with stem loop structures that fold and act as dsRNA precursors, RNAi has been used to induce sequence-specific gene

silencing. Initially, shRNAs were expressed from RNA Pol III promoters, but optimization of shRNA design has led to second-generation synthetic microRNA-based shRNAs, called shRNA-mirs. These consist of synthetic shRNAs embedded within an endogenous miRNA backbone (specifically miR30 for our vectors). When expressed from RNA Pol II promoters such as the MSCV retroviral LTR or tet-inducible TRE, these miR30-based shRNAs have been shown to outperform their standard stem-loop counterparts (Dickins et al., 2005). The Hannon laboratory has produced libraries of microRNA-based shRNAs that target nearly all genes within the human, mouse and rat genomes (http://codex.cshl.edu).

RNAi as a tool for reversible loss of gene function in vivo

The early examples of RNAi application for the study of tumor biology came from mosaic transplant models of lymphoma and hepatocellular carcinoma. Genetically sensitized cells were retrovirally infected *in vitro* with synthetic microRNAs, transplanted into recipient mice and shown to efficiently suppress tumor suppressor gene function *in vivo*, leading to tumor phenotypes (Hemann et al., 2003; Zender et al., 2005). These studies provided the first evidence that RNAi could be used to modulate tumor phenotypes *in vivo* and implied its use in mimicking knockout phenotypes.

Unlike traditional knockout approaches, RNAi-mediated gene silencing does not modify the target locus and therefore one of the most exciting applications of RNAi is the ability for reversible gene expression. By adapting the

tetracycline inducible system, TRE-driven miR30-based shRNAs were able to achieve temporal, DOX-dependent sequence-specific gene knockdown in *in vitro* systems (Dickins et al., 2005). This technology was later expanded for use in transgenic mice by the introduction of a tet-inducible shRNA expression cassette (TRE-miR30) into the mouse genome using standard transgenesis (Dickins et al., 2007). Using this method, we demonstrated that RNAi can cause sufficient knockdown in transgenic mice to recapitulate the phenotypes of knockout mice. Additionally, by crossing these mice to existing tissue-specific tet-transactivator strains, such as LAP-tTA and Eμ-tTA, we were able to spatially, temporally and reversibly regulate *Trp53* gene expression in the liver and B- and T-cell lineages. Other laboratories have also made functionally validated RNAi mouse models using different strategies listed in Table 1.4.

Oncogene dependence, tumor suppressor hypersensitivity and RNAi

Subsequent to numerous observations, the idea of “oncogene dependence” or “oncogene addiction” emerged. This hypothesis claims that tumors can become “addicted” to constitutive activity of an oncogene and they cannot continue to proliferate once the oncogenic stimulus is removed (Weinstein, 2002). Transgenic mouse models that conditionally express oncogenes have supported this concept; they show that several types of cancers regress following removal of the initiating oncogene, even in the presence of additional lesions (Chin et al., 1999; Felsher and Bishop, 1999; Fisher et al., 2001; Tam et al., 1999). More specifically, a recent study showed that repression

of the c-*myc* oncogene induced cellular senescence in diverse tumor types including lymphoma, osteosarcoma, and hepatocellular carcinoma (Wu et al., 2007a). However, this is not the case for all cancers. Osteosarcomas engineered to be deficient in *INK4a* or *Rb* failed to regress after *myc* inactivation (Wu et al., 2007a). Similar results were also seen in a breast cancer model in which only 50% of tumors regress following repression of a *myc* transgene, implying that half of the *myc*-initiated mammary tumors are less dependent on the initiating oncogene. In this cancer model, the cells recovered their malignant properties and were able to generate more aggressive tumors independent of *myc* re-expression (Boxer et al., 2004). This work underscores the progressive nature of cancer and the ability of tumor cells to rapidly acquire new spontaneous genetic lesions, allowing them to escape oncogene dependence.

A parallel concept to oncogene dependence is the idea of “tumor suppressor hypersensitivity”. Overexpression of a wild-type TSG (encoding, for example, p53, Rb, or APC) in human cancer cells lacking that TSG caused marked inhibition of growth, induction of apoptosis, and/or inhibition of tumorigenesis in mice even in the presence of an oncogene (Weinstein, 2000). Surprisingly, correction of just one lesion can have growth-inhibitory effects in cancer cells that contain multiple mutations, suggesting the possibility of a “hypersensitivity” to specific tumor suppressor genes (Weinstein, 2002). However, enforced overexpression of lost tumor suppressor genes may be impractical regarding later therapeutic applications. The use of conditional RNAi, however, allows us to study the effects of restoration of endogenous expression

levels of tumor suppressor genes downregulated in tumors.

Our first transgenic RNAi model demonstrated the potential applications of regulatable RNAi in mice. For the study of cancer, the ability to not only downregulate specific TSGs but to also restore TSG function in developed tumors was revolutionary. Using inducible RNAi technology, our lab successfully demonstrated TSG hypersensitivity by showing that reactivation of endogenous levels of p53 in either transplanted subcutaneous tumors or liver carcinomas derived from H-ras/p53-knockdown MEFS or hepatocytes respectively, was sufficient to cause long lasting tumor regressions (Dickins et al., 2005; Xue et al., 2007). Wen Xue and Lars Zender went further and characterized the response to p53 reactivation in HCC, showing a dramatic induction of senescence in tumors followed by recruitment of and clearance by the innate immune system. The requirement of p53 suppression for maintenance of Eμ-*myc* lymphomas was also shown in fully transgenic tet-inducible RNAi mice (Dickins et al., 2007; Xue et al., 2007). These pivotal studies demonstrated that in specific genetic contexts, continual loss of TSGs is required in order to maintain established tumors.

With further studies, we may be able to pinpoint direct targets whose downregulation could result in increased TSG activity (e.g. PTEN→PIK3CA or Arf→MDM2) and ultimately tumor regression by potentially triggering anti-tumor mechanisms. These studies may also implicate demethylase and histone deacetylase (DNMT/HDAC) inhibitors for reestablishment of candidate targets that are commonly downregulated by promoter hypermethylation (e.g. *Ink4A/ARF*). Furthermore, targets that are mainly downregulated due to an

increased protein turnover may be accessible by specific inhibition of components of the proteasome. Clearly, inducible RNAi technology holds great promise and can help focus and expedite the drug development process. The ability to use shRNA-mir transgenic mice as functional *in vivo* validation would further increase the confidence in pursuing cost- and time-intensive therapeutic developments.

Lung cancer is one in particular in which surgical removal is often the first and most successful treatment, and therapeutics other than surgical treatment of lung cancer are severely lacking. Standard therapies result in a high rate of relapse and toxic side affects, and many new therapeutic are behind in development. Advances in the understanding of the molecular events underlying the development of lung cancer will enable researchers to develop rationally targeted therapies that specifically target proteins used by cancer cells to promote inappropriate growth and survival. Genetic modifications combined with inducible RNAi will create murine lung cancer models that may provide a useful reagent for pre-clinical testing of therapeutics directed against the specific molecular lesions driving tumorigenesis in these mice.

Table 1.4 | Transgenic and targeted mouse models using RNAi.

Method	Promoters	Advantages	Disadvantages	References
Pronuclear injection	H1, mU6 loxP, Zp3	Ubiquitious or conditional	Random integration, multiple copy number, positional effects, laborious screening, variability between founders with same shRNA	(Fedoriw et al., 2004; Hasuwa et al., 2002; Lickert et al., 2005; Stein et al., 2003; Wang et al., 2007)
	CMV pol II	Tissue-specificity, long dsRNA		(Shinagawa and Ishii, 2003)
	TRE_{CMVmin}	Tissue-specificity, regulatable		(Dickins et al., 2007)
Random or lentiviral integration into ES cells	hU6, H1, mU6 loxP	Ubiquitious or conditional	Random integration, multiple copy number, positional effects, laborious screening, variability between founders with same shRNA	(Carmell et al., 2003; Kunath et al., 2003; Rubinson et al., 2003; Tiscornia et al., 2003; Ventura et al., 2004)
Homologous recombination into HPRT-locus	mU6 loxP	Single copy, site-specific, conditional	X-linked and subjected to random X-inactivation; not regulatable	(Oberdoerffer et al., 2005)
Recombinase-mediated cassette exchange (RMCE) into HPRT-locus	TRE loxP	Single copy, site-specific, regulatable	X-linked and subjected to random X-inactivation; never made mice only ES cells	(Wang et al., 2007)
RMCE into Rosa26 locus	H1, hU6, mU6 loxP, H1tetO	Single copy, site-specific, regulatable, Gateway cloning system available for rapid cloning, tissue-specific by CRE	Most are conditional but not reversible, *Rosa26* locus gives variable expression in tissues	(Hitz et al., 2007; Nyabi et al., 2009; Seibler et al., 2007; Seibler et al., 2005; Seidler et al., 2008)
RCAS-TVA retroviral delivery	Rosa26-*LSL*-TVA	Ability to change shRNA easily, tissue-specificity depending on CRE	Mosaic, variability between lines	(Seidler et al., 2008)

1.4 Genetic aberrations in lung cancer

Lung cancer is the leading cause of cancer deaths worldwide (Jemal et al., 2005). According to the United States Cancer Statistics (USCS) documented by the Centers for Disease Control, in 2006 alone, nearly 200,000 people in the US were diagnosed with lung cancer and almost 160,000 others died from it. Forty years ago, patients diagnosed with lung cancer had a 5-year survival rate of only 7%. Despite our increased knowledge on cancer biology, advances in cytotoxic drug development, radiotherapy and patient management, the cure rate remains dismal, as the 5-year survival rate has only improved marginally, from 7% to 14% since 1970. Historically, lung cancer was commonly believed to be a smokers' disease and was strongly linked with small cell lung cancer (SCLC) and squamous cell carcinoma, however more than 10% of all cases also arise in people who have never been smokers, revealing that lung cancer development is not strictly determined by environmental factors but is mostly certainly influenced by genetic predisposition.

Non-small-cell lung cancer (NSCLC) accounts for 85% of all lung cancer cases, with adenocarcinoma being the predominant subtype (Herbst et al., 2008). It is commonly associated with mutations in a few well-characterized oncogenes, including oncogenic *Ras* and mutant *EGFR* (epidermal growth factor receptor), and tumor suppressor genes, *Trp53* and *INK4a*/ARF. Recent data report that activating mutations of the *KRas* oncogene are limited to NSCLC and found in ~10-30% of cases (Miller et al., 2008). Inactivating mutations of *Trp53*

are even more frequent, occurring in roughly 50% of patients (Herbst et al., 2008). Other common inactivating mutations, often due to promoter hypermethylation, involve the *INK4a/ARF* locus, which encodes for both p16 and ARF tumor suppressor proteins. Individually, p16 inactivation is seen in nearly 40-50% of NSCLC cases while ARF suppression occurs less frequently in NSCLC (~20%) but more commonly in small-cell lung cancer (SCLC; ~60%) (Jackson et al., 2001). A more thorough list of genetic mutations commonly found in human lung cancer can be found on Table. 1.5.

Oncogenes and tumor suppressor genes

Briefly, *Kras* is a membrane-associated GTPase signaling protein that regulates proliferation, differentiation and cell survival. Missense mutations at codons 12, 13 and 61 result in constitutive GTPase activity and subsequent signaling (Campbell et al., 1998). They typically exist mutually exclusive to mutations in the *EGFR* kinase domain and generally mark poor prognosis, as they are associated with resistance to *EGFR* inhibitors and chemotherapy (Eberhard et al., 2005; Pao et al., 2005). Furthermore, *Kras* mutations appear to be an early event, detectable in preinvasive lesions of atypical adenomatous hyperplasia (AAHP) and bronchoalveolar carcinoma (Westra, 2000).

Table 1.5 | Genetic Abnormalities Specific in the Lung to Non-Small-Cell Lung Cancer and Small-Cell Lung Cancer. This table was taken from Herbst et al. Lung Cancer. *NJEM.* 359:1367-1380 (2008).

Table 1. Genetic Abnormalities Specific in the Lung to Non–Small-Cell Lung Cancer and Small-Cell Lung Cancer.*

Abnormality	Non–Small-Cell Lung Cancer		Small-Cell Lung Cancer
	Squamous-Cell Carcinoma	Adenocarcinoma	
Precursor			
Lesion	Known (dysplasia)	Probable (atypical adenomatous hyperplasia)	Possible (neuroendocrine field)†
Genetic change	*p53* mutation	*KRAS* mutation (atypical adenomatous hyperplasia in smokers), *EGFR* kinase domain mutation (in nonsmokers)	Overexpression of c-MET
Cancer			
KRAS mutation	Very rare	10 to 30%‡	Very rare
BRAF mutation	3%	2%	Very rare
EGFR			
Kinase domain mutation	Very rare	10 to 40%‡	Very rare
Amplification§	30%	15%	Very rare
Variant III mutation	5%¶	Very rare	Very rare
HER2			
Kinase domain mutation	Very rare	4%	Very rare
Amplification	2%	6%	Not known
ALK fusion‖	Very rare	7%	Not known
MET			
Mutation	12%	14%	13%
Amplification	21%	20%	Not known
TITF-1 amplification	15%	15%	Very rare
p53 mutation	60 to 70%	50 to 70%‡	75%
LKB1 mutation	19%	34%	Very rare
PIK3CA			
Mutation	2%	2%	Very rare
Amplification	33%	6%	4%

* Non–small-cell lung cancer includes squamous-cell carcinoma and adenocarcinoma.
† Neuroendocrine fields have been detected only in tissue surrounding tumors and have been characterized by extremely high rates of allelic loss and by c-MET overexpression (Salgia R: personal communication).
‡ Variations are based in part on smoking profiles.
§ The percentages include increased gene copy numbers from amplification or polysomy and represent percentages from resected cancers. The percentages are higher in primary tumors from patients with metastatic disease. Increased copy numbers have been reported in squamous dysplastic lesions but not in adenocarcinoma precursors.
¶ Genomic *EGFR* variant III mutations have been detected only in lung squamous-cell carcinoma, and these tumors are sensitive preclinically to irreversible EGFR tyrosine kinase inhibitors. The incidence of 5% is substantially lower than that of 30 to 40% for the detection in squamous-cell carcinoma or adenocarcinoma by immunohistochemical analysis or other techniques.
‖ The anaplastic lymphoma kinase (*ALK*) fusion gene (involving chromosome 2p), consisting of parts of *EML4* and *ALK*, is transforming in fibroblasts and occurs in adenocarcinoma but not in other types of non–small-cell lung cancer or other nonlung cancers.

The *Trp53* gene encodes for the p53 tumor suppressor protein, which has often been described as "the guardian of the genome". As a transcriptional regulator, p53 has many anticancer mechanisms and can be activated in

response to DNA damage, oncogene activation or hypoxia, to orchestrate biological outputs such as apoptosis, cell-cycle arrest, senescence or modulation of autophagy (Zilfou and Lowe, 2009). In response to cellular stress, p53 must first be stabilized by various kinases (ATM, ATR, DNA-PK, Chk1 and Chk2) to disrupt interaction with its negative regulator, Mdm2, which promotes ubiquitin-mediated degradation of p53 (Appella and Anderson, 2001). Following its stabilization, p53 sequence-specifically binds DNA to activate or repress a number of target genes, notably activating proapoptotic genes (Bax, Perp, Noxa and PUMA) and cell-cycle regulators (p21), while repressing anti-apoptotic genes (Bcl-2, Bcl-XL and survivin) (Zilfou and Lowe, 2009).

The *INK4a/ARF* locus is also a major player in anti-tumor defenses, encoding for two proteins, $p16^{INK4a}$ (p16) and $p19^{ARF}$ (p19 or $p14^{ARF}$ in humans) through alternative open reading frames using different 5' regulatory regions. These two proteins have non-overlapping functions and regulate distinct tumor suppressor pathways in response to aberrant growth or oncogenic stress, including *Ras* and *myc* signaling (Kim and Sharpless, 2006). Specifically, the *INK4* proteins, including p16, are potent inhibitors of the cell cycle. They function by binding to cyclin-dependent kinases 4 and 6 (cdk4/6) and inhibiting their kinase activity. Subsequently, they activate the Rb pathway, leading to repression of E2F transcription factor activity and growth arrest. p19 also plays a role in tumor suppression, but it does so by binding and inhibiting Mdm2. As a result, expression of p19 indirectly activates p53, a key protein that can initiate apoptosis and/or cause cellular senescence, processes that are important

barriers to tumorigenesis.

Mouse models of lung cancer

Earlier models of lung cancer included inbred strains of mice susceptible to spontaneous and chemically induced tumor development (Tuveson and Jacks, 1999). However, in contrast to the aggressive carcinomas developed in humans, most spontaneous murine pulmonary lesions in these models were less invasive, consisting mainly of hyperplasias and adenomas. For example, systematic treatment of mice with carcinogens, such as vinyl carbamate, was shown to induce proliferative lesions and yield adenocarcinoma formation only at low frequencies. These carcinomas shared many features in common with human pulmonary adenocarcinomas in morphology and genetic alterations, including activation of the *Kras* oncogene and inactivation of the *p16INKa* tumor suppressor (Tuveson and Jacks, 1999). Close examination of these mice indicated progression from hyperplasia, to adenomas, to malignant carcinomas and contributed to our current understanding of human lung tumor progression as a multistep process.

Advances in transgenesis and gene targeting approaches opened up possibilities to manipulate the mouse genome and create custom mouse models for examining the precise roles of cancer genes in lung neoplasia. Several of these models (listed in Table 1.1-1.3) acquired proliferative lesions ranging from hyperplasia to adenocarcinoma. Classic transgenic mouse models of lung cancer were generally based on overexpression of oncogenes in lung tissue, in which

restricted expression was achieved using lung-specific promoters such as the alveolar type II cell-specific surfactant protein C (*SP-C*) promoter (Glasser et al., 1991), the nonciliated secretory cell-specific Clara cell secretory protein (*CCSP*) promoter (Ray et al., 1993; Stripp et al., 1992) and the calcitonin gene-related peptide (*CGRP*) promoter. For example, the *CCSP-T-Ag* model resulted in the transformation of Clara cells of the airways and was useful for the generation of cell-specific cell lines (Magdaleno et al., 1997). Other models that gave rise to pulmonary oncogenic transformation used the *SP-C* promoter to express oncogenes, such as *myc* (Ehrhardt et al., 2001) and *Raf-1* (Kerkhoff et al., 2000). Transgenic models are informative, but they typically presented with numerous lesions that rarely progressed to full blown carcinomas before mice become moribund.

Subsequently, gene targeting brought about many new approaches to lung cancer modeling. Conditional knock-in mutants and binary tet-inducible mice made it possible to specifically regulate gene expression temporally in the lung. One of the most widely used models of lung adenocarcinoma is the conditional mutant *LSL-Kras*^{G12D}, which contains an activated mutant allele at the endogenous *Kras* locus (Jackson et al., 2001). This model overcomes the limitations of most transgenic and carcinogenic models by using adeno-Cre delivery for mutant gene activation, allowing control over the timing and multiplicity of tumor initiation. By crossing *LSL-Kras*^{G12D} mice to others deficient in p53 or p16, cooperations between these lesions were established. In these compound mutants, *Kras* activation cooperated potently with p53 loss, but only

modestly with p16 loss in lung tumorigenesis. In contrast, concomitant p16 and p53 inactivation without the *Kras* mutant allele produced infrequent but highly lethal tumors indicating that the *Kras* mutation initiates tumorigenesis, whereas p16 and p53 constrain tumor progression (Ji et al., 2007); however the cooperation between these lesions is still not well understood.

Genomic approaches to indentify lung cancer aberrations

In addition to the many well-characterized lesions, it is likely that many unknown mutations also exist and contribute to the aggressive nature of lung cancer. In humans, it is thought that more than 10 genetic or epigenetic abnormalities occur before lung tumors become clinically evident (Meuwissen et al., 2001). In order to identify lung cancer-relevant genes, several genome-scale efforts have been initiated that include: (1) systematic genome re-sequencing to identify specific mutations in known lung cancer genes (Paez et al., 2004); (2) comparative genomic hybridization (CGH) array to detect copy number alterations (Lucito et al., 2003); and (3) single-nucleotide polymorphism array analysis to capture point mutations in candidate genes (Zhao et al., 2004). These efforts have proved highly productive in identifying specific mutations and discovering novel lung cancer-specific genomic alterations. For example, re-sequencing approaches identified mutations in the *EGFR* kinase domain in human lung cancer and showed their correlation with patient response to the kinase inhibitors gefitinib and erlotinib (Greulich et al., 2005; Lynch et al., 2004). Additional *in vitro* studies have begun to validate potential gene candidates; in

particular, somatic mutations in *EGFR, BRAF* and *PI3K* kinases have shown to possess transforming activity and further investigation may identify therapeutics with specific kinase inhibitory properties. While results from these *in vitro* studies will be informative, it will still be essential to recapitulate the complex nature of *de novo* tumorigenesis or *in vivo* responses to therapy, both of which can be accomplished in animal models.

1.5 Prelude to research

At the time I began my research at CSHL, the oncogene dependence hypothesis had become more widely accepted, as ongoing clinical success of targeted therapies, such as Gleevec® (imatinib), Herceptin® (trastuzumab), Iressa® (gefitinib) and Tarceva® (erlotinib), continued to demonstrate that some cancers harnessed vulnerabilities to the disruption of dominant oncogenic pathways. These positive therapeutic responses along with animal models mimicking oncogene dependence provided strong grounds for optimism toward controlling cancer more effectively in the future. Regression of tumors following oncogene inhibition gave insight into the critical roles of initiating genetic alterations, showing their importance in the maintenance of early and late staged tumors with malignant phenotypes.

These findings also triggered the question of whether the opposite condition would hold true – whether “tumor hypersensitivity” would render tumors susceptible to tumor suppressor gene reactivation. Prior to the discovery of

RNAi, addressing this question would have posed a difficult feat, as the reexpression of deleted genes was not as simple as downregulating overexpressed oncogenes. The discover of the RNAi machinery and subsequent development of RNAi technology has provided a new means to manipulate gene expression, and this has facilitated the ability to dissect the role of tumor suppressor genes and address this question in understanding their function in tumor maintenance, findings which may have important implications for therapy. Although reconstituting deleted TSGs in patients by gene therapy may be hard to achieve in the near future, these studies will be able to point to other direct targets whose inhibition could indirectly result in increase TSG activity. Such examples were aforementioned.

Several inducible mouse models of lung cancer have characterized the dependence of lung tumors on EGFR and *Kras* mutations, suggesting inhibition of these oncogenes would prove beneficial in patients with NSCLC. While many patients with EGFR mutations have been successfully treated with erlotinib, an EGFR inhibitor, drugs that specifically inhibit *Kras* mutants are still being tested for clinical use. Because of this, lung cancer patients with *Kras* mutations rarely respond to targeted therapies and only marginally to standard cytotoxic therapies. For these patients, it will be crucial to identify other potential targets whose inhibition will inhibit growth in *Kras*-driven lung adenocarcinomas.

For this purpose, I aimed to examine the mechanisms of the most commonly inactivated TSGs, *Trp53* and *INK4a/ARF*, and determine their roles in tumor maintenance of $Kras^{G12D}$-driven lung adenocarcinomas using animals

harboring tet-inducible shRNAs. Unfortunately, our first generation RNAi model harboring an shRNA targeting *Trp53* (p53.1224) was generated using pronuclear injection (Dickins et al., 2007), which proved to be a labor intensive and an unreliable approach and failed to provide mice with potent *INK4a/ARF* suppression.

Therefore, to begin, I first set out to improve RNAi technology in mice and establish a platform for systematic generation of tet-inducible transgenic shRNA mice. Subsequent generations of RNAi mice, also produced by pronuclear injection, failed to produce any functional strains and eventually led to our use of a site-specific targeting method. By adapting a RMCE strategy and optimizing it for integration of tet-inducible shRNA expression cassettes at the *ColA1* locus, we were able to generate an efficient, reliable and scalable approach for generation of RNAi mice.

To establish a lung adenocarcinoma model that could be monitored by bioluminescence, shRNA mice were crossed to *LSL-Kras*^{G12D}, *Rosa26-LSL-luciferase* and CCSP-rtTA to achieve gene regulation specifically in the lung. Owing to the slow rate and high expense of generating quadruple transgenics, we later devised a strategy to re-derive ES cell lines harboring all relevant alleles for the production of lung adenocarcinomas. These ES cells were subsequently used to produce large cohorts of mosaic mice with lung adenocarcinomas, which allowed us to examine the response to reaction of *INK4a/ARF* or *Trp53* in the context of mutant *Kras*. We report distinct response patterns upon TSG restoration: p53 restoration resulted in only a marginal survival benefit while

INK4a/ARF restoration caused rapid but unsustainable tumor regression. We further examined the molecular characteristics of each regression pattern and propose mechanistic cooperative differences between *Trp53* or *INK4a/ARF* and mutant *Kras* that are responsible for the differential outcomes.

1.6 References

Adams, J.M., Harris, A.W., Pinkert, C.A., Corcoran, L.M., Alexander, W.S., Cory, S., Palmiter, R.D., and Brinster, R.L. (1985). The c-myc oncogene driven by immunoglobulin enhancers induces lymphoid malignancy in transgenic mice. Nature *318*, 533-538.

Aguirre, A.J., Bardeesy, N., Sinha, M., Lopez, L., Tuveson, D.A., Horner, J., Redston, M.S., and DePinho, R.A. (2003). Activated *Kras* and $p16^{INK4a/}p19^{ARF}$ deficiency cooperate to produce metastatic pancreatic ductal adenocarcinoma. Genes Dev *17*, 3112-3126.

Andressoo, J.O., Mitchell, J.R., de Wit, J., Hoogstraten, D., Volker, M., Toussaint, W., Speksnijder, E., Beems, R.B., van Steeg, H., Jans, J.*, et al.* (2006). An Xpd mouse model for the combined xeroderma pigmentosum/Cockayne syndrome exhibiting both cancer predisposition and segmental progeria. Cancer Cell *10*, 121-132.

Appella, E., and Anderson, C.W. (2001). Post-translational modifications and activation of p53 by genotoxic stresses. Eur J Biochem *268*, 2764-2772.

Baer, A., and Bode, J. (2001). Coping with kinetic and thermodynamic barriers: RMCE, an efficient strategy for the targeted integration of transgenes. Curr Opin Biotechnol *12*, 473-480.

Balmain, A. (2002). Cancer as a complex genetic trait: tumor susceptibility in humans and mouse models. Cell *108*, 145-152.

Bautch, V.L., Toda, S., Hassell, J.A., and Hanahan, D. (1987). Endothelial cell tumors develop in transgenic mice carrying polyoma virus middle T oncogene. Cell *51*, 529-537.

Beard, C., Hochedlinger, K., Plath, K., Wutz, A., and Jaenisch, R. (2006). Efficient method to generate single-copy transgenic mice by site-specific integration in embryonic stem cells. Genesis *44*, 23-28.

Bell, A.C., and Felsenfeld, G. (2000). Methylation of a CTCF-dependent boundary controls imprinted expression of the Igf2 gene. Nature *405*, 482-485.

Boxer, R.B., Jang, J.W., Sintasath, L., and Chodosh, L.A. (2004). Lack of sustained regression of c-MYC-induced mammary adenocarcinomas following brief or prolonged MYC inactivation. Cancer Cell *6*, 577-586.

Brinster, R.L., Chen, H.Y., Messing, A., van Dyke, T., Levine, A.J., and Palmiter, R.D. (1984). Transgenic mice harboring SV40 T-antigen genes develop characteristic brain tumors. Cell *37*, 367-379.

Campbell, S.L., Khosravi-Far, R., Rossman, K.L., Clark, G.J., and Der, C.J. (1998). Increasing complexity of Ras signaling. Oncogene *17*, 1395-1413.

Capecchi, M.R. (1980). High efficiency transformation by direct microinjection of DNA into cultured mammalian cells. Cell *22*, 479-488.

Capecchi, M.R. (1989). Altering the genome by homologous recombination. Science *244*, 1288-1292.

Carmell, M.A., Zhang, L., Conklin, D.S., Hannon, G.J., and Rosenquist, T.A. (2003). Germline transmission of RNAi in mice. Nat Struct Biol *10*, 91-92.

Chin, L., Tam, A., Pomerantz, J., Wong, M., Holash, J., Bardeesy, N., Shen, Q., O'Hagan, R., Pantginis, J., Zhou, H.*, et al.* (1999). Essential role for oncogenic Ras in tumour maintenance. Nature *400*, 468-472.

Colnot, S., Decaens, T., Niwa-Kawakita, M., Godard, C., Hamard, G., Kahn, A., Giovannini, M., and Perret, C. (2004). Liver-targeted disruption of Apc in mice activates beta-catenin signaling and leads to hepatocellular carcinomas. Proc Natl Acad Sci U S A *101*, 17216-17221.

Cross, J.C. (2001). Factors affecting the developmental potential of cloned mammalian embryos. Proc Natl Acad Sci U S A *98*, 5949-5951.

DePinho, R.A. (2000). The age of cancer. Nature *408*, 248-254.

Derksen, P.W., Liu, X., Saridin, F., van der Gulden, H., Zevenhoven, J., Evers, B., van Beijnum, J.R., Griffioen, A.W., Vink, J., Krimpenfort, P.*, et al.* (2006). Somatic inactivation of E-cadherin and p53 in mice leads to metastatic lobular mammary carcinoma through induction of anoikis resistance and angiogenesis. Cancer Cell *10*, 437-449.

Dickins, R.A., Hemann, M.T., Zilfou, J.T., Simpson, D.R., Ibarra, I., Hannon, G.J., and Lowe, S.W. (2005). Probing tumor phenotypes using stable and regulated synthetic microRNA precursors. Nat Genet *37*, 1289-1295.

Dickins, R.A., McJunkin, K., Hernando, E., Premsrirut, P.K., Krizhanovsky, V., Burgess, D.J., Kim, S.Y., Cordon-Cardo, C., Zender, L., Hannon, G.J.*, et al.* (2007). Tissue-specific and reversible RNA interference in transgenic mice. Nat Genet *39*, 914-921.

Dinulescu, D.M., Ince, T.A., Quade, B.J., Shafer, S.A., Crowley, D., and Jacks, T. (2005). Role of K-ras and Pten in the development of mouse models of endometriosis and endometrioid ovarian cancer. Nat Med *11*, 63-70.

Donehower, L.A., Harvey, M., Slagle, B.L., McArthur, M.J., Montgomery, C.A., Jr., Butel, J.S., and Bradley, A. (1992). Mice deficient for p53 are developmentally normal but susceptible to spontaneous tumours. Nature *356*, 215-221.

Eberhard, D.A., Johnson, B.E., Amler, L.C., Goddard, A.D., Heldens, S.L., Herbst, R.S., Ince, W.L., Janne, P.A., Januario, T., Johnson, D.H.*, et al.* (2005). Mutations in the epidermal growth factor receptor and in KRAS are predictive and prognostic indicators in patients with non-small-cell lung cancer treated with chemotherapy alone and in combination with erlotinib. J Clin Oncol *23*, 5900-5909.

Edelmann, W., Yang, K., Umar, A., Heyer, J., Lau, K., Fan, K., Liedtke, W., Cohen, P.E., Kane, M.F., Lipford, J.R.*, et al.* (1997). Mutation in the mismatch repair gene Msh6 causes cancer susceptibility. Cell *91*, 467-477.

Eggan, K., Akutsu, H., Loring, J., Jackson-Grusby, L., Klemm, M., Rideout, W.M., 3rd, Yanagimachi, R., and Jaenisch, R. (2001). Hybrid vigor, fetal overgrowth, and viability of mice

derived by nuclear cloning and tetraploid embryo complementation. Proc Natl Acad Sci U S A *98*, 6209-6214.

Ehrhardt, A., Bartels, T., Geick, A., Klocke, R., Paul, D., and Halter, R. (2001). Development of pulmonary bronchiolo-alveolar adenocarcinomas in transgenic mice overexpressing murine c-myc and epidermal growth factor in alveolar type II pneumocytes. Br J Cancer *84*, 813-818.

Fedoriw, A.M., Stein, P., Svoboda, P., Schultz, R.M., and Bartolomei, M.S. (2004). Transgenic RNAi reveals essential function for CTCF in H19 gene imprinting. Science *303*, 238-240.

Felsher, D.W., and Bishop, J.M. (1999). Reversible tumorigenesis by MYC in hematopoietic lineages. Mol Cell *4*, 199-207.

Fire, A., Xu, S., Montgomery, M.K., Kostas, S.A., Driver, S.E., and Mello, C.C. (1998). Potent and specific genetic interference by double-stranded RNA in Caenorhabditis elegans. Nature *391*, 806-811.

Fisher, G.H., Wellen, S.L., Klimstra, D., Lenczowski, J.M., Tichelaar, J.W., Lizak, M.J., Whitsett, J.A., Koretsky, A., and Varmus, H.E. (2001). Induction and apoptotic regression of lung adenocarcinomas by regulation of a K-Ras transgene in the presence and absence of tumor suppressor genes. Genes Dev *15*, 3249-3262.

Frese, K.K., and Tuveson, D.A. (2007). Maximizing mouse cancer models. Nat Rev Cancer *7*, 645-658.

Furth, P.A., St Onge, L., Boger, H., Gruss, P., Gossen, M., Kistner, A., Bujard, H., and Hennighausen, L. (1994). Temporal control of gene expression in transgenic mice by a tetracycline-responsive promoter. Proc Natl Acad Sci U S A *91*, 9302-9306.

Glasser, S.W., Korfhagen, T.R., Wert, S.E., Bruno, M.D., McWilliams, K.M., Vorbroker, D.K., and Whitsett, J.A. (1991). Genetic element from human surfactant protein SP-C gene confers bronchiolar-alveolar cell specificity in transgenic mice. Am J Physiol *261*, L349-356.

Gordon, J.W., Scangos, G.A., Plotkin, D.J., Barbosa, J.A., and Ruddle, F.H. (1980). Genetic transformation of mouse embryos by microinjection of purified DNA. Proc Natl Acad Sci U S A *77*, 7380-7384.

Gossen, M., and Bujard, H. (1992). Tight control of gene expression in mammalian cells by tetracycline-responsive promoters. Proc Natl Acad Sci U S A *89*, 5547-5551.

Greulich, H., Chen, T.H., Feng, W., Janne, P.A., Alvarez, J.V., Zappaterra, M., Bulmer, S.E., Frank, D.A., Hahn, W.C., Sellers, W.R.*, et al.* (2005). Oncogenic transformation by inhibitor-sensitive and -resistant EGFR mutants. PLoS Med *2*, e313.

Hanahan, D. (1985). Heritable formation of pancreatic beta-cell tumours in transgenic mice expressing recombinant insulin/simian virus 40 oncogenes. Nature *315*, 115-122.

Hasuwa, H., Kaseda, K., Einarsdottir, T., and Okabe, M. (2002). Small interfering RNA and gene silencing in transgenic mice and rats. FEBS Lett *532*, 227-230.

He, L., and Hannon, G.J. (2004). MicroRNAs: small RNAs with a big role in gene regulation. Nat Rev Genet *5*, 522-531.

Hemann, M.T., Fridman, J.S., Zilfou, J.T., Hernando, E., Paddison, P.J., Cordon-Cardo, C., Hannon, G.J., and Lowe, S.W. (2003). An epi-allelic series of p53 hypomorphs created by stable RNAi produces distinct tumor phenotypes in vivo. Nat Genet *33*, 396-400.

Herbst, R.S., Heymach, J.V., and Lippman, S.M. (2008). Lung cancer. N Engl J Med *359*, 1367-1380.

Heyer, J., Yang, K., Lipkin, M., Edelmann, W., and Kucherlapati, R. (1999). Mouse models for colorectal cancer. Oncogene *18*, 5325-5333.

Hingorani, S.R., Petricoin, E.F., Maitra, A., Rajapakse, V., King, C., Jacobetz, M.A., Ross, S., Conrads, T.P., Veenstra, T.D., Hitt, B.A.*, et al.* (2003). Preinvasive and invasive ductal pancreatic cancer and its early detection in the mouse. Cancer Cell *4*, 437-450.

Hingorani, S.R., Wang, L., Multani, A.S., Combs, C., Deramaudt, T.B., Hruban, R.H., Rustgi, A.K., Chang, S., and Tuveson, D.A. (2005). *Trp53*R172H and *Kras*G12D cooperate to promote chromosomal instability and widely metastatic pancreatic ductal adenocarcinoma in mice. Cancer Cell *7*, 469-483.

Hitz, C., Wurst, W., and Kuhn, R. (2007). Conditional brain-specific knockdown of MAPK using Cre/loxP regulated RNA interference. Nucleic Acids Res *35*, e90.

Hsiao, Y.C., Chang, H.H., Tsai, C.Y., Jong, Y.J., Horng, L.S., Lin, S.F., and Tsai, T.F. (2004). Coat color-tagged green mouse with EGFP expressed from the RNA polymerase II promoter. Genesis *39*, 122-129.

Imren, S., Fabry, M.E., Westerman, K.A., Pawliuk, R., Tang, P., Rosten, P.M., Nagel, R.L., Leboulch, P., Eaves, C.J., and Humphries, R.K. (2004). High-level beta-globin expression and preferred intragenic integration after lentiviral transduction of human cord blood stem cells. J Clin Invest *114*, 953-962.

Izeradjene, K., Combs, C., Best, M., Gopinathan, A., Wagner, A., Grady, W.M., Deng, C.X., Hruban, R.H., Adsay, N.V., Tuveson, D.A.*, et al.* (2007). *Kras*(G12D) and Smad4/Dpc4 haploinsufficiency cooperate to induce mucinous cystic neoplasms and invasive adenocarcinoma of the pancreas. Cancer Cell *11*, 229-243.

Jackson, E.L., Olive, K.P., Tuveson, D.A., Bronson, R., Crowley, D., Brown, M., and Jacks, T. (2005). The differential effects of mutant p53 alleles on advanced murine lung cancer. Cancer Res *65*, 10280-10288.

Jackson, E.L., Willis, N., Mercer, K., Bronson, R.T., Crowley, D., Montoya, R., Jacks, T., and Tuveson, D.A. (2001). Analysis of lung tumor initiation and progression using conditional expression of oncogenic K-ras. Genes Dev *15*, 3243-3248.

Jemal, A., Murray, T., Ward, E., Samuels, A., Tiwari, R.C., Ghafoor, A., Feuer, E.J., and Thun, M.J. (2005). Cancer statistics, 2005. CA Cancer J Clin *55*, 10-30.

Ji, H., Ramsey, M.R., Hayes, D.N., Fan, C., McNamara, K., Kozlowski, P., Torrice, C., Wu, M.C., Shimamura, T., Perera, S.A., *et al.* (2007). LKB1 modulates lung cancer differentiation and metastasis. Nature *448*, 807-810.

Jonkers, J., Meuwissen, R., van der Gulden, H., Peterse, H., van der Valk, M., and Berns, A. (2001). Synergistic tumor suppressor activity of BRCA2 and p53 in a conditional mouse model for breast cancer. Nat Genet *29*, 418-425.

Kerkhoff, E., Fedorov, L.M., Siefken, R., Walter, A.O., Papadopoulos, T., and Rapp, U.R. (2000). Lung-targeted expression of the c-Raf-1 kinase in transgenic mice exposes a novel oncogenic character of the wild-type protein. Cell Growth Differ *11*, 185-190.

Kim, M.J., Cardiff, R.D., Desai, N., Banach-Petrosky, W.A., Parsons, R., Shen, M.M., and Abate-Shen, C. (2002). Cooperativity of Nkx3.1 and Pten loss of function in a mouse model of prostate carcinogenesis. Proc Natl Acad Sci U S A *99*, 2884-2889.

Kim, W.Y., and Sharpless, N.E. (2006). The regulation of INK4/ARF in cancer and aging. Cell *127*, 265-275.

Kistner, A., Gossen, M., Zimmermann, F., Jerecic, J., Ullmer, C., Lubbert, H., and Bujard, H. (1996). Doxycycline-mediated quantitative and tissue-specific control of gene expression in transgenic mice. Proc Natl Acad Sci U S A *93*, 10933-10938.

Kunath, T., Gish, G., Lickert, H., Jones, N., Pawson, T., and Rossant, J. (2003). Transgenic RNA interference in ES cell-derived embryos recapitulates a genetic null phenotype. Nat Biotechnol *21*, 559-561.

Leder, A., Pattengale, P.K., Kuo, A., Stewart, T.A., and Leder, P. (1986). Consequences of widespread deregulation of the c-myc gene in transgenic mice: multiple neoplasms and normal development. Cell *45*, 485-495.

Lickert, H., Cox, B., Wehrle, C., Taketo, M.M., Kemler, R., and Rossant, J. (2005). Dissecting Wnt/beta-catenin signaling during gastrulation using RNA interference in mouse embryos. Development *132*, 2599-2609.

Lois, C., Hong, E.J., Pease, S., Brown, E.J., and Baltimore, D. (2002). Germline transmission and tissue-specific expression of transgenes delivered by lentiviral vectors. Science *295*, 868-872.

Lucito, R., Healy, J., Alexander, J., Reiner, A., Esposito, D., Chi, M., Rodgers, L., Brady, A., Sebat, J., Troge, J.*, et al.* (2003). Representational oligonucleotide microarray analysis: a high-resolution method to detect genome copy number variation. Genome Res *13*, 2291-2305.

Lynch, T.J., Bell, D.W., Sordella, R., Gurubhagavatula, S., Okimoto, R.A., Brannigan, B.W., Harris, P.L., Haserlat, S.M., Supko, J.G., Haluska, F.G.*, et al.* (2004). Activating mutations in the epidermal growth factor receptor underlying responsiveness of non-small-cell lung cancer to gefitinib. N Engl J Med *350*, 2129-2139.

Magdaleno, S.M., Wang, G., Mireles, V.L., Ray, M.K., Finegold, M.J., and DeMayo, F.J. (1997). Cyclin-dependent kinase inhibitor expression in pulmonary Clara cells transformed with SV40 large T antigen in transgenic mice. Cell Growth Differ *8*, 145-155.

Meuwissen, R., Linn, S.C., van der Valk, M., Mooi, W.J., and Berns, A. (2001). Mouse model for lung tumorigenesis through Cre/lox controlled sporadic activation of the K-Ras oncogene. Oncogene *20*, 6551-6558.

Miller, V.A., Riely, G.J., Zakowski, M.F., Li, A.R., Patel, J.D., Heelan, R.T., Kris, M.G., Sandler, A.B., Carbone, D.P., Tsao, A.*, et al.* (2008). Molecular characteristics of bronchioloalveolar carcinoma and adenocarcinoma, bronchioloalveolar carcinoma subtype, predict response to erlotinib. J Clin Oncol *26*, 1472-1478.

Mo, L., Zheng, X., Huang, H.Y., Shapiro, E., Lepor, H., Cordon-Cardo, C., Sun, T.T., and Wu, X.R. (2007). Hyperactivation of Ha-ras oncogene, but not $p16^{INK4a/}p19^{ARF}$ deficiency, triggers bladder tumorigenesis. J Clin Invest *117*, 314-325.

Moody, S.E., Sarkisian, C.J., Hahn, K.T., Gunther, E.J., Pickup, S., Dugan, K.D., Innocent, N., Cardiff, R.D., Schnall, M.D., and Chodosh, L.A. (2002). Conditional activation of Neu in the

mammary epithelium of transgenic mice results in reversible pulmonary metastasis. Cancer Cell *2*, 451-461.

Muller, W.J., Sinn, E., Pattengale, P.K., Wallace, R., and Leder, P. (1988). Single-step induction of mammary adenocarcinoma in transgenic mice bearing the activated c-neu oncogene. Cell *54*, 105-115.

Nyabi, O., Naessens, M., Haigh, K., Gembarska, A., Goossens, S., Maetens, M., De Clercq, S., Drogat, B., Haenebalcke, L., Bartunkova, S.*, et al.* (2009). Efficient mouse transgenesis using Gateway-compatible ROSA26 locus targeting vectors and F1 hybrid ES cells. Nucleic Acids Res *37*, e55.

O'Gorman, S., Fox, D.T., and Wahl, G.M. (1991). Recombinase-mediated gene activation and site-specific integration in mammalian cells. Science *251*, 1351-1355.

Oberdoerffer, P., Kanellopoulou, C., Heissmeyer, V., Paeper, C., Borowski, C., Aifantis, I., Rao, A., and Rajewsky, K. (2005). Efficiency of RNA interference in the mouse hematopoietic system varies between cell types and developmental stages. Mol Cell Biol *25*, 3896-3905.

Olive, K.P., Tuveson, D.A., Ruhe, Z.C., Yin, B., Willis, N.A., Bronson, R.T., Crowley, D., and Jacks, T. (2004). Mutant p53 gain of function in two mouse models of Li-Fraumeni syndrome. Cell *119*, 847-860.

Opitz, O.G., Harada, H., Suliman, Y., Rhoades, B., Sharpless, N.E., Kent, R., Kopelovich, L., Nakagawa, H., and Rustgi, A.K. (2002). A mouse model of human oral-esophageal cancer. J Clin Invest *110*, 761-769.

Oshima, H., Matsunaga, A., Fujimura, T., Tsukamoto, T., Taketo, M.M., and Oshima, M. (2006). Carcinogenesis in mouse stomach by simultaneous activation of the Wnt signaling and prostaglandin E2 pathway. Gastroenterology *131*, 1086-1095.

Paez, J.G., Janne, P.A., Lee, J.C., Tracy, S., Greulich, H., Gabriel, S., Herman, P., Kaye, F.J., Lindeman, N., Boggon, T.J.*, et al.* (2004). EGFR mutations in lung cancer: correlation with clinical response to gefitinib therapy. Science *304*, 1497-1500.

Pao, W., Miller, V.A., Politi, K.A., Riely, G.J., Somwar, R., Zakowski, M.F., Kris, M.G., and Varmus, H. (2005). Acquired resistance of lung adenocarcinomas to gefitinib or erlotinib is associated with a second mutation in the EGFR kinase domain. PLoS Med *2*, e73.

Potts, W., Tucker, D., Wood, H., and Martin, C. (2000). Chicken beta-globin 5'HS4 insulators function to reduce variability in transgenic founder mice. Biochem Biophys Res Commun *273*, 1015-1018.

Quaife, C.J., Pinkert, C.A., Ornitz, D.M., Palmiter, R.D., and Brinster, R.L. (1987). Pancreatic neoplasia induced by ras expression in acinar cells of transgenic mice. Cell *48*, 1023-1034.

Rangarajan, A., Hong, S.J., Gifford, A., and Weinberg, R.A. (2004). Species- and cell type-specific requirements for cellular transformation. Cancer Cell *6*, 171-183.

Rangarajan, A., and Weinberg, R.A. (2003). Opinion: Comparative biology of mouse versus human cells: modelling human cancer in mice. Nat Rev Cancer *3*, 952-959.

Ray, M.K., Magdaleno, S., O'Malley, B.W., and DeMayo, F.J. (1993). Cloning and characterization of the mouse Clara cell specific 10 kDa protein gene: comparison of the 5'-flanking region with the human rat and rabbit gene. Biochem Biophys Res Commun *197*, 163-171.

Reilly, K.M., Loisel, D.A., Bronson, R.T., McLaughlin, M.E., and Jacks, T. (2000). Nf1;*Trp53* mutant mice develop glioblastoma with evidence of strain-specific effects. Nat Genet *26*, 109-113.

Rubinson, D.A., Dillon, C.P., Kwiatkowski, A.V., Sievers, C., Yang, L., Kopinja, J., Rooney, D.L., Zhang, M., Ihrig, M.M., McManus, M.T.*, et al.* (2003). A lentivirus-based system to functionally silence genes in primary mammalian cells, stem cells and transgenic mice by RNA interference. Nat Genet *33*, 401-406.

Ruther, U., Komitowski, D., Schubert, F.R., and Wagner, E.F. (1989). c-fos expression induces bone tumors in transgenic mice. Oncogene *4*, 861-865.

Sansom, O.J., Griffiths, D.F., Reed, K.R., Winton, D.J., and Clarke, A.R. (2005). Apc deficiency predisposes to renal carcinoma in the mouse. Oncogene *24*, 8205-8210.

Sansom, O.J., Meniel, V., Wilkins, J.A., Cole, A.M., Oien, K.A., Marsh, V., Jamieson, T.J., Guerra, C., Ashton, G.H., Barbacid, M.*, et al.* (2006). Loss of Apc allows phenotypic manifestation of the transforming properties of an endogenous K-ras oncogene in vivo. Proc Natl Acad Sci U S A *103*, 14122-14127.

Santoni-Rugiu, E., Nagy, P., Jensen, M.R., Factor, V.M., and Thorgeirsson, S.S. (1996). Evolution of neoplastic development in the liver of transgenic mice co-expressing c-myc and transforming growth factor-alpha. Am J Pathol *149*, 407-428.

Sauer, B., and Henderson, N. (1989). Cre-stimulated recombination at loxP-containing DNA sequences placed into the mammalian genome. Nucleic Acids Res *17*, 147-161.

Schmidt, E.V., Pattengale, P.K., Weir, L., and Leder, P. (1988). Transgenic mice bearing the human c-myc gene activated by an immunoglobulin enhancer: a pre-B-cell lymphoma model. Proc Natl Acad Sci U S A *85*, 6047-6051.

Schuster-Gossler, K., Lee, A.W., Lerner, C.P., Parker, H.J., Dyer, V.W., Scott, V.E., Gossler, A., and Conover, J.C. (2001). Use of coisogenic host blastocysts for efficient establishment of germline chimeras with C57BL/6J ES cell lines. Biotechniques *31*, 1022-1024, 1026.

Seibler, J., Kleinridders, A., Kuter-Luks, B., Niehaves, S., Bruning, J.C., and Schwenk, F. (2007). Reversible gene knockdown in mice using a tight, inducible shRNA expression system. Nucleic Acids Res *35*, e54.

Seibler, J., Kuter-Luks, B., Kern, H., Streu, S., Plum, L., Mauer, J., Kuhn, R., Bruning, J.C., and Schwenk, F. (2005). Single copy shRNA configuration for ubiquitous gene knockdown in mice. Nucleic Acids Res *33*, e67.

Seidler, B., Schmidt, A., Mayr, U., Nakhai, H., Schmid, R.M., Schneider, G., and Saur, D. (2008). A Cre-loxP-based mouse model for conditional somatic gene expression and knockdown in vivo by using avian retroviral vectors. Proc Natl Acad Sci U S A *105*, 10137-10142.

Shinagawa, T., and Ishii, S. (2003). Generation of Ski-knockdown mice by expressing a long double-strand RNA from an RNA polymerase II promoter. Genes Dev *17*, 1340-1345.

Sinn, E., Muller, W., Pattengale, P., Tepler, I., Wallace, R., and Leder, P. (1987). Coexpression of MMTV/v-Ha-ras and MMTV/c-myc genes in transgenic mice: synergistic action of oncogenes in vivo. Cell *49*, 465-475.

Smith, D.J., Stevens, M.E., Sudanagunta, S.P., Bronson, R.T., Makhinson, M., Watabe, A.M., O'Dell, T.J., Fung, J., Weier, H.U., Cheng, J.F*., et al.* (1997). Functional screening of 2 Mb of human chromosome 21q22.2 in transgenic mice implicates minibrain in learning defects associated with Down syndrome. Nat Genet *16*, 28-36.

Stein, P., Svoboda, P., and Schultz, R.M. (2003). Transgenic RNAi in mouse oocytes: a simple and fast approach to study gene function. Dev Biol *256*, 187-193.

Stewart, T.A., Pattengale, P.K., and Leder, P. (1984). Spontaneous mammary adenocarcinomas in transgenic mice that carry and express MTV/myc fusion genes. Cell *38*, 627-637.

Stripp, B.R., Sawaya, P.L., Luse, D.S., Wikenheiser, K.A., Wert, S.E., Huffman, J.A., Lattier, D.L., Singh, G., Katyal, S.L., and Whitsett, J.A. (1992). cis-acting elements that confer lung epithelial cell expression of the CC10 gene. J Biol Chem *267*, 14703-14712.

Tam, R.C., Lin, C.J., Lim, C., Pai, B., and Stoisavljevic, V. (1999). Inhibition of CD28 expression by oligonucleotide decoys to the regulatory element in exon 1 of the CD28 gene. J Immunol *163*, 4292-4299.

Teng, Y., Sun, A.N., Pan, X.C., Yang, G., Yang, L.L., Wang, M.R., and Yang, X. (2006). Synergistic function of Smad4 and PTEN in suppressing forestomach squamous cell carcinoma in the mouse. Cancer Res *66*, 6972-6981.

Thomas, K.R., and Capecchi, M.R. (1987). Site-directed mutagenesis by gene targeting in mouse embryo-derived stem cells. Cell *51*, 503-512.

Thomas, K.R., Folger, K.R., and Capecchi, M.R. (1986). High frequency targeting of genes to specific sites in the mammalian genome. Cell *44*, 419-428.

Tiscornia, G., Singer, O., Ikawa, M., and Verma, I.M. (2003). A general method for gene knockdown in mice by using lentiviral vectors expressing small interfering RNA. Proc Natl Acad Sci U S A *100*, 1844-1848.

Tuveson, D.A., and Jacks, T. (1999). Modeling human lung cancer in mice: similarities and shortcomings. Oncogene *18*, 5318-5324.

Tuveson, D.A., and Jacks, T. (2002). Technologically advanced cancer modeling in mice. Curr Opin Genet Dev *12*, 105-110.

Van Dyke, T., and Jacks, T. (2002). Cancer modeling in the modern era: progress and challenges. Cell *108*, 135-144.

Vasquez, K.M., Marburger, K., Intody, Z., and Wilson, J.H. (2001). Manipulating the mammalian genome by homologous recombination. Proc Natl Acad Sci U S A *98*, 8403-8410.

Ventura, A., Meissner, A., Dillon, C.P., McManus, M., Sharp, P.A., Van Parijs, L., Jaenisch, R., and Jacks, T. (2004). Cre-lox-regulated conditional RNA interference from transgenes. Proc Natl Acad Sci U S A *101*, 10380-10385.

Voinnet, O., Vain, P., Angell, S., and Baulcombe, D.C. (1998). Systemic spread of sequence-specific transgene RNA degradation in plants is initiated by localized introduction of ectopic promoterless DNA. Cell *95*, 177-187.

Wang, J., Theunissen, T.W., and Orkin, S.H. (2007). Site-directed, virus-free, and inducible RNAi in embryonic stem cells. Proc Natl Acad Sci U S A *104*, 20850-20855.

Wang, S., Gao, J., Lei, Q., Rozengurt, N., Pritchard, C., Jiao, J., Thomas, G.V., Li, G., Roy-Burman, P., Nelson, P.S.*, et al.* (2003). Prostate-specific deletion of the murine Pten tumor suppressor gene leads to metastatic prostate cancer. Cancer Cell *4*, 209-221.

Weinstein, I.B. (2000). Disorders in cell circuitry during multistage carcinogenesis: the role of homeostasis. Carcinogenesis *21*, 857-864.

Weinstein, I.B. (2002). Cancer. Addiction to oncogenes--the Achilles heal of cancer. Science *297*, 63-64.

West, A.G., and Fraser, P. (2005). Remote control of gene transcription. Hum Mol Genet *14 Spec No 1*, R101-111.

Westra, W.H. (2000). Early glandular neoplasia of the lung. Respir Res *1*, 163-169.

Williams, R.L., Courtneidge, S.A., and Wagner, E.F. (1988). Embryonic lethalities and endothelial tumors in chimeric mice expressing polyoma virus middle T oncogene. Cell *52*, 121-131.

Wilson, C., Bellen, H.J., and Gehring, W.J. (1990). Position effects on eukaryotic gene expression. Annu Rev Cell Biol *6*, 679-714.

Wu, C.H., van Riggelen, J., Yetil, A., Fan, A.C., Bachireddy, P., and Felsher, D.W. (2007a). Cellular senescence is an important mechanism of tumor regression upon c-Myc inactivation. Proc Natl Acad Sci U S A *104*, 13028-13033.

Wu, R., Hendrix-Lucas, N., Kuick, R., Zhai, Y., Schwartz, D.R., Akyol, A., Hanash, S., Misek, D.E., Katabuchi, H., Williams, B.O.*, et al.* (2007b). Mouse model of human ovarian endometrioid adenocarcinoma based on somatic defects in the Wnt/beta-catenin and PI3K/Pten signaling pathways. Cancer Cell *11*, 321-333.

Xiao, A., Yin, C., Yang, C., Di Cristofano, A., Pandolfi, P.P., and Van Dyke, T. (2005). Somatic induction of Pten loss in a preclinical astrocytoma model reveals major roles in disease progression and avenues for target discovery and validation. Cancer Res *65*, 5172-5180.

Xue, W., Zender, L., Miething, C., Dickins, R.A., Hernando, E., Krizhanovsky, V., Cordon-Cardo, C., and Lowe, S.W. (2007). Senescence and tumour clearance is triggered by p53 restoration in murine liver carcinomas. Nature *445*, 656-660.

Zamore, P.D., Tuschl, T., Sharp, P.A., and Bartel, D.P. (2000). RNAi: double-stranded RNA directs the ATP-dependent cleavage of mRNA at 21 to 23 nucleotide intervals. Cell *101*, 25-33.

Zender, L., Spector, M.S., Xue, W., Flemming, P., Cordon-Cardo, C., Silke, J., Fan, S.T., Luk, J.M., Wigler, M., Hannon, G.J.*, et al.* (2006). Identification and validation of oncogenes in liver cancer using an integrative oncogenomic approach. Cell *125*, 1253-1267.

Zender, L., Xue, W., Cordon-Cardo, C., Hannon, G.J., Lucito, R., Powers, S., Flemming, P., Spector, M.S., and Lowe, S.W. (2005). Generation and analysis of genetically defined liver carcinomas derived from bipotential liver progenitors. Cold Spring Harb Symp Quant Biol *70*, 251-261.

Zhao, X., Li, C., Paez, J.G., Chin, K., Janne, P.A., Chen, T.H., Girard, L., Minna, J., Christiani, D., Leo, C.*, et al.* (2004). An integrated view of copy number and allelic alterations in the cancer genome using single nucleotide polymorphism arrays. Cancer Res *64*, 3060-3071.

Zhou, Z., Flesken-Nikitin, A., Corney, D.C., Wang, W., Goodrich, D.W., Roy-Burman, P., and Nikitin, A.Y. (2006). Synergy of p53 and Rb deficiency in a conditional mouse model for metastatic prostate cancer. Cancer Res *66*, 7889-7898.

Zilfou, J.T., and Lowe, S.W. (2009). Tumor Suppressive Functions of p53. Cold Spring Harb Perspect Biol *1*, a001883.

Chapter 2

RNAi Mouse Models using Transgenesis

2.1 Introduction

RNAi is a useful tool for sequence-specific gene suppression that can be used to phenocopy knockout models and therefore accelerate loss-of-gene function studies. It provides the ability to control gene expression without interruption of the endogenous gene, which makes it a very powerful approach. We and others have previously shown that tet-inducible shRNA cassettes can be introduced into the genome by retro- or lentivral expression vectors (Dickins et al., 2005; Stegmeier et al., 2005) for gene specific knockdown *in vitro.* More recently, we have shown that they can also be integrated into the mouse genome by classical transgenesis using pronuclear injection methods to gain conditional gene expression in mice (Dickins et al., 2007).

Although pronuclear injection is an effective and widely used method to generate transgenic mice, this approach has several limitations, specifically the inability to control integration site and copy number, both of which translate into laborious screening of founder lines. Despite these limitations, it is one of the most rapid and simplest methods for producing transgenic mice. Additionally, it requires less elaborate cloning strategies to produce transgenes for this procedure, thus making it a highly attractive method.

In this study, we made strides to improve upon our first generation RNAi mouse model by addressing the limitations of pronuclear injection. We modified the transgene configuration to improve shRNA efficacy and provide a reporter of shRNA expression in order to decrease the need for high copy number

integrations and expedite the screening process. We also attempted to decrease the affect of position-effect variegation by flanking the tet-inducible transgene with insulator sequences, which are thought to prevent transgene silencing by blocking the spread of heterochromatin (Potts et al., 2000). Although no additional functional founders were identified from the second and third generation mice, this study demonstrates the importance of the integration site position within the genome for shRNA expression in transgenic mice and spearheaded the move toward site-specific targeting in ES cells.

2.2 Results

2.2.1 First generation RNAi mouse models

For rapid introduction of a tet-regulatable shRNA into the mouse genome, a transgene comprised of the tet-responsive TRE-CMV promoter (Gossen and Bujard, 1992) upstream of an shRNA targeting murine *Trp53* (referred to as p53.1224) (Dickins et al., 2005) was injected into fertilized zygotes using standard pronuclear injection procedures (Gordon et al., 1980). Several founder lines harboring the TRE-p53.1224 transgene (Fig. 2.1A) were tested for their ability to express p53.1224 by isolating transgenic mouse embryonic fibroblasts (MEFs) from each of nine founder lines and infecting them with retrovirus expressing tTA (tet-off), which transactivates the TRE promoter in the absence of doxycycline. Only two lines, A and D (data not shown for line D), showed

marked, tTA-dependent *Trp53* knockdown in MEFs (Fig. 2.1B) that was fully reversible upon addition of doxycycline (Fig. 2.1C).

We observed an even lower efficiency for founder lines carrying the TRE-p16/p19.478 transgene, harboring an shRNA designed to target the common exon 2 of both *INK4a* and *ARF* genes encoding for the p16 and p19 proteins respectively. Only one of six founders (line F) showed knockdown, however, there was substantial variation in knockdown levels in the MEFs established from different embryos (Fig. 2.2A,B). The variation suggested that founder F harbored multiple transgene integrations but this was not confirmed by Southern blot. Bitransgenic F-A MEFs treated with doxycycline (harboring TRE-p16/p19.478/Rosa-rtTA) displayed the most potent knockdown of p16 and p19 proteins, which resulted in a proliferation phenotype demonstrated by their ability to form colonies when plated at low density (Fig. 2.2C). However, the knockdown was insufficient to fully recapitulate the proliferation effect seen in $ARF^{-/-}$ MEFs; in fact, F-A MEFs formed ~60-70% less colonies than $ARF^{-/-}$ (Fig.2.2C). For that reason, we terminated line F and did not further characterize the line. Together, these results demonstrated that classical transgenesis, although inefficient, could be used to generate transgenic tet-regulatable RNAi mice with reversible gene expression. Moreover, these results highlighted the need for potent shRNAs that can substantially knockdown target genes in order to phenocopy knockout models.

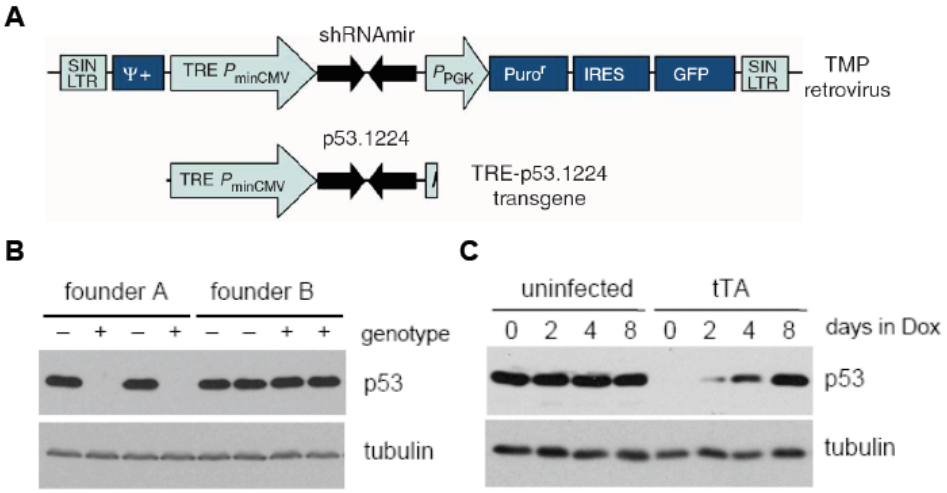

Figure 2.1 | Germline transmission of a functional TRE-p53.1224 cassette. *A,* Diagram of the TRE-p53.1224 transgene, derived from the TMPp53.1224 retroviral vector. *B, Trp53* protein blot of MEFs of indicated TRE-p53.1224 genotype (+ indicates transgenic) isolated from two different TRE-p53.1224 founder lines (A and B), infected with tTA. Note that *Trp53* knockdown is only observed in line A. *C, Trp53* protein blot of TRE-p53.1224 transgenic MEFs infected with tTA and cultured in doxcycline (Dox) for various periods. Uninfected controls are shown. Adapted from Dickins *et al. Nat Genet.* 2007; 39(7):914-21.

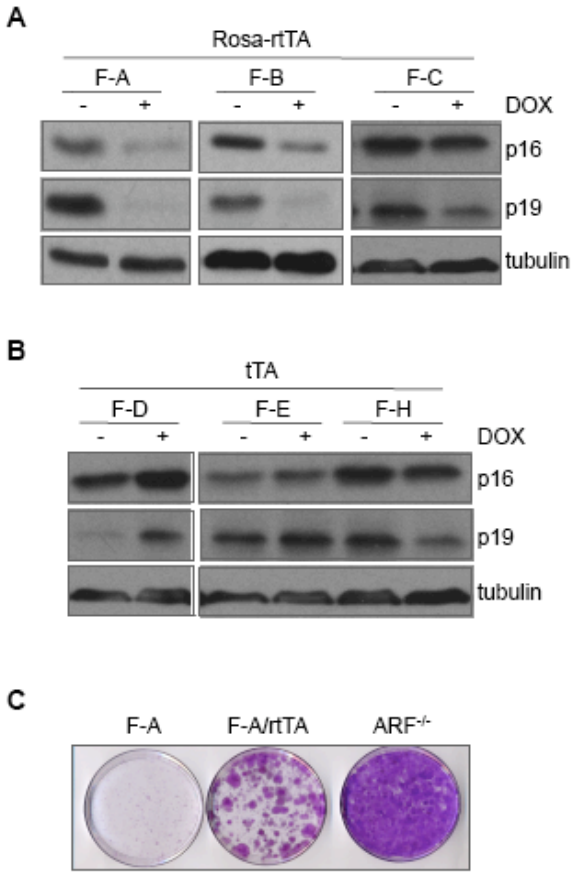

Figure 2.2 | Germline transmission of a TRE-p16/p19.478 cassette. *A,* Western blots of MEFs isolated from bitransgenic embryos resulting from a cross between TRE-p16/p19.478 founder F and Rosa-rtTA mice. MEFs were treated with or without DOX for 4 d. The p16/p19.478 shRNA is designed to target the transcript encoding both proteins. Note that marked p16 and p19 knockdown are only observed in embryos F-A and F-B, suggesting multiple integrations of the TRE-p16/p19.478 cassette in founder F. *B,* p16INK4a and p19ARF western blot of MEFs from line F embryos infected with tTA and treated with or without DOX for 4 d. *C*, Colony formation assay for bitransgenic TRE-p16/p19.478/Rosa-rtTA transgenic MEFs, line F-A plated at low density and maintained in media containing DOX. $ARF^{-/-}$ MEFs were plated for comparison.

2.2.2 Optimizing RNAi efficiency

Following production of our first generation RNAi mouse models, a study demonstrated enhanced miR30-based shRNA (shRNA-mir) efficacy by addition of a 'spacer' element between the CMV promoter and the miR30 cassette using a lentiviral system (Stegmeier et al., 2005). We reasoned we could also optimize shRNA-mir expression from our tet-inducible retroviral vectors and include a fluorescent transgene to report shRNA expression. To do so, we modified the TMP vector by inserting a GFP cDNA upstream (TRE-GFP-miR30-PGKpuro – TGMP) of the mir30 cassette (Fig.2.3A). During the cloning process, we also generated an intermediary TMGP vector (TRE-miR30-GFP-PGKpuro) carrying the miR30 cassette between TRE and GFP (Fig.2.3A). We then assessed knockdown of *Trp53* by p53.1224 in each configuration in primary MEFs by retroviral integration at low multiplicity of infection (MOI) to avoid possible misinterpretation of high copy number integrations. The presence of the GFP cDNA between TRE and miR30 both enhanced knockdown, visible by western blot and colony formation, in comparison to TMP and TMGP vectors and importantly allowed robust expression of GFP to serve as a reporter for shRNA expression (Fig. 2.3B-D) (Stegmeier et al., 2005). Note that the TMGP vector gave no GFP expression likely due to the lack of a polyA sequence following GFP (Fig.2.3B).

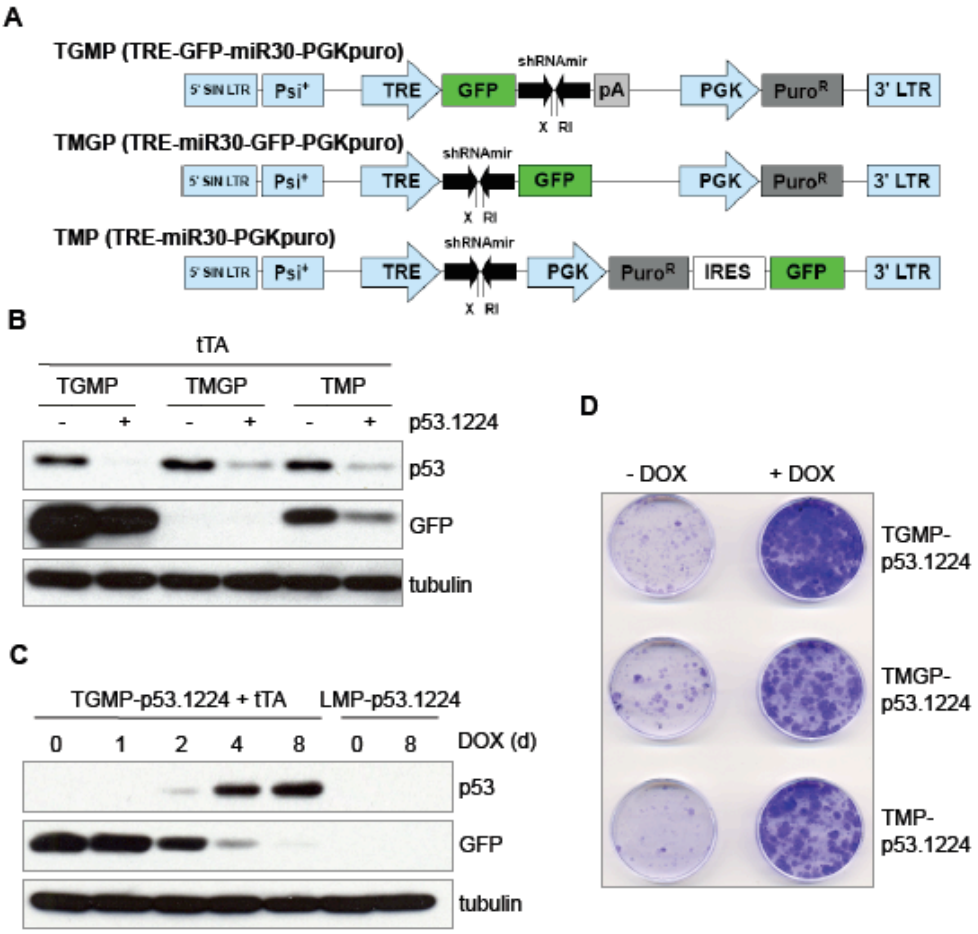

Figure 2.3 | TGMP enhances knockdown and provides a biomarker for shRNA expression. *A,* Schematic diagram comparing the TGMP, TMGP and TMP retroviral vectors. *B,* Western blot analysis reveals enhanced p53.1224 efficacy in infected tTA-expressing MEFs in the context of the TGMP retroviral vector in comparison to TMGP and TMP. *C,* Time course of *Trp53* re-expression and GFP downregulation upon DOX treatment in retrovirally infected TGMP-p53.1224;tTA MEFs. LMP (LTR-miR30-PGKpuro) vector is a constitutive retroviral vector. *D,* Colony formation assay for TGMP-, TMGP- and TMP-p53.1224 infected tTA-MEFs plated at low density.

Given the enhanced efficacy for p53.1224, we wanted to test whether we could improve knockdown of p16 and p19 using the TGMP vector. We first tested additional shRNAs using the constitutive retroviral vector MGP (MSCV-GFP-PGKpuro), which is similar to TMGP in that it also places the miR30 cassette in the 3'UTR of GFP. Of four shRNAs tested, p16/p19.478 proved most effective in suppressing both p16 and p19 (representative data in Fig. 2.4A). Additionally, we observed substantial and reversible knockdown of the target proteins both by western blot and colony formation, when using p16/p19.478 in the TGMP vector in comparison to the LMP (LTR-mir30-PGKpuro), which expresses the shRNA from the strong LTR promoter (Fig. 2.4B-C). As a result, we moved forward with RNAi mouse production using the TGM configuration for shRNA-mir expression.

2.2.3 Second generation RNAi mouse models by transgenesis

While standard pronuclear injection may require laborious and time-consuming screening protocols to identify functional founders, the approach is simple and allows rapid generation of multiple founder lines in which to test for reversible knockdown. Additionally, the speed and ease of generating transgenes suitable for pronuclear injection made this approach more appealing for the generation of RNAi mouse models than ES cell targeting, which requires elaborate cloning of vectors with large homology arms. For two different shRNAs, the TGMP vector improved knockdown considerably (Figs. 2.3 and 2.4); therefore, we assumed the same would hold true in a transgenic setting.

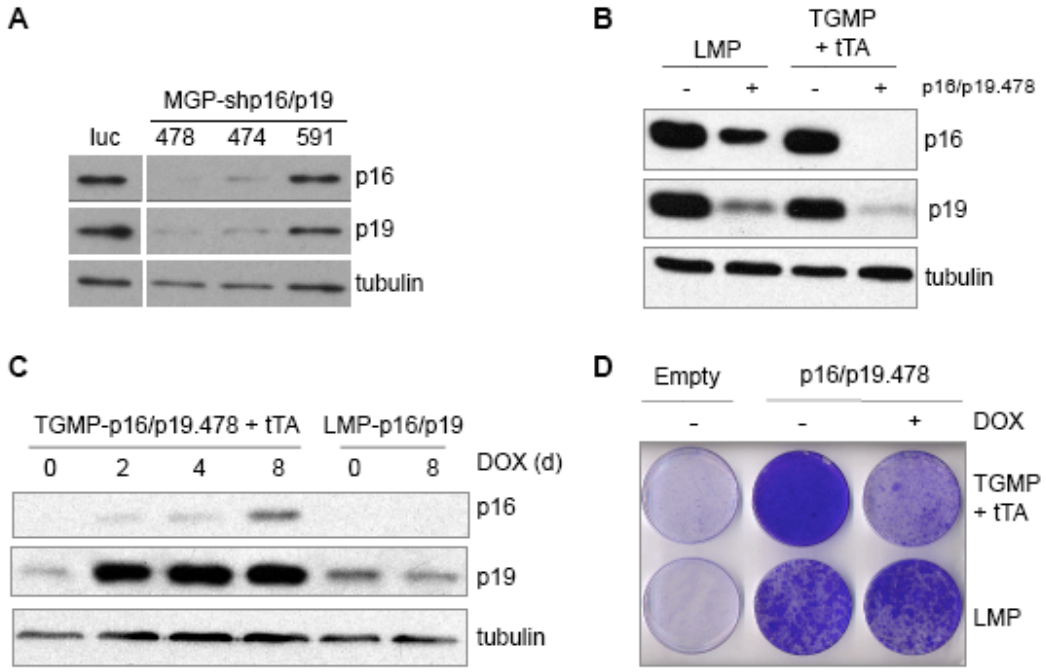

Figure 2.4 | Dual specificity knockdown of *INK4a* and *ARF* with a single shRNA. *A,* Validation of 3 different shRNAs targeting *INK4a/ARF.* p16 and p19 western blot of MEFs infected with the constitutive retroviral MGP (MSCV-GFP-PGKpuro) vector containing each shRNA. sh-luc.1309 was used as a control. *B,* p16 and p19 western blot with sh-p16/p19.478 comparing two vector configurations: LMP and TGMP. *C,* Time course of p16 and p19 re-expression upon DOX treatment in retrovirally infected TGMP-p16/p19.478/tTA in late-passage MEFs. *D,* Colony formation assay for LMP- and TMP-p16/p19.478/tTA infected MEFs plated at low density.

Moreover, use of the GFP biomarker to visualize shRNA-mir expression should expedite and simplify screening founders for functional shRNAs.

To test whether the TGM configuration would further enhance knockdown in transgenic mice, we isolated two transgenes we named Salt and Pepper, either lacking or including a polyA sequence 3' of the miR30 cassette respectively (Fig. 2.5A). At the time, it was unclear whether a polyA-tail was necessary for proper GFP translation and miR30 processing; hence, we generated second generation mice by pronuclear injection of either Salt or Pepper transgenes. We chose to use p53.1224 because we could directly compare these founders to our first generation TRE-p53.1224 founders.

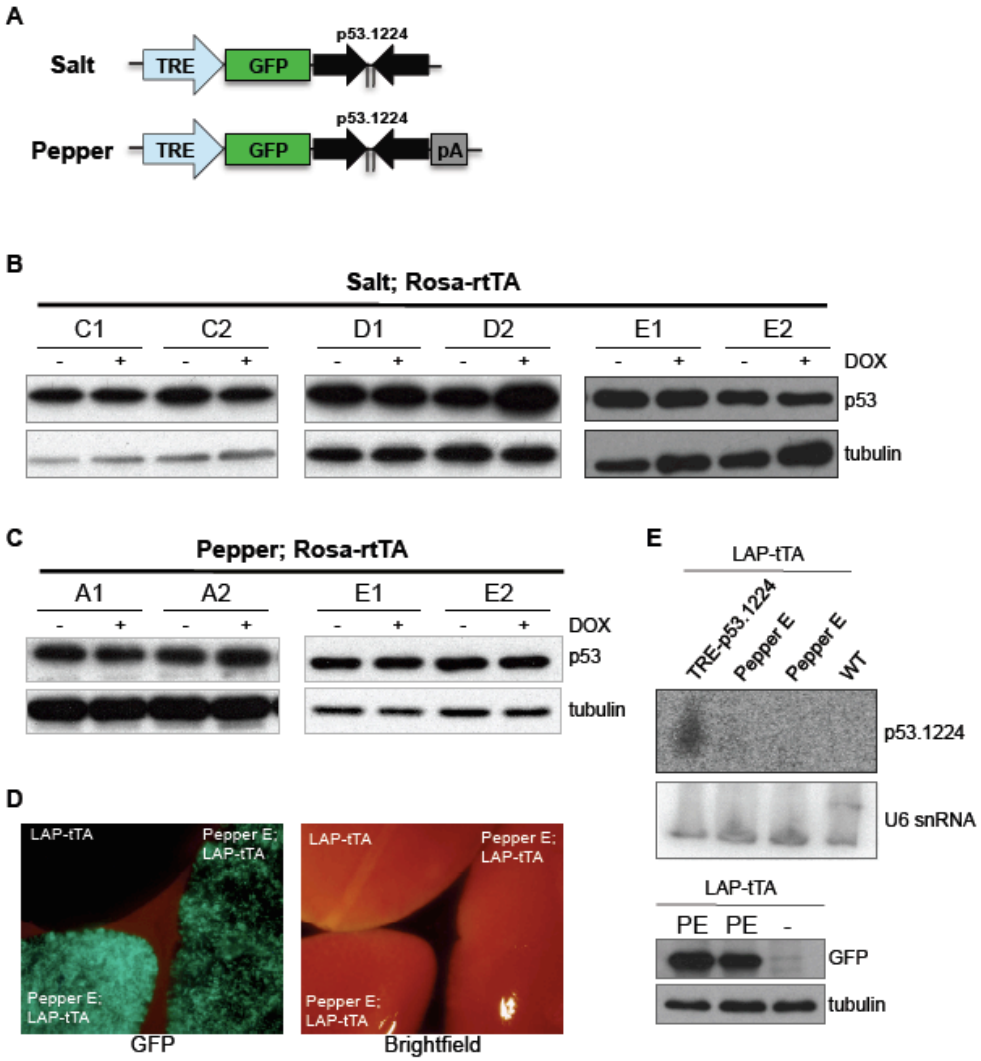

Figure 2.5 | Salt and Pepper transgenic RNAi mouse lines confer no knockdown. *A,* Diagram of the Salt (TGM) and Pepper (TGMpA) transgenes, derived from the TGMP retroviral vector (Fig. 2.3). *B-C, Trp53* protein blot of bitransgenic MEFs of the indicated genotype, isolated from three different Salt founder lines C, D and E. *(B)* or two different Pepper founder lines A and E *(C)*. Note that *Trp53* knockdown is not observed in all lines. *D,* GFP and brightfield images of adult livers harvested from bitransgenic Pepper E/LAP-tTA. *E,* Small RNA blot for expression of p53.1224 siRNA *(top)* and western blot for GFP expression *(bottom)* in adult livers isolated from bitransgenic TRE-p53.1224/LAP-tTA and Pepper E/LAP-tTA mice. U6 snRNA is shown as a loading control.

For each of the Salt and Pepper transgenes, five founders genotyped positive out of 20 and 18 respectively (Table 2.1). Founders Salt A and B failed to transmit the transgene to three separate F_1 generations and thus were not further characterized. Primary bitransgenic MEFs were isolated from crosses between

Rosa-rtTA mice and the remaining founder lines and treated with doxycycline to transactivate GFP and p53.1224 expression (representative data in Fig 2.5B,C). By fluorescence microscopy, GFP was either undetectable, weakly to moderately visible, or strong as in the case for Pepper B/Rosa-rtTA MEFs (Table 2.1). In all cases, however, expression was heterogeneous throughout the population ranging between 10-80% GFP positivity and did not correspond to *Trp53* knockdown (Fig. 2.5B,C; Table 2.1).

Rosa26 has been previously described as a weak promoter that might not be capable of driving rtTA expression sufficient for shRNA production at levels that translate into gene target suppression (Beard et al., 2006; Dickins et al., 2007). Therefore, despite these findings in MEFs, we continued to examine other tissues using other ubiquitous or tissue-specific tet-transactivator strains that were available in our lab. Several Salt and Pepper strains were crossed to either Eμ-tTA (Eμ-SRα αcontrol element) mice, previously shown to drive tet-regulated Myc overexpression leading to an immature T cell disease, (Felsher and Bishop, 1999) or LAP-tTA (liver-enriched transcriptional activator protein; also known as C/EBPβ) mice that express tTA specifically in differentiated hepatocytes (Sotillo et al., 2007). Bitransgenic Salt- or Pepper;Eμ-tTA mice displayed no GFP in peripheral blood or harvested spleens and thymi and were therefore not examined further (data not shown). In contrast, bitransgenic Salt- or Pepper/LAP-tTA mice showed varying degrees of GFP expression in liver tissue (Fig. 2.5D,E; Table 2.1).

Trp53 siRNA was detectable by small RNA northern and able to affect

Trp53 expression in liver tissue isolated from TRE-p53.1224/LAP-tTA mice (Dickins et al., 2007). To determine whether *Trp53* expression was affected in Pepper E/LAP-tTA mice, we directly compared the siRNA expression in liver tissue from TRE-p53.1224/LAP-tTA and Pepper E/LAP-tTA mice, of which was undetectable in the latter (Fig. 2.5E). Given these results, we did not further character these mice.

We also examined GFP expression in Pepper A and B lines using the CMV-rtTA mouse strain previously used to regulate tet-on cDNA overexpression in tissues of adult mice (Kistner et al., 1996). To determine whether the transgene could be activated in utero, pregnant females were fed doxycycline in their food pellets 1 week prior to giving birth. Compared to single transgenic littermates, 2 day old bitransgenic Pepper B/CMV-rtTA pups showed strong GFP in the their skin (Fig. 2.6A). This preliminary GFP screen warranted a thorough examination in the adults. To do so, we determined GFP levels by western blot of tissues collected from 6 wk old bitransgenic Pepper A- and Pepper B;LAP-tTA mice on dox for 1 wk (Fig. 2.6B). Unexpectedly, we did not observe GFP in all tissues previously shown to express detectable *Trp53* siRNA in TRE-p53.1224/CMV-rtTA mice (Dickins et al., 2007) and decided further characterization of these Salt and Pepper strains would be futile.

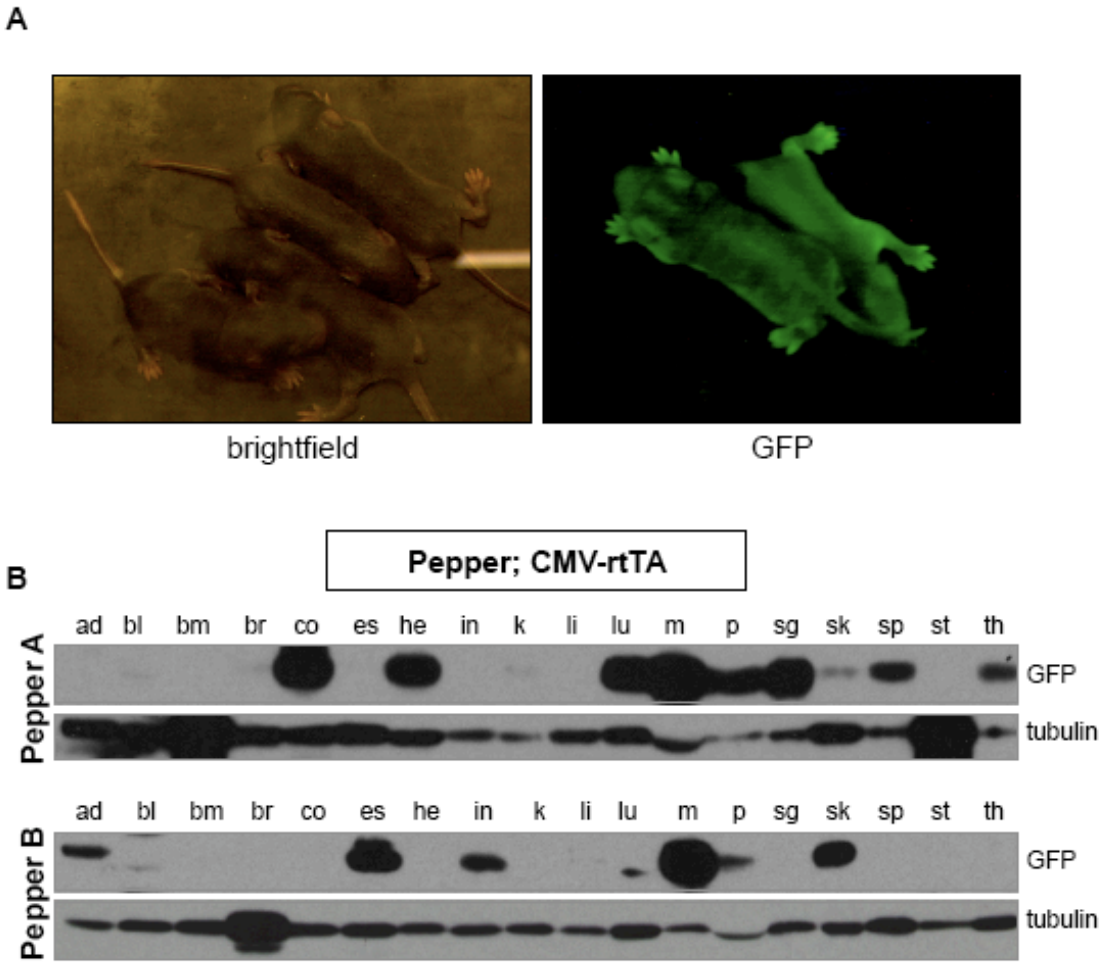

Figure 2.6 | Global GFP expression is variable between Pepper founder lines. *A,* Pepper B;CMV-rtTA double transgenic pups (postnatal d2) and single transgenic littermates (left) from pregnant moms fed DOX 1 wk prior to birth. Only double transgenic mice display GFP expression (right). *B,* GFP western blot on different tissues harvested from double transgenic Pepper/CMV-rtTA mice. CMV-rtTA drives ubiquitous expression of the reverse tet-transactivator (rtTA). ad- adipose, bl- bladder, bm- bone marrow, co- colon, es- esophagus, he- heart, in- intestine, k- kidney, li- liver, lu- lung, m- muscle, p- pancreas, sg- salivary gland, sk- skin, sp- spleen, st- stomach, th- thymus.

Table 2.1 | Summary of Salt and Pepper transgenic RNAi mouse lines. Five out of 20 and five out 18 founder mice genotyped positive for the Salt (TGM-p53.1224) and Pepper (TGM-p53.1224-pA) transgenes respectively. Salt founders A and B did not transmit the transgene to F1 generations and could not be further evaluated. MEFs derived from founders Salt C and D did not express GFP nor confer p53 knockdown by western blot. Salt C and D expressed GFP within adult livers but were not further characterized. Only Pepper E showed strong but heterogeneous GFP expression in MEFs; knockdown was not noted by western blot. Pepper E; LAP-tTA mice showed strongly GFP positivity in adult livers but p53.1224 siRNA was undetectable by small RNA northern (Fig. 2.5).

Second generation transgenic founders					
SALT	GENDER	NOTES	MEFs (GFP)	MEFs (WB)	LAP-tTA
A	F	No germline transmission	N/A	N/A	N/A
B	F	No germline transmission	N/A	N/A	N/A
C	M		Negative	No knockdown	Strong GFP
D	M		Negative	No knockdown	Weak GFP
E	F		Weak heterogeneous expression	No knockdown	N/A
PEPPER	GENDER	NOTES	MEFs (GFP)	MEFs (WB)	LAP-tTA
A	M		Moderate heterogeneous expression	No knockdown	Negative GFP
B	M		Moderate heterogeneous expression	No knockdown	N/A
C	F	Found dead	N/A	N/A	N/A
D	M	Not breeding well	Negative	No knockdown	N/A
E	M		Strong heterogeneous expression	No knockdown	Moderate GFP/ no detectable siRNA

2.2.4 Third generation insulated RNAi mouse models

Although no second generation founder with functional p53.1224 expression was identified, the presence of a GFP biomarker greatly expedited the screening process of these founder lines and clearly demonstrated the variability in expression between each line which was not observable in the first generation mice that lacked a visible marker. Copy number and integration site of transgenes cannot be controlled in transgenic mice generated by pronuclear injection; however, owing to the ease and simplicity of this procedure, several groups were able to decrease the position-effect variegation between founder lines by flanking the transgene with insulator sequences (Guglielmi et al., 2003; Hsiao et al., 2004; Potts et al., 2000) (Fig. 1.2).

To test whether insulator sequences would increase efficiency and consistent GFP and shRNA expression between founder lines, we generated a third RNAi mouse model using the H19 insulator sequences (Bell and Felsenfeld, 2000; Kaffer et al., 2000) from the pWhere vector (InvivGen). The H19TGM-p53.1224 transgene (Fig. 2.7A) integrated into 4 of 12 founder lines, 2 of which did not transmit the transgene to F_1 progeny (Table 2.2). Founders B and C both produced MEFs that lacked GFP expression and *Trp53* knockdown when combined with either Rosa-rtTA and culture in dox-containing media (Fig. 2.7B) or infected with tTA (Fig. 2.7C). These initial but quick observations were ample evidence to discontinue screening and terminate the lines. Together, these results illustrated the limitations of pronuclear injection, revealing the laborious

and time-consuming screening protocols required to identify functional founders due to the inability to control copy number and integration site.

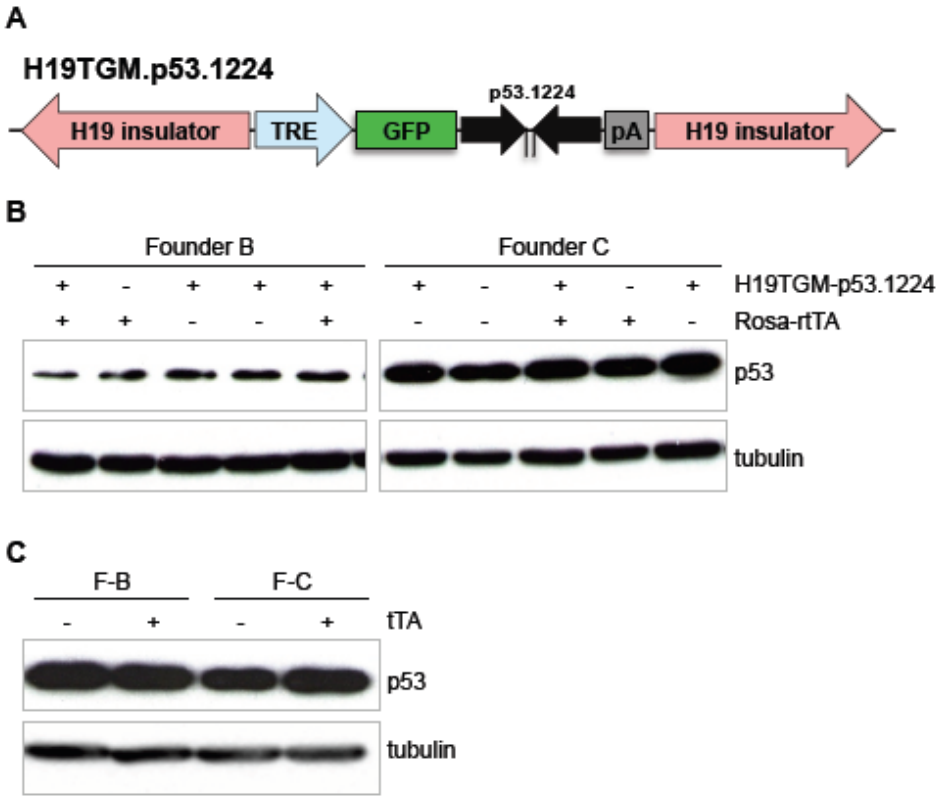

Figure 2.7 | H19TGM-p53.1224 transgenic RNAi mouse lines confer no knockdown. *A,* Diagram of H19TGM-p53.1224 transgene. The TGM cassette was derived from the TGMP retroviral vector (Fig. 2.3) and cloned into the pWhere vector containing H19 insulator sequences (Invivogen). *B-C, Trp53* protein blot of bitransgenic MEFs of the indicated genotype *(B)* or single transgenic MEFs infected with MSCV-tTA, *(C)* isolated from two different H19TGM founder lines B and C).

Table 2.2 | Summary of H19TGM-p53.1224 transgenic RNAi mouse lines. Four out of 12 founder mice genotyped positive for the H19TGM-p53.1224 transgene. Founders B and C did not transmit the transgene to F1 generations and could not be further evaluated. Eμ-tTA expresses the tet-transactivator in B- and T-cell lineages.

Third generation H19 insulated transgenic founders					
	GENDER	NOTES	MEFs (GFP)	MEFs (WB)	Eμ-tTA
A	F	No germline transmission	N/A	N/A	N/A
B	M		Negative	Negative	Negative
C	M		Negative	No knockdown	Negative
D	F	No germline transmission	N/A	N/A	N/A

2.3 Discussion

Our first generation RNAi mouse model demonstrates that pronuclear injection can be used to produce transgenic mice harboring tet-inducible shRNA cassettes; however, this method is inefficient in that it requires thorough screening of numerous founder lines to identify those with functional and widespread shRNA expression. Despite these limitations, we were able to identify two functional founders harboring TRE-p53.1224. In contrast, we identified only 1 amongst 8 founders with a functional TRE-p16/p19.478 cassette (line F), which only moderately knocked down p16 and p19. Furthermore, MEFs derived from F_1 generation embryos displayed highly variable knockdown, suggesting that founder F harbored multiple integrations. The other nonfunctional

founders likely integrated the transgene into genomically silent loci or carried low transgene copy number insufficient for potent knockdown.

In an effort to maximize shRNA efficiency and simplify and accelerate the screening process, we altered the configuration of the tet-regulatable shRNA expression cassette to TGM (Fig. 2.3A). This configuration added a visual biomarker of shRNA expression and placed the miR30 cassette further downstream from the TRE promoter in the 3' UTR of GFP, which in comparison to TMP, creates a longer mRNA transcript encoding the miRNA. We speculate that the longer mRNA transcript allows the endogenous miRNA processing machinery to bind more efficiently, thus more effectively producing an abundance of siRNA that translates into enhanced RNAi-mediated post-transcriptional gene silencing. By retroviral integration, we show that the potency of both p53.1224 and p16/p19.478 was significantly increased in the TGM configuration, even when integrated at low MOI. Therefore we presumed that the TGM configuration would decrease the need for high copy number integration in transgenic mice, thus reducing the potential for off-target effects (Snove and Rossi, 2006) and making the integration site within the genome the critical factor for determining shRNA potency.

Using GFP expression for initial screening purposes, we were able to significantly expedite the screening process of the second generation founders harboring the TGM cassette. As anticipated from the minimal and heterogeneous expression of GFP, no knockdown was observed by western blot of MEFs isolated from these strains (Fig. 2.3). Moreover, the dramatic variability in GFP

clearly illustrated the affect of random integrations. In fact, the strongest GFP expression observed in tissues harvested from these transgenic lines was still significantly lower than seen when TGM was retrovirally integrated into MEFs at low MOI (data not shown); therefore, we were not surprised by the lack of gene knockdown or detectable siRNA. These results demonstrate that shRNA-mirs must be transcribed at higher levels than GFP in order to be efficiently processed and achieve observable knockdown.

Other groups using transgenesis were able to decrease variability and increase the percentage of functional founders by using insulator sequences to protect transgenes from genomic silencing (Hsiao et al., 2004; Potts et al., 2000). Pronuclear injection of a transgene harboring H19 insulator sequences (Bell and Felsenfeld, 2000; Kaffer et al., 2000) flanking the TGM cassette resulted in only two fertile third generation founders, both of which gave rise to MEFs that lacked GFP expression when transduced with tTA. From these results, it remains unclear as to whether H19 insulators improve transgenic efficiency. In hindsight however, the chicken H24 insulators (Potts et al., 2000) may have provided a more dramatic effect than the H19 insulators in decreasing position-effect variegation, but use of these required much more detailed cloning that may have taken months to complete. Taken together, these results demonstrate the need to minimize position-effect variegation by moving toward a site-specific integration method into ES cells in which expression would be more predictable.

RNAi holds great promise, but the limitations of standard transgenesis prevent us from maximizing its potential in transgenic mice. Unlike cDNA

transgenes used for overexpression of proteins, which encode mRNAs that can be amplified into protein molecules, miRNA transcripts are cleaved and believed to produce siRNAs at approximately a 1:1 ratio; therefore, it is presumed that they must be expressed at relatively high concentrations to produce sufficient levels of siRNA to achieve post-transcriptional gene silencing that will translate into the expected phenotype. This may explain why shRNA potency is more drastically affected by the position of the genomic integration site. Altogether, these results implicate pronuclear injection as a futile approach for generating multiple founders with different shRNAs. The inability to control copy number and integration site makes it difficult to predict whether shRNA potency *in vitro* will translate into an expected phenotype *in vivo*. Random integration would also make it difficult to compare different shRNAs and interpret the numerous phenotypes that may result from variable knockdown. After production of three generations of founders by classical transgenesis, it is clear that site-specific targeting into a defined, transcriptionally accessible locus in ES cells would be a more valuable approach for producing conditional RNAi mice.

2.4 References

Beard, C., Hochedlinger, K., Plath, K., Wutz, A., and Jaenisch, R. (2006). Efficient method to generate single-copy transgenic mice by site-specific integration in embryonic stem cells. Genesis *44*, 23-28.

Bell, A.C., and Felsenfeld, G. (2000). Methylation of a CTCF-dependent boundary controls imprinted expression of the Igf2 gene. Nature *405*, 482-485.

Dickins, R.A., Hemann, M.T., Zilfou, J.T., Simpson, D.R., Ibarra, I., Hannon, G.J., and Lowe, S.W. (2005). Probing tumor phenotypes using stable and regulated synthetic microRNA precursors. Nat Genet *37*, 1289-1295.

Dickins, R.A., McJunkin, K., Hernando, E., Premsrirut, P.K., Krizhanovsky, V., Burgess, D.J., Kim, S.Y., Cordon-Cardo, C., Zender, L., Hannon, G.J.*, et al.* (2007). Tissue-specific and reversible RNA interference in transgenic mice. Nat Genet *39*, 914-921.

Felsher, D.W., and Bishop, J.M. (1999). Reversible tumorigenesis by MYC in hematopoietic lineages. Mol Cell *4*, 199-207.

Gordon, J.W., Scangos, G.A., Plotkin, D.J., Barbosa, J.A., and Ruddle, F.H. (1980). Genetic transformation of mouse embryos by microinjection of purified DNA. Proc Natl Acad Sci U S A *77*, 7380-7384.

Gossen, M., and Bujard, H. (1992). Tight control of gene expression in mammalian cells by tetracycline-responsive promoters. Proc Natl Acad Sci U S A *89*, 5547-5551.

Guglielmi, L., Le Bert, M., Truffinet, V., Cogne, M., and Denizot, Y. (2003). Insulators to improve expression of a 3(')IgH LCR-driven reporter gene in transgenic mouse models. Biochem Biophys Res Commun *307*, 466-471.

Hsiao, Y.C., Chang, H.H., Tsai, C.Y., Jong, Y.J., Horng, L.S., Lin, S.F., and Tsai, T.F. (2004). Coat color-tagged green mouse with EGFP expressed from the RNA polymerase II promoter. Genesis *39*, 122-129.

Kaffer, C.R., Srivastava, M., Park, K.Y., Ives, E., Hsieh, S., Batlle, J., Grinberg, A., Huang, S.P., and Pfeifer, K. (2000). A transcriptional insulator at the imprinted H19/Igf2 locus. Genes Dev *14*, 1908-1919.

Kistner, A., Gossen, M., Zimmermann, F., Jerecic, J., Ullmer, C., Lubbert, H., and Bujard, H. (1996). Doxycycline-mediated quantitative and tissue-specific control of gene expression in transgenic mice. Proc Natl Acad Sci U S A *93*, 10933-10938.

Potts, W., Tucker, D., Wood, H., and Martin, C. (2000). Chicken beta-globin 5'HS4 insulators function to reduce variability in transgenic founder mice. Biochem Biophys Res Commun *273*, 1015-1018.

Snove, O., Jr., and Rossi, J.J. (2006). Toxicity in mice expressing short hairpin RNAs gives new insight into RNAi. Genome Biol *7*, 231.

Sotillo, R., Hernando, E., Diaz-Rodriguez, E., Teruya-Feldstein, J., Cordon-Cardo, C., Lowe, S.W., and Benezra, R. (2007). Mad2 overexpression promotes aneuploidy and tumorigenesis in mice. Cancer Cell *11*, 9-23.

Stegmeier, F., Hu, G., Rickles, R.J., Hannon, G.J., and Elledge, S.J. (2005). A lentiviral microRNA-based system for single-copy polymerase II-regulated RNA interference in mammalian cells. Proc Natl Acad Sci U S A *102*, 13212-13217.

2.5 Author Contributions

Ross Dickins (R.D.) designed the TMP vector and first generation RNAi mouse models. Sang Yong Kim (S.Y.K.) performed pronuclear injections for all transgenics. Prem K. Premsrirut (P.K.P.) and Johannes Zuber (J.Z.) designed the TGM vector. P.K.P. designed transgenes for Salt and Pepper lines and the H19TGM line. R.D. conducted experiments (Fig. 2.1). P.K.P conducted experiments (Fig. 2.2-2.7). Kristin Diggins-Lehet and Janelle Simon (J.S.) tailed, weaned and cared for the animal colonies.

Chapter 3

RNAi Mouse Models using Recombinase-Mediated Cassette Exchange

A rapid and scalable system for studying gene function in mice using conditional RNA interference

Prem K. Premsrirut[1,2], Lukas E. Dow[1], , Sang Yong Kim[1], Colin D. Malone[1,3], Claudio Scuoppo[1,3], Cornelius Miething[1], Johannes Zuber[1], Ross A. Dickins[1,5], Gregory J. Hannon[1,4] and Scott W. Lowe[1,4*]

[1]Cold Spring Harbor Laboratory, Cold Spring Harbor, New York 11724, USA. [2]Stony Brook University, Medical Scientist Training Program, Stony Brook, New York 11794, USA. [3]Watson School of Biological Sciences and [4]Howard Hughes Medical Institute, Cold Spring Harbor, New York 11724, USA. [5]Molecular Medicine Division, Walter & Eliza Hall Institute of Medical Research, Parkville 3052, Australia.

*Correspondence should be addressed to S.W.L. (lowe@cshl.edu)

Abstract

RNA interference is a powerful tool for reversible control of gene expression, not only in cell-based systems, but also *in vivo*. To date the promise of regulatable RNAi transgenic mice has yet to be realized because the reproducible generation of these animals remains a significant technical limitation. By combining optimized fluorescence-coupled miR30-based shRNA technology with high efficiency ES cell targeting, we have developed a flexible and scalable pipeline for the rapid and reliable production of tet-regulated shRNA transgenic mice. As proof of principle, we have generated six novel doxycycline-regulated shRNA transgenic lines targeting the bioluminescence reporter *luciferase*, pluripotency regulator Oct4 and the tumor suppressor genes p53, p16, p19 and APC. Each shows strong doxycycline-dependent knockdown of its target protein, without disrupting endogenous miRNA processing. This system provides a platform for the large-scale production of RNAi transgenic mice targeting any gene in the mammalian genome.

3.1 Introduction

Genetically engineered mice are invaluable tools for understanding mammalian biology. They can be systematically manipulated and analyzed to define the genetic components that contribute to human disease and identify therapeutic approaches to combat those diseases. Traditionally, manipulation of gene expression in the mouse has relied on either the overexpression of transgenic cDNAs, or modification (deletion/knock-in) of endogenous genes using homologous recombination (Capecchi, 2005). The subsequent development of inducible transgenics and Cre-LoxP conditional knock-in/knockout models has added immense versatility to mouse modeling, however these approaches still require extensive labor and relatively high cost to produce and identify a single, functional genetically-engineered mouse.

More recently, RNA interference (RNAi) has been adapted to suppress gene expression in transgenic mice (Dickins et al., 2007), showing it is an effective alternative to conventional knockout approaches. RNAi regulates gene silencing through post-transcriptional repression, a process that is triggered endogenously by small, non-coding RNAs known as microRNAs (miRNAs) (He and Hannon, 2004). We have previously described the use of synthetic miRNA-based expression cassettes to trigger silencing of specific gene targets (Dickins et al., 2005). In this context, short hairpin RNAs (shRNAs) embedded within the endogenous miR30 backbone can be manipulated to target any endogenous transcript. Importantly, like naturally occurring miRNAs, miR30-based shRNAs

(shRNA-miRs) can be efficiently expressed from polymerase II promoters, enter the endogenous miRNA processing machinery to produce 21-22nt mature siRNAs and are capable of suppressing gene expression when present at single copy in the genome. When expressed from promoters such as tetracycline regulated elements (TREs) in cells that also express a tet-transactivator protein (either tTA or rtTA), shRNA-miR expression, and thus gene silencing, can be controlled by treatment with tetracycline or more commonly, doxycycline (DOX). By manipulating the timing and duration of DOX treatment and/or the expression of tTA or rtTA, shRNA-miRs can be used to inhibit endogenous gene expression in a conditional, ubiquitous or tissue-specific fashion in vivo (Dickins et al., 2007; Furth et al., 1994). Such systems have the powerful advantage that they act without modifying the genomic locus and, as such, are reversible.

A variety of RNAi-based mouse models have been successfully produced using traditional methods that include pronuclear DNA injection (Dickins et al., 2007; Fedoriw et al., 2004; Hasuwa et al., 2002; Lickert et al., 2005; Stein et al., 2003) or lenti-viral infection of zygotes or ES cells (Rubinson et al., 2003; Ventura et al., 2004), however these techniques result in random genomic insertions of the shRNA expression cassette and are therefore prone to copy number and position effect variegation. As has been noted for transgenic overexpression of protein coding cDNAs (Beard et al., 2006), these drawbacks can be overcome by utilizing recombinase-mediated cassette exchange (RMCE) to integrate single copy shRNA cassettes into well-defined loci such as the *HPRT* (Wang et al., 2007) or *Rosa26* locus (Hitz et al., 2007). Unlike homologous

recombination that relies on rare targeting events, RMCE systems (Hitz et al., 2007; Nyabi et al., 2009; Seibler et al., 2005; Seidler et al., 2008) efficiently introduce transgenes into pre-targeted genomic loci by promoting FlpE or Cre-mediated plasmid-chromosome recombination between compatible FRT or loxP sites. Because of this, RMCE remains a significant improvement over conventional homologous recombination schemes as it allows for fast, consistent and efficient production of genetically modified mice without the need for elaborate and customized gene targeting vectors.

Here, we describe the development of a rapid and reliable system to generate doxycycline-regulated RNAi mouse models with high efficiency and minimal labor. Specifically, we utilize the Flp/FRT recombinase system (Buchholz et al., 1998) to target DOX-regulatable shRNA-miRs) downstream of the endogenous *Collagen type 1* (*ColA1*) gene (Beard et al., 2006). Our system allows for fast, single-step delivery of any shRNA-miR into the mouse genome. Moreover, we have adapted the configuration of the shRNA-miR expression cassette to include a GFP reporter, which acts both as a 'spacer' element that enhances knockdown and serves as an *in vivo* biomarker of shRNA expression. These improvements establish a platform that can be used for large-scale production of ES cells and mice with spatial, temporal and reversible control of any endogenous gene.

3.2 Results

To create a rapid, flexible and scalable system for producing shRNA transgenic mice, we set out to reduce the time, cost and variability associated with the development of each individual transgenic strain. We reasoned that the ideal system should provide potent and regulatable gene silencing, trackable shRNA expression, be cheap, high throughput and adaptable to allow conditional, tissue-specific gene knockdown. In an effort to develop a versatile shRNA-miR targeting construct, we tested whether we could optimize the miR30-based expression cassette to include a fluorescent transgene to report shRNA expression without compromising gene silencing. To do this we tested knockdown efficiency in different retroviral vector configurations that linked miR30 transcription to a GFP cDNA. First, a retroviral DOX-inducible shRNA-miR vector (TMP) (Dickins et al., 2007) was modified by inserting GFP either upstream (TRE-GFP-miR30-pgkPuro – TGMP) or downstream (TRE-miR30-GFP-pgkPuro – TMGP) of the miR30 cassette (Supplementary Fig. 1a). We then assessed each configuration by retroviral integration at low multiplicity of infection (MOI) into primary mouse embryonic fibroblasts (MEFs), using a potent shRNA-miR targeting the tumor suppressor gene *Trp53* (Dickins et al., 2005). The presence of a GFP 'spacer' between TRE and miR30 (TGM) both enhanced knockdown in comparison to TMP and TMGP vectors and importantly allowed robust expression of GFP to serve as a reporter for shRNA expression (Supplementary Fig. 1b,c) (Stegmeier et al., 2005).

3.2.1 Site-specific targeting in ES cells

To allow efficient generation of targeted ES cells harboring a single tet-regulatable mir30-based cassette we adapted the *ColA1* recombinase-mediated targeting system previously described by Jaenisch and colleagues (Beard et al., 2006). This system allows for rapid and efficient targeting of transgenes to pre-engineered 'KH2' ES cells by FRT-mediated recombination. Briefly, KH2 ES cells contain an FRT-hygro-pA "homing" cassette downstream of the *ColA1* gene on mouse chromosome 11 (Supplementary Fig. 3.2A), as well as a reverse tet-transactivator (M2rtTA) targeted to the *Rosa26* locus (referred to as Rosa-rtTA). Following coelectroporation of pCAGs-FLPe and the targeting vector, transient expression of FLPe recombinase in ES cells mediates recombination between the FRT site at the *ColA1* locus and those present on the targeting vector (Beard et al., 2006) (outlined in Supplementary Fig. 3.2A). Importantly, the configuration of the targeting vector and homing cassette restores hygromycin resistance only upon correct integration. Consequently, the highly stringent *ColA1* approach confers precise recombination and therefore obviates the need to screen numerous clones.

To generate the targeting construct, we modified the pBS31-*ColA1* vector (Beard et al., 2006) to facilitate cloning of miR30-based shRNAs into the TGM design (Fig. 3.1A). Using this modified targeting vector, *ColA1*-TGM Flp-In (hereafter referred to as pCol-TGM), nearly every shRNA from the Hannon-Elledge genome-wide library (Paddison et al., 2004) or RNAi codex library (Olson

et al., 2006) can be inserted into the miR30 backbone in a single *XhoI* /*EcoRI* subcloning step

Following electroporation, hygromycin selection and expansion of individual clones, cells were screened for GFP expression upon DOX treatment. Approximately 95% of hygromycin resistant clones expressed GFP when treated with DOX and nearly 100% of dual-selected, hygro^{R}-GFP positive clones showed correct targeting as determined by Southern blot analysis (Supplementary Fig. 3.2B). With highly stringent dual selection approach, we were able to reduce the number of clones screened to only 4-6 clones for each individual shRNA targeted, making it feasible to generate multiple ES cell clones, carrying different shRNAs simultaneously and with minimal effort. Moreover, the majority of ES clones showed a single transgenic insertion at the expected size (Supplementary Fig. 3.2B,C) and we observed minimal variation in GFP-shRNA expression between ES cells lines harboring different shRNAs.

Using the pipeline detailed in (Supplementary Fig. 3.3), we generated several independent ES cell lines harboring an shRNA-mir targeting the firefly bioluminescence reporter gene, *luciferase* (TG-luc.1309) (Silva et al., 2005). We also knocked-in a number of endogenous genes, including the pluripotency transcriptional regulator, *Pou5f1* (TG-Oct4.468) and the tumor suppressor genes *Trp53* (TG-p53.1224), *ARF* (TG-p19.157), *Adenomatous Polyposis Coli* (*APC*) (TG-APC.9365), and the transcript that encodes the tumor suppressors p16INK4a and p19ARF (TG-p16/p19.478).

To validate the effectiveness of single-copy shRNA-miRs targeted to the *ColA1* locus, we first confirmed knockdown in 5 independently selected TG-luc.1309/Rosa-rtTA ES cell clones transduced with retrovirus expressing *luciferase*. Bioluminescence imaging following DOX treatment showed a consistent 70-75% knockdown of *luciferase* activity in each clone tested (representative data in Fig. 1b). In addition, significant suppression of endogenous protein expression was observed in selected TG-p53.1224/Rosa-rtTA, TG-Oct4.468/Rosa-rtTA and TG-APC.9365/Rosa-rtTA ES cell clones after DOX treatment and this knockdown was fully reversible upon DOX withdrawal (Fig. 1c,d). Importantly, as described earlier, GFP expression strongly correlated with gene knockdown and thus could be used as a visual biomarker of shRNA-miR expression. (Fig. 1c,d). Induction of p53.1224 or Oct4.468 in these ES cells mimicked the effect of gene loss as DOX-treated TG-p53.1224/Rosa-rtTA ES cells displayed decreased sensitivity to the DNA damaging agent Adriamycin (Supplemental Fig. 4a) (Hong and Stambrook, 2004; Schmitt et al., 2002) while TG-Oct4.468/Rosa-rtTA ES cells treated with DOX, but not untreated cells, underwent differentiation toward a trophoblast lineage (Fig. 1e; Supplementary Fig. 4b), characteristic of what is observed following deletion of Oct4 in ES cells (Niwa et al., 2000). Together these results show that DOX-dependent expression of a single shRNA-miR transgene at the *ColA1* locus can induce dramatic gene knockdown and mimic loss of function phenotypes in ES cells.

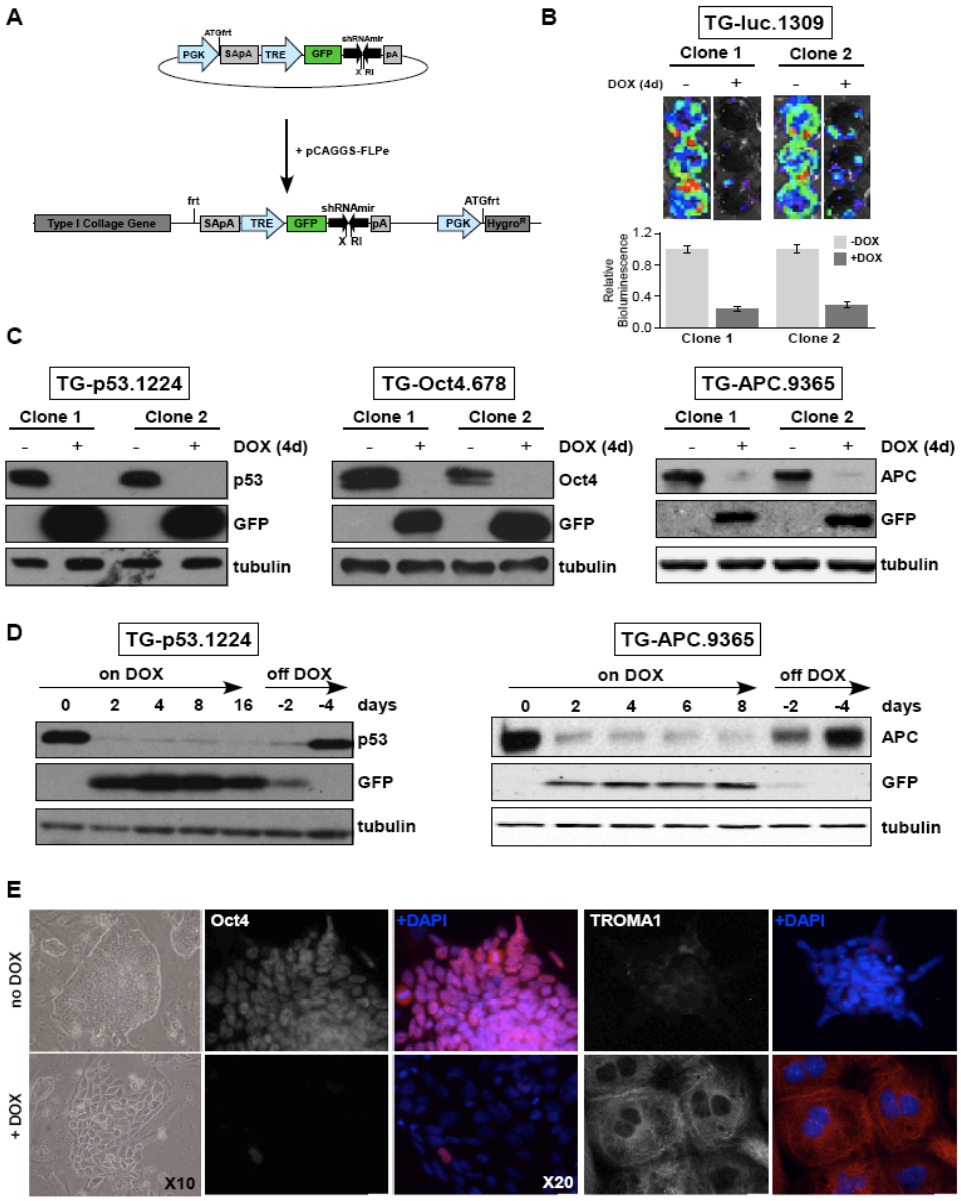

Figure 3.1 | TRE-driven shRNA-mirs targeted to the *Col1A1* locus can drive robust DOX-dependent gene knockdown in ES cells. *A,* Schematic diagram of the pColTGM vector. Coelectroporation of pColTGM and pCAGGS-Flpe recombinase promotes integration of pColTGM to restore hygromycin resistance. *B,* (*Top*) Luminescent images of two independent clones containing luc.1309;Rosa-rtTA. Cells were infected with MSCV-*luciferase* and treated 48h post- infection with DOX for 4 days. (*Bottom*) The images were quantified to assess *luciferase* knockdown. *C,* Western blot analyses of representative DOX-treated ES cell clones containing Rosa-rtTA and TG-p53.1224, TG-Oct4.678 or TG-APC.9365. *D,* Western blot analyses of TG-p53.1224 and TG-APC.9365 clones treated with doxycycline for 8 days and then shifted to normal media for 2, 4 or 8 days prior to harvest. All cells containing p53.1224 were treated with Adriamycin (0.5μg/ml) for 2hr prior to harvest (*C-D*). *E,* Brightfield and immunofluorescence images of TG-Oct4.678;Rosa-rtTA cells treated with DOX for 7d. Cells were stained with antibodies against Oct4, the trophoectoderm marker, TROMA1 and proliferation marker, Ki67.

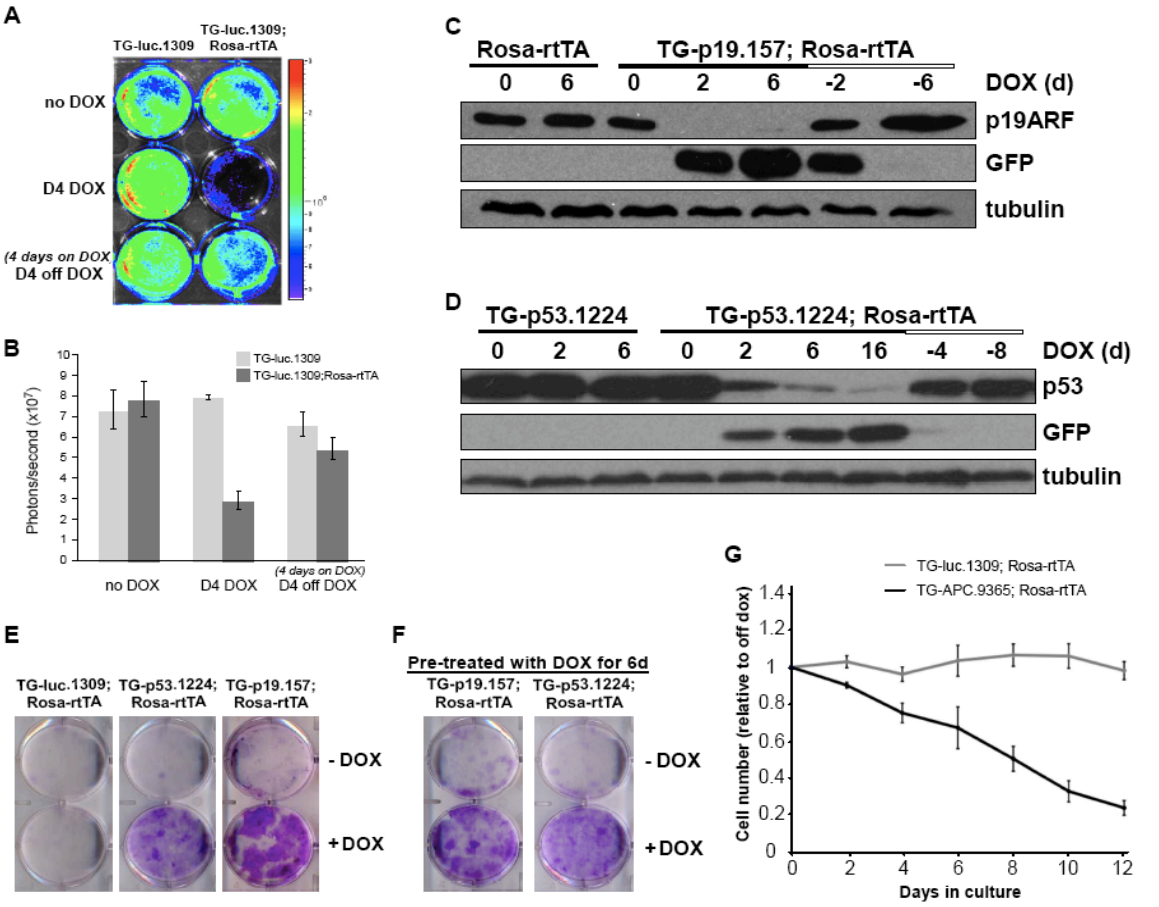

Figure 3.2 | Reversible knockdown of gene targets in primary mouse embryonic fibroblasts derived from *Col1A1*-TGM ES-cell derived mice. *A,* Bioluminescence imaging of TG-luc.1309 and TG-luc.1309;Rosa-rtTA MEFs infected with *MSCV-luciferase*. MEFs were treated with DOX, then shifted into DOX-free media as for the days indicated. All cells were treated with luciferin prior to imaging. *B,* Quantification of the bioluminescence signal to assess *luciferase* knockdown. (*C-D*) Western blot analysis of MEFs harvested from a cross between C57BL/6 WT mice and *C,* TG-p19.157;Rosa-rtTA and *D,* TG--p53.1224;Rosa-rtTA founder mice. Time course were performed on MEFs cultured in DOX-containing media then shifted to normal media. Littermate Rosa-rtTA or TG-p53.1224 MEFs are also shown. All TG-p53.1224 containing MEFs were treated for 2hr with Adriamycin (0.5μg/ml) to induce *Trp53* stabilization prior to harvest. *E,* Colony formation assay of Rosa-rtTA MEFs containing either TG-luc.1309, TG-p53.1224 or TG-p19.157 plated at low density and cultured with or without DOX for 12d. *F,* MEFs pre-treated with DOX for 10d were plated at low density and culture with or without DOX for 12d. *G,* Proliferation of DOX-treated TG-luc.1309;Rosa-rtTA and TG-APC.9365;Rosa-rtTA MEFs relative to off-DOX populations.

3.2.2 Functional validation in cells derived from RNAi mice

Following validation of knockdown in the ES cell clones, we generated fully ES cell-derived transgenic mice using tetraploid embryo complementation, eliminating the need to screen litters for germline transmission, thus accelerating mouse production and reducing the costs of establishing a colony (Schuster-Gossler et al., 2001). To test the potency and reversibility of each shRNA-mir in each transgenic line, we isolated mouse embryonic fibroblast (MEFs) carrying the TGM-shRNA-mir and Rosa-rtTA and performed immunoblotting for the target protein in the absence and presence of DOX. As expected, DOX treatment resulted in significant depletion of *luciferase* activity in double transgenic (TG-luc.1309;Rosa-rtTA), but not single transgenic (TG-luc.1309 alone) MEFs (Fig 3.2A,B). Moreover, this knockdown was rapidly reversible upon DOX withdrawal (Fig. 3.2A,B). In MEFs derived from each of the TG-p53.1224, TG-p16/p19.478 and TG-p19.157 shRNA-mir founder lines we observed substantial DOX-dependent knockdown of the target protein that was fully reversible upon DOX withdrawal (Fig. 3.2C,D; Supplementary Fig. 5).

Several of the genes we targeted are known to have proliferation phenotypes in MEFs, enabling us to examine whether we could phenocopy the effects of gene deletion using our system. Similar to gene deletion, suppression of either p53 or ARF in this system promoted immortalization as demonstrated by their ability to form colonies when plated at low density (Fig. 3.2E). Additionally, TG-p53.1224;Rosa-rtTA and TG-p19.157;Rosa-rtTA MEFs pretreated with DOX

lost their ability to form colonies when removed from DOX-containing media, indicating that DOX withdrawal restores tumor suppressor function and reverts the immortalized phenotype (Fig. 3.2F). Conversely, induction of APC.9365 in MEFs caused a progressive proliferation arrest consistent with what has been described following activation of Wnt signaling in MEFs via overexpression of stable mutant β-catenin (Fig. 3.2G) (Damalas et al., 2001).

3.2.3 Conservation of the miRNA profile

Recent studies have highlighted potential complications of expressing exogenous shRNAs due to saturation of the miRNA processing machinery (Grimm et al., 2006). To address whether shRNA-mir expression in our system disrupts endogenous miRNA expression, we examined global miRNA expression in bitransgenic TG-luc.1309/Rosa-rtTA transgenic MEFs, as these cells express a functional shRNA (Fig. 3.2A,B) with no known target in mouse cells and should therefore not affect the biological regulation of specific miRNA transcripts. We anticipated this would provide a simple readout for gene knockdown of an ectopically expressed *luciferase* transgene as well as a control to distinguish non-specific effects of shRNA-mir expression (Dickins et al., 2005). To do this we cloned small RNAs (Malone et al., 2009) from single (TG-luc.1309) and double-transgenic (TG-luc.1309/Rosa-rtTA) MEFs cultured in DOX-containing or DOX-free media for 4 days. Solexa deep-sequencing revealed that while there was a substantial DOX-dependent induction of luc.1309 shRNA, this induction did not

affect the expression profiles of all 319 detected miRNAs (Fig. 3.3; Supplementary Fig. 3.6). In fact, endogenous miRNA expression remained virtually unchanged despite luc.1309 expression; only small changes, both increases and decreases, of individual miRNAs were observed (generally less than two-fold). This indicates that induction of an exogenous miRNA did not cause a general suppression of endogenous miRNAs, as previously publications report. We also noted a basal level of luc.1309 expression, which likely reflects a low-level leakiness from the TRE promoter in MEFs that does not appear to be sufficient to cause gene knockdown in TG-p53.1224, TG-p19.157,TG-p16/p19.478 or TG-APC.9365 MEFs (Fig. 3.2C,D; Supplementary Fig. 3.5, data no shown). Moreover, leaky expression from this promoter appears to be cell type specific as we have not observed significant DOX-independent GFP expression in other cell types, including cultured ES cells and multiple hematopoetic cell types from transgenic mice (data not shown). Together, these results demonstrate that tet-regulated shRNA-mirs expressed from the *ColA1* locus allow potent, reversible silencing of gene expression without disrupting endogenous miRNA processing.

A

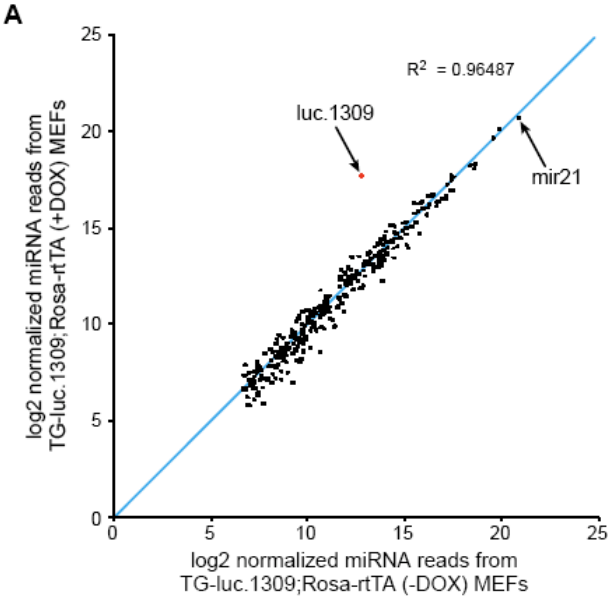

B

miRNA	Normalized Reads	
	-DOX	+DOX
mmu-miR-21	1818873	1703510
mmu-miR-22	946310	1126022
mmu-miR-143	761747	834027
mmu-miR-29b	400981	333784
mmu-miR-29a	389143	285289
mmu-miR-24	328930	312654
mmu-let-7i	189515	210355
mmu-let-7f	176965	126538
mmu-miR-31	167143	183385
mmu-let-7c	166497	217007
mmu-miR-125b-5p	159742	128726
mmu-miR-130a	143896	161989
mmu-miR-199b	139458	93004
mmu-let-7a	136054	107188
mmu-miR-26a	120847	96290
mmu-miR-16	105034	85699
mmu-let-7d	102163	71860
mmu-miR-27b	101483	84696
mmu-miR-103	88202	110605
mmu-miR-20a	84479	106212
Luc.1309	3998	103734

Figure 3.3 | Induction of shRNA-miR does not affect endogenous miRNA processing. *A,* Scatter plot representing normalized abundance of 319 expressed miRNAs from DOX-treated and untreated TG-luc.1309;Rosa-rtTA MEFs. R^2 correlation coefficient excludes TG-luc.1309 reads. *B,* Number of normalized reads obtained for the top 20 miRNAs and luc.1309 expressed in MEFs.

3.2.4 Gene regulation in *luciferase* reporter mice

To evaluate the dynamics of reversible gene silencing in adult mice, we bred mice that express *luciferase* from the endogenous *Rosa26* promoter [by crossing *Rosa26-LSL-luciferase* (Safran et al., 2003) to a germline Cre-deleter strain, Stra11-Cre (Sadate-Ngatchou et al., 2008)] and crossed these to TG-luc.1309/Rosa-rtTA mice to produce triple transgenics (TG-luc.1309/Rosa-rtTA/Rosa-*luciferase*, or shluc/R/RL). *Rosa26* activity is reportedly high in embryonic tissues (Soriano, 1999; Srinivas et al., 2001), therefore, we first tested knockdown in E17.5 embryos harvested from pregnant females DOX-treated for

8 days. Triple transgenic embryos showed marked induction of GFP expression and ~75% knockdown of the bioluminescent signal compared to controls (Fig. 4a-c), consistent with the level of knockdown we have observed in ES cells and transgenic MEFs with this shRNA-miR (Fig. 1b, 2a,b). To evaluate the reversibility of knockdown in adult mice we next measured *luciferase* activity longitudinally in the skin of triple transgenic mice treated with DOX for 4 days and then removed from treatment. Strikingly, after only 4 days of DOX-treatment, shluc/R/RL animals displayed significant suppression of *luciferase* activity (and high GFP expression) compared to untreated triple transgenic controls (Fig. 4d-f) and mice expressing *luciferase* but not the luc.1309 shRNA-miR (not shown). Moreover, this suppression was completely reversible and 12 days following DOX withdrawal, *luciferase* activity returned to basal levels.

To evaluate knockdown in individual tissues we sacrificed animals after 4 days of DOX treatment and imaged individual organs for GFP and bioluminescence. In accordance with previous publications we observed significant variation in the level of Rosa-rtTA-mediated GFP induction between different organs (Beard et al., 2006). Significantly however, tissues that displayed strong induction (> 20 fold) of GFP expression (skin, intestine, spleen, thymus and liver) showed significant *luciferase* knockdown, validating our transgenic system and highlighting the utility of GFP-marked shRNA expression *in vivo*. (Supplementary Fig. 7).

During our *in vivo* testing we noted that the presence of two Rosa-rtTA transgenic alleles increased the DOX-dependent expression of GFP-shRNA-

miRs relative to a single allele (not shown). This indicated that not only was rtTA expression from the *Rosa26* promoter tissue restricted (Supplementary Fig. 3.7) it was also not promoting maximal expression from the TRE in most tissues. To overcome this limitation, we sought to develop a stronger, more ubiquitous, tet-transactivator strain expressing the third-generation, highly sensitive reverse tet-transactivator (rtTA3) downstream of the strong CAG promoter (Niwa et al., 1991). We screened over 70 founder animals generated by standard pronuclear injection to identify a strain that contained a single genomic insertion of CAG-rtTA3 (Supplementary Fig. 3.8) and showed strong DOX-dependent induction of TRE-GFP-miR30 in multiple tissues (Supplementary Fig. 3.9). We then generated triple transgenic mice carrying TG-luc.1309/CAG-rtTA3/Rosa-*luciferase* (shluc/C3/RL) and imaged individual organs after 4 days of DOX treatment. In contrast to shluc/R/RL mice, shluc/C3/RL triple transgenics showed robust induction of GFP in almost all tissues examined and consistent with previous results, tissues that expressed high levels of GFP displayed a largely dose-dependent knockdown of *luciferase* activity (Supplementary Fig. 9). These results clearly demonstrate that expression of GFP-shRNA-miR from the TRE promoter at the ColA1 locus is possible in almost all adult mouse tissues and that gene silencing can be controlled coordinately *in vivo* by doxycycline treatment and the restricted expression of a tet-transactivator protein.

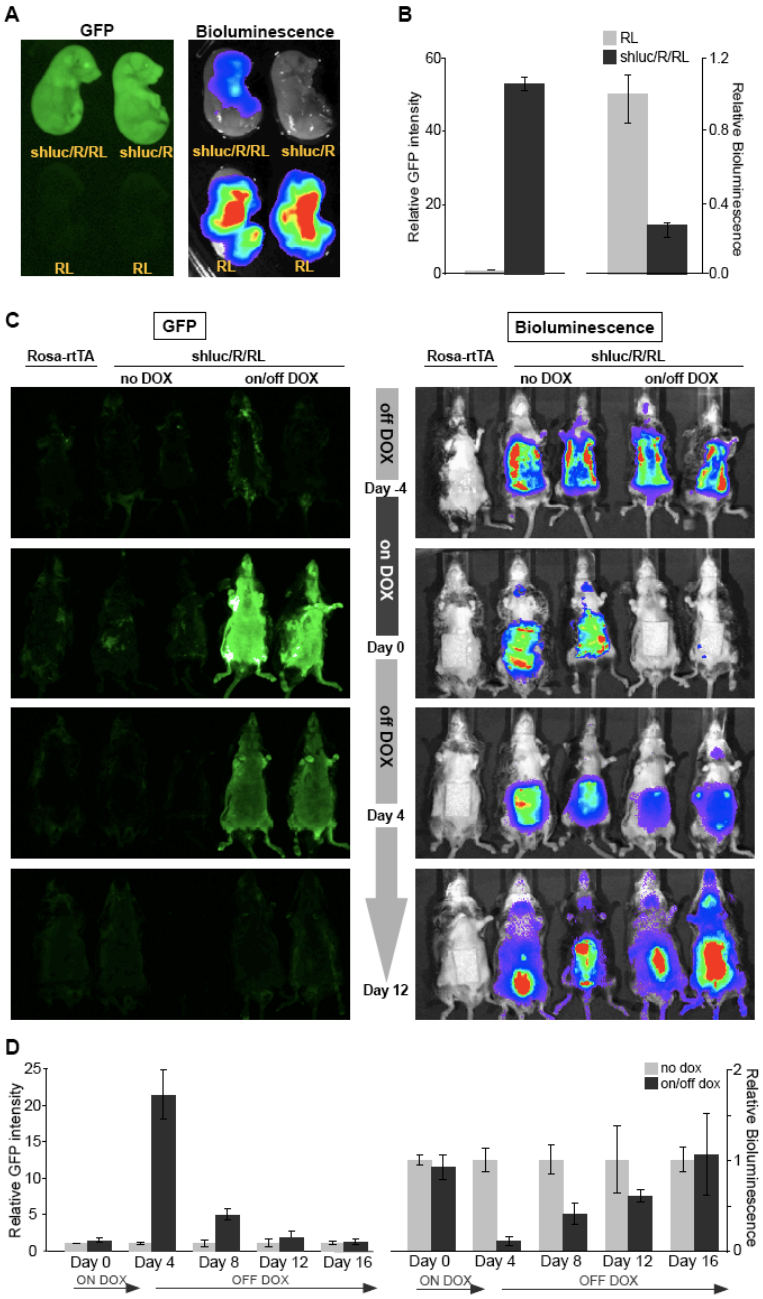

Figure 3.4 | Reversible GFP-marked DOX-dependent knockdown in live animals. *A,* GFP and bioluminescent images of E17.5 embryos sacrificed from a DOX-treated pregnant female. *B,* Relative GFP intensity and *C*, bioluminescence with standard error (n=6) between RL and shluc/R/RL embryos. *D, In vivo* luminescent time course imaging of TG-luc.1309;Rosa-rtTA;Rosa-*luciferase* (shluc/R/RL) triple transgenics and controls. Serial luminescent images were captured every 4 days beginning with untreated animals followed by 4d of DOX treatment delivered in food pellets. After 4d, animals were placed on their regular diet and imaged. *E,* Relative GFP intensity and *F,* bioluminescence quanitfication with standard error (n=3) between untreated and DOX-treated shluc/R/RL animals over time.

3.2.5 Recapitulating phenotypes in RNAi mice

Finally, we examined whether our shRNA transgenic system would enable study of gene function during development and in adult mice. As a proof of principle, we examined the phenotype of the TG-APC.9365 transgenic mouse, as normal APC function is known to be essential for proper embryonic development and homeostasis of a variety of adult tissues (Moser et al., 1990). While homozygous APC mutant mice do not survive beyond 6-8 days of development (Moser et al., 1990), here we took advantage of the inducible nature of our model to bypass the early lethality of APC mutants and investigate the requirement for APC expression beyond embryonic day 8 (E8). For this purpose we used Rosa-rtTA to drive shRNA-miR expression as we observed significant *luciferase* knockdown using this allele in embryos (Fig. 4a-c). To knockdown APC *in utero*, wild type females crossed to TG-APC.9365/TG-luc.1309/Rosa-rtTA triple transgenic males were fed DOX at 8.5dpc (E8.5) and embryos were analyzed at E14.5 and E18.5. This breeding scheme ensured that the control (TG-luc.1309) and test (TG-APC.9365) transgenes segregate in the F1 generation providing appropriate littermate controls for each experiment. After only 2 days of DOX-treatment APC knockdown was detectable in TG-APC.9365/Rosa-rtTA bi-transgenic embryos compared to TG-luc.1309/Rosa-rtTA and TG-APC.9365 (no Rosa-rtTA) controls (Fig. 5a). By E14.5 TG-APC.9365/Rosa-rtTA embryos displayed a prominent *hydrops fetalis* phenotype, characterized by a pronounced fetal edema (Fig. 5b) and both limb and forelimb digits appeared stunted relative

to TG-luc.1309/Rosa-rtTA littermate controls (Fig. 5b, arrows). By E18.5, TG-APC.9365/Rosa-rtTA bi-transgenic embryos showed accumulating edema and no DOX-treated TG-APC.9365/Rosa-rtTA animals survived to birth.

We next assessed the effect of post-natal depletion of APC using the same breeding strategy but starting DOX treatment on the day of birth. Similar to what has been described using K14-Cre/APC$^{flox/flox}$ animals (Kuraguchi et al., 2006), post-natal depletion of APC resulted in a stunted development of the snout in newborn mice, most evident 18 days after birth (P18) (Fig. 5d). Continued DOX treatment throughout juvenile development promoted excessive hair growth due to a prolonged anagen phase of the hair cycle (Fig. 5e). However, paradoxically, long-term DOX treatment of these mice resulted in progressive hair loss and at 5-6 months of age APC.9365/Rosa-rtTA animals were almost entirely hairless (Fig. 5e). Near identical phenotypes have been described in transgenic mice that overexpress mutant β-catenin or Wnt1 in the epidermis (Castilho et al., 2009; Van Mater et al., 2003), underscoring the efficacy of the transgenic shRNA system to model consequences of hyperphysiological Wnt activation. Interestingly, although transient Wnt activation is sufficient to hyperactivate the hair cycle (Van Mater et al., 2003), hair loss required sustained Wnt activation as mice withdrawn from DOX treatment after 4 weeks (although runted) did not show hair loss similar to controls (Fig. 5f). It will be interesting to determine the developmental stage at which hair loss can no longer be reversed. Importantly, we have confirmed that both the embryonic and postnatal defects described above are due to APC knockdown as an

independent transgenic line carrying a different APC hairpin displays identical phenotypes (not shown). Together these results show that temporally controlled deregulation of Wnt signaling via APC depletion can both recapitulate predicted phenotypes observed in other genetic models and be used to identify novel gene functions that would not have been possible using existing technologies. Overall these data establish that regulated expression of a single copy miR30-based shRNA in transgenic mice can be adapted to effectively investigate gene function during mammalian development and/or in adult mice.

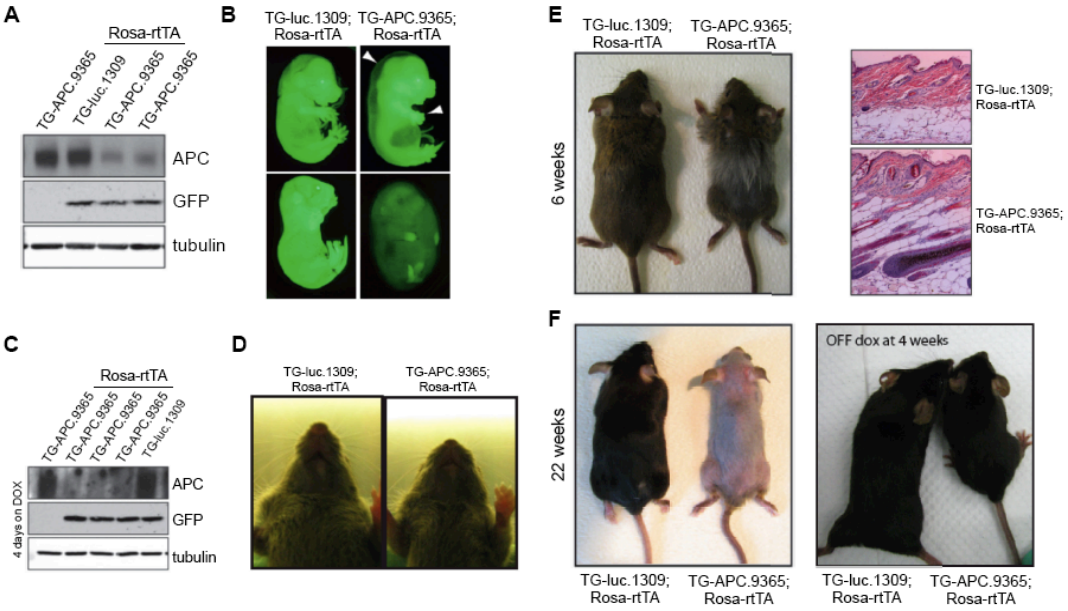

Figure 3.5 | APC knockdown by RNAi recapitulates null phenotypes. *A,* Western blot of whole protein lysates from E10.5 embryos on DOX for 2 days. *B,* GFP images of embryos treated with DOX from E8.5 and analysed at E14.5 and E18.5 as indicated. Arrows indicate fluid accumulation along the dorsal ridge and defects in limb and digit development apparent at E14.5. *C,*Western blot of whole protein lysate for E18.5 epidermis, on DOX for 4 days. *D,* Representative photographs of TG-luc.1309/Rosa-rtTA and TG-APC.9365;Rosa-rtTA double transgenic mice at P18, on DOX since birth. *E-F, Left.* Photograph of TG-luc.1309;Rosa-rtTA and TG-APC.9365;Rosa-rtTA double transgenic mice 6 weeks of age (*E)* or 22 weeks of age (*F)* on DOX since birth. *Right*. H&E sections of skin taken from 6 week old double transgenic mice as indicated. *F, Right.* Photograph of TG-luc.1309;Rosa-rtTA and TG-APC.9365;Rosa-rtTA double transgenic, on dox at birth and taken off DOX at 4 weeks of age. Although runted, the TG-APC.9365;Rosa-rtTA mouse does not show hair loss like mice continually exposed to DOX.

3.3 Discussion

The production of constitutive and conditional knockout mice has revolutionized the study of gene function in mammals but it entails laborious, time-consuming and/or expensive procedures to build primary models. While transgenic shRNA 'knockdown' mice provide a potential alternative, challenges associated with reproducible production of such strains with effective knockdown has curtailed their widespread use. By adapting the Flp/FRT recombinase system for rapid introduction of DOX-regulatable shRNA-miRs, we have developed an efficient platform suitable for large-scale generation of ES cells and transgenic mice with reversible, RNAi-mediated inhibition of gene expression. In fact, such is the ease of scaling the system that during the initial development phase, we have been able to generate and validate over 100 ES cell lines and 30 mouse strains harboring different shRNA-miRs in less than 2 years with minimal labor (unpublished data). Moreover, the platform is flexible such that it is not only valuable for the production of mice bearing 'knockdown' shRNA-miR cassettes, but also for the expression of other non-coding RNAs. In fact, with our optimized pipeline now in place, we have established a collaboration with the NCI and expanded our efforts to produce a repository of ~1500 DOX-regulatable ES cell lines containing all known endogenous miRNAs.

Previous iterations of transgenic shRNA mouse technologies have shown that RNAi can be effectively used to recapitulate loss of function phenotypes in mice (Dickins et al., 2007; Hitz et al., 2009; Wang et al., 2007), although none of

these systems have effectively streamlined the approach such that it can be quickly and easily applied for multiple targets. To improve power and efficiency, we have: 1. Accelerated the production of RNAi transgenic mice by moving to a site-specific targeting method using the *ColA1* genomic locus, which is accessible in a broad range of tissues and overcomes variability among founder mice produced by pronuclear injection. 2. Optimized the miR30-based shRNA cassette to provide more efficient gene silencing and expression of a GFP reporter, which can be used as a surrogate marker for shRNA-miR expression *in vivo* and during ES cell clone selection and 3. Designed the pCol-TGM targeting vector such that any of the validated shRNA-miRs from the Elledge-Hannon and Codex (http://codex.cshl.org) genome-wide libraries can be substituted using a single XhoI/EcoRI cloning step. While such a system will not replace gene targeting to create precise genetic lesions, it is now feasible to develop shRNA-miR transgenic animals to evaluate the function of any mammalian gene.

In contrast to gene targeting, shRNA-miR expression does not modify the genomic locus of the target gene and thus one of the most exciting applications of RNAi technology in mice is the potential to temporally and reversibly control gene expression in a tissue-specific manner. In this regard our transgenic design is flexible, as the tet-transactivator and TRE-GFP-miR are physically separated in the genome in contrast to 'all-in-one' approaches used in other systems (Seibler et al., 2007). This separation means that through breeding to the more than 100 existing tissue specific tet-transactivator strains (http://www.zmg.uni-mainz.de), shRNA-miR expression can be directed and regulated in specific tissues in the

mouse. Using a new ubiquitous CAG-rtTA3 tet-transactivator strain that shows greater and more widespread induction of TRE-GFP than other strains we have tested (including Rosa-rtTA, Actin-rtTA and CMV-rtTA; not shown), we showed that GFP-shRNA-miR expression from the *ColA1* targeting locus is possible in almost all tissues. Importantly, we noted that in every setting in which we saw substantial GFP expression, we also observed gene silencing, indicating that when expressed, the shRNA-miR transcript was processed effectively in all cases. Although some organs, such as the brain, spleen and lung showed lower GFP expression and reduced *luciferase* knockdown (Supplementary Fig. 8), we believe this is likely due to the inaccessibility of DOX to the cells (in the case of brain) or sub-optimal rtTA expression in some tissues in the CAG-rtTA3 line, as tissue-specific expression of tet-transactivators in CCSP-rtTA (Tichelaar et al., 2000) and Vav-tTA (Kim et al., 2007) strains can promote shRNA-miR expression and gene silencing in the lung and in B-cells (Premsrirut et al, in preparation; unpublished data).

In all, we combine a state-of-the-art fluorescent-coupled miR30-based gene silencing cassette with recombinase-mediated ES cell targeting and tetraploid embryo complementation to provide a platform for fast and reliable generation of DOX-regulated RNAi transgenic mice. This system is adaptable to the study of both stable and transient loss of function phenotypes *in vivo*. In addition, the flexible design of the targeting vector enables the expression of different fluorescent reporters or tandem shRNA-miRs (unpublished data). Still, it should be noted that not all shRNAs act as effective gene silencing triggers at

single copy in the genome. In fact before ES cell targeting, we regularly test up to 10 shRNAs per gene to identify the most potent sequences. For those genes with which effective shRNA-miRs are particularly difficult to identify, we have now developed a high-throughput screening methodology to find the most potent shRNAs (Fellmann et al submitted); these shRNAs can then be directly applied to transgenic mouse production. Indeed we have already implemented this workflow to generate transgenic mice harboring the most potent shRNA sequences against cMyc and Mcl1 (Fellmann et al, submitted; unpublished data). In the future we anticipate this system will be invaluable for studies ranging from embryonic and postnatal development, to normal mammalian physiology and ultimately the biology of disease and therapeutic strategies to treat disease.

Supplementary Figures

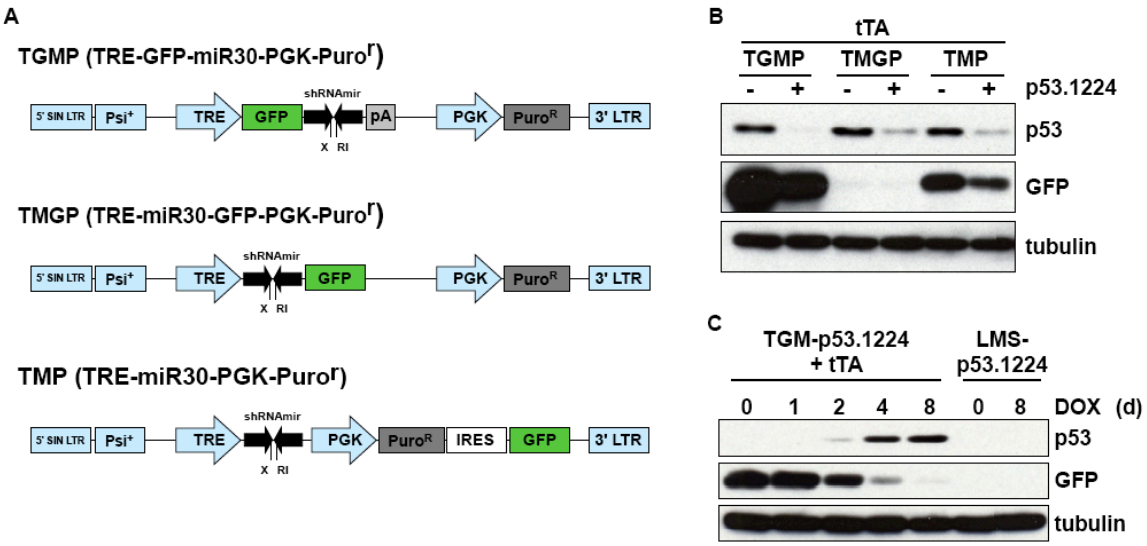

Supplementary Figure 3.1 | TGMP enhances knockdown and provides a biomarker for shRNA expression. *A,* Schematic diagram comparing the TGMP, TMGP and TMP retroviral vectors. *B,* Western blot analysis reveals enhanced p53.1224 efficacy in infected tTA-expressing MEFs in the context of the TGMP retroviral vector in comparison to TMGP and TMP. *C,* Time course of *Trp53* re-expression and GFP downregulation upon DOX treatment in retrovirally infected TGMP-p53.1224;tTA MEFs.

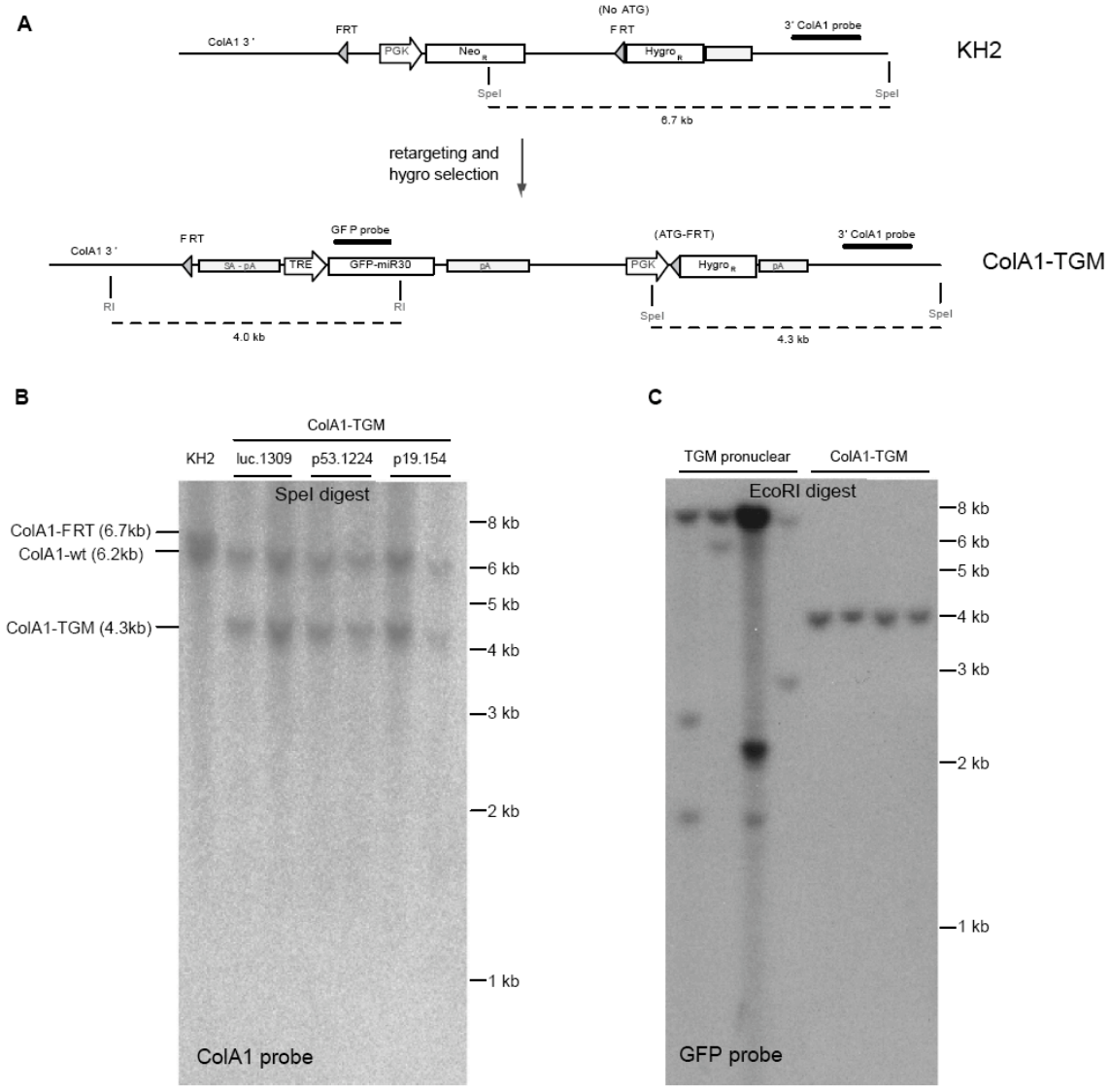

Supplementary Fig. 3.2 | Strategy for Flp/FRT RMCE at the *ColA1* locus in KH2 mES cells. *A,* Schematic representation of the downstream region of the *ColA1* locus after placement of an frt-hygro-pA "homing" cassette by homologous recombination. The "FRT homing cassette" consists of PGK-Neo^R and a nonfunctional Hygro^R cassette with no ATG site or promoter. Coelectroporation of the pColTGM and pCAGGs-Flpe recombinase vectors promotes inter- and intrachromosomal recombination at the *ColA1* locus downstream of the Type I Collagen gene, resulting in excision of PGK-Neo^R and integration of the pColTGM. Correct integration restores hygromycin resistance. *B,* Representative results of southern blot analysis of hygromycin resistant-GFP positive DOX treated clones using the ColA1 probe. *C,* Southern blot analysis of transgenic animals generated by pronuclear injection and Flp/FRT RMCE using a GFP probe to determine multiple integrations.

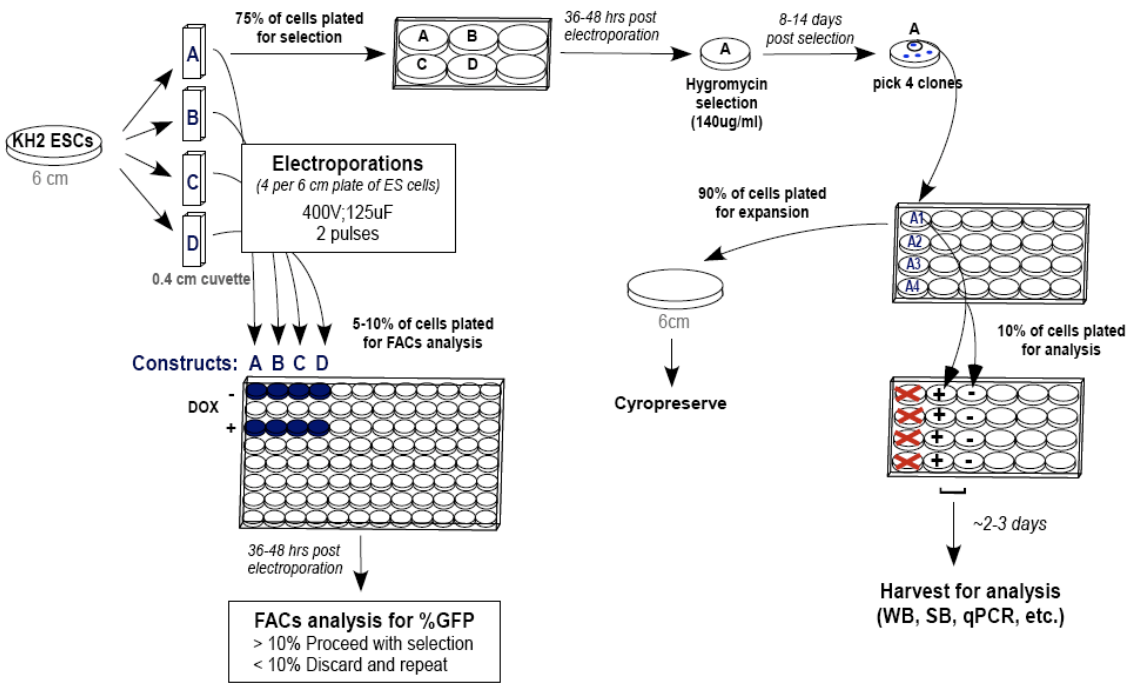

Supplementary Figure 3.3 | Optimized pipeline for rapid and efficient generation of *Col1A1* targeted ES cell clones. One confluent 6cm plate of KH2 ES cells can be used for 4 separate electroporations to generate unique ES cell lines. Immediately following electroporation, a small fraction of ES cells were plated in normal or DOX-containing media for GFP expression by FACs analysis 48 hours later to assess electroporation efficiency. If FACs revealed greater than 10% GFP positive cells, the cells were plated in hygromycin-containing media (140µg/ml) for 10-14 days until colonies were visible. For each independent electroporation, 4-6 clones were picked and expanded for functional knockdown analyses and mice production.

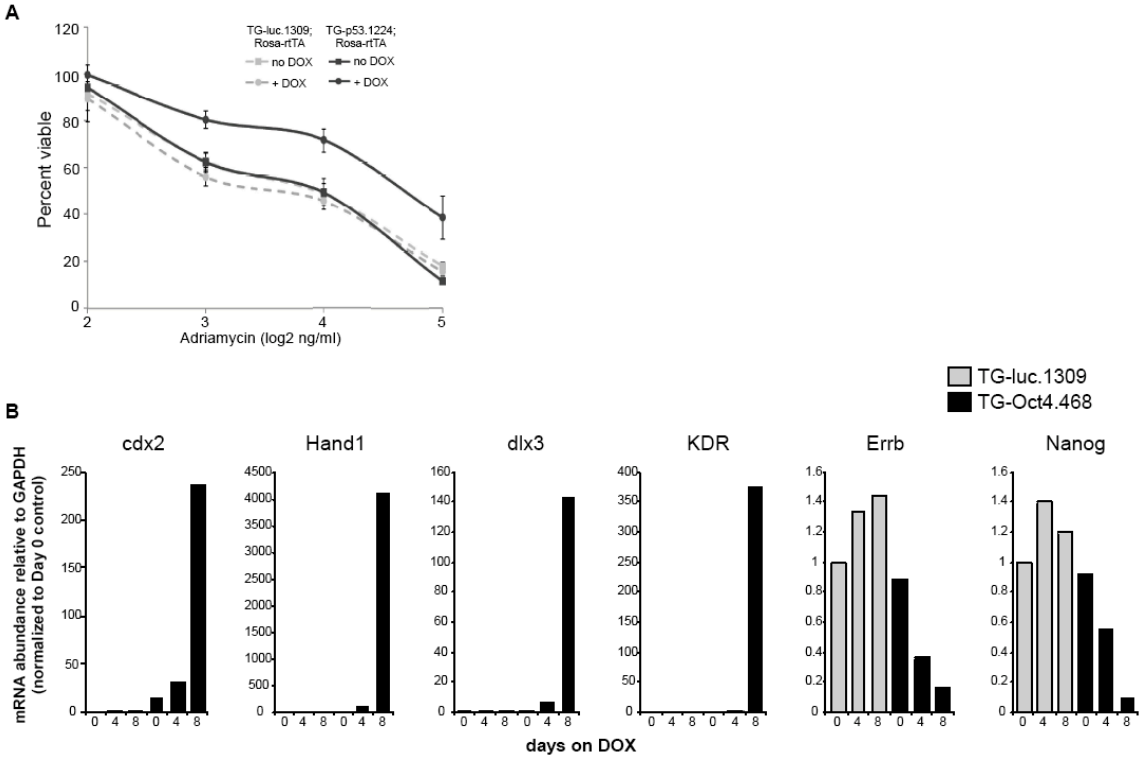

Supplementary Figure 3.4 | DOX-induced gene repression causes phenotypic changes ES cell clones. *A,* DOX-treated TG-p53.1224;Rosa-rtTA ES cells exhibit impaired DNA damage response. Rosa-rtTA ES cells with either TG-p53.1224 or TG-luc.1309 were pre-treated with or without DOX for 4 days, then subjected to various concentrations of Adriamycin (0.4-256 ng/ml). Cell viability was assessed 18hr post Adriamycin treatment by propridium iodide staining and FACs analysis. *B,* DOX-induced repression of *Pou5f1* in TG-Oct.678;Rosa-rtTA ES cells promotes differentiation toward trophoectoderm. Quantitative real-time PCR analysis of markers of trophoectoderm (cdx2, Hand1, dlx3 KDR) and embryonic stem cells (Errb and Nanog) reveal a shift in cell type.

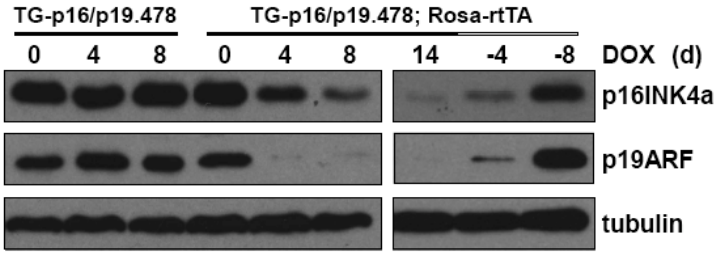

Supplementary Figure 3.5 | Reversible knockdown of gene targets in primary mouse embryonic fibroblasts derived from *ColA1*-TGM ES-cell derived mice. Western blot analysis of MEFs harvested from a cross between C57BL/6 WT mice and TG-p16/p19.478;Rosa-rtTA founder mice. Time course were performed on MEFs cultured in DOX-containing media then shifted to normal media.

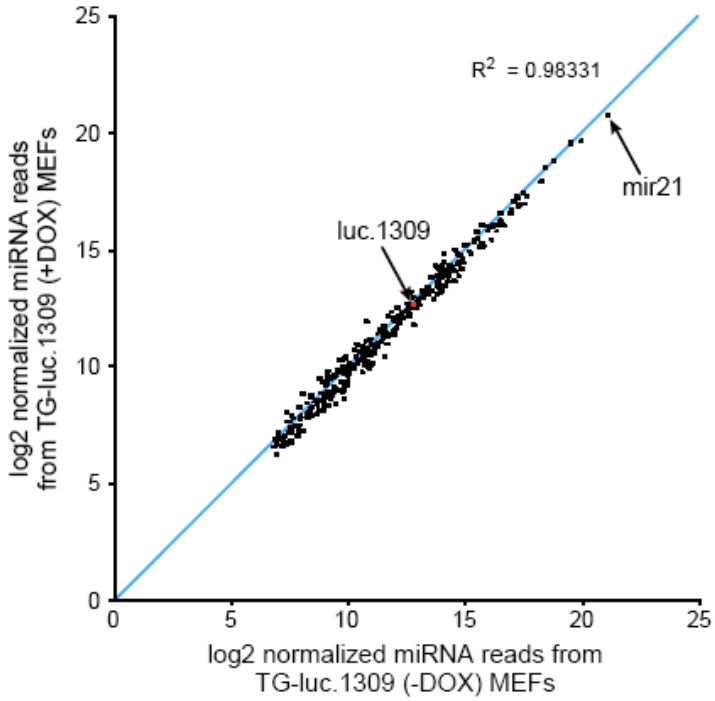

Supplementary Figure 3.6 | Induction of shRNA-miR does not affect endogenous miRNA processing. Scatter plot representing normalized abundance of 319 expressed miRNAs from DOX-treated and untreated TG-luc.1309 MEFs.

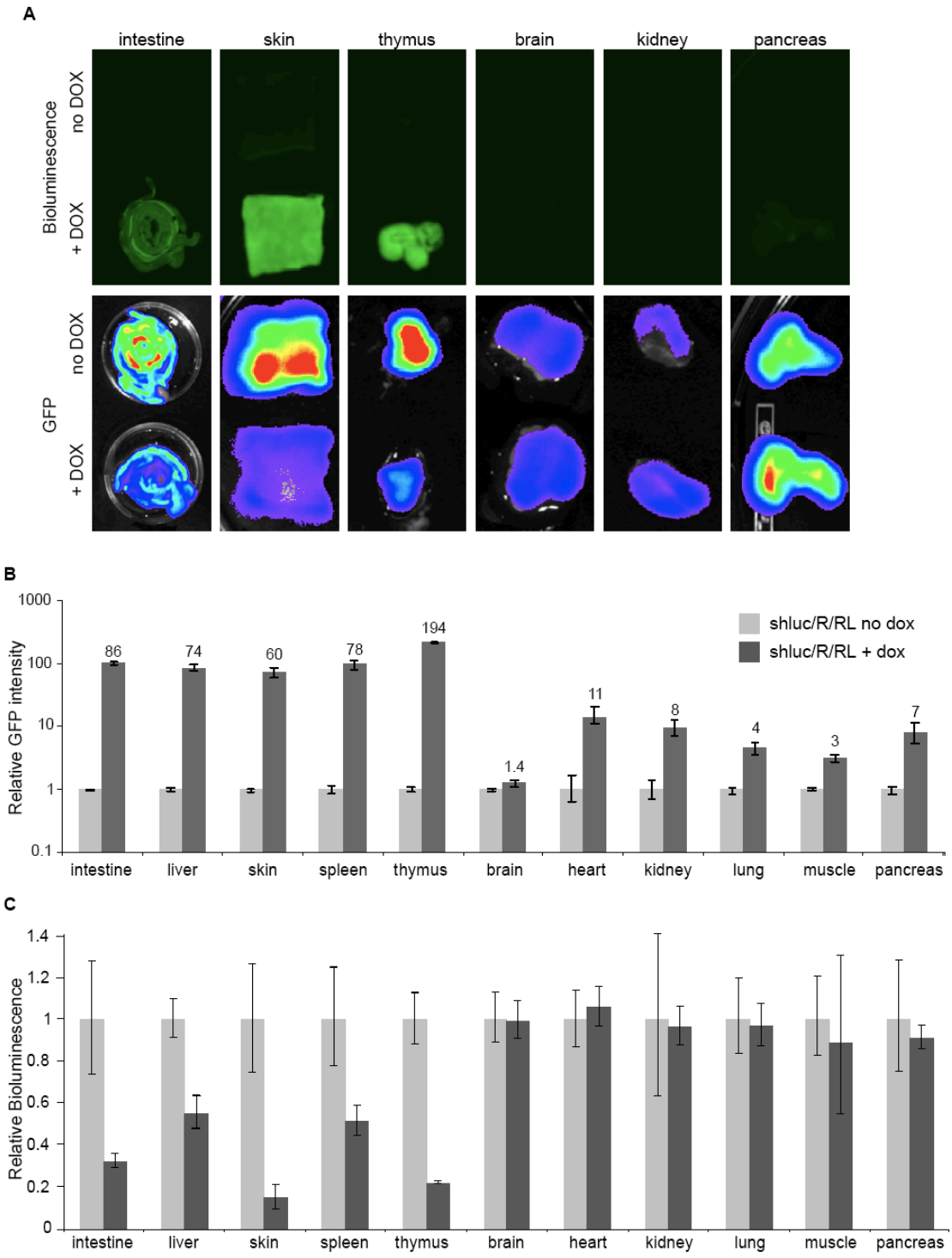

Supplementary Figure 3.7 | DOX-dependent knockdown in GFP-marked organs of Rosa-rtTA mice. *A,* Representative GFP and bioluminescent images of organs harvested from untreated and DOX-treated shluc/R/RL mice. *B,* Relative GFP intensity and C, bioluminescence quantification with standard error (n=3) between organs harvested from untreated and DOX-treated mice.

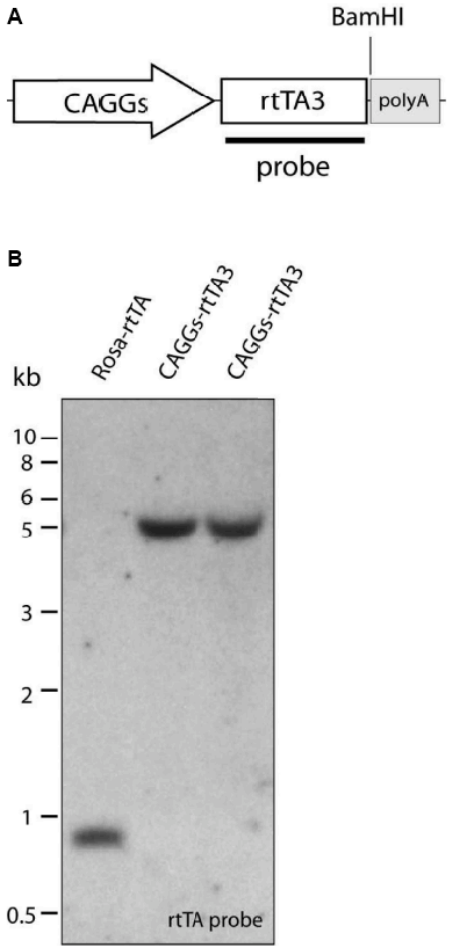

Supplementary Figure 3.8 | Generation of CAG-rtTA3 mice. *A,* Schematic of CAGGs-rtTA3 construct injected into fertilized zygotes to produce founder animals. *B* Southern blot of genomic DNA digested with BamHI from Rosa-rtTA (control) and two representative F2 generation CAGGs-rtTA3 mice indicating a single genomic integration of CAGGs-rtTA3.

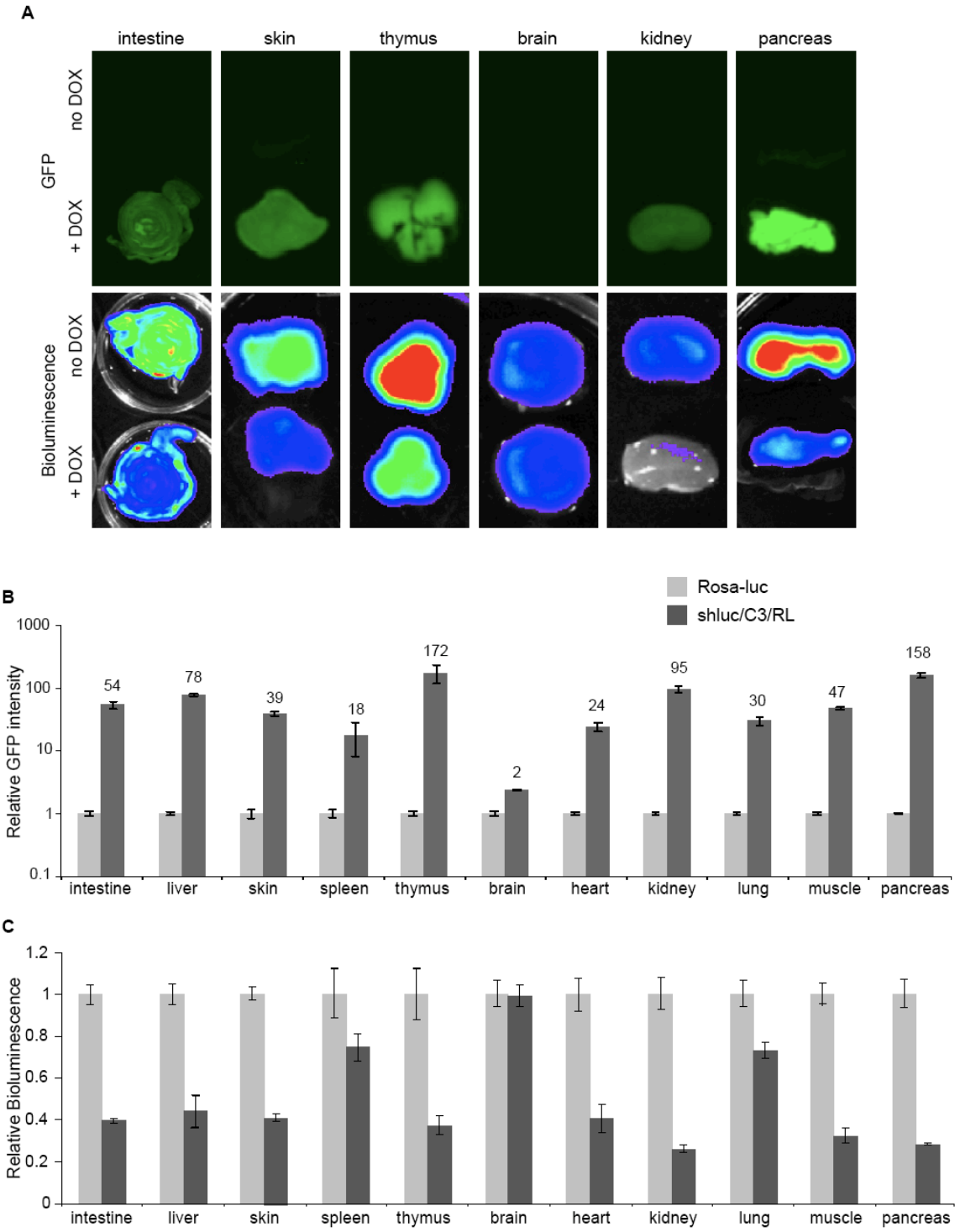

Supplementary Figure 3.9 | DOX-dependent knockdown in GFP-marked organs of CAG-rtTA3 mice. *A,*Representative GFP and bioluminescent images of organs harvested from untreated and DOX-treated shluc/C3/RL mice. *B,* Relative GFP intensity and *C,* bioluminescence quantification with standard deviation (n=2) between organs harvested from untreated and DOX-treated mice.

3.4 References

Beard, C., Hochedlinger, K., Plath, K., Wutz, A., and Jaenisch, R. (2006). Efficient method to generate single-copy transgenic mice by site-specific integration in embryonic stem cells. Genesis *44*, 23-28.

Buchholz, F., Angrand, P.O., and Stewart, A.F. (1998). Improved properties of FLP recombinase evolved by cycling mutagenesis. Nat Biotechnol *16*, 657-662.

Capecchi, M.R. (2005). Gene targeting in mice: functional analysis of the mammalian genome for the twenty-first century. Nat Rev Genet *6*, 507-512.

Castilho, R.M., Squarize, C.H., Chodosh, L.A., Williams, B.O., and Gutkind, J.S. (2009). mTOR mediates Wnt-induced epidermal stem cell exhaustion and aging. Cell Stem Cell *5*, 279-289.

Damalas, A., Kahan, S., Shtutman, M., Ben-Ze'ev, A., and Oren, M. (2001). Deregulated beta-catenin induces a p53- and ARF-dependent growth arrest and cooperates with Ras in transformation. EMBO J *20*, 4912-4922.

Dickins, R.A., Hemann, M.T., Zilfou, J.T., Simpson, D.R., Ibarra, I., Hannon, G.J., and Lowe, S.W. (2005). Probing tumor phenotypes using stable and regulated synthetic microRNA precursors. Nat Genet *37*, 1289-1295.

Dickins, R.A., McJunkin, K., Hernando, E., Premsrirut, P.K., Krizhanovsky, V., Burgess, D.J., Kim, S.Y., Cordon-Cardo, C., Zender, L., Hannon, G.J.*, et al.* (2007). Tissue-specific and reversible RNA interference in transgenic mice. Nat Genet *39*, 914-921.

Fedoriw, A.M., Stein, P., Svoboda, P., Schultz, R.M., and Bartolomei, M.S. (2004). Transgenic RNAi reveals essential function for CTCF in H19 gene imprinting. Science *303*, 238-240.

Furth, P.A., St Onge, L., Boger, H., Gruss, P., Gossen, M., Kistner, A., Bujard, H., and Hennighausen, L. (1994). Temporal control of gene expression in transgenic mice by a tetracycline-responsive promoter. Proc Natl Acad Sci U S A *91*, 9302-9306.

Grimm, D., Streetz, K.L., Jopling, C.L., Storm, T.A., Pandey, K., Davis, C.R., Marion, P., Salazar, F., and Kay, M.A. (2006). Fatality in mice due to oversaturation of cellular microRNA/short hairpin RNA pathways. Nature *441*, 537-541.

Hasuwa, H., Kaseda, K., Einarsdottir, T., and Okabe, M. (2002). Small interfering RNA and gene silencing in transgenic mice and rats. FEBS Lett *532*, 227-230.

He, L., and Hannon, G.J. (2004). MicroRNAs: small RNAs with a big role in gene regulation. Nat Rev Genet *5*, 522-531.

Hitz, C., Steuber-Buchberger, P., Delic, S., Wurst, W., and Kuhn, R. (2009). Generation of shRNA transgenic mice. Methods Mol Biol *530*, 101-129.

Hitz, C., Wurst, W., and Kuhn, R. (2007). Conditional brain-specific knockdown of MAPK using Cre/loxP regulated RNA interference. Nucleic Acids Res *35*, e90.

Hong, Y., and Stambrook, P.J. (2004). Restoration of an absent G1 arrest and protection from apoptosis in embryonic stem cells after ionizing radiation. Proc Natl Acad Sci U S A *101*, 14443-14448.

Kim, W.I., Wiesner, S.M., and Largaespada, D.A. (2007). Vav promoter-tTA conditional transgene expression system for hematopoietic cells drives high level expression in developing B and T cells. Exp Hematol *35*, 1231-1239.

Kuraguchi, M., Wang, X.P., Bronson, R.T., Rothenberg, R., Ohene-Baah, N.Y., Lund, J.J., Kucherlapati, M., Maas, R.L., and Kucherlapati, R. (2006). Adenomatous polyposis coli (APC) is required for normal development of skin and thymus. PLoS Genet *2*, e146.

Lickert, H., Cox, B., Wehrle, C., Taketo, M.M., Kemler, R., and Rossant, J. (2005). Dissecting Wnt/beta-catenin signaling during gastrulation using RNA interference in mouse embryos. Development *132*, 2599-2609.

Malone, C.D., Brennecke, J., Dus, M., Stark, A., McCombie, W.R., Sachidanandam, R., and Hannon, G.J. (2009). Specialized piRNA pathways act in germline and somatic tissues of the Drosophila ovary. Cell *137*, 522-535.

Moser, A.R., Pitot, H.C., and Dove, W.F. (1990). A dominant mutation that predisposes to multiple intestinal neoplasia in the mouse. Science *247*, 322-324.

Niwa, H., Miyazaki, J., and Smith, A.G. (2000). Quantitative expression of Oct-3/4 defines differentiation, dedifferentiation or self-renewal of ES cells. Nat Genet *24*, 372-376.

Niwa, H., Yamamura, K., and Miyazaki, J. (1991). Efficient selection for high-expression transfectants with a novel eukaryotic vector. Gene *108*, 193-199.

Nyabi, O., Naessens, M., Haigh, K., Gembarska, A., Goossens, S., Maetens, M., De Clercq, S., Drogat, B., Haenebalcke, L., Bartunkova, S.*, et al.* (2009). Efficient mouse transgenesis using Gateway-compatible ROSA26 locus targeting vectors and F1 hybrid ES cells. Nucleic Acids Res *37*, e55.

Olson, A., Sheth, N., Lee, J.S., Hannon, G., and Sachidanandam, R. (2006). RNAi Codex: a portal/database for short-hairpin RNA (shRNA) gene-silencing constructs. Nucleic Acids Res *34*, D153-157.

Paddison, P.J., Silva, J.M., Conklin, D.S., Schlabach, M., Li, M., Aruleba, S., Balija, V., O'Shaughnessy, A., Gnoj, L., Scobie, K.*, et al.* (2004). A resource for large-scale RNA-interference-based screens in mammals. Nature *428*, 427-431.

Rubinson, D.A., Dillon, C.P., Kwiatkowski, A.V., Sievers, C., Yang, L., Kopinja, J., Rooney, D.L., Zhang, M., Ihrig, M.M., McManus, M.T.*, et al.* (2003). A lentivirus-based system to functionally silence genes in primary mammalian cells, stem cells and transgenic mice by RNA interference. Nat Genet *33*, 401-406.

Sadate-Ngatchou, P.I., Payne, C.J., Dearth, A.T., and Braun, R.E. (2008). Cre recombinase activity specific to postnatal, premeiotic male germ cells in transgenic mice. Genesis *46*, 738-742.

Safran, M., Kim, W.Y., Kung, A.L., Horner, J.W., DePinho, R.A., and Kaelin, W.G., Jr. (2003). Mouse reporter strain for noninvasive bioluminescent imaging of cells that have undergone Cre-mediated recombination. Mol Imaging *2*, 297-302.

Schmitt, C.A., Fridman, J.S., Yang, M., Baranov, E., Hoffman, R.M., and Lowe, S.W. (2002). Dissecting p53 tumor suppressor functions in vivo. Cancer Cell *1*, 289-298.

Schuster-Gossler, K., Lee, A.W., Lerner, C.P., Parker, H.J., Dyer, V.W., Scott, V.E., Gossler, A., and Conover, J.C. (2001). Use of coisogenic host blastocysts for efficient establishment of germline chimeras with C57BL/6J ES cell lines. Biotechniques *31*, 1022-1024, 1026.

Seibler, J., Kleinridders, A., Kuter-Luks, B., Niehaves, S., Bruning, J.C., and Schwenk, F. (2007). Reversible gene knockdown in mice using a tight, inducible shRNA expression system. Nucleic Acids Res *35*, e54.

Seibler, J., Kuter-Luks, B., Kern, H., Streu, S., Plum, L., Mauer, J., Kuhn, R., Bruning, J.C., and Schwenk, F. (2005). Single copy shRNA configuration for ubiquitous gene knockdown in mice. Nucleic Acids Res *33*, e67.

Seidler, B., Schmidt, A., Mayr, U., Nakhai, H., Schmid, R.M., Schneider, G., and Saur, D. (2008). A Cre-loxP-based mouse model for conditional somatic gene expression and knockdown in vivo by using avian retroviral vectors. Proc Natl Acad Sci U S A *105*, 10137-10142.

Silva, J.M., Li, M.Z., Chang, K., Ge, W., Golding, M.C., Rickles, R.J., Siolas, D., Hu, G., Paddison, P.J., Schlabach, M.R.*, et al.* (2005). Second-generation shRNA libraries covering the mouse and human genomes. Nat Genet *37*, 1281-1288.

Soriano, P. (1999). Generalized lacZ expression with the ROSA26 Cre reporter strain. Nat Genet *21*, 70-71.

Srinivas, S., Watanabe, T., Lin, C.S., William, C.M., Tanabe, Y., Jessell, T.M., and Costantini, F. (2001). Cre reporter strains produced by targeted insertion of EYFP and ECFP into the ROSA26 locus. BMC Dev Biol *1*, 4.

Stegmeier, F., Hu, G., Rickles, R.J., Hannon, G.J., and Elledge, S.J. (2005). A lentiviral microRNA-based system for single-copy polymerase II-regulated RNA interference in mammalian cells. Proc Natl Acad Sci U S A *102*, 13212-13217.

Stein, P., Svoboda, P., and Schultz, R.M. (2003). Transgenic RNAi in mouse oocytes: a simple and fast approach to study gene function. Dev Biol *256*, 187-193.

Tichelaar, J.W., Lu, W., and Whitsett, J.A. (2000). Conditional expression of fibroblast growth factor-7 in the developing and mature lung. J Biol Chem *275*, 11858-11864.

Van Mater, D., Kolligs, F.T., Dlugosz, A.A., and Fearon, E.R. (2003). Transient activation of beta -catenin signaling in cutaneous keratinocytes is sufficient to trigger the active growth phase of the hair cycle in mice. Genes Dev *17*, 1219-1224.

Ventura, A., Meissner, A., Dillon, C.P., McManus, M., Sharp, P.A., Van Parijs, L., Jaenisch, R., and Jacks, T. (2004). Cre-lox-regulated conditional RNA interference from transgenes. Proc Natl Acad Sci U S A *101*, 10380-10385.

Wang, J., Theunissen, T.W., and Orkin, S.H. (2007). Site-directed, virus-free, and inducible RNAi in embryonic stem cells. Proc Natl Acad Sci U S A *104*, 20850-20855.

3.5 Author contributions

R.D. designed the TMP vector and first generation RNAi mouse models. S.Y.K. performed pronuclear injections and tetraploid embryo complementation for all transgenics. P.K.P andJ.Z. designed the TGM vector. P.K.P. designed pColTGM targeting vector and conducted all ES targeting and experiments (Fig. 3.1-3.4; Supplementary Fig. 3.1, 3.3-3.9). Luke Dow (L.E.D) conducted experiments Fig. 3.1E, 3.2G, 3.5; Supplementary Fig. 3.2, 3.4B, 3.8-3.9). Colin Malone (C.M.) helped with Fig 3.3 data analysis. J.S., Danielle Grace (D.G.) and Jaqueline Cappellani (J.C.) tailed, weaned and cared for the animal colonies.

Chapter 4

Modeling Lung Adenocarcinoma using RNAi Mice

4.1 Introduction

Lung cancer is the leading cause of cancer deaths in the US, with an estimated 160,000 people projected to die of the disease each year (Jemal et al., 2005). Despite our increased knowledge on cancer biology, advances in cytotoxic drug development, radiotherapy and patient management, the cure rate remains dismal, as the 5-year survival rate has only improved marginally, from 7% to 14% since 1970. Non-small-cell lung cancer (NSCLC) accounts for 85% of all lung cancer cases, with adenocarcinoma being the predominant subtype now accounting for >40% of all lung cancer cases (Herbst et al., 2008). Analysis of resected tumors has identified several frequent molecular changes (Forgacs et al., 2001). Recent data report that activating mutations of the *KRas* oncogene are limited to NSCLC and found in ~10-30% of cases (Miller et al., 2008). Inactivating mutations of the tumor suppressor gene (TSG), *Trp53,* are even more frequent, occurring in roughly 50% of patients (Herbst et al., 2008). Other common inactivating mutations, often due to promoter hypermethylation, involve the *INK4a/ARF* locus, which encodes both the $p16^{INK4a}$ (Ink4a) and $p19^{ARF}$ (ARF) tumor suppressor proteins. Individually, p16 inactivation is seen in nearly 40-50% of NSCLC cases while ARF suppression occurs less frequently in NSCLC (~20%) but more commonly in small-cell lung cancer (SCLC; ~60%) (Jackson et al., 2001).

The proposed precursor cells of peripheral lung adenocarcinomas include metaplastic mucin-producing cells, type II alveolar cells and Clara cells, whose

major product is the Clara cell specific protein (CCSP or CC10) (Greenberg et al., 1987). For specific gene expression in respiratory epithelial cells, transgenic mice expressing a reverse tet-transactivator (rtTA) protein under control of regulatory elements from the rat CCSP gene were generated (Tichelaar et al., 2000) and used to build binary tet-inducible mice in which oncogene expression could be regulated temporally in the lung (Fisher et al., 2001; Politi et al., 2006). Surprisingly, in these mice, the rCCSP promoter drives rtTA expression not only in Clara cells, which are nonciliated bronchiolar epithelial cells, but also in type II alveolar epithelial cells, which may be due to species differences or positional effects that influence transcriptional activity of the exogenous rCCSP promoter (Tichelaar et al., 2000).

Several inducible mouse models of lung cancer have characterized the dependence of lung adenocarcinomas on oncogenic FGF-7, EGFR and *Kras*, demonstrating tumor regression after inhibition of the initiating oncogenic stimulus (Fisher et al., 2001). These studies highlight the potential therapeutic benefits of oncogene inhibition in patients with NSCLC and in fact, treatment with erlotinib, an EGFR inhibitor, has proved successful in many patients with EGFR mutations (Neal and Sequist; Shepherd, 2005; Shepherd et al., 2005). Unfortunately, no targeted therapies that specifically inhibit *Kras* mutants have been approved for clinical use in patients. Currently, only one targeted therapy against mutant *Kras*, salirasib (farnesylthiosalicylic acid), has shown success in a xenograft model of human lung cancer (Zundelevich et al., 2007) and is currently in Phase I/II clinical trials. Because of this, lung cancer patients with *Kras*

mutations have relied primarily on standard cytotoxic therapies. For these patients, it will be beneficial to identify other potential gene targets whose inhibition will interfere with growth in *Kras*-driven lung adenocarcinomas. A better understanding of the roles of TSGs and whether their inactivation is critical for tumor maintenance will help guide the development of new generation therapeutics.

To examine the mechanisms of TSGs and their role in tumor maintenance in the presence of oncogenic *Kras*, we make use of the CCSP-rtTA transgenic mice and tet-regulated shRNA mice (Chapter 3) to achieve TSG suppression specifically in lung epithelial cells. To establish $Kras^{G12D}$-driven lung adenocarcinomas, binary tet-inducible shRNA mice are further crossed to *LSL*-$Kras^{G12D}$ animals to generate compound transgenic alleles. We report the development of lung adenocarcinomas in these compound transgenic mice following treatment with intranasal Adeno-Cre and TSG suppression by DOX administration. Furthermore, these lung adenocarcinomas were indistinguishable from previous mouse models of lung adenocarcinoma that utilized knockout alleles.

Owing to the slow rate and high expense of generating multi-allelic transgenic mice, we later devised a strategy to re-derive ES cell lines harboring all relevant alleles for the production of lung adenocarcinomas. These ES cells were subsequently used to produce large cohorts of mosaic mice with lung adenocarcinomas, which allowed us to examine the response to reactivation of $p16^{INK4a}$/Arf or p53 in the context of mutant *Kras*. We report distinct response

patterns upon TSG restoration: p53 restoration resulted in only a marginal survival benefit while *INK4a/ARF* restoration caused rapid but unsustainable tumor regression. We further examined the molecular characteristics of each regression pattern and propose mechanistic cooperative differences between *Trp53* or *INK4a/ARF* and mutant *Kras* that are responsible for the differential outcomes.

4.2 Results

4.2.1 Establishing the lung adenocarcinoma model

To generate mice in which we could regulate expression of specific TSGs, we took advantage of the previously described tet-inducible RNAi mice harboring single copy shRNAs downstream of the *ColA1* locus targeting either *INK4a/ARF* or *Trp53* (referred to as TG-p16/p19.478 or TG-p53.1224 respectively) (Chapter 3; Premsrirut et al., submitted). For control, RNAi mice harboring an shRNA targeting the firefly *luciferase* gene (referred to as TG-luc.1309) was used. To achieve tissue-specific control of shRNA expression, TG-p16/p19.478, TG-p53.1224 and TG-luc.1309 mice were crossed to a line of transgenic mice (*CCSP*-rtTA mice, referred to as *R*; refer to Table 4.1 for detailed nomenclature) that restricted expression of the reverse tetracycline transactivator protein (rtTA) to epithelial cells of the lung (Tichelaar et al., 2000). To discern relationships among pulmonary tumor suppressor mechanisms, the bitransgenic progeny were

intercrossed to a conditionally activatable *Lox-Stop-Lox Kras*^{G12D} (hereafter called *Kras* or *K*) mouse strain (Jackson et al., 2001) to attain triple transgenics (Fig. 4.1;Table 4.1). The resulting triple transgenics (*p53RK*, *p16/p19RK, lucRK*; refer to Table 4.1 for nomenclature) cohorts were of mixed background and caution was warranted in comparing these cohorts; hence littermate controls were used for comparison. Mice were inoculated with adenoviral Cre recombinase (adeno-Cre) by inhalation to promote *Kras* expression in a small percentage of pulmonary cells (Jackson et al., 2001) and simultaneously started on a doxycycline-containing diet to induce shRNA expression in lung epithelial cells.

To determine whether we could noninvasively monitor and quantify lung tumor progression in triple transgenic animals, we applied positron emission tomography that had been specifically tailored for imaging of small animals (microPET) (Fig. 4.2A) as previously described using ^{18}F-FDG (radioactive fluorodeoxyglucose) (Woo et al., 2008). This approach, which is commonly used in the clinics, would allow visualization and quantification of tumor burden longitudinally in the same animal (Woo et al., 2008). Additionally, it may allow tracking of metastatic disease (Woo et al., 2008). These efforts proved unsuccessful, as microPET failed to clearly distinguish large lung tumors that were unmistakably noted when the lungs were removed and examined *ex vivo* (Fig 4.2A,B; data not shown). Rather, high uptake of ^{18}F-FDG was observed in the thoracic region representing the heart, which made it difficult to identify lung tumors within the region. ^{18}F-FDG biodistribution in normal mice and tumor-

bearing mice is known to be affected by various experimental animal conditions: feeding, environment temperature, anesthesia and so on (Woo et al., 2008), which further complicates interpretation of the data. Additionally, *ex vivo* measurements of harvested organs failed to detect increased ^{18}F-FDG uptake in the lung tissue (Fig. 4.2C).

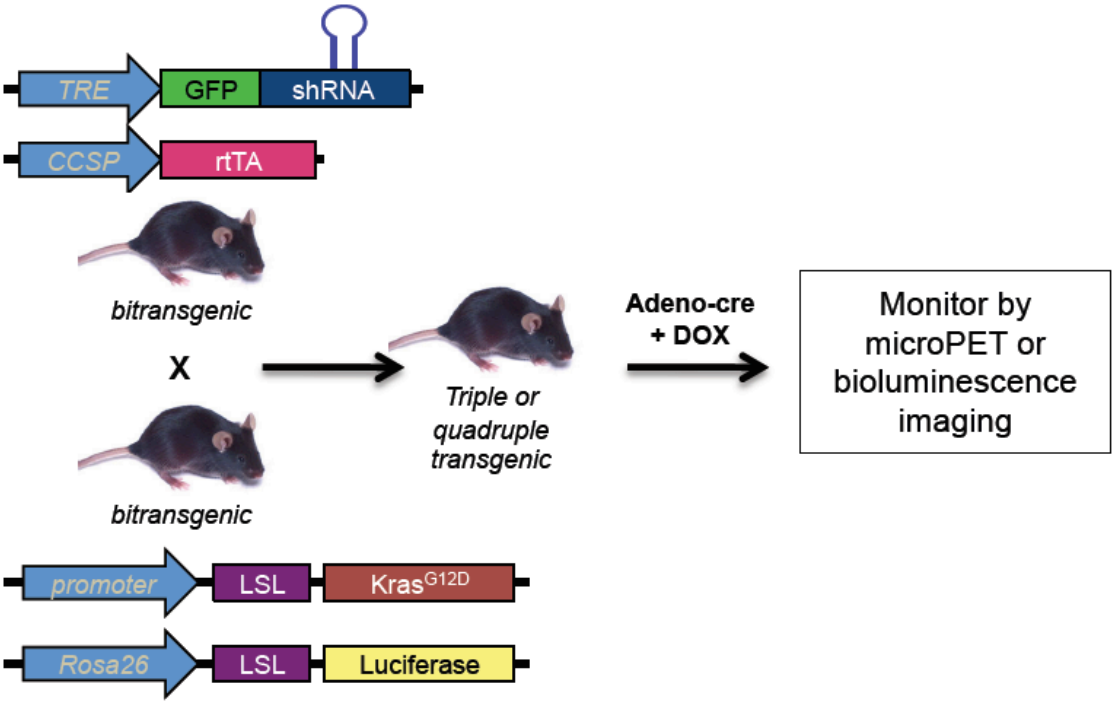

Figure 4.1 | Multi transgenic-allelic crosses for generation of an RNAi-mediated lung adenocarcinoma model. Schematic representation of transgenic alleles crossed to produce either triple transgenic mice carrying 1) a tet-inducible GFP-marked shRNA-mir (*ColA1*-TRE-GFP-mir30), 2) CCSP-rtTA (clara cell secretory protein) and 3) LSL-Kras^{G12D} or quadruple transgenics bearing the additional *Rosa26-LSL-luciferase*. Mice were infected with adeno-cre via nasal inhalation and treated with dox in their food pellets at 4-6 wk of age. Triple transgenic tumor-bearing mice were examined noninvasively by microPET imaging. Quadruple transgenic mice were monitored by bioluminescence signal.

Table 4.1 | Mouse nomenclature. Initial crosses lacked the LSL-luciferase transgene.

Strain name	Alleles
KL	LSL-Kras^{G12D}/LSL-luc
RKL	CCSP-rtTA/LSL-Kras^{G12D}/ LSL-luc
p16/p19RKL	TG-p16/p19.478; CCSP-rtTA/LSL-Kras^{G12D}/LSL-luc
p53RKL	TG-p53.1224/CCSP-rtTA/ LSL-Kras^{G12D}/LSL-luc
lucRK	TG-luc.1309/CCSP-rtTA/ LSL-Kras^{G12D}
renRKL	TG-ren.713/CCSP-rtTA/LSL-Kras^{G12D}/LSL-luc

To incorporate a detectable marker within tumorigenic cells that permits serial, noninvasive imaging of animals, triple transgenics were intercrossed to a conditionally activatable *Rosa26-Lox-Stop-Lox luciferase* reporter strain (LSL-luc, or *L*) (Safran et al., 2003). TG-luc.1309 control animals were replaced with TG-ren.713 (harboring shRen.713 targeting renilla *luciferase*) to avoid downregulation of the *luciferase* reporter by luc.1309. Additional littermate control strains included all mice carrying the *Kras* allele without an shRNA (*K, RK, KL,* and *RKL*). Tumor latency and histopathology for these four control genotypes as well as *lucRK, renRK* and *renRKL* animals was similar whether with DOX or untreated; therefore, for simplicity, these mice were grouped together for analyses and hereafter referred to as *Kras* only. Additionally, triple transgenics without the *luciferase* reporter showed no variance from quadruple transgenics

and were used when bioluminescence imaging was not required.

4.2.2 TSG inhibition by RNAi cooperates with *Kras^{G12D}*

Compound mutant strains carrying either p53$^{flox/flox}$ or p16^{INK4a}/Arf$^{-/-}$ alleles and *LSL-Kras^{G12D}* have previously been used to show potent or modest cooperation with oncogenic *Kras* and p53 or p16$^{INK4a/}$p19^{ARF} loss respectively, in lung tumorigenesis (Ji et al., 2007). Similarly, using mice with DOX-inducible shRNAs targeting p53 or p16$^{INK4a/}$p19^{ARF}, we have demonstrated *Kras* cooperation with suppression of either target gene (Fig. 4.3). Bioluminescence imaging revealed tumor onset as early as 4 or 6 weeks post infection (w.p.i). in *p53RKL* or *p16/p19RKL* animals respectively. By 8 weeks, *p53RKL* animals displayed a markedly increased tumor burden (Fig. 4.3A) and developed symptoms of disease, such as weight loss and rapid shallow breathing. In contrast, *p16/p19RKL* animals displayed only a moderate increase in tumor burden in comparison to *KL* controls at 8 w.p.i. (Fig. 4.3A). At this time point, macroscopic observations of lungs from animals with p53 suppression revealed high tumor multiplicity and an irregular surface; tumors were highly variable in size and marked by GFP expression (Fig. 4.3B). In contrary, p16$^{INK4a/}$p19^{ARF} suppression resulted in fewer and smaller GFP positive areas within the lung (Fig. 4.3B). Additionally, the surface of *p16/p19RKL* lungs was mostly smooth and comparable to lungs from *Kras* animals. By microscopic examination, multiple tumors were present in both *p53RK* and *p16/p19RK* lungs; *lucRK*

animals showed no tumor growth and only few regions with hyperplastic growth (Fig. 4.3C). *p16/p19RK* lungs contained numerous non-invasive adenomas and well-differentiated tumors; however, those with the *p53RK* genotype had highly dysplastic lesions containing features of poorly differentiated adenocarcinomas with large sheets of dysplastic cells, abnormal mitoses and multinucleate giant cells with pleomorphic chromatin patterns (Fig. 4.4). (Fig. 4.3C; Table 4.2).

To assess the extent of progression for each genotype at different time points following adeno-Cre inhalation, mice were euthanized and lungs were examined histologically and scored for tumor burden (Fig. 4.4; Fig.4.5A ;Table 4.2). Tumors were graded in a blinded manner by pathologist Dr. Ken Shroyer (Stony Brook University) on a scale of 1-3 with grade 3 indicating the most advanced tumor phenotype. The criteria for each grade were as follows: Grade 1 tumors were comprised of well-differentiated cells having uniform nuclei and no signs of invasion. Grade 2 tumors had moderately differentiated cell types with uniform but slightly enlarged nuclei showing prominent nucleoli and still show minimal invasiveness. Grade 3 tumors had poorly-differentiated cells with large, pleomorphic nuclei exhibiting a high degree of nuclear atypia, including abnormal mitoses and hyperchromatism and contained multinucleate giant cells. Additionally, grade 3 tumors showed signs of invasion into surrounding regions.

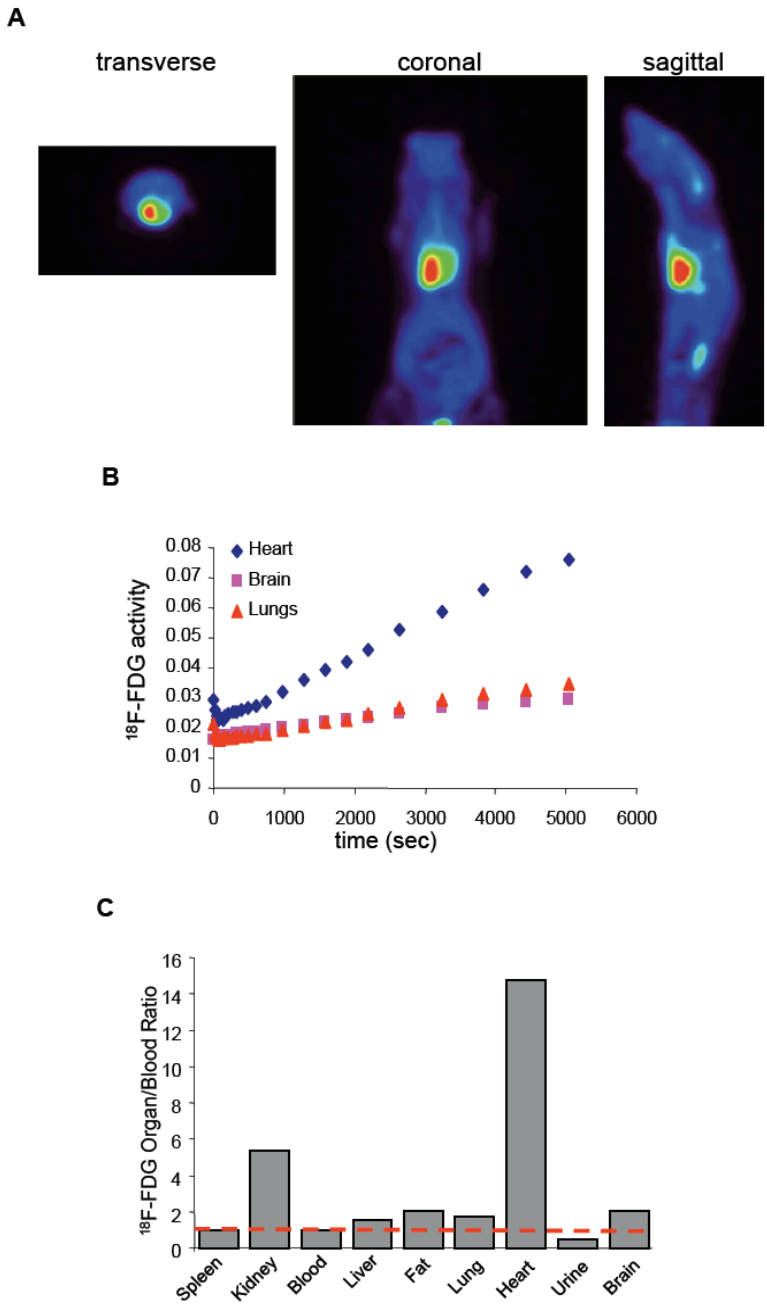

Figure 4.2 | MicroPET imaging analysis of tumor-burdened mice. *A,* MicroPET images of a *p16/p19RK* mouse 14 weeks post adeno-cre infection (w.p.i) following tail vein injection of 400μCu of ^{18}F-FDG (radioactive fluorodeoxyglucose). *B,* ^{18}F-FDG activity measured in select tissues over time. *C,* Global ^{18}F-FDG distribution to organs of *p16/p19RK* mouse from *A* measured ex vivo.

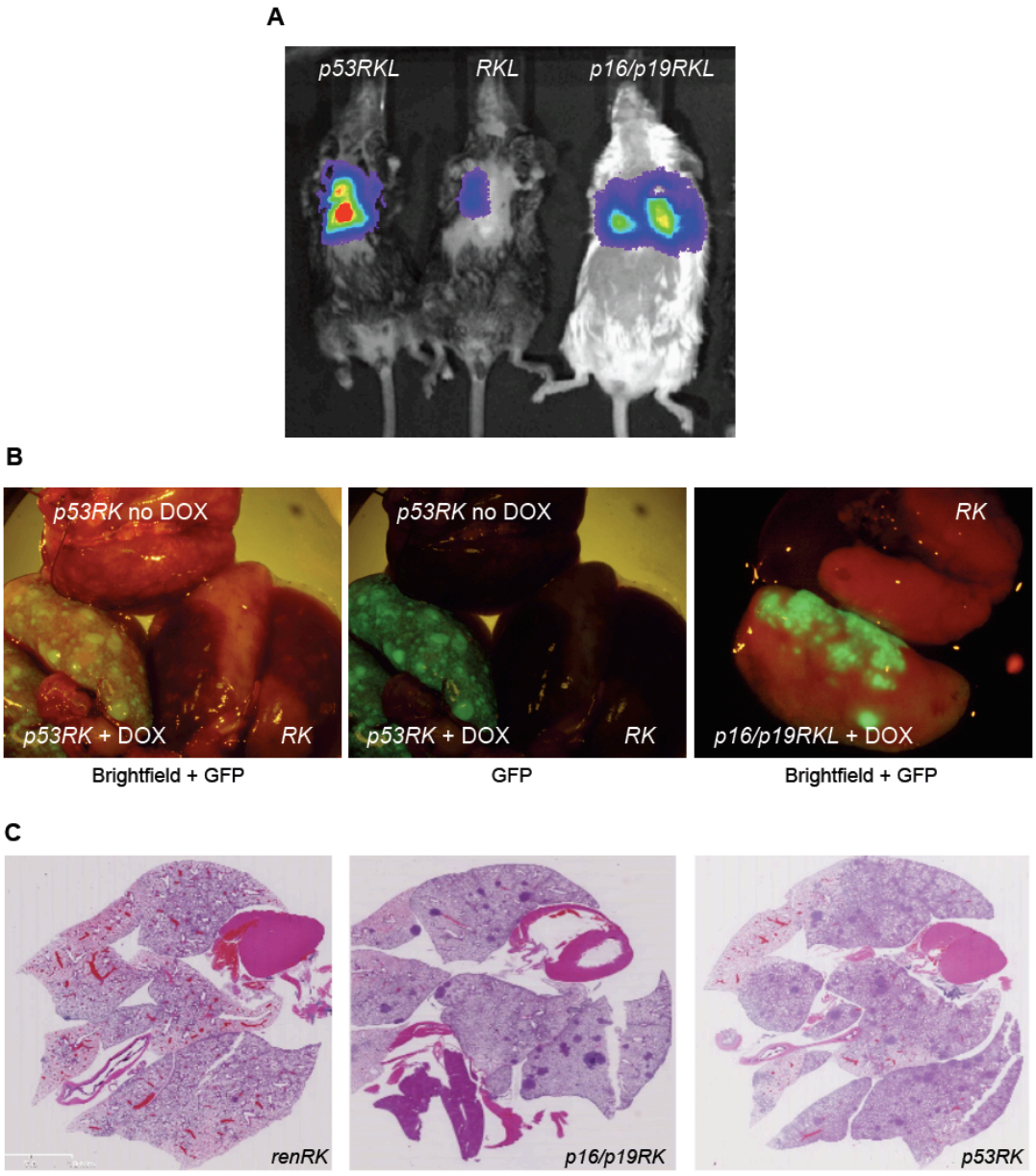

Figure 4.3 | CCSP-rtTA drives functional p16/p19.748 and p53.1224 expression to cooperate with Kras^{G12D} in lung tumorigenesis. *A,* Bioluminescence imaging of *p53RKL, RKL and p16/p19RKL* mice (left to right) 8 w.p.i and maintained on a DOX-diet. *B,* Macroscopic images of *RK*, *p53RK* and *p16/p19RK* lungs harvested at 8 weeks post adeno-cre. *C,* H&E stains of whole lung sections from quadruple transgenic mice 8 wk post adeno-cre.

Table 4.2 | Histopathological features of Kras^{G12D} driven lung adenocarcinomas. Lungs were grossly classified at 8-20 weeks post adeno-cre infection (w.p.i.) by features representing Grade 1 (well-differentiated), Grade 2 (moderately differentiated) and Grade 3 (poorly differentiated) murine lung tumors.

Genotype	8-10 w.p.i.	11-14 w.p.i.	16-20 w.p.i.
KL, RKL and Ren-RKL	Few non-invasive small focal adenomas	Infiltrative adenomas or Grade 1 adenocarcinomas	Grade 1-2, small areas with Grade 3 adenocarcinoma; minimally infiltrative
p16/p19RKL	Adenomas to Grade 1; non-infiltrative pattern	Grade 2-3 adenocarcinomas; mitotic activity visible	Grade 1, mostly Grade 2-3 adenocarcinoma
p53RKL	Grade 2-3 adenocarcinoma; poorly differentiated; grade III nuclei, pleomorphic chromatin pattern	Grade 3 adenocarcinomas; focally high grade nuclei; many multinucleated tumor cells	**Grade 3 adenocarcinoma; poorly differentiated with necrosis; acute and chronic inflammation visible

≥ 3 mice, 2 sections from each subject were examined at each time interval.
**only 2 mice survived to 16 w.p.i.

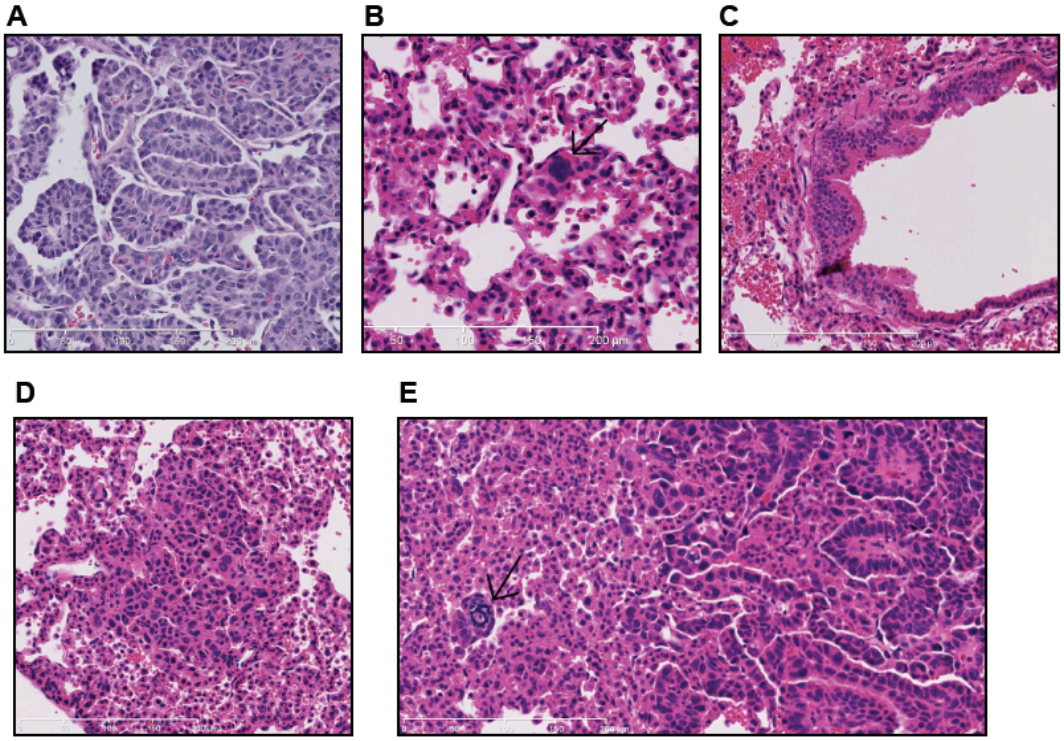

Figure 4.4 | *p53RKL* mice display features of high grade adenocarcinomas. *A,* Grade 1 lesions seen 6-8 w.p.i show well-differentiated cells with a glandular pattern. *B,* Grade 2 lesions have hyperplastic regions with multinucleated tumors cells (*arrow*), some irregular nuclei and *C,* hyperproliferative bronchiolar epithelium. *D,* Grade 3 lesions exhibit pleomorphic nuclei with prominent nucleoli and irregular borders. *E,* Advanced grade 3 lesions have multipleomorphic nucleated cells (*arrow*) with invasive borders.

Histopathological examination of tumor sections revealed that TSG knockdown by RNAi resulted in pulmonary neoplasias with features analogous to those seen in corresponding knockout models combined with $Kras^{G12D}$ activation (Fisher et al., 2001; Jackson et al., 2005; Ji et al., 2007). *p53RKL* animals showed striking similarities to previously characterized models, (Jackson et al., 2005; Ji et al., 2007) harboring lesions characteristic of high grade lung adenocarcinoma, including multinucleated cells with prominent nucleoli, invasive borders and areas with pleomorphic tumor cells (Table 4.2; Fig. 4.4). Furthermore, differences in survival rates were statistically significant between

cohorts (p<.0001). Median survival for *p53RK* animals was 11 weeks (*n=10*), compared to 20 weeks for *p16/p19RK* (*n=4*) or 23 weeks for *Kras* mice (*n=22*) (Fig. 4.5B,C), similar to previous reports (Ji et al., 2007). Triple transgenics that were treated with adeno-Cre but not with DOX treatment had survival rates similar to *Kras* controls (Fig. 4.5B,C), suggesting that shRNA expression was both rtTA and DOX-dependent and not leaky.

4.2.3 Tumor suppressor gene reactivation by conditional RNAi

To examine the effects of restoring TSG activity in established lung tumors, triple transgenic *p53RK* and *p16/p19RK* animals were withdrawn from DOX treatment when they displayed signs of disease at ~8 or 14-16 w.p.i. respectively. DOX removal did not affect the median survival of *p16/p19RK* animals (Fig. 4.5C) but gross macroscopic differences were apparent between lungs taken from animals that had been removed for 1 or 6 weeks from or maintained on DOX treatment (Fig. 4.6A). After ~30 days of DOX withdrawal, the lung surfaces appeared smooth and lacked both surface nodules and GFP expression. In contrast, animals kept on DOX had numerous large GFP positive tumors encompassing the entire surface of the lung (Fig. 4.6A). Histological analyses also showed striking differences: surprisingly, tumor multiplicity was similar in both cases but tumor morphology was distinct in each case. Tumors from animals with continuous $p16^{INK4a/}p19^{ARF}$ suppression were comprised of

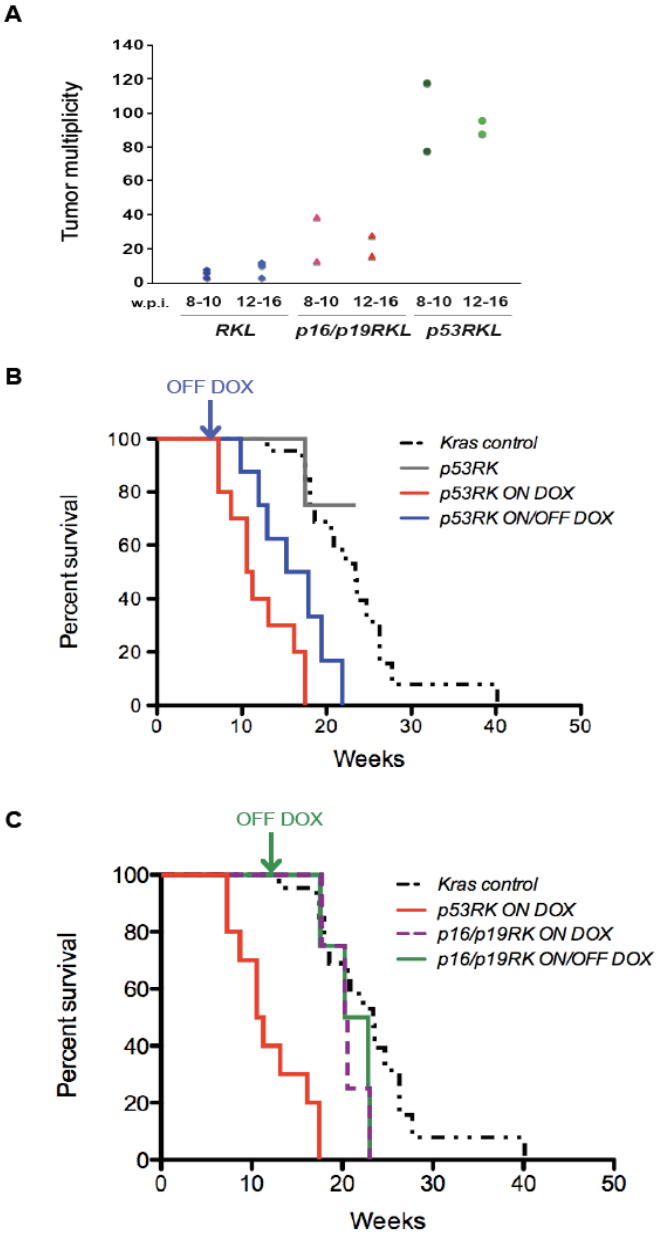

Figure 4.5 | *p16/p19RK* and *p53RK* mice display multifocal lesions and decreased survival. *A,* Quantification of lesions present in lungs of *p16/p19RK* and *p53RK* mice at various time points following adeno-cre and DOX treatment (*n=2*). For each mice, two cross-sections from each lung lobe was examined and scored for lesions that progressed beyond dysplastic hyperplasia. *B-C,* Kaplan-meier curves comparing survival of *p53RK, p16/p19RK and Kras* controls treated with adeno-cre and DOX. Median survival was 24 w.p.i for *Kras controls* (*n*=22), 11 w.p.i. for *p53RK* (*n=10*), 20 w.p.i. for *p16/p19RK* (*n=4*) mice (p<.0001). Median survival for *p53RK* treated with adeno-cre but not DOX but was similar to Kras control (*n=3*). *p53RK* mice removed from DOX treatment ~8 w.p.i. (*n=7)* and *p16/p19RK* mice removed from DOX ~14-16 w.p.i. (*n*=4) had a median survival of 16.6 and 21.6 weeks respectively.

moderately to poorly differentiated cells that were tightly compacted, whereas tumors from animals with restored $p16^{INK4a/}p19^{ARF}$ activity appeared less compact and more differentiated and glandular (Fig. 4.6B). Alveolar macrophage infiltration was noted within pockets of the tumors (Fig. 4.6B). While DOX withdrawal did not affect median survival of *p16/p19RK* animals, it prolonged the survival of *p53RK* animals by an average of 5.6 weeks. However, these animals still succumbed to disease substantially before *Kras* controls (~6 weeks), suggesting that p53 restoration was not sufficient to fully revert lung tumorigenesis to *Kras* control levels.

To observe the effects of p53 and $p16^{INK4a/}p19^{ARF}$ restoration at earlier time points, mice were monitored by bioluminescence imaging and then removed from DOX treatment at tumor onset, which was ~4-5 weeks for *p53RKL* animals and ~6-8 weeks for *p16/p19RKL* mice. Bioluminescence imaging showed rapid tumor regression in *p16/p19RKL* mice only 5 days following DOX removal (Fig. 4.7). Serial imaging revealed a continued decrease in bioluminescence levels that remained steady for an additional 3 weeks. However, ~4-5 weeks following DOX removal, *p16/p19RKL* mice relapsed with an even more accelerated disease than that observed in *Kras* controls (Fig. 4.7). Macroscopically, the lungs were mostly smooth with a few small GFP positive nodules in comparison to

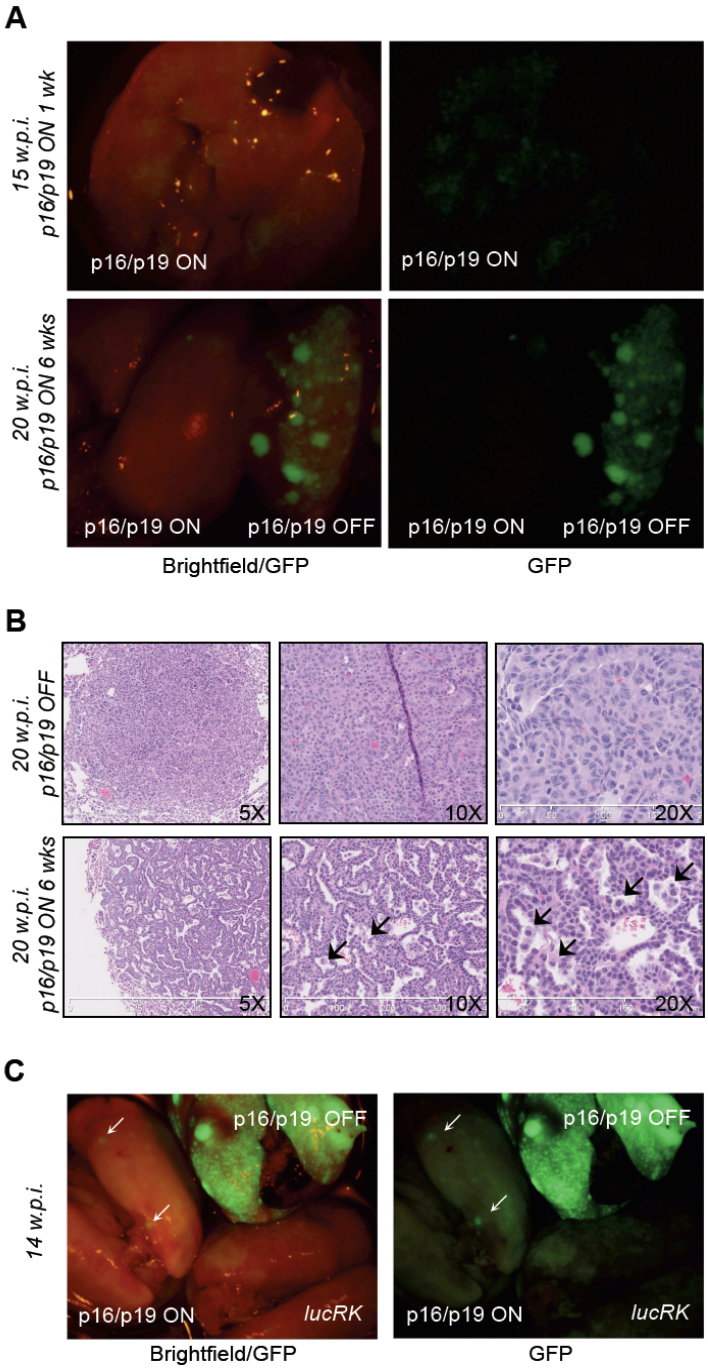

Figure 4.6 | p16^{INK4a}/p19^{ARF} restoration induces tumor morphology alterations both macro- and microscopically. *A,* Brightfield and GFP images of whole lungs from *p16/p19RK* mice after 1 week (*top*) or 6 weeks (*bottom*) following DOX removal. *B,* H & E stains of lung sections from mice 20 w.p.i either on DOX (*top*) or off DOX for 6 weeks (*bottom*). Alveolar macrophages were noted between the tumor cells (*arrows*) (*B*). *C*, Brightfield and GFP images of lungs 14 w.p.i. from *p16/p19RKL* and *lucRK* animals maintained on DOX (*top, bottom right*) and *p16/p19RKL* removed from DOX for 6 weeks (from Fig. 4.6; bottom left).

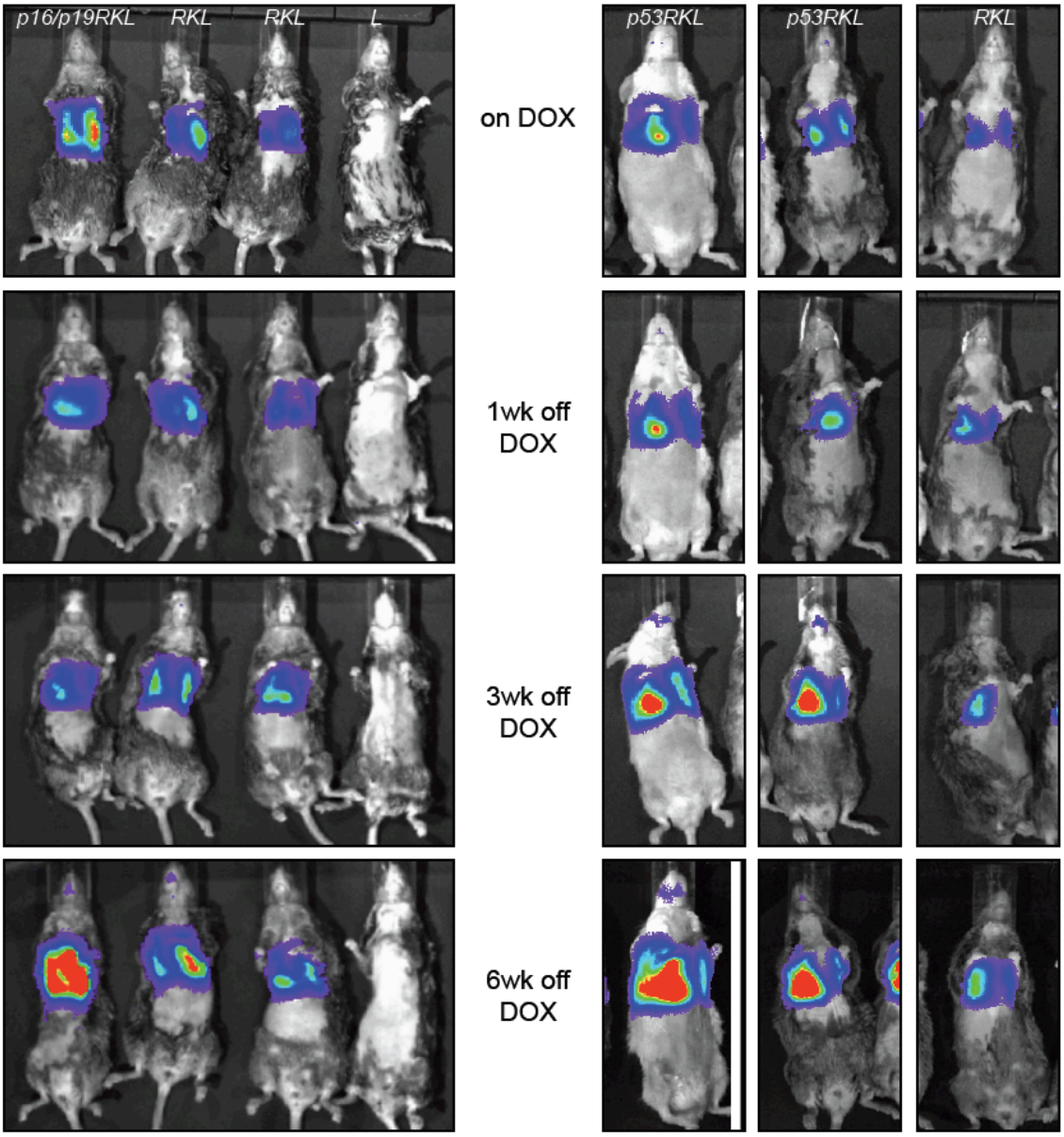

Figure 4.7 | Reactivation of Ink4a/Arf, not p53, elicits partial regression in established tumors. (*Left*) Serial bioluminescence images of *p16RKL*, *RKL* and *L* animals 8 w.p.i and DOX treatment (*top*) and 1, 3 and 6 weeks following DOX withdrawal. (*Right*) Serial bioluminescence images of *p53RKL* and *RKL* animals 5 w.p.i and DOX treatment (*top*) and 1, 3 and 6 weeks following DOX withdrawal.

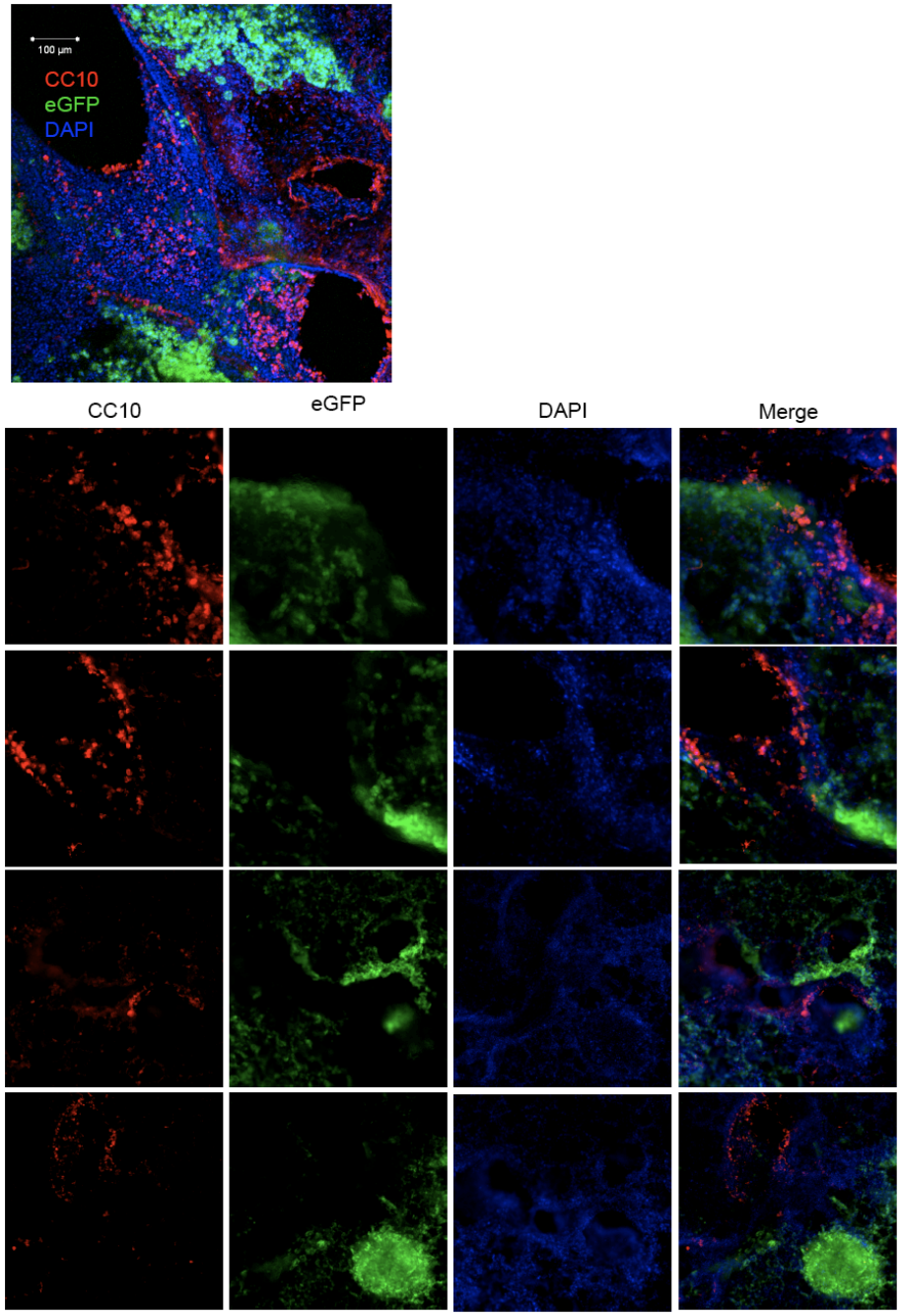

Figure 4.8 | *p53RKL* tumors do not express CC10. Confocal immunofluorescence microscopy images of lungs from *p53RKL* animals 8 w.p.i. with DOX treatment. Sections were stained with an antibody to detect the CC10 protein, a protein normally highly expressed in bronchiolar Clara cells, and DAPI. CC10 staining overlaps with GFP in <1% of cells. Images taken from multiple lung lobes of one mouse.

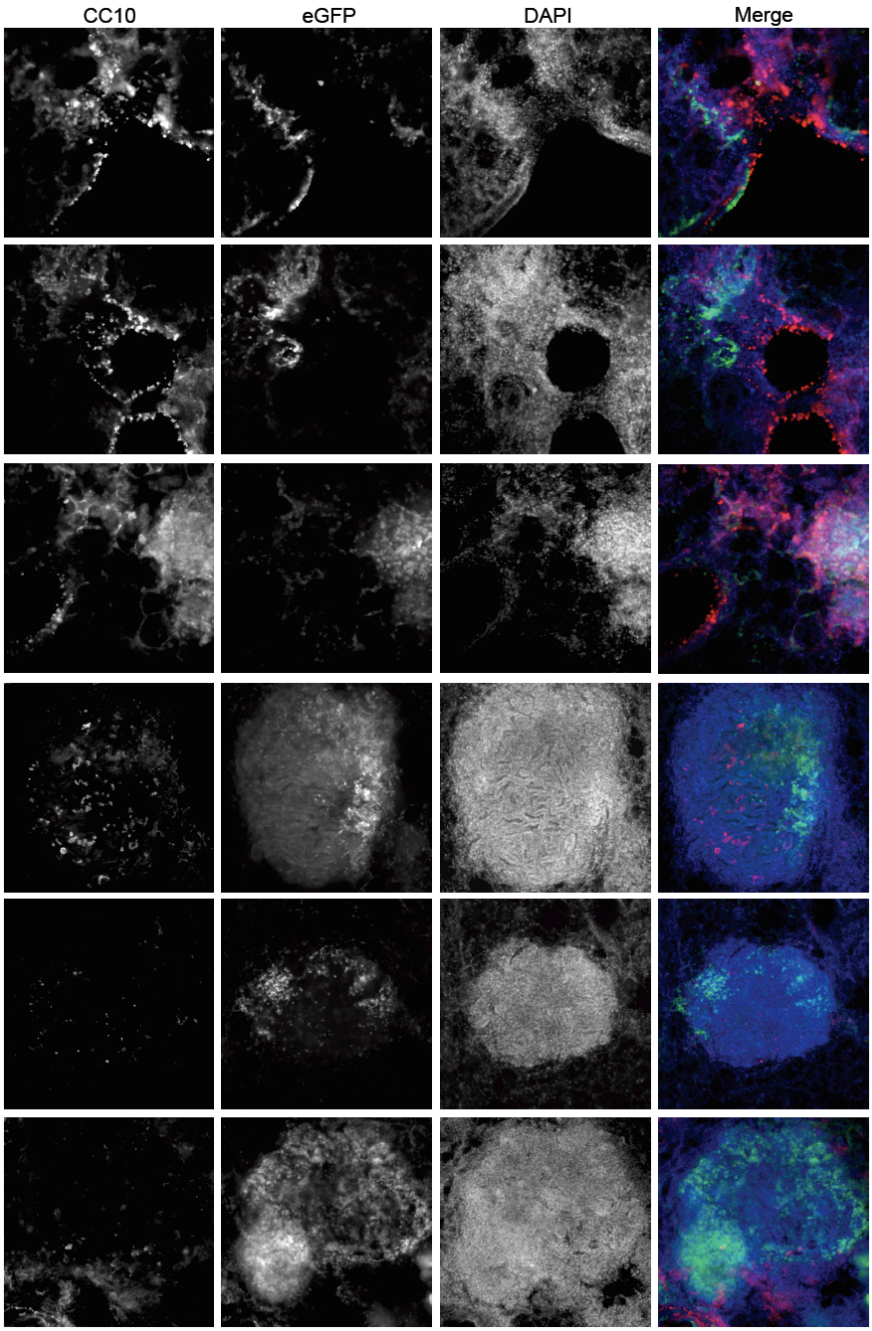

Figure 4.9 | CC10 is expressed in *p53RKL* tumors following p53 restoration. Confocal immunofluorescence images of lungs from *p53RKL* animals 9 w.p.i. and 1 week following DOX withdrawal. Sections were stained for CC10 and DAPI. CC10 expressed is expressed primarily in non-GFP regions of tumors; overlap of CC10 and GFP is seen <1%. Images were taken from multiple lobes of one mouse.

animals that were maintained on DOX (Fig. 4.6C).In comparison, *p53RKL* animals failed to show any decrease in bioluminescence levels in response to DOX withdrawal (Fig. 4.7). Response patterns varied in each animal with no indication of tumor regression. This may be attributable to the low level resolution of bioluminescence imaging, which cannot detect individual tumors. Therefore, to further examine the response to p53 reactivation in individual *p53RKL* tumors, confocal microscopy was performed on lung tumors collected serially from animals prior to and following DOX withdrawal. Immunofluorescence showed <1% overlap of CC10 and GFP staining, thus revealing a lack of CC10 expression in advanced GFP-positive tumors taken from *p53RKL* animals 8 w.p.i with DOX treatment (Fig. 4.8). Interestingly, following 1 week after DOX withdrawal, CC10 expression was observed in the tumors but did not overlap in GFP positive areas (Fig. 4.9). As expected, GFP signal decreased after 1 week, but full repression of GFP generally occurs ~10-14 days after DOX withdrawal.

To examine the behavior of the lung tumor cells *in vitro*, advanced tumors from *p16/p19RKL* and *p53RKL* animals that were maintained on DOX were harvested, digested and grown in culture on DOX. After 1 week in culture, differentiated “dome-shaped” vacuolized GFP-positive *p16/p19RKL* cells began to grow steadily as clusters and maintained this morphology after 3 weeks in culture (Fig. 4.10). Conversely, <20% of the *p53RKL* tumor cells had a differentiated morphology; rather, most cells had a spindle shape and long projections resembling mesenchymal cells (Fig. 4.10). After 1 week in culture, >99% of the *p53RKL* cells appeared mesenchymal-like and GFP-negative.

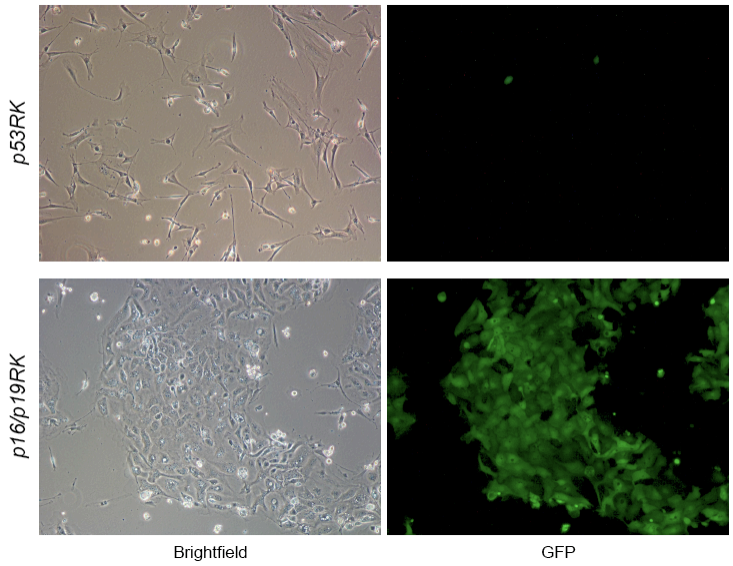

Figure 4.10 | *p16/p19RKL*, but not *p53RKL*, tumor cells maintain GFP expression and a differentiated morphology *in vitro*. Brightfield and GFP images of lung tumor cells from *p53RK* (*top*) and *p16RKL* (*bottom*) grown *in vitro* in LHC-9 media containing DOX (1µg/ml) for 3 weeks.

4.2.4 Speedy mouse models

Owing to the slow rate and high expense of producing multi-allelic transgenic mice with the correct genetic configurations, we devised an alternative "speedy" mouse models strategy based on the re-derivation of embryonic stem cells from mice with the relevant alleles in place (Fig. 4.11A). As a proof of principle, we harvested E3.5 embryos collected from *p16/p19R* females that had been crossed to *Kras* males and established ES cell lines from these blastocysts using established protocols (Nagy et al., 2003). ES cells genotyped as *p16/p19RK* were expanded *in vitro* and subsequently used to generate mosaic mice by blastocyst injection into C/57BL6/J albino host embryos (Fig. 4.11B). Using this method, we generated ~40 triple transgenic chimeras simultaneously,

many of which acquired lung adenocarcinomas within 10-14 weeks, similar to fully transgenic mice generated by intercrossing strains.

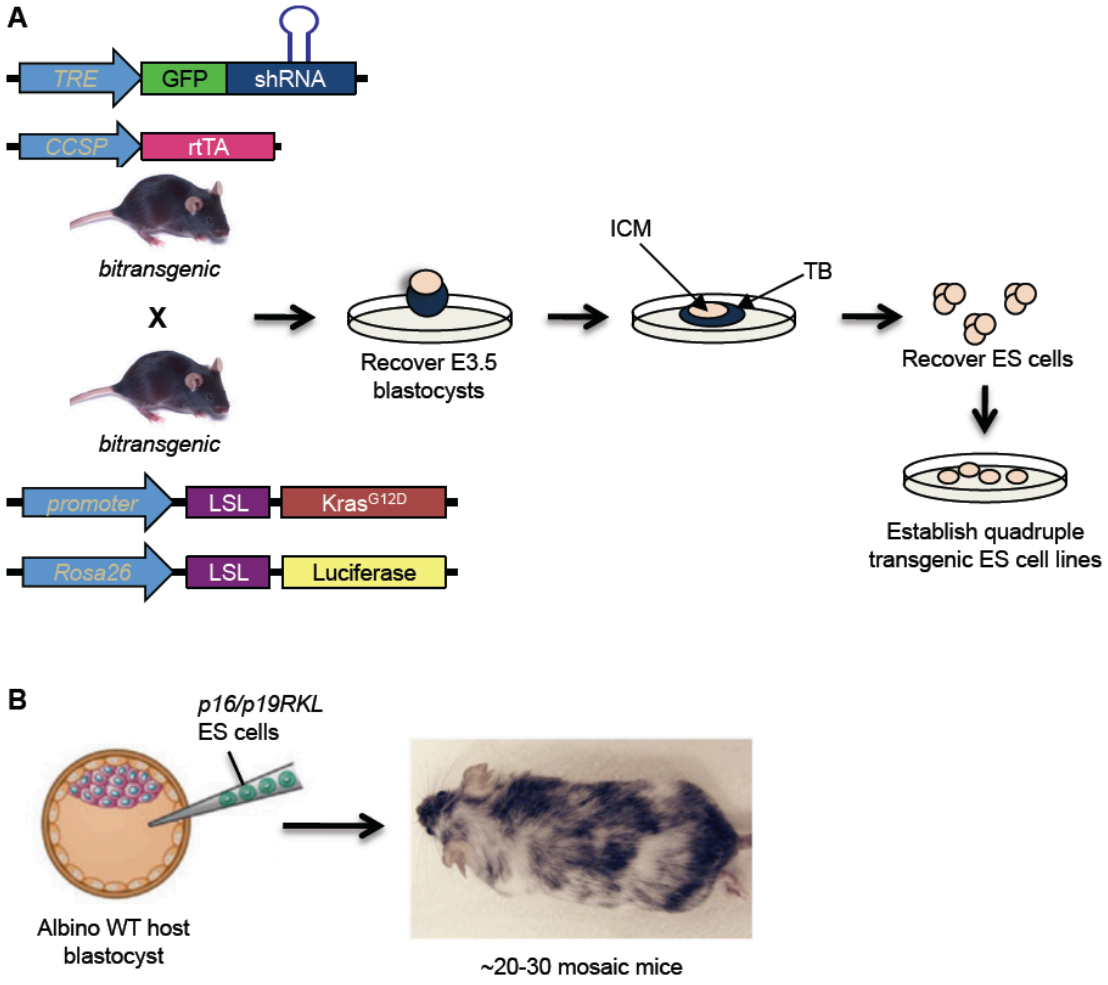

Figure 4.11 | Speedy mouse production pipeline. *A,* Schematic diagram of ES cell derivation. E3.5 blastocysts are recovered from a cross between bitransgenic mice. The inner cell mass (ICM) is separated from trophoblasts (TB) ~ 5d post collection and cultured for ~ 1wk to produce ES cell lines carrying four alleles for lung tumorigenesis. *B, p16/p19RKL* ES cells are injected into WT albino host blastocysts to generate mosaic mice applicable for adeno-cre delivery at 6-8 wk of age.

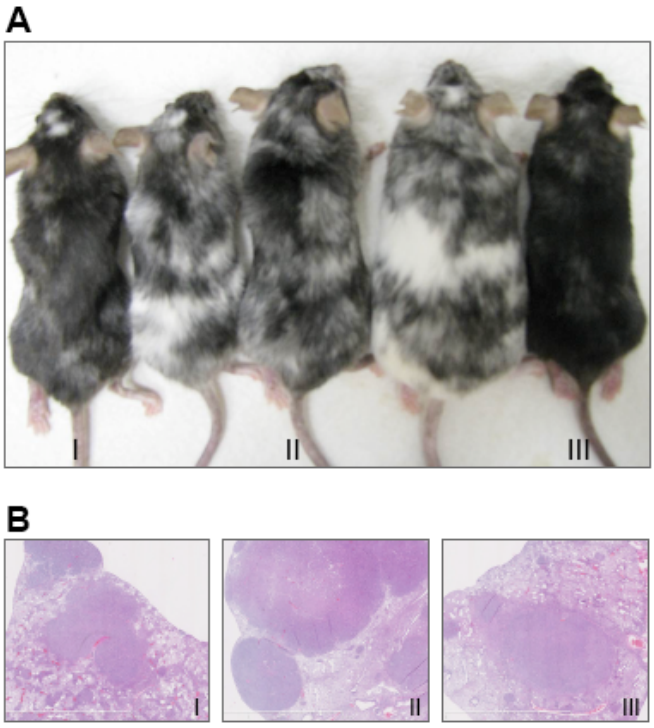

Figure 4.12 | Chimerism correlates with tumor burden. *A,* Representative *p16/p19RK* chimeric mice generated by blastocyst injection from re-derived ES cells. Mice with a higher degree of black coat color (representing the transgenic alleles) exhibit marked cachexia in comparison to those with a more mixed coat color 10 wk w.p.i. *B,* Corresponding lung sections from mice in *A*, displaying considerable tumor burden.

Table 4.3 | Number of chromosomes in *L48* ES cells following RMCE.

ES cells	37	38	39	40	41
X4	0	3(9%)	1(3%)	28(88%)	0
W3	4(13%)	1(3%)	4(12%)	22(69%)	1(3%)
Y5	0	2(6%)	5(16%)	25(78%)	0
Z6	1 (3%)	3(9%)	6 (19%)	22 (69%)	0

32 cells were evaluated for each clone

At 16 w.p.i. the degree of cachexia was notably more pronounced in mice with a higher degree of black coat color, which represents the transgenic alleles (Fig. 4.12A). Histological evaluation also confirmed that the tumor burden was more substantial in mice with a higher degree of chimerism, as determined by

coat color (Fig. 4.12B). Mice with a lesser degree of chimerism succumbed at much later time points. Interestingly, these mice displayed fewer but grossly larger tumors than their fully transgenic counterparts (data not shown). From these preliminary studies, it was evident that re-derived ES cell lines would greatly expedite our ability to generate large cohorts of animals to study tumor pathology and maintenance in much greater detail.

To allow for integration of different shRNAs into the re-derived ES cells, we established additional ES cells that contained the *ColA1* homing cassette (referred to as *CHC*) (Chapter 3; Supplementary Fig. 3.2) in addition to *RKL* alleles. Two ES cell lines (L17 and L48) were injected into blastocysts and tested for their ability to contribute to mouse production. L48 ES cells successfully gave rise to chimeras in which 8 out of 9 displayed >85% degree of black coat color. On the other hand, mice generated from L17 ES cells displayed high variability (5-95%) in coat color ranging between 30-40% for the majority of animals. These mice were inoculated with adeno-Cre and are currently being monitored biweekly by bioluminescence.

To establish large cohorts of quadruple transgenics with p53.1224, p16/p19.478 and ren.713 shRNAs, L48 ES cells were targeted and selected as previously described in Chapter 3. Southern blot analyses revealed correct targeting of 95% of the clones clones (data not shown). Prior to blastocyst injection, the percent of euploidy cells within the population was determined Table 4.3. To determine if the number of injected cells corresponds to total chimeric contribution, 5, 10 or 15 cells were injected into blastocysts for each ES

cell line. The percentage of chimeric pups obtained is listed in Table 4.4. These mice will be administered adeno-Cre when they reach 4-6 weeks of age and used for further tumor maintenance studies.

Table 4.4 | Summary of chimeras born after blastocyst injection.

ES-Clone Name	# of ES cell Injected Per Blastocyst	Number of Pups	Chimeras Pups	Dead Chimeras Pups	Number of Wild type	Percentage of Chimerism (Coat color)
p53L48	5	6 (24%)	5 (83%)	0	1(17%)	70,80,80,100,100%
	10	5 (20%)	3 (60%)	5 (100%)	2 (40%)	N/A
	15	9 (30%)	7 (78%)	2 (28.6%)	2 (22%)	20,30,40,50,70%
p16/p19L48	5	15 (62.5%)	11 (73.3%)	7 (63.7%)	4 (26.7%)	20,50,50,60%
	10	11 (40%)	10 (91%)	3 (27.3%)	1 (9%)	15,15,40,40,40,50,60%
	15	11 (41%)	10 (91%)	3 (27.3%)	1 (9%)	15,30,30,40,50,50,50%
**p19L48*	5	13 (50%)	7 (54%)	7 (100%)	6 (46%)	N/A
	10	9 (36%)	3 (34%)	1 (11%)	6 (67%)	60,70%
	15	13 (50%)	4 (3%)	2 (50%)	9 (69%)	5%,80%
renL48	5	13 (52%)	9 (69%)	5 (56%)	4 (31%)	15,30,50,50%
	10	9 (39%)	6 (67%)	6 (100%)	3(33%)	N/A
	15	9 (39%)	6 (67%)	4 (67%)	3 (33%)	30.50%

*Observed some chimeras pups were abnormal and chimeras were not health

4.3 Discussion

We have described the first use of regulatable RNAi *in vivo* to recapitulate *de novo* lung tumorigenesis in mice and study the effects of TSG restoration on tumor maintenance, which could not have previously been done using knockout animals. In the presence of oncogenic *Kras*, RNAi-mediated silencing of either p53 or $p16^{INK4a/}p19^{ARF}$ accelerated tumor pathogenesis and gave rise to more advanced disease than *Kras* activation alone. The median survival, tumor burden

and histopathological features of *p53RKL* and *p16/p19RKL* animals were markedly similar to those previously described for knockout models (Ji et al., 2007). Furthermore, close histological analyses of tumors derived from these animals revealed that they were indistinguishable from lung adenocarcinomas produced by knockout mice strains (Table 4.2; Fig. 4.4) (Jackson et al., 2005; Ji et al., 2007).

With the use of RNAi, we were able to investigate the effects of endogenous TSG reactivation in established tumors. Median survival was increased for *p53RK* animals upon p53 reactivation but remained unaltered following $p16^{INK4a/}p19^{ARF}$ restoration (Fig. 4.5B,C). While this would suggest that p53 reactivation promoted some degree of tumor regression, bioluminescence imaging showed the opposite effect (Fig. 4.7). Tumor regression was observed in *p16/p19RKL* animals, whereas no clear pattern was noted in *p53RKL* mice. Several explanations are warranted for these observations. First, disease onset was substantially different for these two cohorts and therefore the time of DOX removal also varied. For a more precise comparison, DOX removal will need to be synchronized in future studies. Second, mice can survive with very little lung capacity (Bates and Irvin, 2003) and therefore, survival is a somewhat poor measure of lung tumor burden and aggressiveness of the disease. For example, mice with many large but distal tumors can survive much longer than those that acquire tumors more proximally that tend to compress the airways and decrease lung and heart function to a greater degree. Finally, most animals within the survival study did not have the *luciferase* allele, and therefore it was not possible

to precisely measure tumor onset or burden prior to removal from DOX. For these reasons, the survival benefit may not accurately reflect a therapeutic response.

To understand the cellular effects of TSG reactivation, we examined the response microscopically. We report several findings upon TSG reactivation in lung tissue from *p16/p19RKL* and *p53RKL* animals. Most striking was the degree of differentiation of the tumor cells both *in vivo* and *in vitro*. Our investigation suggests that loss of p53 in the presence of oncogenic *Kras* causes tumor cells to either “de-differentiate” or “trans-differentiate” to a more poorly differentiated state. CC10 is known to be highly expressed in Clara cells, which are described as nonciliated bronchiolar epithelial cells, (Linnoila et al., 2000), however immunofluorescence staining showed that tumors from *p53RKL* kept on DOX lacked CC10 expression (Fig 4.8). *In vitro* studies of *p53RKL* tumor cells also provide further evidence that some type of differentiation has occurred. These cells do not have the typical epithelial “dome-shaped” morphology of Clara cells with secretory vacuolization (Linnoila et al., 2000) but rather resemble mesenchymal-like cells with a spindle-shaped morphology (Fig.4.10). Whether this is in fact “de-differentiation” or epithelial-to-mesenchymal transition (EMT) has yet to be determined. Further assessment of mesenchymal markers (e.g. vimentin, fibronectin, snail, slug, twist, MMPs, increased migration, invasion and scattering) (Bates and Irvin, 2003) and respiratory epithelial cellular markers (e.g. SP-C) will enable a more precise characterization of the differentiation status of these tumor cells.

In stark contrast, *de novo* lung tumors with oncogenic *Kras* and $p16^{INK4a/}p19^{ARF}$ loss are typically comprised of moderate-to-well-differentiated cells that maintain their "dome-shaped" morphology even when cultured *in vitro* (Fig. 4.10). *p16/p19RK* tumor cells cluster and appear to sustain cell-to-cell adhesions *in vitro*. While additional assessment of cellular markers, such as CC10 and SP-C, will be necessary to clearly define the differentiation status of *p16/p19RK* lung tumor cells, we predict these analyses will provide further evidence that loss of $p16^{INK4a/}p19^{ARF}$ does not promote the "de-differentiation" seen in *p53RKL* tumors. We hypothesize that the different cellular response to TSG reactivation in *p16/p19RKL* and *p53RKL* animals is dependent upon their differentiation status. Furthermore, we propose that more well-differentiated lung adenocarcinomas that maintain epithelial characteristics will better respond to TSG reactivation and potentially regress. Indeed, partial regression of *p16/p19RKL* tumors was observed upon TSG reactivation, but whether regression occurred through a senescence or apoptotic pathway has yet to be determined. Previously, studies in a model of hepatocellular carcinoma suggest that TSG reactivation in the presence of oncogenic *Kras* may trigger tumor cell senescence and an senescence-associated secretory phenotype that promotes recruitment of members of the innate immune system that participate in tumor clearance (Xue et al., 2007). Consistent with this notion, preliminary histological analyses of lung lesions following $p16^{INK4a/}p19^{ARF}$ restoration revealed an inflammatory response, predominantly consisting of alveolar macrophage infiltration within areas of disseminating tumor tissue (Fig. 4.6B). Whether these

immune cells are being recruited and contribute to tumor regression has yet to be determined. Finally, we hypothesize that the relapse seen in *p16/p19RKL* animals can be attributed to mutations in p53 or members of the p53 pathway.

To further understand the differential response to p53 or $p16^{INK4a/}p19^{ARF}$ restoration, we will first need to characterize the gene expression signatures of these tumors and determine which key signaling pathways are responsible for their differentiation status. This can be done by array analyses of tumor samples from *p53RKL* and *p16/p19RKL* animals that are maintained on DOX. Recent studies have demonstrated that overexpression of Mad2 in the presence of oncogenic *Kras* causes genomic instability, which is sufficient to accelerate *Kras*-driven murine lung tumorigenesis (Sotillo et al., 2007). Furthermore, these *Kras*/Mad2 tumors respond accordingly to the oncogene addiction phenomenon and regress upon *Kras* inhibition; however, recurrence of these tumors is markedly elevated in comparison to tumors with *Kras* activation alone. Genomic instability caused by loss of p53 has frequently been reported (Zilfou and Lowe, 2009) and could also provide an explanation for the lack of tumor regression in *p53RKL* animals upon TSG reactivation. We will also need to determine whether p53 but not $p16^{INK4a/}p19^{ARF}$ loss causes genomic instability in the tumor cells, which would explain the accelerated tumorigenesis seen in *p53RKL* animals.

Another key player that may contribute to the differential response is NFκB. Previous studies have shown that overexpression of oncogenic forms of Ras result in NFκB activation (Finco et al., 1997; Hanson et al., 2004), whereas wildtype p53 has been shown to anatagonize NFκB activity (Huang et al., 2007;

Kawauchi et al., 2008; Ravi et al., 1998). Additionally, a previous study has shown that activation of the NFκB pathway is required for the development of murine lung adenocarcinomas with concomitant loss of p53 and expression of oncogenic *Kras* (Meylan et al., 2009). Meylan and collegues also reported that this requirement was dependent on p53 status and that inhibition of the NFκB pathway, from the time of tumor initiation or after tumor progression, resulted in significantly reduced lung tumor development. Additionally, NFκB has been reported to repress an epithelial phenotype by regulating mesechymal genes that promote and maintain an invasive phenotype in aggressive cancers (Min et al., 2008). In our model, it is possible that activation of the NFκB pathway is not activated in *p16/p19RKL* tumors with wildtype p53, but is active in *p53RKL* tumors and promoting EMT in the lung adenocarcinomas of *p53RKL* animals. This may explain the "de-differentiation" observed. If so, in addition to p53 restoration, *p53RKL* tumors may require inhibition of the NFκB pathway in order for tumor regression to occur. Administration of an NFκB inhibitor, such as dehydroxymethylepoxyquinomicin (DHMEQ) (Horie et al., 2006), at the time of DOX withdrawal and observing tumor responsiveness can test this hypothesis.

In addition to studying the effects of TSG reactivation in established lung adenocarcinomas, we devised a strategy that allows for rapid generation of animals with multiple transgenic alleles for the study of lung tumorigenesis. Our re-derivation strategy provided several advantages over traditional breeding schemes: First, these ES cells can undergo Flpe-mediated recombination to incorporate different tet-inducible shRNAs, thus allowing us to examine the roles

of multiple TSGs without establishing expansive breeding colonies. Second, these ES cells can be used to make chimeric mice that will give rise to tumors surrounded by normal WT tissue – a scenario that more closely resembles the human disease. Finally, large cohorts of mice can be rapidly established simultaneously providing sufficient animals necessary for statistically rigorous studies. Blastocyst injection into albino host embryos resulted in chimeric mice comprised of a mixture host and targeted ES cells, which is most evident by the black and white coat color of the chimeric mice. It would be most beneficial if we could control the level of chimerism in animals established by blastocysts injection. Our preliminary experiments to address this issue were inconclusive, but further trials will be performed to assess whether we can limit the variable chimerism seen in our newborn litters. Alternatively, we can use tetraploid embryo complementation to derive fully ES-cell derived mice (Schuster-Gossler et al., 2001).

We have recently generated *p53RKL*, *p16/p19RKL* and *renRKL* chimeric animals to continue our studies and more thoroughly characterize the response to TSG reactivation. We believe further studies will allow us to determine the gene expression patterns of *p53RK* and *p16/p19RK* lung tumors both before and after TSG restoration. With this information, we may be able to distinguish the critical pathways that render *p16RK*, and not *p53RK*, tumors vulnerable TSG reactivation, important findings that could play a role in identifying new therapeutics.

4.4 References

Bates, J.H., and Irvin, C.G. (2003). Measuring lung function in mice: the phenotyping uncertainty principle. J Appl Physiol *94*, 1297-1306.

Finco, T.S., Westwick, J.K., Norris, J.L., Beg, A.A., Der, C.J., and Baldwin, A.S., Jr. (1997). Oncogenic Ha-Ras-induced signaling activates NF-kappaB transcriptional activity, which is required for cellular transformation. J Biol Chem *272*, 24113-24116.

Fisher, G.H., Wellen, S.L., Klimstra, D., Lenczowski, J.M., Tichelaar, J.W., Lizak, M.J., Whitsett, J.A., Koretsky, A., and Varmus, H.E. (2001). Induction and apoptotic regression of lung adenocarcinomas by regulation of a K-Ras transgene in the presence and absence of tumor suppressor genes. Genes Dev *15*, 3249-3262.

Forgacs, E., Zochbauer-Muller, S., Olah, E., and Minna, J.D. (2001). Molecular genetic abnormalities in the pathogenesis of human lung cancer. Pathol Oncol Res *7*, 6-13.

Greenberg, S.D., Fraire, A.E., Kinner, B.M., and Johnson, E.H. (1987). Tumor cell type versus staging in the prognosis of carcinoma of the lung. Pathol Annu *22 Pt 2*, 387-405.

Hanson, J.L., Hawke, N.A., Kashatus, D., and Baldwin, A.S. (2004). The nuclear factor kappaB subunits RelA/p65 and c-Rel potentiate but are not required for Ras-induced cellular transformation. Cancer Res *64*, 7248-7255.

Herbst, R.S., Heymach, J.V., and Lippman, S.M. (2008). Lung cancer. N Engl J Med *359*, 1367-1380.

Horie, R., Watanabe, M., Okamura, T., Taira, M., Shoda, M., Motoji, T., Utsunomiya, A., Watanabe, T., Higashihara, M., and Umezawa, K. (2006). DHMEQ, a new NF-kappaB inhibitor, induces apoptosis and enhances fludarabine effects on chronic lymphocytic leukemia cells. Leukemia *20*, 800-806.

Huang, W.C., Ju, T.K., Hung, M.C., and Chen, C.C. (2007). Phosphorylation of CBP by IKKalpha promotes cell growth by switching the binding preference of CBP from p53 to NF-kappaB. Mol Cell *26*, 75-87.

Jackson, E.L., Olive, K.P., Tuveson, D.A., Bronson, R., Crowley, D., Brown, M., and Jacks, T. (2005). The differential effects of mutant p53 alleles on advanced murine lung cancer. Cancer Res *65*, 10280-10288.

Jackson, E.L., Willis, N., Mercer, K., Bronson, R.T., Crowley, D., Montoya, R., Jacks, T., and Tuveson, D.A. (2001). Analysis of lung tumor initiation and progression using conditional expression of oncogenic K-ras. Genes Dev *15*, 3243-3248.

Jemal, A., Murray, T., Ward, E., Samuels, A., Tiwari, R.C., Ghafoor, A., Feuer, E.J., and Thun, M.J. (2005). Cancer statistics, 2005. CA Cancer J Clin *55*, 10-30.

Ji, H., Ramsey, M.R., Hayes, D.N., Fan, C., McNamara, K., Kozlowski, P., Torrice, C., Wu, M.C., Shimamura, T., Perera, S.A.*, et al.* (2007). LKB1 modulates lung cancer differentiation and metastasis. Nature *448*, 807-810.

Kawauchi, K., Araki, K., Tobiume, K., and Tanaka, N. (2008). p53 regulates glucose metabolism through an IKK-NF-kappaB pathway and inhibits cell transformation. Nat Cell Biol *10*, 611-618.

Linnoila, R.I., Szabo, E., DeMayo, F., Witschi, H., Sabourin, C., and Malkinson, A. (2000). The role of CC10 in pulmonary carcinogenesis: from a marker to tumor suppression. Ann N Y Acad Sci *923*, 249-267.

Meylan, E., Dooley, A.L., Feldser, D.M., Shen, L., Turk, E., Ouyang, C., and Jacks, T. (2009). Requirement for NF-kappaB signalling in a mouse model of lung adenocarcinoma. Nature *462*, 104-107.

Miller, V.A., Riely, G.J., Zakowski, M.F., Li, A.R., Patel, J.D., Heelan, R.T., Kris, M.G., Sandler, A.B., Carbone, D.P., Tsao, A.*, et al.* (2008). Molecular characteristics of bronchioloalveolar

carcinoma and adenocarcinoma, bronchioloalveolar carcinoma subtype, predict response to erlotinib. J Clin Oncol *26*, 1472-1478.

Min, C., Eddy, S.F., Sherr, D.H., and Sonenshein, G.E. (2008). NF-kappaB and epithelial to mesenchymal transition of cancer. J Cell Biochem *104*, 733-744.

Nagy, A., Gertsenstein, M., Vintersten, K., and Behringer, R. (2003). Manipulating the mouse embryo : a laboratory manual, 3 edn (Cold Spring Harbor, Cold Spring Harbor Laboratory Press).

Neal, J.W., and Sequist, L.V. First-line use of EGFR tyrosine kinase inhibitors in patients with NSCLC containing EGFR mutations. Clin Adv Hematol Oncol *8*, 119-126.

Politi, K., Zakowski, M.F., Fan, P.D., Schonfeld, E.A., Pao, W., and Varmus, H.E. (2006). Lung adenocarcinomas induced in mice by mutant EGF receptors found in human lung cancers respond to a tyrosine kinase inhibitor or to down-regulation of the receptors. Genes Dev *20*, 1496-1510.

Ravi, R., Mookerjee, B., van Hensbergen, Y., Bedi, G.C., Giordano, A., El-Deiry, W.S., Fuchs, E.J., and Bedi, A. (1998). p53-mediated repression of nuclear factor-kappaB RelA via the transcriptional integrator p300. Cancer Res *58*, 4531-4536.

Safran, M., Kim, W.Y., Kung, A.L., Horner, J.W., DePinho, R.A., and Kaelin, W.G., Jr. (2003). Mouse reporter strain for noninvasive bioluminescent imaging of cells that have undergone Cre-mediated recombination. Mol Imaging *2*, 297-302.

Schuster-Gossler, K., Lee, A.W., Lerner, C.P., Parker, H.J., Dyer, V.W., Scott, V.E., Gossler, A., and Conover, J.C. (2001). Use of coisogenic host blastocysts for efficient establishment of germline chimeras with C57BL/6J ES cell lines. Biotechniques *31*, 1022-1024, 1026.

Shepherd, F.A. (2005). A targeted approach to reducing lung cancer mortality. J Clin Oncol *23*, 3173-3174.

Shepherd, F.A., Rodrigues Pereira, J., Ciuleanu, T., Tan, E.H., Hirsh, V., Thongprasert, S., Campos, D., Maoleekoonpiroj, S., Smylie, M., Martins, R.*, et al.* (2005). Erlotinib in previously treated non-small-cell lung cancer. N Engl J Med *353*, 123-132.

Sotillo, R., Hernando, E., Diaz-Rodriguez, E., Teruya-Feldstein, J., Cordon-Cardo, C., Lowe, S.W., and Benezra, R. (2007). Mad2 overexpression promotes aneuploidy and tumorigenesis in mice. Cancer Cell *11*, 9-23.

Tichelaar, J.W., Lu, W., and Whitsett, J.A. (2000). Conditional expression of fibroblast growth factor-7 in the developing and mature lung. J Biol Chem *275*, 11858-11864.

Woo, S.K., Lee, T.S., Kim, K.M., Kim, J.Y., Jung, J.H., Kang, J.H., Cheon, G.J., Choi, C.W., and Lim, S.M. (2008). Anesthesia condition for (18)F-FDG imaging of lung metastasis tumors using small animal PET. Nucl Med Biol *35*, 143-150.

Xue, W., Zender, L., Miething, C., Dickins, R.A., Hernando, E., Krizhanovsky, V., Cordon-Cardo, C., and Lowe, S.W. (2007). Senescence and tumour clearance is triggered by p53 restoration in murine liver carcinomas. Nature *445*, 656-660.

Zilfou, J.T., and Lowe, S.W. (2009). Tumor Suppressive Functions of p53. Cold Spring Harb Perspect Biol *1*, a001883.

Zundelevich, A., Elad-Sfadia, G., Haklai, R., and Kloog, Y. (2007). Suppression of lung cancer tumor growth in a nude mouse model by the Ras inhibitor salirasib (farnesylthiosalicylic acid). Mol Cancer Ther *6*, 1765-1773.

4.5 Author Contributions

Jacob Hooker of Brookhaven National Laboratories performed experiments and data analyses for Fig. 4.2. Dr. Kenneth Shroyer of Stony Brook Medical School perfomed histological analyses to generated data in Fig. 4.4 and Table 4.2. Matthew Camiolo performed immunofluorescence microscopy in Fig. 4.8-4.9. S.Y.K. performed the first round of ES-cell derivation and taught the procedure for re-derivation of the *L48* ES cells. J.S., J.C. and D.G were responsible for animal husbandry and assisted with mouse imaging. Shirley Guo assisted with *L48* ES cell targeting. All other experiments were performed by P.K.P.

Chapter 5

Discussion and Perspectives

5.1 Experimental conclusions

At the start of my thesis project, RNAi technology was expanding in all directions, which opened up avenues to explore biology in unprecedented ways. The ability to not only suppress endogenous gene expression, but to be able to control it – turning genes off and then on again – was a revolutionary feat in genetic research. I predicated my PhD studies with this in mind, hoping to utilize the potential of RNAi technology to study the role of tumor suppressor genes in cancer biology.

However, before I could begin to address these questions, I felt that it was imperative to first set out to improve regulatable RNAi technology in transgenic mice. In the beginning, I was confronted with many challenges and endured disappointing defeats, but these trials and tribulations effectively forced a turn to new directions and the development of tools that would later result in several major advances in RNAi technology, ES cell targeting and mouse production. Briefly, the outcomes that resulted from this thesis project are listed as follows:

First, as discussed in Chapter 2, modification of our primary tet-regulatable shRNA vector (TMP; Fig. 2.1A) gave rise to the TGM vector (Fig. 2.2A), which substantially improved shRNA efficacy and incorporated an invaluable fluorescence biomarker of shRNA expression. This vector currently serves as a template for the majority of shRNA expression vectors in our lab.

Second, numerous failed attempts of establishing conditional transgenic shRNA mice by pronuclear injection (described in Chapter 2) resulted in our

reliance on ES cells and the subsequent successful use of RMCE to efficiently deliver tet-regulated shRNA expression cassettes to a defined genomic locus in ES cells (Chapter 3). By using RMCE and designing the pCol-TGM targeting vector (Fig. 3.1A) to accept any shRNA from the Hannon-Elledge genome wide library (Paddison et al., 2004) or RNAi codex library (Olson et al., 2006), we were able to streamline targeting, and produce a pipeline for rapid generation of correctly-targeted ES cell clones harboring different shRNAs. In only 2 years of using this pipeline, we produced and validated GFP-marked shRNA expression in over 100 ES lines carrying different shRNAs. This effort led to the development of an RNAi ES cell facility that is currently contracted by the National Cancer Institute to produce ~1500 ES cell clones harboring all known endogenous mouse miRNAs.

Third, with the efforts of Dr. Sang Yong Kim, tetraploid embryo complementation, once a novel and arduous procedure for our lab, has now become a successful and standard protocol performed at the gene targeting facility of CSHL. This procedure has eliminated the need for a chimeric intermediate, and therefore greatly accelerated our ability to establish and characterize founder lines. Since its implementation less than 3 years ago, we have validated over 35 founder lines harboring unique shRNAs.

Fourth, owing to the slow rate and high expense of producing quadruple transgenic mice with the correct genetic configurations to model lung adenocarcinoma using RNAi, we devised a novel approach to re-derive ES cells harboring the relevant alleles for production of “mosaic” models (Chapter 4). By

doing so, we bypassed the need for a large and complex breeding colony and increased the speed at which we could generate quadruple transgenics by an order of magnitude faster than if we relied on standard genetic crosses. Additionally, we were able to re-derive several ES lines with *LSL-Kras*, CCSP-rtTA, LSL-luc and the shRNA "homing" cassette (hereafter referred to as CHC, or *ColA1* homing cassette), allowing us to subsequently retarget these cells with many other shRNAs or even cDNAs (Table 5.1). Therefore, this system greatly accelerates the rate at which we can study genetic interactions and tumor maintenance genes in the lung adenocarcinoma system.

Lastly, we believe the ES cell re-derivation approach can be applied to build a number of complex mouse models, which can be utilized to study a wide range of disease processes even beyond the scope of cancer – in areas including but not limited to developmental, neurological or even autoimmune pathology. Owing to our expertise in cancer, we have recently been awarded several grants and established numerous collaborations in effort to expand the development of sophisticated mouse models to study a number of cancers including lung, pancreatic, ovarian and breast cancer. These models will not only serve to identify new genetic contributors of tumor development, they will also be used to discover and validate potential therapeutic drug targets.

5.2 Lessons learned from transgenesis

When I first joined the Lowe lab, the use of RNAi in transgenic mice was only in its infancy. Still, having realized its potential, many labs had already invested substantial efforts toward the goal of achieving stable and heritable RNAi-mediated gene regulation in mice. The most common approach used to incorporate shRNA expression cassettes into the mouse genome was classical transgenesis, whereby the transgene was simply delivered to a gene targeting facility and injected into the pronucleus of fertilized zygotes (Dickins et al., 2007; Fedoriw et al., 2004; Hasuwa et al., 2002; Lickert et al., 2005; Shinagawa and Ishii, 2003; Stein et al., 2003; Wang et al., 2007). In approximately 3-4 weeks time, founder mice were produced and investigators began their work by screening multiple founders to identify those with potent shRNA expression.

From our lab's perspective, standard transgenesis was most desirable, primarily because an alternative site-directed method would require integration into embryonic stem cells. These are historically more expensive to maintain in culture and were not currently being used in our lab. For this reason, I originally relied on pronuclear injection and sought ways to improve shRNA expression in order to overcome the hurdles imposed by this method.

The first improvement transpired from reconfiguration of the elements within the shRNA expression cassette to TRE-GFP-miR30 (TGM; Fig. 2.2A). We tested multiple shRNAs including p53.1224 and p16/p19.748 in the TGM setting and all shRNAs showed consistent and enhanced knockdown, in comparison to

the TRE-miR30 configuration. Following these results, we redesigned many of the existing expression vectors in the lab in order to maximize shRNA potency in all settings, including constitutive expression vectors commonly used in RNAi screens. We further adopted this configuration as the standard template for future vector designs.

From our second generation RNAi mice discussed in Chapter 2, we quickly learned that this enhanced efficiency still could not overcome the constraints of random transgene integrations, which are often prone to varying degrees of heterochromatic silencing. By observing the level of GFP expression in various tissues throughout the mice and comparing the GFP levels between founder lines (Fig. 2.6), it was clear that position-effect variegation would make it impossible to control for shRNA potency, which ultimately would be determined by the integration site. We were quick to realize that screening founders with weak or heterogeneous shRNA expression is only possible if the shRNA provides a proliferative advantage, such as p53.1224. In this case, those cells with more potent gene suppression would eventually out grow the others and give rise to a more clonal population. In contrast, without reliable expression, we knew it would not be feasible to screen for shRNAs with neutral or negative proliferative effects, such as control shRNAs (luc.1309 and ren.713) or killer hairpins that target essential genes (rpa3.457). Their efficiency would be immeasurable in a heterogeneous population because evaluation of their effectiveness would present confounding results.

We therefore made an effort with the use of insulators to protect the transgene from heterochromatic gene silencing – an approach that proved successful for several groups using chicken HS4 insulator sequences (Guglielmi et al., 2003; Hsiao et al., 2004; Potts et al., 2000). However, the HS4 sequences contained many enzymatic restriction sites necessary for cloning shRNAs into the TGM cassette. Use of these insulators would have required destruction of these restriction sites and sequential rounds of testing to ensure that this manipulation did not affect their function. Instead, we chose an alternative – the pWhere vector (Invivogen), a commercially available vector with 5' and 3' H19 insulator arms flanking a multiple cloning site. Supporting literature suggested these sequences work in a similar manner to the chicken HS4 insulators and are responsible for influencing differential expression at the imprinted Igf2 locus in mice (Bell and Felsenfeld, 2000; Kaffer et al., 2000).

This effort also failed. While we cannot draw any clear conclusions regarding the use of H19 insulators, our limited experience with these sequences suggests that they may have many unknown functions that play a role in fertility and influence survival. Compared to other transgenes (Fig. 2.1A; 2.5A), which integrated and were transmitted to F_1 progeny at expected frequencies, the H19TGM (Fig. 2.7A) and H19TMG (not discussed) transgenes resulted in fewer founders, and of those, ~50% were sterile. Additionally, in contrast to the Salt and Pepper founders, which displayed some GFP expression, tissues isolated from the H19TGM founders lacked even minimal GFP expression (data not

shown). Therefore, we chose to abandon further investigation of these founders and move toward a more promising method to produce RNAi mice.

5.3 A move toward ES cells and ES cell-derived mice

After numerous rounds of pronuclear injection and the establishment of three generations of founders harboring tet-regulatable shRNAs, it was clear that we had exhausted our efforts using standard transgenesis and needed to turn to a more reliable method for the generation of shRNA transgenic mice. For this purpose, we chose to use a recombinase-mediated cassette exchange (RMCE) strategy that takes advantage of the Flp/FRT recombinase system (Zhu et al., 1995; Zhu and Sadowski, 1995) and directs recombination of transgenes into the *ColA1* locus (Beard et al., 2006). Unlike homologous recombination, an infrequent event that relies on the endogenous enzymatic machinery, RMCE systems (Hitz et al., 2007; Nyabi et al., 2009; Seibler et al., 2005; Seidler et al., 2008) are very efficient for introducing transgenes into the pre-targeted loci. This is because they utilize exogenous FlpE or Cre recombinases to promote intra- and interchromosomal recombination of the FRT or loxP sites, respectively, within the targeted locus and on the targeting vector.

As discussed in detail in Chapter 3, the *ColA1* RMCE system was exceptionally designed for high-efficiency because it necessarily requires correct integration of the targeting vector in order to recover expression of the post-selection hygromycin resistance cassette (Beard et al., 2006). By combining this

high efficiency ES cell targeting system with our optimized fluorescence reported, miR30-based shRNA technology, we were able to develop a flexible and scalable pipeline with integrated “go/no go” checkpoints that estimated electroporation efficiency and GFP-shRNA expression at early time points. These checkpoints served as quality control measures tracking progress that ultimately predicted failure rates and reduced culturing costs. With these in place, we defined a pipeline that can produce hundreds of effective transgenic ES cells and mice per year with minimal labor and expense. Since then we adopted an even more cost-effective 96-well formatted pipeline using Amaxa® Nucleofector technology illustrated in Fig. 5.1. With our optimized pipeline now in place, we were able to establish multiple collaborations, including those aforementioned with the NCI, and to expand our efforts to produce hundreds of ES cell lines now available to the research community.

For targeting purposes, we used V6.5 F_1 hybrid ES cells, which harbor genetic heterozygosity, a crucial parameter for post-natal survival of mice entirely derived from ES cells produced by tetraploid embryo complementation. Although tetraploid embryo complementation had never been performed at our gene targeting facility, we still requested production of fully ES cell-derived mice in order to eliminate the need for a chimeric intermediate and subsequent screening for germline transmission. Dr. SY Kim, a vital member of the gene targeting facility’s research team, learned the procedure and succeeded at reproducing these efforts, resulting in the production of many viable litters of fully ES cell-derived mice. His perseverance has been instrumental in accelerating the

establishment of founder lines and our ability to perform studies using these mice.

Table 5.1 Future ES cell lines for cancer models. *ColA1* homing cassette (CHC) and *LSL-luciferase* will be included in all models.

ES cell genetic configuration	Tetracycline-transactivator strain	Cancer Model	Purpose	Cre-delivery
$p53^{R270H}$ *LSL-Kras*^{G12D}	CCSP-rtTA	Lung Adenocarinoma	Drug target identification/ validation	Nasal administration
	CAGs-LSL-rtTA3 or CAGs-rtTA3		Local and systemic drug toxicity studies	
$p53^{R172H}$ *LSL-Kras*^{G12D} PDX-Cre	CAGs-LSL-rtTA3 or CAGs-rtTA3	Pancreatic cancer	Oncogene/TSG cooperativity; Drug target identification/ validation	NA
$p53^{flox/flox}$ *LSL-Kras*^{G12D}	CAGs-LSL-rtTA3 or CAGs-rtTAs	Lung adenocarcinoma, ovarian epithelial cancer, colon carcinoma	Oncogene/TSG cooperativity; drug target identification/ validation; local and systemic drug toxicity studies	Local injection

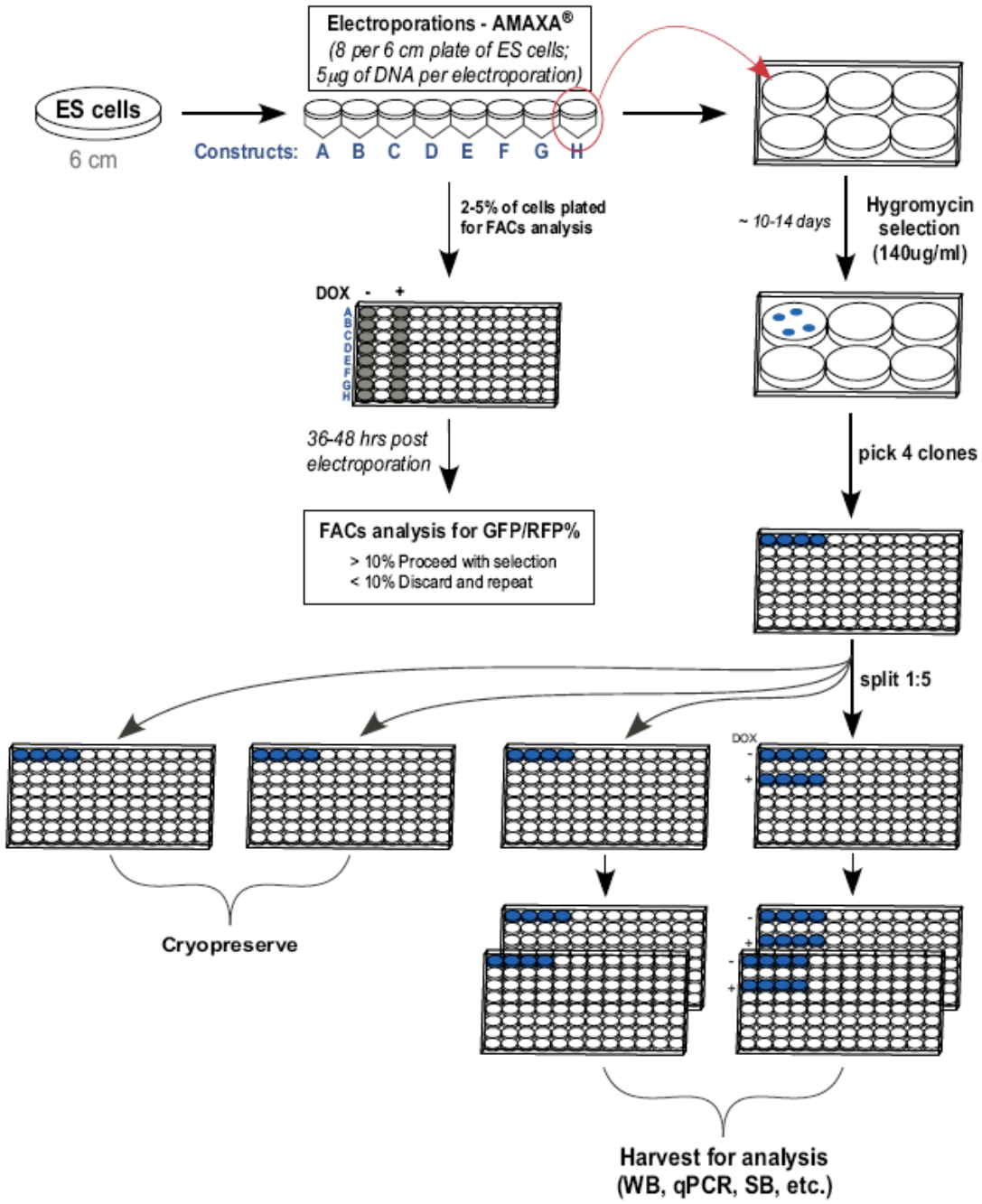

Figure 5.1 | Schematic of AMAXA® Nucleofector ES cell targeting pipeline.

5.4 Tumor suppressor genes in tumor maintenance

At the start of my thesis, substantial compelling evidence supporting the "oncogene dependence" phenomenon had come not only from mouse models of cancer (Chin et al., 1999; Felsher and Bishop, 1999; Fisher et al., 2001; Moody et al., 2002; Soucek et al., 2008), but also from ongoing success in the clinic with targeted therapies (Neal and Sequist; Shepherd, 2005; Shepherd et al., 2005). Following these findings, the notion of "tumor suppressor hypersensitivity" was under question and it was proposed that some tumors might require continual TSG inactivation in order for tumors to maintain themselves. Prior to the discovery of RNAi, the only feasible means to test this hypothesis *in vivo* other than gene therapy, was either by use of dominant-negative mutants that could be conditionally expressed or use of knockout/knock-in models in which an inducible transgene could be activated following tumor development. Both of these situations are presented with caveats: 1) dominant-negative mutants may have additional functions beyond suppression of the target gene; and 2) overexpression of a TSG may not be physiologically relevant.

However, by using RNAi to mediate gene suppression, the genomic locus of the target gene is not modified and thus temporal and reversible control of endogenous TSG could be realized. In fact, two studies, one in a model of HCC and the other in a model of Eμ-myc-driven lymphomagenesis from our lab demonstrated that tet-inducible RNAi could achieve temporal gene regulation and restore TSG activity in established tumors (Dickins et al., 2007; Xue et al.,

2007). Both of these studies highlight the role of p53 inactivation in tumor maintenance and suggest that restoration of the p53 pathway could provide therapeutic benefits for cancer patients (Dickins et al., 2007; Xue et al., 2007).

NSCLC is a deadly disease with few treatment options that have been shown to provide long-term benefits to only a small number of patients (Herbst et al., 2008). Both p53 and $p16^{INK4a/}p19^{ARF}$ have been noted to play crucial roles in lung tumorigenesis, and therefore I chose to further investigate the mechanisms by which p53 and $p16^{INK4a/}p19^{ARF}$ loss contribute to tumor initiation and maintenance. Because oncogenic *Kras* mutations are often found in combination with either p53 or $p16^{INK4a/}p19^{ARF}$ loss in human lung tumors, I developed mouse models of lung adenocarcinomas that have concomitant $Kras^{G12D}$ expression and RNAi-mediated suppression of either p53 or $p16^{INK4a/}p19^{ARF}$ TSGs.

Using the mouse models we describe in Chapter 4, I provide further evidence that RNAi can be used *in vivo* to phenocopy knockout mice. Both *p53RK* and *p16/p19RK* animals developed tumors that were indistinguishable from compound knockout/knock-in mutants and provided platforms in which tumor maintenance could be studied. In accordance to previous reports (Dickins et al., 2007; Xue et al., 2007), I anticipated tumors would regress upon TSG restoration even in the presence of oncogenic *Kras*; however, this was not entirely the case. I noted that following p53 restoration in advanced tumors, survival was increased but no change was documented by bioluminescence (Fig. 4.5-4.6). Because bioluminescence imaging can only detect tumor burden at low resolution, I interpreted the bioluminescence results as an average overview of

how multiple heterogenic tumors respond to p53 restoration. Therefore, the combined survival and bioluminescence data suggested that some tumors regress while others either remain static or show no response.

To determine whether some tumors were responding, I resorted to *in vitro* studies and fluorescence microscopy to observe what was occurring in individual tumors. Unexpectedly, most tumor cells from *p53RK* had a mesenchymal-like morphology that was uncharacteristic of respiratory epithelial cells. Fluorescence microscopy also confirmed that *p53RK* tumors lacked CC10 staining, a marker of bronchiolar epithelial cells. Surprisingly, CC10 expression was observed in tumors 1 week following p53 restoration, and this staining was mutually exclusive to GFP-marked tissue, in which p53 restoration had not yet occurred. In addition to follow-up studies at later time points after DOX withdrawal, it would be interesting to observe tumors at earlier time points for CC10, SP-C and other epithelial markers to determine whether they are in fact derived from Clara cells or type II alveolar epithelial cells. These studies would enable us to understand the role of p53 and the cooperation between p53 and oncogenic *Kras*. My studies indicate that concomitant oncogenic *Kras* and p53 loss promotes a type of “de-differentiation” that induces a shorter tumor onset and distinguishes it morphologically from *p16/p19RK* tumors, which do respond to TSG reactivation. A clearer understanding of the gene expression patterns of *p53RK* tumors and how they differ from *p16/p19RK* tumors will provide clues to why the tumors behave differently following TSG reactivation.

On the other hand, *p16/p19RK* tumors responded as seen by bioluminescence imaging when DOX was removed after 8 w.p.i (Fig 4.5). This was not the case when DOX was removed at later time points between 14-16 w.p.i. (Fig. 4.6) likely because the tumors were more advanced and have acquired additional mutations that render them resistant to $p16^{INK4a}$/$p19^{ARF}$ reactivation. It will be interesting to observe the effects of $p16^{INK4a/}p19^{ARF}$ reactivation in more detail at an earlier time point and determine whether reactivation can fully extinguish the oncogenic *Kras* stimulus that initiates lung tumorigenesis.

Finally, our study stressed the importance of identifying the genetic aberrations within individual tumors. Both p53 and $p16^{INK4a/}p19^{ARF}$ loss cooperated with oncogenic *Kras* and promoted disease with features of high-grade tumors, but our study suggested that p53 and $p16^{INK4a/}p19^{ARF}$ used alternative mechanisms to accelerate disease. It is likely that p53 loss promoted genomic instability (Zilfou and Lowe, 2009) or augmented NFκB activity (Meylan et al., 2009), both which may have contributed to the aggressiveness of *p53RK* lung tumors. p53 status may ultimately predict therapeutic response. Knowing this would prevent patients from undergoing toxic treatment regimes that would have no benefits but decrease patients' quality of life. Further studies described in Chapter 4, would enable us to characterize the gene signatures in *p53RK* and *p16/p19RK* tumors that may provide possible explanations to the differential mechanistic roles p53 and $p16^{INK4a/}p19^{ARF}$ play in *Kras*-driven lung tumorigenesis.

5.5 ES cell re-derivation for speedy mouse models

As discussed in Chapter 4, for the initial establishment of the lung adenocarcinoma mouse model, only three transgenes were required: (1) *LSL-Kras*^{G12D} to initiate lung tumorigenesis upon Cre-driven recombination (Jackson et al., 2001); (2) *ColA1*-TRE-GFP-shRNA; and (3) CCSP-rtTA (Tichelaar et al., 2000) to drive tet-regulated tumor suppressor gene inactivation in lung epithelial cells. However, after preliminary trials using microPET imaging failed to detect lung tumors in the mice, it became evident that a fourth allele, *Rosa26-LSL-luciferase* (Safran et al., 2003), would be necessary for serial *in vivo* imaging of tumors in live mice. From past experience, we knew it would be difficult to obtain large cohorts of quadruple transgenic mice at a reasonable rate, even if a large and costly breeding colony were established for this purpose. We later confirmed that our apprehension was well founded. Even after homozygous crosses (*ColA1*$^{shRNA/shRNA}$*; CCSPrtTA*$^{T/T}$ X *Rosa26*$^{luc/luc}$*; Kras*$^{LSL/WT}$*)* were established to increase the expected frequency of quadruple transgenics to 50% of the resulting progeny, the actual frequency observed was never greater than 25% in each litter. In addition, identification of quadruple transgenics requires laborious animal husbandry involving weaning, tailing for genomic DNA extraction, followed by multiple rounds of PCR-based genotyping, all which make animal studies prohibitively expensive and labor intensive.

With this in mind, I conceived of an alternative strategy that would bypass the breeding requirement and improve the rate of production of multi-allelic transgenic mice, hence the term “speedy mouse models”. Rather than produce progeny from multi-allelic crosses, we could attempt to re-derive our own ES cell lines from E3.5 embryos, cryopreserve the lines with the correct genetic configuration and then produce multi-allelic transgenic mice whenever needed (Fig. 4.9). Most ES cell lines are obtained from a commercial source, as the success rate for the establishment of ES cell lines is relatively low for inexperienced laboratories. For such a method to work, we would have to consider several factors, particularly the genetic background of the mice, which significantly influences the ease of ES cell establishment and developmental potential. In our case, the backgrounds of each mouse strain varied and therefore our ES cell lines would contain the genetic heterozygosity that would support their establishment. And secondly, we would need to provide careful culturing conditions to ensure viability and pluripotency is maintained throughout the process.

Shortly after making this initial proposal, the potentials of such an approach were revealed. In addition to having a steady supply of ES cells that could be used for mass and simultaneous generation of multi-allelic transgenic mice, our re-derived ES cells could contain the CHC allele, giving us the flexibility to later target many different shRNAs to the locus. With our application of these ES cells, we could rapidly generate mice to study multiple genes in the same context. In theory, this methodology enables us to perform small-scale screens *in*

vivo without any further *in vitro* genetic manipulations or transplantations, processes known to introduce genetic abnormalities and often produce confounding results. Furthermore, rather than using tetraploid embryo complementation, as we had used for our RNAi transgenic mice (discussed in Chapter 3), we could use blastocyst injection to generate mosaic mice. An advantage of mosaicism is that it addresses the common criticism perceived when using fully transgenic mice – that every cell in the mouse contains the transgenic modifications. The argument claims that fully transgenic mice are not completely physiologically relevant because all cells within the mice have the potential to give rise to a phenotype or create a dysfunctional microenvironment. Chimeric mice, on the other hand, contain a mixture of transgenic and WT cells and will therefore give rise to tumors surrounded by genetically normal tissues, similar to what occurs in humans.

During the time period in which the idea was conceived, we had just received the *Rosa26-LSL-luciferase* strain and were limited in their numbers. We also lacked a CHC mouse; therefore, with the help of S.Y. Kim, we proceeded with a preliminary, proof-of-principle trial to validate the approach and re-derived ES cell lines from a cross that would otherwise give rise to triple *p16/p19RK* transgenic mice (shown in Chapter 4). Using blastocyst injection of *p16/p19RK* ES cells, we generated ~40 triple transgenic chimeras simultaneously. What proved most remarkable in these mice was that the degree of tumor burden highly correlated to the degree of chimerism, as determined by the percent of black coat color, following intranasal adeno-Cre and DOX administration. All mice

with >75% black coat color acquired lung adenocarcinomas within 8-12 w.p.i. (similar to non-chimeric triple transgenics; Fig.4.12). On the other hand, mice with <50% succumbed 2-4 months later and those with <1% still show no signs of disease (data not shown). Histological examination of lung tumors from mice with <50% chimerism also revealed interesting results previously not identified in the fully transgenic mice; they had far fewer but grossly large tumors, a feature that may more closely mimic human lung cancer, a diagnosis in which patients typically develop a single lung tumor that progresses over time to metastatic disease. It has yet to be determined whether these mice showed signs of metastatic disease, but we are confident that our ongoing investigation will lead to a more conclusive pathological report.

Since then, we have been able to re-derive additional ES cell lines (L17 and L48) and test whether they would produce mosaic mice harboring *RKL* and the *ColA1* homing cassette. The L48 ES cell line successfully gave rise to mice with ~75-95% chimerism, while the majority of L17 mice ranged between 5-40%. These mice were recently treated with adeno-Cre and are currently being monitored by bioluminescence imaging for tumor onset. For future studies, we chose to carry on with the L48 line and to first assess whether these cells can undergo RMCE and still maintain pluripotency for murine development. As it was desirable to compare the chimeric animals to their germline transgenic counterparts, we targeted these cells with the same shRNAs previously described (p53.1224, p19.157, p16/p19.478 and ren.713). Only recently, L48 targeted cells were injected into blastocysts and we currently await their birth. We

envision that these mice will be a valuable resource to assess the differential responses to TSG reactivation; and given that we will have a larger cohort from the start, we will be able to investigate the dynamics of tumor maintenance in further detail. We have also begun cloning new shRNAs that will be targeted within the L48 line in order to identify and validate novel genes that cooperate with *Kras*^{G12D} to promote lung tumorigenesis.

These preliminary results were extremely promising and informative. We quickly realized that our approach would revolutionize the development and application of genetically engineered mouse models. For all fields of biological study and cancer biology in particular, the cost and speed of generating experimental cohorts have remained the biggest challenges associated with the use of genetically modified mouse models. For drug discovery and understanding toxicity, in which *in vivo* studies are mandatory, researchers and pharmaceutical companies have relied on alternatives such as xenograft models. While xenograft models have worked the best at satisfying the criteria of speed, they have proved to be problematic with few predictive achievements, poor correlation to human disease and many notable failures (Sharpless and Depinho, 2006). Not to mention, xenograft models often use mice with compromised immune systems, which is a fundamental flaw that may present mixed results.

In a relevant *Nature* review, Sharpless and DePinho define the key factors that constitute a 'good' murine model while also pointing out a number of deficiencies in existing ones used for cancer drug development (Sharpless and Depinho, 2006). In essence, tractable murine models must include moderate

penetrance and short latency of single tumors and be engineered with alleles that are representative of the human disease – all without sacrificing the ability to accurately recapitulate the evolution of the tumor microenvironment and the acquisition of cooperating lesions. In addition, they must be cost-effective and simplistic in colony management and technical use. Our “all-in-one” ES cell prototype is well suited to meet these requirements. It simultaneously addresses the many technical hurdles previously described that greatly curtail their use and possesses many desirable features that can be tailored to tackle the specific question at hand. For the initial set-up and re-derivation protocol, it does, however, require particular expertise and animal husbandry costs, but these are radically offset by the speed in which mice can be produced. We believe our approach addresses these problems and more precisely models the stochastic nature of human cancers. Already our *p16/p19RK* chimeras have demonstrated that it is possible to limit the occurrence of multi-focal lung tumors without affecting penetrance and only marginally increasing tumor onset. Importantly, this mosaic setting appears to drastically prolong survival in comparison to their fully transgenic counterparts, likely due to the decreased tumor multiplicity. We believe that this prolonged survival more faithfully translates into an environment with expanded opportunities to acquire secondary genetic or epigenetic events, and with careful serial measurements and examination of these tumors, we may begin to unravel and identify new genetic lesions that are contributing to lung tumor growth.

5.6 Identifying and validating drug targets using speedy mouse models

The “speedy mouse model” technology carries with it enormous potential in its ability to rapidly engineer complex mouse models with numerous genetic modifications. Given that the same initiating lesions are commonly observed in a broad spectrum of cancers, we can easily build upon previous models and expand our scope without having to start from “ground zero.” For example, by adding a fifth transgenic allele, $p53^{R270H}$, a dominant-negative p53 mutant (Olive et al., 2004), to our previous model, we will have created a model in which we can screen for and validate potential therapeutic targets of lung adenocarcinoma. Together, activation of both $Kras^{G12D}$ and $p53^{R270H}$ in itself will give rise to therapeutically resistant lung tumors that carry the most common genetic abnormalities seen in human lung adenocarcinoma that are poor prognostic indicators of survival (Jackson et al., 2005).

In brief detail, we will re-derive ES cells containing *LSL-*$Kras^{G12D}$; CCSP-rtTA, $p53^{R270H}$, *LSL-luciferase*, and CHC (or *CHC;RKL;*$p53^{m}$ for simplicity; Table 5.1). Prior to chimeric mouse production, we will use RMCE to incorporate shRNAs that will inhibit candidate genes and potential therapeutic targets. Following adeno-Cre delivery, we will monitor the mice by bioluminescence imaging, and once detected, we will treat the mice with doxycycline to induce RNAi-mediated gene silencing that may disrupt tumor growth and/or induce tumor regression. For control purposes, we will use the rpa3.457 shRNA that

targets an essential replication factor required for cell survival. In transplant models of acute myeloid leukemia, this shRNA has already been shown to be effective in killing highly chemo-resistant leukemic cells harboring aberrant genotypes (Zuber et al., 2009). We reason we will see similar effects in lung tumors even in the presence of *Kras* and p53 abnormalities.

In order to narrow our list candidate genes, we have established a collaborative effort with Scott Power's laboratory at CSHL. Currently, they are conducting genome-wide RNAi screens in 6 human cell lines and established mouse transplant models to uncover any genetic dependencies that will potentially lead to the discovery of a new generation of therapeutic targets. Their screen will serve as a preliminary genetic filter to limit the number candidates genes we will test *in vivo*. In addition, we will employ literature searches to identify potentially interesting candidates. For example, recent studies from both Jacks and Hahn laboratories suggest targeting members of the NF-κB pathway as a potential effective strategy for treating lung adenocarcinomas (Barbie et al., 2009; Meylan et al., 2009). We anticipate that this model will serve as an invaluable tool to effectively validate potential candidates as true targets.

Our system also offers tremendous flexibility for wide application beyond the lung adenocarcinoma model. By simply varying the tissue-specific tet-transactivator, a diverse array of cancer models may be constructed for gene and drug validation using this same method. Furthermore, we can use an alternative approach to tissue-specific promoters, which incorporates the use of CAGs-*LSL*-rtTA3, a new conditional tet-transactivator strain generated by Luke Dow, a

postdoctoral fellow in the Lowe lab. This strain will allow us to make use of the numerous existing and functionally validated tissue-specific Cre strains available without having to rely on different tet-transactivator strains for each tissue examined. Alternatively, we can deliver adeno-Cre directly to the tissue of interest for gene activation and/or deletion as we have previously done to establish the lung adenocarcinoma model. With this new technology at hand, we envision building a number of new models including one for pancreatic cancer, which already is in progress and will combine the following alleles: *LSL-Kras*^{G12D}; *LSL*-p53^{R172H}; *LSL-luciferase*; CHC; CAGs-*LSL*-rtTA3 and PDX-Cre for pancreas-specific Cre-mediated activation (Aguirre et al., 2003) (Table 5.1).

Finally, we foresee the possibility of creating models that are not solely limited to drug target identification and validation, but also directed at the testing of drug toxicity in live animals. Such efforts to test toxicity have already been made by Katie McJunkin, a graduate student within our lab. By crossing ubiquitous tet-transactivator strains (e.g. Rosa-rtTA, CMV-rtTA, CAGs-rtA3) to a mouse harboring a tet-inducible rpa3.457 shRNA, we were able to observe the effects of this killer shRNA on all tissues within the mouse. Because this shRNA targets an essential component of the DNA replication machinery, its knockdown mimicked many of the toxic effects observed in patients following chemotherapy – primarily destroying the tissue architecture in highly proliferative organs such as the intestine and causing dramatic weight loss and malnutrition. This proof-of-principle study indicates that a drug targeting rpa3 would not be useful in the clinic because of the overwhelming side effects observed. Moving forward, for

future drug toxicity studies, by simply changing the tissue-specific tet-transactivator to the strong, ubiquitous CAGs-rtTA3 allele (discussed in Chapter 3), we can build separate mouse models that resemble our existing multi-allelic cancer models but also possess the ability for global gene knockdown. In theory, we can test these models side-by-side and observe both tissue-specific and global effects of gene silencing. These results will have important implications for the future of drug therapy, by being able to examine possible negative side effects that are common and often render drugs intolerable for use. Lastly, and of practical importance, we must not fail to mention the financial impact these models could have for the drug development industry. Each year, pharmaceutical and biotech companies invest billions of dollars to identify and test the functionality of millions of compounds, some of which show promise *in vitro* and/or xenograft models – only later do they come to realize the harmful side effects in patients which ultimately result in their suspension and/or prevent further pharmacological use. With these drug toxicity models, pharmaceutical companies can gain valuable information that will help direct their efforts toward the development of effective and tolerable therapeutics without having to first exhaust considerable resources towards inevitably flawed pharmaceuticals.

5.7 Future perspectives

Before embarking on my PhD journey, I endured two grueling but important years of medical school education. During these two years, I gained

critical knowledge essential to understanding normal development as well as the many disease processes that occur in humans. This knowledge served not only to prepare me with the ability to solve clinical problems and understand the pathophysiology behind well-characterized diseases, it also exposed me to the many unexplainable phenomena clinicians face everyday. By far, cancer was the disease that perplexed me most – why our own bodies would give rise to such disarray and further, why our bodies would fail to recognize this chaos. With new therapeutics rapidly coming to life, it was still unclear to me the disparity in treatment results: why some patients with the same disease responded with great success while others showed little or even worse, no signs of improvement at all. With enormous progress in research and rapidly expanding technology, why had so many questions regarding cancer still remained unanswered?

With a continuously growing family history of cancer, I set out with the goal to not only to study the disease itself, but to also have an impact on how we can better treat the disease and prolong survival, all while increasing patients' quality of life. I also aimed at conducting research that would help dissect the intricacies of tumor biology so we could understand not just how to suppress the disease but also eradicate it. From my medical school experience, I was exposed to the clinical point of view, constantly reminded to treat patients as a whole, with a clear understanding of the interdependence of one organ on another – for example, a physician cannot independently treat a patient's liver without affecting the entire person. This invaluable lesson always helped me throughout my PhD career to remember the bigger picture – the patient.

With this understanding, I entered my PhD years and quickly began working with an important and powerful model organism – the mouse. For obvious reasons, there will never be a perfect model organism of human disease, but the mouse is by far one of the most tractable, genetically modifiable organisms invaluable in its capability to faithfully mimic human disease and predict outcomes in patients in response to therapy. The mouse has given us the ability to observe cancer from a different perspective outside of the clinic – a purely genetic perspective. By altering its genetic makeup through a gene-by-gene approach, we have been able to slowly disentangle the overwhelming pieces of the cancer puzzle and identify gene mutations that create growth advantages and others that render vulnerabilities, therefore providing opportunities to target cancers for destruction. By expanding upon existing technologies and creating a method for rapid engineering of mouse models, my research will provide pivotal tools to enable continuing research to further tease apart and better understand the complex signaling pathways, pharmacological interactions, molecular and biological processes together that contribute to disease.

What has proved most exciting to me is learning how we can better model human disease, not just by combining genetic mutations, but also by using our ability to modify genetic factors which in turn create a more physiological environment within the mouse that better reflects what occurs in humans. For example, I have been given an opportunity to create a new mouse model of ovarian cancer. For this, the genetic combination that will best reflect the human

disease is similar to that observed in both the lung and pancreatic models: an activating mutation in *Kras* and inactivation of p53 specifically in ovarian epithelial cells (Bast et al., 2009). While these two lesions will likely promote ovarian epithelial hyperplasia and possibly tumors, they fail to take into account the physiological and/or hormonal changes that also occur in the typical patient with ovarian cancer. These women are predominantly of peri- or postmenopausal age and therefore are experiencing significant changes within the ovary and also systemically: (1) a reduction or depletion of oocytes; (2) a reduction in circulating steroid hormone levels (e.g. estrogen and progesterone); and (3) a dramatic increase in gonadotropic hormones (e.g. LH and FSH) (Vanderhyden, 2005). Several animal models have demonstrated that premature ovarian failure resulting from induced depletion of germ cells consistently yields ovarian surface epithelial hyperplasia with invasion into the stroma and development of ovarian adenomas, both believed to be precursors to ovarian cancer (Craig et al.; Duncan and Chada, 1993; Hoyer et al., 2009). A model that will best represent ovarian cancer in humans will not only incorporate the most common genetic changes but also induce postmenopausal changes that are found to exist in the majority of patients. To accomplish this, I will engineer a model that combines our shRNA technology with existing genetic tools to recapitulate menopause by the loss of oocytes. Specifically, I will clone a transgene that uses the oocyte-specific promoter, *ZP3* (a zona pellucida glycoprotein), to express the rpa3.457 shRNA and therefore cause destruction of the oocytes. With this allele, we will create several murine models of ovarian cancer containing various genetic

combinations that direct specific tumor types. These models will serve as tools to either identify genes that contribute to tumor development or validate potential therapeutic targets of ovarian cancer. Moreover, from a therapeutic point of view, drastic endocrinological changes may alter therapeutic responses, and therefore a model that incorporates these changes will likely serve as a better predictor of therapeutic outcome.

The possibility to create a sophisticated model of ovarian cancer is only the beginning. Although my PhD training has come to an end, I plan to continue my collaborations to design even more complex models of human disease. I endeavor to apply what I have learned in the lab as I transition toward the clinical wards to complete my MD/PhD training. Throughout the course of my work, I have learned a great deal about the genetics of cancer. However, such knowledge is not without ethical responsibilities and considerations of societal constructs. My PhD career has transformed me into a mouse modeler and given me enormous insight into our capabilities to genetically manipulate and engineer animals tailored for our specific use. It is a power that comes with many responsibilities, as these genetic insights in mice can be prospectively translated and potentially engineered in humans. With the completion of the Human Genome Project and the dramatic decrease in the cost for genomic sequencing, we will soon enter an age of gene information overload and we will need to prepare our collective society for how we will use the new DNA knowledge that will certainly emerge in the not so distant future. As history has taught us, we must examine and foresee the possibilities that will arise from this genetic

evolution. We must pave the road and define ethical boundaries, in order to prevent the misuse of genetic information and protect patient privacy. As I prepare myself for reentry into the clinical wards, I realize that I will undoubtedly face many ethical dilemmas involving genetic testing and manipulation. As a future MD/PhD, I hope to help patients cope with and make informed decisions in response to the increasing genetic information that will be available to them.

Finally, during my PhD career, I have faced failure, endured humiliation, persevered in spite of exhaustion, and taken enormous risks when simpler alternatives were in sight. Most importantly, I have taught myself that “if there is a will, there is a way.” I thank my parents, family and friends for instilling within me that *will*.

5.8 References

Aguirre, A.J., Bardeesy, N., Sinha, M., Lopez, L., Tuveson, D.A., Horner, J., Redston, M.S., and DePinho, R.A. (2003). Activated *Kras* and $p16^{INK4a/}p19^{ARF}$ deficiency cooperate to produce metastatic pancreatic ductal adenocarcinoma. Genes Dev *17*, 3112-3126.

Barbie, D.A., Tamayo, P., Boehm, J.S., Kim, S.Y., Moody, S.E., Dunn, I.F., Schinzel, A.C., Sandy, P., Meylan, E., Scholl, C.*, et al.* (2009). Systematic RNA interference reveals that oncogenic KRAS-driven cancers require TBK1. Nature *462*, 108-112.

Bast, R.C., Jr., Hennessy, B., and Mills, G.B. (2009). The biology of ovarian cancer: new opportunities for translation. Nat Rev Cancer *9*, 415-428.

Beard, C., Hochedlinger, K., Plath, K., Wutz, A., and Jaenisch, R. (2006). Efficient method to generate single-copy transgenic mice by site-specific integration in embryonic stem cells. Genesis *44*, 23-28.

Bell, A.C., and Felsenfeld, G. (2000). Methylation of a CTCF-dependent boundary controls imprinted expression of the Igf2 gene. Nature *405*, 482-485.

Chin, L., Tam, A., Pomerantz, J., Wong, M., Holash, J., Bardeesy, N., Shen, Q., O'Hagan, R., Pantginis, J., Zhou, H.*, et al.* (1999). Essential role for oncogenic Ras in tumour maintenance. Nature *400*, 468-472.

Craig, Z.R., Davis, J.R., Marion, S.L., Barton, J.K., and Hoyer, P.B. 7,12-dimethylbenz[a]anthracene induces sertoli-leydig-cell tumors in the follicle-depleted ovaries of mice treated with 4-vinylcyclohexene diepoxide. Comp Med *60*, 10-17.

Dickins, R.A., McJunkin, K., Hernando, E., Premsrirut, P.K., Krizhanovsky, V., Burgess, D.J., Kim, S.Y., Cordon-Cardo, C., Zender, L., Hannon, G.J.*, et al.* (2007). Tissue-specific and reversible RNA interference in transgenic mice. Nat Genet *39*, 914-921.

Duncan, M.K., and Chada, K.K. (1993). Incidence of tubulostromal adenoma of the ovary in aged germ cell-deficient mice. J Comp Pathol *109*, 13-19.

Fedoriw, A.M., Stein, P., Svoboda, P., Schultz, R.M., and Bartolomei, M.S. (2004). Transgenic RNAi reveals essential function for CTCF in H19 gene imprinting. Science *303*, 238-240.

Felsher, D.W., and Bishop, J.M. (1999). Reversible tumorigenesis by MYC in hematopoietic lineages. Mol Cell *4*, 199-207.

Fisher, G.H., Wellen, S.L., Klimstra, D., Lenczowski, J.M., Tichelaar, J.W., Lizak, M.J., Whitsett, J.A., Koretsky, A., and Varmus, H.E. (2001). Induction and apoptotic regression of lung adenocarcinomas by regulation of a K-Ras transgene in the presence and absence of tumor suppressor genes. Genes Dev *15*, 3249-3262.

Guglielmi, L., Le Bert, M., Truffinet, V., Cogne, M., and Denizot, Y. (2003). Insulators to improve expression of a 3(')IgH LCR-driven reporter gene in transgenic mouse models. Biochem Biophys Res Commun *307*, 466-471.

Hasuwa, H., Kaseda, K., Einarsdottir, T., and Okabe, M. (2002). Small interfering RNA and gene silencing in transgenic mice and rats. FEBS Lett *532*, 227-230.

Herbst, R.S., Heymach, J.V., and Lippman, S.M. (2008). Lung cancer. N Engl J Med *359*, 1367-1380.

Hitz, C., Wurst, W., and Kuhn, R. (2007). Conditional brain-specific knockdown of MAPK using Cre/loxP regulated RNA interference. Nucleic Acids Res *35*, e90.

Hoyer, P.B., Davis, J.R., Bedrnicek, J.B., Marion, S.L., Christian, P.J., Barton, J.K., and Brewer, M.A. (2009). Ovarian neoplasm development by 7,12-dimethylbenz[a]anthracene (DMBA) in a chemically-induced rat model of ovarian failure. Gynecol Oncol *112*, 610-615.

Hsiao, Y.C., Chang, H.H., Tsai, C.Y., Jong, Y.J., Horng, L.S., Lin, S.F., and Tsai, T.F. (2004). Coat color-tagged green mouse with EGFP expressed from the RNA polymerase II promoter. Genesis *39*, 122-129.

Jackson, E.L., Olive, K.P., Tuveson, D.A., Bronson, R., Crowley, D., Brown, M., and Jacks, T. (2005). The differential effects of mutant p53 alleles on advanced murine lung cancer. Cancer Res *65*, 10280-10288.

Jackson, E.L., Willis, N., Mercer, K., Bronson, R.T., Crowley, D., Montoya, R., Jacks, T., and Tuveson, D.A. (2001). Analysis of lung tumor initiation and progression using conditional expression of oncogenic K-ras. Genes Dev *15*, 3243-3248.

Kaffer, C.R., Srivastava, M., Park, K.Y., Ives, E., Hsieh, S., Batlle, J., Grinberg, A., Huang, S.P., and Pfeifer, K. (2000). A transcriptional insulator at the imprinted H19/Igf2 locus. Genes Dev *14*, 1908-1919.

Lickert, H., Cox, B., Wehrle, C., Taketo, M.M., Kemler, R., and Rossant, J. (2005). Dissecting Wnt/beta-catenin signaling during gastrulation using RNA interference in mouse embryos. Development *132*, 2599-2609.

Meylan, E., Dooley, A.L., Feldser, D.M., Shen, L., Turk, E., Ouyang, C., and Jacks, T. (2009). Requirement for NF-kappaB signalling in a mouse model of lung adenocarcinoma. Nature *462*, 104-107.

Moody, S.E., Sarkisian, C.J., Hahn, K.T., Gunther, E.J., Pickup, S., Dugan, K.D., Innocent, N., Cardiff, R.D., Schnall, M.D., and Chodosh, L.A. (2002). Conditional activation of Neu in the mammary epithelium of transgenic mice results in reversible pulmonary metastasis. Cancer Cell *2*, 451-461.

Neal, J.W., and Sequist, L.V. First-line use of EGFR tyrosine kinase inhibitors in patients with NSCLC containing EGFR mutations. Clin Adv Hematol Oncol *8*, 119-126.

Nyabi, O., Naessens, M., Haigh, K., Gembarska, A., Goossens, S., Maetens, M., De Clercq, S., Drogat, B., Haenebalcke, L., Bartunkova, S.*, et al.* (2009). Efficient mouse transgenesis using Gateway-compatible ROSA26 locus targeting vectors and F1 hybrid ES cells. Nucleic Acids Res *37*, e55.

Olive, K.P., Tuveson, D.A., Ruhe, Z.C., Yin, B., Willis, N.A., Bronson, R.T., Crowley, D., and Jacks, T. (2004). Mutant p53 gain of function in two mouse models of Li-Fraumeni syndrome. Cell *119*, 847-860.

Olson, A., Sheth, N., Lee, J.S., Hannon, G., and Sachidanandam, R. (2006). RNAi Codex: a portal/database for short-hairpin RNA (shRNA) gene-silencing constructs. Nucleic Acids Res *34*, D153-157.

Paddison, P.J., Silva, J.M., Conklin, D.S., Schlabach, M., Li, M., Aruleba, S., Balija, V., O'Shaughnessy, A., Gnoj, L., Scobie, K.*, et al.* (2004). A resource for large-scale RNA-interference-based screens in mammals. Nature *428*, 427-431.

Potts, W., Tucker, D., Wood, H., and Martin, C. (2000). Chicken beta-globin 5'HS4 insulators function to reduce variability in transgenic founder mice. Biochem Biophys Res Commun *273*, 1015-1018.

Safran, M., Kim, W.Y., Kung, A.L., Horner, J.W., DePinho, R.A., and Kaelin, W.G., Jr. (2003). Mouse reporter strain for noninvasive bioluminescent imaging of cells that have undergone Cre-mediated recombination. Mol Imaging *2*, 297-302.

Seibler, J., Kuter-Luks, B., Kern, H., Streu, S., Plum, L., Mauer, J., Kuhn, R., Bruning, J.C., and Schwenk, F. (2005). Single copy shRNA configuration for ubiquitous gene knockdown in mice. Nucleic Acids Res *33*, e67.

Seidler, B., Schmidt, A., Mayr, U., Nakhai, H., Schmid, R.M., Schneider, G., and Saur, D. (2008). A Cre-loxP-based mouse model for conditional somatic gene expression and knockdown in vivo by using avian retroviral vectors. Proc Natl Acad Sci U S A *105*, 10137-10142.

Sharpless, N.E., and Depinho, R.A. (2006). The mighty mouse: genetically engineered mouse models in cancer drug development. Nat Rev Drug Discov *5*, 741-754.

Shepherd, F.A. (2005). A targeted approach to reducing lung cancer mortality. J Clin Oncol *23*, 3173-3174.

Shepherd, F.A., Rodrigues Pereira, J., Ciuleanu, T., Tan, E.H., Hirsh, V., Thongprasert, S., Campos, D., Maoleekoonpiroj, S., Smylie, M., Martins, R.*, et al.* (2005). Erlotinib in previously treated non-small-cell lung cancer. N Engl J Med *353*, 123-132.

Shinagawa, T., and Ishii, S. (2003). Generation of Ski-knockdown mice by expressing a long double-strand RNA from an RNA polymerase II promoter. Genes Dev *17*, 1340-1345.

Soucek, L., Whitfield, J., Martins, C.P., Finch, A.J., Murphy, D.J., Sodir, N.M., Karnezis, A.N., Swigart, L.B., Nasi, S., and Evan, G.I. (2008). Modelling Myc inhibition as a cancer therapy. Nature *455*, 679-683.

Stein, P., Svoboda, P., and Schultz, R.M. (2003). Transgenic RNAi in mouse oocytes: a simple and fast approach to study gene function. Dev Biol *256*, 187-193.

Tichelaar, J.W., Lu, W., and Whitsett, J.A. (2000). Conditional expression of fibroblast growth factor-7 in the developing and mature lung. J Biol Chem *275*, 11858-11864.

Vanderhyden, B.C. (2005). Loss of ovarian function and the risk of ovarian cancer. Cell Tissue Res *322*, 117-124.

Wang, J., Theunissen, T.W., and Orkin, S.H. (2007). Site-directed, virus-free, and inducible RNAi in embryonic stem cells. Proc Natl Acad Sci U S A *104*, 20850-20855.

Xue, W., Zender, L., Miething, C., Dickins, R.A., Hernando, E., Krizhanovsky, V., Cordon-Cardo, C., and Lowe, S.W. (2007). Senescence and tumour clearance is triggered by p53 restoration in murine liver carcinomas. Nature *445*, 656-660.

Zhu, X.D., Pan, G., Luetke, K., and Sadowski, P.D. (1995). Homology requirements for ligation and strand exchange by the FLP recombinase. J Biol Chem *270*, 11646-11653.

Zhu, X.D., and Sadowski, P.D. (1995). Cleavage-dependent ligation by the FLP recombinase. Characterization of a mutant FLP protein with an alteration in a catalytic amino acid. J Biol Chem *270*, 23044-23054.

Zilfou, J.T., and Lowe, S.W. (2009). Tumor Suppressive Functions of p53. Cold Spring Harb Perspect Biol *1*, a001883.

Zuber, J., Radtke, I., Pardee, T.S., Zhao, Z., Rappaport, A.R., Luo, W., McCurrach, M.E., Yang, M.M., Dolan, M.E., Kogan, S.C.*, et al.* (2009). Mouse models of human AML accurately predict chemotherapy response. Genes Dev *23*, 877-889.

Chapter 6

Material and Methods

6.2 Materials and methods

Retroviral vectors, transgene cassettes and targeting constructs

The retroviral SIN-TRE-GFP-miR30-PGK-Puro (TGMP) vector was generated by modification of the SIN-TRE-PIG vector (Dickins et al., 2005). We generated GFP and miR30 fragments by PCR, digested them with SalI or AgeI/BamHI respectively, and cloned them in sequentially into SIN-TRE-PIG digested with XhoI/EcoRV, yielding SIN-TRE-GFP-miR30 (TGM). To add a selectable marker, we digested the TGM vector with *Bgl* II/ *BamHI* restriction enzymes and ligated the fragment into MSCV-PGKpuro-SIN to generate TGMP.

The pWhere vector containing H19 insulator sequences was obtained from Invivogen. The TGM fragment was isolated by BglII/NheI restriction enzymes from pTGMP and ligated into and cloned into the MCS (multiple cloning site) of pWhere using BamHI/NheI restriction enzymes. The p53.1224 shRNA was cloned into pWhere-TGM by XhoI/EcoRI. The pWhere-TGM-p53.1224 vector was digested with BglII/NheI or BglII/HpaI or PacI restriction enzymes to generate the Salt, Pepper and H19TGM transgene fragments, respectively (1.2-kb, 1.5-kb and 6.2-kb in size).

The pBS31 flp-in and pCAGGS-FLPe-puro vectors and ColA1 3' probe were generously provided by the Jaensich laboratory (Beard et al., 2006). To generate the pColTGM flp-in vector, we first destroyed the XhoI site in the pBS31 flp-in vector by XhoI digestion, klenow treatment and blunt religation. We generated a GFP-miR30 PCR fragment, digested it with MfeI and ligated into the

pBS31 flp-in vector digested with EcoRI. 110-bp XhoI-EcoRI DNA fragments encoding shRNA-mirs targeting p53, INK4a/ARF, ARF and *luciferase* were subcloned into pColTGM. Cloning strategies and primer sequences are available on request.

Transgenic mice

Transgenic mice were generated by standard pronuclear injection procedures of the transgene fragments previously described. All founders were generated on a C57BL/6 background. Mice were genotyped by PCR using the primers listed in Table 6.1. Other mouse lines used were LAP-tTA (Kistner et al., 1996), Rosa26-M2rtTA (Beard et al., 2006), CMV-rtTA (Wiekowski et al., 2001) , CAGs-rtTA3 (Chapter 3), CCSP-rtTA (Tichelaar et al., 2000) , *LSL-Kras*^{G12D} (Jackson et al., 2001), and Rosa26-*LSL-luciferase* (Safran et al., 2003). CAG-rtTA3 mice were generated using pronuclear injection and genotyped by PCR (Table 6.1). rtTA3 Southern blots were performed on genomic DNA digested with BamHI, using a probe covering the coding region of rtTA3.

Isolation of genomic DNA

Tail fragments were digested overnight at 55°C in lysis buffer with Proteinase K, boiled at 95°C for 15 min and centrifuged at 13,000 rpm for 5 min. PCR primers are listed on Table 6.1.

Isolation, culture and retroviral infection of mouse embryonic fibroblasts

Mouse embryonic fibroblasts (MEFs) were isolated from E13.5 (embryonic day) embryos with the head and fetal liver removed. The embryonic tissue was manually dissected into small pieces and further digested with 0.05% trypsin-EDTA for 45 min. Cultures were maintained in DMEM containing 10% FBS. Doxycycline (Sigma) was refreshed in cell culture medium (1μg/mL) every 2 days. Retroviral-mediated gene transfer was performed using Phoenix packaging cells (G. Nolan, Stanford University, Stanford, CA) as described (Schmitt et al., 2002). Population doubling and colony formation assays were as described.

Immunoblotting

Fresh tumor tissue or cell pellets were lysed in RIPA or Laemmli buffer using a tissue homogenizer. Equal amounts of protein (16 μg) were separated on 10-15% SDS-polyacrylamide gels, and then transferred to PVDF membranes. The blots were probed with antibodies against p53 (Vector Laboratories, IMX25, 1:1000), Tubulin (B-5-1-2, Sigma; 1:5000), p16 (Santa Cruz, M156, 1:500), p19 (5-C3-1, Affinity BioReagents, MA1-16665, 1:500), Oct4 (MAB4305, Millipore), (APC (FE-9, Calbiochem) and GFP-HRP (Hypromatrix, 1:10,000).

Small RNA Northern blot

To isolate total RNA, we lysed cultured cells in 1 ml of Trizol (Invitrogen). We separated 30 g of RNA on a denaturing acrylamide gel, transferred it to Hybond N+ membrane (Amersham) and probed it with end-labeled oligonucleotides complementary to predicted siRNAs.

ES cell culture, targeting and expression analysis

The pColTGM-shRNA targeting vectors were introduced into KH2 ES cells by coelectroporation of 50 µg pColTGM-shRNA with 25 µg pCAGGS-FLPe at 400 V and 125 µF using two pulses in a Gene PulserII (Bio-Rad, Hercules, CA). Immediately following electroporation, small subpopulations of ES cells were plated in DOX-containing media for 36-48 h and screened for GFP expression by flow cytometry (Guava EasyCyte, Guava Technologies) to assess the elecroporation efficiency. Only cultures with >10% GFP expression were continued and selected in 140 µg/ml hygromycin. DNA from GFP positive, hygromycin-resistant picked clones were digested with SpeI and analyzed for correct targeting using the ColA1 3' probe. In most cases, Southern blot analyses showed a single transgenic integration in the ES cells clones when compared to founder mice generated by pronuclear injection (Supplementary Fig. 2c). However, we have observed that 10-20% of clones show additional random integration and as such recommend that Southern blots be performed prior to mouse production.

ES cell cultures were maintained on irradiated (4.0 Gy) primary mouse embryonic fibroblasts derived from the DR4 mouse strain (Tucker et al., 1997). To test ES cells containing TGM-shLuc.1309 for functional *luciferase* knockdown, we infected ES cells with MSCV-IRES-*luciferase* (Zuber et al., 2009) and treated cells with 1µg/ml doxycycline-hyclate (Sigma) for 4 days prior to qualitative bioluminescence imaging (IVIS100, Caliper LifeSciences). For all *Trp53* protein

blots in Figure 2 and Figure 3, cells were treated with 1μg/ml adriamycin for 2–4 h to induce *Trp53*. To assess survival of ES cells following DNA damage, 50,000 ES cells, pre-treated with and without dox for 4 days, were plated on gelatin-coated 96-well plates. Cells were treated with Adriamycin (0.4-256 ng/ml) for 12 h, stained with propidium iodide (1 μg/ml) and counted by flow cytometry (Guava EasyCyte, Gauva Technologies). MEF cultures and protein blotting were performed as described previously (Dickins et al., 2005).

ES cell-derived mice

ES cell-derived mice containing cTGM-shRNAs were generated by tetraploid embryo complementation (Eggan et al., 2002). Founder mice were backcrossed onto C57BL/6 and crossed to other mouse lines including Vav-tTA (Kim et al., 2007) and *Rosa26-luciferase* (Safran et al., 2003). *Rosa26-luciferase* mice were produced from a cross between Rosa26-*LSL-luciferase* females and Stra8-Cre males (Sadate-Ngatchou et al., 2008). Mice were genotyped by PCR using shRNA-specific forward primers and a RGBpA common reverse primer (Table 6.1), yielding a 250-bp product. Doxycycline was administered to mice in food pellets (625mg/kg) from Harlan Teklad. The Cold Spring Harbor Animal Care and Use Committee approved all procedures described in this work.

RNA isolation, cloning and bioinformatic analysis

RNA was extracted, purified, cloned and analyzed as previously described (Malone et al., 2009). Briefly, RNA was purified from ~1.0×10^6 MEFs after

extraction using TRIZOL® reagent (Invitrogen™), followed by phenol/choloroform/isoamyl alcohol and chloroform purifications. After 5' and 3' adapter ligations and PCR, 18-29nt small RNA libraries were sequenced on the Illumina®/Solexa™ platform. Sequence reads were first clipped and redundant sequences collapsed; any sequencing artifacts (unclipped or low-complexity sequences) were removed from any further analysis. Then, structural RNA degradation products from tRNAs, rRNAs, snoRNAs, snRNAs and smRNAs were also filtered from analysis. The number of remaining sequences were scaled to determine normalization factors for cross-comparison of all libraries (Supplementary Table 1). Remaining sequences were then mapped against the latest *Mus musculus* miRBase catalog (http://www.mirbase.org/), and the full-length *luciferase* shRNA vector sequence to determine miRNA abundances in all sequenced libraries (Supplementary Tables 1 and 2). Annotated sequencing reads were then scaled for subsequent analysis, using the determined normalization factors.

RNA extraction and quantitative real-time PCR

Total RNA was harvested using TRizol reagent according to the manufacturers instructions (Invitrogen, Carlsbad, CA). For quantitative analysis of mRNA levels, cDNA was created from 1ug total RNA using random primers and MultiScribe reverse transcriptase (Applied Biosystems) and amplified by PCR with SYBR Green® dye detection method (Applied Biosystems, Warrington UK) as per manufacturers specifications. Primers were described previously

(Niwa et al and Kado et al BBRC 2008, Takahashi and Yamanaka Cell 2006) and PCR product detection was performed on the IQ5 iCycler (BioRad) under standard conditions.

Image acquisition and manipulation

Brightfield images of cells were captured on a Nikon TE2000-S inverted microscope (Nikon, Tokyo, Japan) using a 10X objective (Nikon, NA 0.3) and a Spot Insight QE CCD camera (Diagnostic Instruments, Sterling Heights, MI). Fluorescence and H&E stained sections were imaged on a Zeiss Axioscope Imager Z.1 using a 10x objective (Zeiss NA 0.3) and an ORCA/ER CCD camera (Hamamatsu Photonics, Hamamatsu, Japan). Whole embryo GFP fluorescence images were acquired on a Nikon SMZ1500 dissecting scope equipped with a DXM1200F CCD camera (Nikon). For bioluminescence imaging, mice were anesthetized with isoflurane, and ventral hair removed using Nair. Topical application to the ventral area was performed using felt applicators soaked in a luciferin-DMSO solution (5.6mg/ml in 40% DMSO-PBS). Bioluminescent imaging was performed 10 min following luciferin-DMSO treatment using an IVIS100 imaging system (Caliper LifeSciences). Tissues and embryos were submerged in luciferin-DMSO prior to imaging. *Image manipulation:* Raw .tif files were processed using Image J freeware (rsb.info.nih.gov/ij) and Photoshop CS software (Adobe Systems Inc., San Jose, CA) to measure greyscale levels and apply false coloring. MicroPET imaging was performed at Brookhaven National Laboratory according the previous studies (Woo et al., 2008).

Intranasal adeno-*Cre *administration

Adeno-Cre was purchased from the University of Iowa Gene Transfer Vector Core. Adeno-Cre:CaPi coprecipitates were generated by mixing 2.5 µl of Adeno-Cre (2.5 x 10^7 PFU), 121.9 µl MEM and 0.6 µl of $CaCl_2$ and letting sit for ~20 prior to use. Mice were anesthetized with 2% isoflurane and using a pipette tip, 125 µl of Adeno-Cre:CaPi was pipetted into the nostrils of each mouse.

Histopathology and immunofluorescence

Lung plucks were first inflated with either PBS or 10% buffered formalin and embedded them in paraffin, then stained sections (5 m) with hematoxylin and eosin (H&E) according to standard protocols. For tumor burden analyses (Fig. 4.5A), all lung lobes were orientated in the same manner and 2 cross sections 5 mm apart where taken toward the mid-section. NDP view software (Hamamatsu) was used for tumor quantification. For detection of CC10, fresh lung slices were prepared fixed in paraformaldehyde for 10 min and then incubated first in 10% normal goat serum for 30 min and then at 4 °C with CC10 primary antibody (rabbit antibody, Seven Hills Bioreagents, WRAB-CCSP). We next incubated the slices with biotinylated goat rabbit-specific immunoglobulins (Vector Laboratories) at 1:500 dilution for 30 min and then with avidin–biotin peroxidase complexes (1:25; Vector Laboratories) for 30 min.

Tumor digestion for single cell suspension

Tumor were harvested into cold PBS and cut to small pieces manually with

scissors and then digested with digestion media [10% Trypsin-EDTA (0.25%), 10% Collagenase IV (10 mg/ml in HBSS, 10% Dispase (4mg/ml) in Hank's Buffered Salt Solution (HBSS, Sigma)] for 45 min. Digestions were filtered through 100 µm filters, treated with ACK buffer for 5 min and plated in LHC-9 media (Gibco) with 10% FBS and Pen-strep.

Derivation of Murine ES Cell Lines

Provided by: CSHL Gene Targeting and Transgenic Mouse Shared Resource

Materials and Reagents

Feeder layer-Mouse embryonic fibroblast cells: CF-1

Mouse fibroblast MEF (CF-1) : ATCC .cat#:SCRC-1040

Mineral oil: Cooper Sergical cat#:4008-5

M2 medium (Millipore. cat #: MR-015-D. 50 ml)

KSOM +AA medium (Millipore. cat#: MR-121-D. 50 ml)

Phosphate-buffered saline (PBS)-Ca/Mg free (Invitrogen. cat#14190-144. 500ml)

1X -0.25% Typsin-EDTA (Invitrogen. cat#:25200-056. 100ml)

10X -0.50% Typsin-EDTA (Invitrogen. cat# 15400-054 100ml)

Mitomycine-C (Roche. cat#: 107409. 2mg)

0.1% Gelatin with ultrapure water (Millipore. cat#:ES-006-B. 500ml)

Tyrode's solution acidic (Sigma. cat# T1788. 100ml)

ES-SR Culture Medium (500 ml)

Knockout Dulbecco's modified Eagle's medium

(Invitrogen:Cat# 10829-018):425 ml

20% knockout Serum-Replacement (SR)

(Invitrogen. Cat. no. 10828-028):75 ml

Nonessential amino acids

(Invitrogen:NEAA):5 ml

Penicillin-Streptomycin-Glutamine

(Invitrogen:PSG):5 ml

2-mercaptoethanol (Sigma): dissolve 7 micro liters of 2-ME in 5 ml of PSG

Recombinant mouse Leukemia inhibitor factor (LIF): 50 micro liters (1,000U/ml)
Chemicon International Cat # :ESGRO-1107

Remove of Zona Pellucida

The blastocysts were cultured in 50 micro liter drops of Acid's for 2 minutes to dissolve the zona pellucida. After removed zona pellucida was washed approximately two to three times in a M2 medium and cultured 4-well feeder layer plates.

Preparation of MEF Feeder Layers

We used a feeder layer of mouse CF-1 embryonic fibroblasts (MEF) that was obtained from ATCC. We have used MEFs from different mouse strains and they did not differ ability to support the process of ES cell derivation. We normally used the early passage between 3-5 of MEFs. The more than passage number 6 of MEFs were have lower viability during the derivation ES cells. The MEF cells were mitotically inactivated by treatment with mitomycin-C for 2 hours.

Superovulation and blastocysts collection
Day 1 PMSG (pregnant mare's serum gonadotropin) Injection: 2:45PM
Day 3 hCG (human chorionic gonadotropin) injection: 2-3PM PM
mated with stud male
Day 4 Plugged females: morning
Day 6 Preapre of feeder layer in 4 well plates: afternoon
Day 7 Blastocysts collection: 9-10AM
ES-SR medium change for feeder plates
blastocyst culture in feeder layer: 3-5PM
Day 10 ES-SR medium change
Day 11 ES-SR medium change and Prepare of feeder plates for ICM cells

Day 12 ES-SR medium changes
Day 13 ICM cells disaggregation and culture in feeder layer
Day 14 ES-SR medium changes
Day 15 Observe of small ES cell-like colonies

Procedure

1. Day before prepared of KSOM+AA blastcysts culture five 80 micro liter of drops. In 60 mm tissue culture dishes and covered mineral oil and put into 37 degree CO2 incubator.
2. Flush the blastocysts from the uterine horns with M2 medium in 60 mm tissue culture dishes.
3. Collection of blastocysts (9AM) and cultured until develop to expanded blastocysts (3-4 PM).
4. Removed zona pelluida by Tyrode's solution Acid's and washed in M2
5. Wash with PBS and add of 1 ml of ES/SR medium for CF-1 feeder layer 4-well plates for balstocysts culture.
6. Culture of one blastocyst in per-4-well plate.
7. After 2 –3 days of culture-the blastocysts was attach to the surface of tissue culture dish with spreading of the trophoblast cells.
8. After 6 days cultured and ICM outgrowth selected
9. Aspirate the media from the 4 wells and add 0.5 ml of PBS to the wells
10. Place 4 X 30 micro liter drops of trypsin-EDTA (0.5%-10X-dilutied (1:9) with PBS) in 6 mm plate
11. Using pulled Pasteur pipette with fine capillary –gently ICM clump and remove it from trophoblat cells and place it into a Trypsin drop
12. Incubate 5 minutes
13. Using pulled basteur pipette: Break up the ICM into smaller clumps pf the cells (about 10 –15 cells)
14. Transfer cells suspension into fresh feeder 4-well contain ES/SR media
15. Repeat the procedure with rest of ICMs
16. Change the ES/SR medium after overnight incubation
17. After 3 days: Observe of ES cell-like colonies. Watch colonies growth everyday
18. Large ES like colonies can disaggregated individually in the 6-well plate

Table 6.1 | PCR primers

Transgene	Forward primer	Reverse primer	Product
Salt / Pepper / H19TGM	AAGTGAAAGTCGAGC TCGGTACCCG	TGAGCAAAGACCCCAA CGAGAA	240 bp
rtTA[1]	GCTTGGTGTAGAGCA GCCTACAC	CAGCGCTGAGTGCATA TAACGCG	358bp
Rosa-rtTA[2]	A: AAAGTCGCTCTGA GTTGTTAT B: GCGAAGAGTTTGT CCTCAACC	C: GGAGCGGGAGAAA TGGATATG	300 bp WT allele 500 bp rtTA allele
CAGs-rtTA[3]	CAGGGCGGGGTTCGG CTTCT	AGTCTACTCATGGTTG TGGCCA	300 bp
ColA1-TGM-shRNA	AATCATCCCAGGTGC ACAGCATTGCGG	ColA1-rev: CTTTGAGGGCTCATGA ACCTCCCAGG SApA-rev: ATCAAGGAAACCCTGG ACTACTGCG	218 bp WT allele 283 bp targeted allele
p53.1224	TGTATTACACATGTAC TTGTAGTGG	GAAAGAACAATCAAGG GTCC	~240 bp
p16/p19.478	GATGTAAACACAAAGA GCACC	GAAAGAACAATCAAGG GTCC	~240 bp
p19.157	CAGATGTATGTTCACG AAAGC	GAAAGAACAATCAAGG GTCC	~240 bp
Oct4.468	ACAGATGTAAAACTGT TCTAGCTC	GAAAGAACAATCAAGG GTCC	~240 bp
luc.1309	GATGTATTAATCAGAG ACTTC	CACCCTGAAAACTTTG CCCC	~240 bp
LSL-Kras^{G12D}	WT: GTCGACAAGCTC ATCGCCC Mutant: CCATGGCTTG AGTAACTCTGC	CGCAGATGTAGAGCAG CG	500 bp WT allele 550 bp mutant allele
LSL-luciferase	WT: CGTGATCTGCAA CTCCAGTC LUC: CCAGGGATTTCA GTCGATGT	WT: GGAGCGGGAGAA ATGGATATG LUC: AATCTGACGCAG GCAGTTCT	450 bp WT allele 180 bp *luciferase* allele
CHC	GGATGTGGAATGTGT GCGAG	WT: GGATGTGGAATG TGTGCGAG pArev: CTTTGAGGGCT CATGAACCTCCCAGG	218 bp WT allele 352 bp CHC allele

Reference List

Adams, J.M., Harris, A.W., Pinkert, C.A., Corcoran, L.M., Alexander, W.S., Cory, S., Palmiter, R.D., and Brinster, R.L. (1985). The c-myc oncogene driven by immunoglobulin enhancers induces lymphoid malignancy in transgenic mice. Nature *318*, 533-538.

Aguirre, A.J., Bardeesy, N., Sinha, M., Lopez, L., Tuveson, D.A., Horner, J., Redston, M.S., and DePinho, R.A. (2003). Activated Kras and Ink4a/Arf deficiency cooperate to produce metastatic pancreatic ductal adenocarcinoma. Genes Dev *17*, 3112-3126.

Andressoo, J.O., Mitchell, J.R., de Wit, J., Hoogstraten, D., Volker, M., Toussaint, W., Speksnijder, E., Beems, R.B., van Steeg, H., Jans, J.*, et al.* (2006). An Xpd mouse model for the combined xeroderma pigmentosum/Cockayne syndrome exhibiting both cancer predisposition and segmental progeria. Cancer Cell *10*, 121-132.

Appella, E., and Anderson, C.W. (2001). Post-translational modifications and activation of p53 by genotoxic stresses. Eur J Biochem *268*, 2764-2772.

Baer, A., and Bode, J. (2001). Coping with kinetic and thermodynamic barriers: RMCE, an efficient strategy for the targeted integration of transgenes. Curr Opin Biotechnol *12*, 473-480.

Balmain, A. (2002). Cancer as a complex genetic trait: tumor susceptibility in humans and mouse models. Cell *108*, 145-152.

Barbie, D.A., Tamayo, P., Boehm, J.S., Kim, S.Y., Moody, S.E., Dunn, I.F., Schinzel, A.C., Sandy, P., Meylan, E., Scholl, C.*, et al.* (2009). Systematic RNA interference reveals that oncogenic KRAS-driven cancers require TBK1. Nature *462*, 108-112.

Bast, R.C., Jr., Hennessy, B., and Mills, G.B. (2009). The biology of ovarian cancer: new opportunities for translation. Nat Rev Cancer *9*, 415-428.

Bates, J.H., and Irvin, C.G. (2003). Measuring lung function in mice: the phenotyping uncertainty principle. J Appl Physiol *94*, 1297-1306.

Bautch, V.L., Toda, S., Hassell, J.A., and Hanahan, D. (1987). Endothelial cell tumors develop in transgenic mice carrying polyoma virus middle T oncogene. Cell *51*, 529-537.

Beard, C., Hochedlinger, K., Plath, K., Wutz, A., and Jaenisch, R. (2006). Efficient method to generate single-copy transgenic mice by site-specific integration in embryonic stem cells. Genesis *44*, 23-28.

Bell, A.C., and Felsenfeld, G. (2000). Methylation of a CTCF-dependent boundary controls imprinted expression of the Igf2 gene. Nature *405*, 482-485.

Boxer, R.B., Jang, J.W., Sintasath, L., and Chodosh, L.A. (2004). Lack of sustained regression of c-MYC-induced mammary adenocarcinomas following brief or prolonged MYC inactivation. Cancer Cell *6*, 577-586.

Brinster, R.L., Chen, H.Y., Messing, A., van Dyke, T., Levine, A.J., and Palmiter, R.D. (1984). Transgenic mice harboring SV40 T-antigen genes develop characteristic brain tumors. Cell *37*, 367-379.

Buchholz, F., Angrand, P.O., and Stewart, A.F. (1998). Improved properties of FLP recombinase evolved by cycling mutagenesis. Nat Biotechnol *16*, 657-662.

Campbell, S.L., Khosravi-Far, R., Rossman, K.L., Clark, G.J., and Der, C.J. (1998). Increasing complexity of Ras signaling. Oncogene *17*, 1395-1413.

Capecchi, M.R. (1980). High efficiency transformation by direct microinjection of DNA into cultured mammalian cells. Cell *22*, 479-488.

Capecchi, M.R. (1989). Altering the genome by homologous recombination. Science *244*, 1288-1292.

Capecchi, M.R. (2005). Gene targeting in mice: functional analysis of the mammalian genome for the twenty-first century. Nat Rev Genet *6*, 507-512.

Carmell, M.A., Zhang, L., Conklin, D.S., Hannon, G.J., and Rosenquist, T.A. (2003). Germline transmission of RNAi in mice. Nat Struct Biol *10*, 91-92.

Castilho, R.M., Squarize, C.H., Chodosh, L.A., Williams, B.O., and Gutkind, J.S. (2009). mTOR mediates Wnt-induced epidermal stem cell exhaustion and aging. Cell Stem Cell *5*, 279-289.

Chin, L., Tam, A., Pomerantz, J., Wong, M., Holash, J., Bardeesy, N., Shen, Q., O'Hagan, R., Pantginis, J., Zhou, H.*, et al.* (1999). Essential role for oncogenic Ras in tumour maintenance. Nature *400*, 468-472.

Colnot, S., Decaens, T., Niwa-Kawakita, M., Godard, C., Hamard, G., Kahn, A., Giovannini, M., and Perret, C. (2004). Liver-targeted disruption of Apc in mice activates beta-catenin signaling and leads to hepatocellular carcinomas. Proc Natl Acad Sci U S A *101*, 17216-17221.

Craig, Z.R., Davis, J.R., Marion, S.L., Barton, J.K., and Hoyer, P.B. 7,12-dimethylbenz[a]anthracene induces sertoli-leydig-cell tumors in the follicle-depleted ovaries of mice treated with 4-vinylcyclohexene diepoxide. Comp Med *60*, 10-17.

Cross, J.C. (2001). Factors affecting the developmental potential of cloned mammalian embryos. Proc Natl Acad Sci U S A *98*, 5949-5951.

Damalas, A., Kahan, S., Shtutman, M., Ben-Ze'ev, A., and Oren, M. (2001). Deregulated beta-catenin induces a p53- and ARF-dependent growth arrest and cooperates with Ras in transformation. EMBO J *20*, 4912-4922.

DePinho, R.A. (2000). The age of cancer. Nature *408*, 248-254.

Derksen, P.W., Liu, X., Saridin, F., van der Gulden, H., Zevenhoven, J., Evers, B., van Beijnum, J.R., Griffioen, A.W., Vink, J., Krimpenfort, P.*, et al.* (2006). Somatic inactivation of E-cadherin and p53 in mice leads to metastatic lobular mammary carcinoma through induction of anoikis resistance and angiogenesis. Cancer Cell *10*, 437-449.

Dickins, R.A., Hemann, M.T., Zilfou, J.T., Simpson, D.R., Ibarra, I., Hannon, G.J., and Lowe, S.W. (2005). Probing tumor phenotypes using stable and regulated synthetic microRNA precursors. Nat Genet *37*, 1289-1295.

Dickins, R.A., McJunkin, K., Hernando, E., Premsrirut, P.K., Krizhanovsky, V., Burgess, D.J., Kim, S.Y., Cordon-Cardo, C., Zender, L., Hannon, G.J.*, et al.* (2007). Tissue-specific and reversible RNA interference in transgenic mice. Nat Genet *39*, 914-921.

Dinulescu, D.M., Ince, T.A., Quade, B.J., Shafer, S.A., Crowley, D., and Jacks, T. (2005). Role of K-ras and Pten in the development of mouse models of endometriosis and endometrioid ovarian cancer. Nat Med *11*, 63-70.

Donehower, L.A., Harvey, M., Slagle, B.L., McArthur, M.J., Montgomery, C.A., Jr., Butel, J.S., and Bradley, A. (1992). Mice deficient for p53 are developmentally normal but susceptible to spontaneous tumours. Nature *356*, 215-221.

Duncan, M.K., and Chada, K.K. (1993). Incidence of tubulostromal adenoma of the ovary in aged germ cell-deficient mice. J Comp Pathol *109*, 13-19.

Eberhard, D.A., Johnson, B.E., Amler, L.C., Goddard, A.D., Heldens, S.L., Herbst, R.S., Ince, W.L., Janne, P.A., Januario, T., Johnson, D.H.*, et al.* (2005). Mutations in the epidermal growth factor receptor and in KRAS are predictive and prognostic indicators in patients with non-small-cell lung cancer treated with chemotherapy alone and in combination with erlotinib. J Clin Oncol *23*, 5900-5909.

Edelmann, W., Yang, K., Umar, A., Heyer, J., Lau, K., Fan, K., Liedtke, W., Cohen, P.E., Kane, M.F., Lipford, J.R.*, et al.* (1997). Mutation in the mismatch repair gene Msh6 causes cancer susceptibility. Cell *91*, 467-477.

Eggan, K., Akutsu, H., Loring, J., Jackson-Grusby, L., Klemm, M., Rideout, W.M., 3rd, Yanagimachi, R., and Jaenisch, R. (2001). Hybrid vigor, fetal overgrowth, and viability of mice derived by nuclear cloning and tetraploid embryo complementation. Proc Natl Acad Sci U S A *98*, 6209-6214.

Eggan, K., Rode, A., Jentsch, I., Samuel, C., Hennek, T., Tintrup, H., Zevnik, B., Erwin, J., Loring, J., Jackson-Grusby, L.*, et al.* (2002). Male and female mice derived from the same embryonic stem cell clone by tetraploid embryo complementation. Nat Biotechnol *20*, 455-459.

Ehrhardt, A., Bartels, T., Geick, A., Klocke, R., Paul, D., and Halter, R. (2001). Development of pulmonary bronchiolo-alveolar adenocarcinomas in transgenic mice overexpressing murine c-myc and epidermal growth factor in alveolar type II pneumocytes. Br J Cancer *84*, 813-818.

Fedoriw, A.M., Stein, P., Svoboda, P., Schultz, R.M., and Bartolomei, M.S. (2004). Transgenic RNAi reveals essential function for CTCF in H19 gene imprinting. Science *303*, 238-240.

Felsher, D.W., and Bishop, J.M. (1999). Reversible tumorigenesis by MYC in hematopoietic lineages. Mol Cell *4*, 199-207.

Finco, T.S., Westwick, J.K., Norris, J.L., Beg, A.A., Der, C.J., and Baldwin, A.S., Jr. (1997). Oncogenic Ha-Ras-induced signaling activates NF-kappaB transcriptional activity, which is required for cellular transformation. J Biol Chem *272*, 24113-24116.

Fire, A., Xu, S., Montgomery, M.K., Kostas, S.A., Driver, S.E., and Mello, C.C. (1998). Potent and specific genetic interference by double-stranded RNA in Caenorhabditis elegans. Nature *391*, 806-811.

Fisher, G.H., Wellen, S.L., Klimstra, D., Lenczowski, J.M., Tichelaar, J.W., Lizak, M.J., Whitsett, J.A., Koretsky, A., and Varmus, H.E. (2001). Induction and apoptotic regression of lung adenocarcinomas by regulation of a K-Ras transgene in the presence and absence of tumor suppressor genes. Genes Dev *15*, 3249-3262.

Forgacs, E., Zochbauer-Muller, S., Olah, E., and Minna, J.D. (2001). Molecular genetic abnormalities in the pathogenesis of human lung cancer. Pathol Oncol Res *7*, 6-13.

Frese, K.K., and Tuveson, D.A. (2007). Maximizing mouse cancer models. Nat Rev Cancer *7*, 645-658.

Furth, P.A., St Onge, L., Boger, H., Gruss, P., Gossen, M., Kistner, A., Bujard, H., and Hennighausen, L. (1994). Temporal control of gene expression in transgenic mice by a tetracycline-responsive promoter. Proc Natl Acad Sci U S A *91*, 9302-9306.

Glasser, S.W., Korfhagen, T.R., Wert, S.E., Bruno, M.D., McWilliams, K.M., Vorbroker, D.K., and Whitsett, J.A. (1991). Genetic element from human surfactant protein SP-C gene confers bronchiolar-alveolar cell specificity in transgenic mice. Am J Physiol *261*, L349-356.

Gordon, J.W., Scangos, G.A., Plotkin, D.J., Barbosa, J.A., and Ruddle, F.H. (1980). Genetic transformation of mouse embryos by microinjection of purified DNA. Proc Natl Acad Sci U S A *77*, 7380-7384.

Gossen, M., and Bujard, H. (1992). Tight control of gene expression in mammalian cells by tetracycline-responsive promoters. Proc Natl Acad Sci U S A *89*, 5547-5551.

Greenberg, S.D., Fraire, A.E., Kinner, B.M., and Johnson, E.H. (1987). Tumor cell type versus staging in the prognosis of carcinoma of the lung. Pathol Annu *22 Pt 2*, 387-405.

Greulich, H., Chen, T.H., Feng, W., Janne, P.A., Alvarez, J.V., Zappaterra, M., Bulmer, S.E., Frank, D.A., Hahn, W.C., Sellers, W.R.*, et al.* (2005). Oncogenic transformation by inhibitor-sensitive and -resistant EGFR mutants. PLoS Med *2*, e313.

Grimm, D., Streetz, K.L., Jopling, C.L., Storm, T.A., Pandey, K., Davis, C.R., Marion, P., Salazar, F., and Kay, M.A. (2006). Fatality in mice due to oversaturation of cellular microRNA/short hairpin RNA pathways. Nature *441*, 537-541.

Guglielmi, L., Le Bert, M., Truffinet, V., Cogne, M., and Denizot, Y. (2003). Insulators to improve expression of a 3(')IgH LCR-driven reporter gene in transgenic mouse models. Biochem Biophys Res Commun *307*, 466-471.

Hanahan, D. (1985). Heritable formation of pancreatic beta-cell tumours in transgenic mice expressing recombinant insulin/simian virus 40 oncogenes. Nature *315*, 115-122.

Hanson, J.L., Hawke, N.A., Kashatus, D., and Baldwin, A.S. (2004). The nuclear factor kappaB subunits RelA/p65 and c-Rel potentiate but are not required for Ras-induced cellular transformation. Cancer Res *64*, 7248-7255.

Hasuwa, H., Kaseda, K., Einarsdottir, T., and Okabe, M. (2002). Small interfering RNA and gene silencing in transgenic mice and rats. FEBS Lett *532*, 227-230.

He, L., and Hannon, G.J. (2004). MicroRNAs: small RNAs with a big role in gene regulation. Nat Rev Genet *5*, 522-531.

Hemann, M.T., Fridman, J.S., Zilfou, J.T., Hernando, E., Paddison, P.J., Cordon-Cardo, C., Hannon, G.J., and Lowe, S.W. (2003). An epi-allelic series of p53 hypomorphs created by stable RNAi produces distinct tumor phenotypes in vivo. Nat Genet *33*, 396-400.

Herbst, R.S., Heymach, J.V., and Lippman, S.M. (2008). Lung cancer. N Engl J Med *359*, 1367-1380.

Heyer, J., Yang, K., Lipkin, M., Edelmann, W., and Kucherlapati, R. (1999). Mouse models for colorectal cancer. Oncogene *18*, 5325-5333.

Hingorani, S.R., Petricoin, E.F., Maitra, A., Rajapakse, V., King, C., Jacobetz, M.A., Ross, S., Conrads, T.P., Veenstra, T.D., Hitt, B.A.*, et al.* (2003). Preinvasive and invasive ductal pancreatic cancer and its early detection in the mouse. Cancer Cell *4*, 437-450.

Hingorani, S.R., Wang, L., Multani, A.S., Combs, C., Deramaudt, T.B., Hruban, R.H., Rustgi, A.K., Chang, S., and Tuveson, D.A. (2005). *Trp53*R172H and KrasG12D cooperate to promote chromosomal instability and widely metastatic pancreatic ductal adenocarcinoma in mice. Cancer Cell *7*, 469-483.

Hitz, C., Steuber-Buchberger, P., Delic, S., Wurst, W., and Kuhn, R. (2009). Generation of shRNA transgenic mice. Methods Mol Biol *530*, 101-129.

Hitz, C., Wurst, W., and Kuhn, R. (2007). Conditional brain-specific knockdown of MAPK using Cre/loxP regulated RNA interference. Nucleic Acids Res *35*, e90.

Hong, Y., and Stambrook, P.J. (2004). Restoration of an absent G1 arrest and protection from apoptosis in embryonic stem cells after ionizing radiation. Proc Natl Acad Sci U S A *101*, 14443-14448.

Horie, R., Watanabe, M., Okamura, T., Taira, M., Shoda, M., Motoji, T., Utsunomiya, A., Watanabe, T., Higashihara, M., and Umezawa, K. (2006). DHMEQ, a new NF-kappaB inhibitor, induces apoptosis and enhances fludarabine effects on chronic lymphocytic leukemia cells. Leukemia *20*, 800-806.

Hoyer, P.B., Davis, J.R., Bedrnicek, J.B., Marion, S.L., Christian, P.J., Barton, J.K., and Brewer, M.A. (2009). Ovarian neoplasm development by 7,12-dimethylbenz[a]anthracene (DMBA) in a chemically-induced rat model of ovarian failure. Gynecol Oncol *112*, 610-615.

Hsiao, Y.C., Chang, H.H., Tsai, C.Y., Jong, Y.J., Horng, L.S., Lin, S.F., and Tsai, T.F. (2004). Coat color-tagged green mouse with EGFP expressed from the RNA polymerase II promoter. Genesis *39*, 122-129.

Huang, W.C., Ju, T.K., Hung, M.C., and Chen, C.C. (2007). Phosphorylation of CBP by IKKalpha promotes cell growth by switching the binding preference of CBP from p53 to NF-kappaB. Mol Cell *26*, 75-87.

Imren, S., Fabry, M.E., Westerman, K.A., Pawliuk, R., Tang, P., Rosten, P.M., Nagel, R.L., Leboulch, P., Eaves, C.J., and Humphries, R.K. (2004). High-level beta-globin expression and preferred intragenic integration after lentiviral transduction of human cord blood stem cells. J Clin Invest *114*, 953-962.

Izeradjene, K., Combs, C., Best, M., Gopinathan, A., Wagner, A., Grady, W.M., Deng, C.X., Hruban, R.H., Adsay, N.V., Tuveson, D.A.*, et al.* (2007). Kras(G12D) and Smad4/Dpc4 haploinsufficiency cooperate to induce mucinous cystic neoplasms and invasive adenocarcinoma of the pancreas. Cancer Cell *11*, 229-243.

Jackson, E.L., Olive, K.P., Tuveson, D.A., Bronson, R., Crowley, D., Brown, M., and Jacks, T. (2005). The differential effects of mutant p53 alleles on advanced murine lung cancer. Cancer Res *65*, 10280-10288.

Jackson, E.L., Willis, N., Mercer, K., Bronson, R.T., Crowley, D., Montoya, R., Jacks, T., and Tuveson, D.A. (2001). Analysis of lung tumor initiation and progression using conditional expression of oncogenic K-ras. Genes Dev *15*, 3243-3248.

Jemal, A., Murray, T., Ward, E., Samuels, A., Tiwari, R.C., Ghafoor, A., Feuer, E.J., and Thun, M.J. (2005). Cancer statistics, 2005. CA Cancer J Clin *55*, 10-30.

Ji, H., Ramsey, M.R., Hayes, D.N., Fan, C., McNamara, K., Kozlowski, P., Torrice, C., Wu, M.C., Shimamura, T., Perera, S.A*., et al.* (2007). LKB1 modulates lung cancer differentiation and metastasis. Nature *448*, 807-810.

Jonkers, J., Meuwissen, R., van der Gulden, H., Peterse, H., van der Valk, M., and Berns, A. (2001). Synergistic tumor suppressor activity of BRCA2 and p53 in a conditional mouse model for breast cancer. Nat Genet *29*, 418-425.

Kaffer, C.R., Srivastava, M., Park, K.Y., Ives, E., Hsieh, S., Batlle, J., Grinberg, A., Huang, S.P., and Pfeifer, K. (2000). A transcriptional insulator at the imprinted H19/Igf2 locus. Genes Dev *14*, 1908-1919.

Kawauchi, K., Araki, K., Tobiume, K., and Tanaka, N. (2008). p53 regulates glucose metabolism through an IKK-NF-kappaB pathway and inhibits cell transformation. Nat Cell Biol *10*, 611-618.

Kerkhoff, E., Fedorov, L.M., Siefken, R., Walter, A.O., Papadopoulos, T., and Rapp, U.R. (2000). Lung-targeted expression of the c-Raf-1 kinase in transgenic mice exposes a novel oncogenic character of the wild-type protein. Cell Growth Differ *11*, 185-190.

Kim, M.J., Cardiff, R.D., Desai, N., Banach-Petrosky, W.A., Parsons, R., Shen, M.M., and Abate-Shen, C. (2002). Cooperativity of Nkx3.1 and Pten loss of function in a mouse model of prostate carcinogenesis. Proc Natl Acad Sci U S A *99*, 2884-2889.

Kim, W.I., Wiesner, S.M., and Largaespada, D.A. (2007). Vav promoter-tTA conditional transgene expression system for hematopoietic cells drives high level expression in developing B and T cells. Exp Hematol *35*, 1231-1239.

Kim, W.Y., and Sharpless, N.E. (2006). The regulation of INK4/ARF in cancer and aging. Cell *127*, 265-275.

Kistner, A., Gossen, M., Zimmermann, F., Jerecic, J., Ullmer, C., Lubbert, H., and Bujard, H. (1996). Doxycycline-mediated quantitative and tissue-specific control of gene expression in transgenic mice. Proc Natl Acad Sci U S A *93*, 10933-10938.

Kunath, T., Gish, G., Lickert, H., Jones, N., Pawson, T., and Rossant, J. (2003). Transgenic RNA interference in ES cell-derived embryos recapitulates a genetic null phenotype. Nat Biotechnol *21*, 559-561.

Kuraguchi, M., Wang, X.P., Bronson, R.T., Rothenberg, R., Ohene-Baah, N.Y., Lund, J.J., Kucherlapati, M., Maas, R.L., and Kucherlapati, R. (2006). Adenomatous polyposis coli (APC) is required for normal development of skin and thymus. PLoS Genet *2*, e146.

Leder, A., Pattengale, P.K., Kuo, A., Stewart, T.A., and Leder, P. (1986). Consequences of widespread deregulation of the c-myc gene in transgenic mice: multiple neoplasms and normal development. Cell *45*, 485-495.

Lickert, H., Cox, B., Wehrle, C., Taketo, M.M., Kemler, R., and Rossant, J. (2005). Dissecting Wnt/beta-catenin signaling during gastrulation using RNA interference in mouse embryos. Development *132*, 2599-2609.

Linnoila, R.I., Szabo, E., DeMayo, F., Witschi, H., Sabourin, C., and Malkinson, A. (2000). The role of CC10 in pulmonary carcinogenesis: from a marker to tumor suppression. Ann N Y Acad Sci *923*, 249-267.

Lois, C., Hong, E.J., Pease, S., Brown, E.J., and Baltimore, D. (2002). Germline transmission and tissue-specific expression of transgenes delivered by lentiviral vectors. Science *295*, 868-872.

Lucito, R., Healy, J., Alexander, J., Reiner, A., Esposito, D., Chi, M., Rodgers, L., Brady, A., Sebat, J., Troge, J.*, et al.* (2003). Representational oligonucleotide microarray analysis: a

high-resolution method to detect genome copy number variation. Genome Res *13*, 2291-2305.

Lynch, T.J., Bell, D.W., Sordella, R., Gurubhagavatula, S., Okimoto, R.A., Brannigan, B.W., Harris, P.L., Haserlat, S.M., Supko, J.G., Haluska, F.G.*, et al.* (2004). Activating mutations in the epidermal growth factor receptor underlying responsiveness of non-small-cell lung cancer to gefitinib. N Engl J Med *350*, 2129-2139.

Magdaleno, S.M., Wang, G., Mireles, V.L., Ray, M.K., Finegold, M.J., and DeMayo, F.J. (1997). Cyclin-dependent kinase inhibitor expression in pulmonary Clara cells transformed with SV40 large T antigen in transgenic mice. Cell Growth Differ *8*, 145-155.

Malone, C.D., Brennecke, J., Dus, M., Stark, A., McCombie, W.R., Sachidanandam, R., and Hannon, G.J. (2009). Specialized piRNA pathways act in germline and somatic tissues of the Drosophila ovary. Cell *137*, 522-535.

Meuwissen, R., Linn, S.C., van der Valk, M., Mooi, W.J., and Berns, A. (2001). Mouse model for lung tumorigenesis through Cre/lox controlled sporadic activation of the K-Ras oncogene. Oncogene *20*, 6551-6558.

Meylan, E., Dooley, A.L., Feldser, D.M., Shen, L., Turk, E., Ouyang, C., and Jacks, T. (2009). Requirement for NF-kappaB signalling in a mouse model of lung adenocarcinoma. Nature *462*, 104-107.

Miller, V.A., Riely, G.J., Zakowski, M.F., Li, A.R., Patel, J.D., Heelan, R.T., Kris, M.G., Sandler, A.B., Carbone, D.P., Tsao, A.*, et al.* (2008). Molecular characteristics of bronchioloalveolar carcinoma and adenocarcinoma, bronchioloalveolar carcinoma subtype, predict response to erlotinib. J Clin Oncol *26*, 1472-1478.

Min, C., Eddy, S.F., Sherr, D.H., and Sonenshein, G.E. (2008). NF-kappaB and epithelial to mesenchymal transition of cancer. J Cell Biochem *104*, 733-744.

Mo, L., Zheng, X., Huang, H.Y., Shapiro, E., Lepor, H., Cordon-Cardo, C., Sun, T.T., and Wu, X.R. (2007). Hyperactivation of Ha-ras oncogene, but not Ink4a/Arf deficiency, triggers bladder tumorigenesis. J Clin Invest *117*, 314-325.

Moody, S.E., Sarkisian, C.J., Hahn, K.T., Gunther, E.J., Pickup, S., Dugan, K.D., Innocent, N., Cardiff, R.D., Schnall, M.D., and Chodosh, L.A. (2002). Conditional activation of Neu in the mammary epithelium of transgenic mice results in reversible pulmonary metastasis. Cancer Cell *2*, 451-461.

Moser, A.R., Pitot, H.C., and Dove, W.F. (1990). A dominant mutation that predisposes to multiple intestinal neoplasia in the mouse. Science *247*, 322-324.

Muller, W.J., Sinn, E., Pattengale, P.K., Wallace, R., and Leder, P. (1988). Single-step induction of mammary adenocarcinoma in transgenic mice bearing the activated c-neu oncogene. Cell *54*, 105-115.

Nagy, A., Gertsenstein, M., Vintersten, K., and Behringer, R. (2003). Manipulating the mouse embryo : a laboratory manual, 3 edn (Cold Spring Harbor, Cold Spring Harbor Laboratory Press).

Neal, J.W., and Sequist, L.V. First-line use of EGFR tyrosine kinase inhibitors in patients with NSCLC containing EGFR mutations. Clin Adv Hematol Oncol *8*, 119-126.

Niwa, H., Miyazaki, J., and Smith, A.G. (2000). Quantitative expression of Oct-3/4 defines differentiation, dedifferentiation or self-renewal of ES cells. Nat Genet *24*, 372-376.

Niwa, H., Yamamura, K., and Miyazaki, J. (1991). Efficient selection for high-expression transfectants with a novel eukaryotic vector. Gene *108*, 193-199.

Nyabi, O., Naessens, M., Haigh, K., Gembarska, A., Goossens, S., Maetens, M., De Clercq, S., Drogat, B., Haenebalcke, L., Bartunkova, S.*, et al.* (2009). Efficient mouse transgenesis using Gateway-compatible ROSA26 locus targeting vectors and F1 hybrid ES cells. Nucleic Acids Res *37*, e55.

O'Gorman, S., Fox, D.T., and Wahl, G.M. (1991). Recombinase-mediated gene activation and site-specific integration in mammalian cells. Science *251*, 1351-1355.

Oberdoerffer, P., Kanellopoulou, C., Heissmeyer, V., Paeper, C., Borowski, C., Aifantis, I., Rao, A., and Rajewsky, K. (2005). Efficiency of RNA interference in the mouse hematopoietic system varies between cell types and developmental stages. Mol Cell Biol *25*, 3896-3905.

Olive, K.P., Tuveson, D.A., Ruhe, Z.C., Yin, B., Willis, N.A., Bronson, R.T., Crowley, D., and Jacks, T. (2004). Mutant p53 gain of function in two mouse models of Li-Fraumeni syndrome. Cell *119*, 847-860.

Olson, A., Sheth, N., Lee, J.S., Hannon, G., and Sachidanandam, R. (2006). RNAi Codex: a portal/database for short-hairpin RNA (shRNA) gene-silencing constructs. Nucleic Acids Res *34*, D153-157.

Opitz, O.G., Harada, H., Suliman, Y., Rhoades, B., Sharpless, N.E., Kent, R., Kopelovich, L., Nakagawa, H., and Rustgi, A.K. (2002). A mouse model of human oral-esophageal cancer. J Clin Invest *110*, 761-769.

Oshima, H., Matsunaga, A., Fujimura, T., Tsukamoto, T., Taketo, M.M., and Oshima, M. (2006). Carcinogenesis in mouse stomach by simultaneous activation of the Wnt signaling and prostaglandin E2 pathway. Gastroenterology *131*, 1086-1095.

Paddison, P.J., Silva, J.M., Conklin, D.S., Schlabach, M., Li, M., Aruleba, S., Balija, V., O'Shaughnessy, A., Gnoj, L., Scobie, K.*, et al.* (2004). A resource for large-scale RNA-interference-based screens in mammals. Nature *428*, 427-431.

Paez, J.G., Janne, P.A., Lee, J.C., Tracy, S., Greulich, H., Gabriel, S., Herman, P., Kaye, F.J., Lindeman, N., Boggon, T.J.*, et al.* (2004). EGFR mutations in lung cancer: correlation with clinical response to gefitinib therapy. Science *304*, 1497-1500.

Pao, W., Miller, V.A., Politi, K.A., Riely, G.J., Somwar, R., Zakowski, M.F., Kris, M.G., and Varmus, H. (2005). Acquired resistance of lung adenocarcinomas to gefitinib or erlotinib is associated with a second mutation in the EGFR kinase domain. PLoS Med *2*, e73.

Politi, K., Zakowski, M.F., Fan, P.D., Schonfeld, E.A., Pao, W., and Varmus, H.E. (2006). Lung adenocarcinomas induced in mice by mutant EGF receptors found in human lung cancers respond to a tyrosine kinase inhibitor or to down-regulation of the receptors. Genes Dev *20*, 1496-1510.

Potts, W., Tucker, D., Wood, H., and Martin, C. (2000). Chicken beta-globin 5'HS4 insulators function to reduce variability in transgenic founder mice. Biochem Biophys Res Commun *273*, 1015-1018.

Quaife, C.J., Pinkert, C.A., Ornitz, D.M., Palmiter, R.D., and Brinster, R.L. (1987). Pancreatic neoplasia induced by ras expression in acinar cells of transgenic mice. Cell *48*, 1023-1034.

Rangarajan, A., Hong, S.J., Gifford, A., and Weinberg, R.A. (2004). Species- and cell type-specific requirements for cellular transformation. Cancer Cell *6*, 171-183.

Rangarajan, A., and Weinberg, R.A. (2003). Opinion: Comparative biology of mouse versus human cells: modelling human cancer in mice. Nat Rev Cancer *3*, 952-959.

Ravi, R., Mookerjee, B., van Hensbergen, Y., Bedi, G.C., Giordano, A., El-Deiry, W.S., Fuchs, E.J., and Bedi, A. (1998). p53-mediated repression of nuclear factor-kappaB RelA via the transcriptional integrator p300. Cancer Res *58*, 4531-4536.

Ray, M.K., Magdaleno, S., O'Malley, B.W., and DeMayo, F.J. (1993). Cloning and characterization of the mouse Clara cell specific 10 kDa protein gene: comparison of the 5'-flanking region with the human rat and rabbit gene. Biochem Biophys Res Commun *197*, 163-171.

Reilly, K.M., Loisel, D.A., Bronson, R.T., McLaughlin, M.E., and Jacks, T. (2000). Nf1;*Trp53* mutant mice develop glioblastoma with evidence of strain-specific effects. Nat Genet *26*, 109-113.

Rubinson, D.A., Dillon, C.P., Kwiatkowski, A.V., Sievers, C., Yang, L., Kopinja, J., Rooney, D.L., Zhang, M., Ihrig, M.M., McManus, M.T.*, et al.* (2003). A lentivirus-based system to

functionally silence genes in primary mammalian cells, stem cells and transgenic mice by RNA interference. Nat Genet *33*, 401-406.

Ruther, U., Komitowski, D., Schubert, F.R., and Wagner, E.F. (1989). c-fos expression induces bone tumors in transgenic mice. Oncogene *4*, 861-865.

Sadate-Ngatchou, P.I., Payne, C.J., Dearth, A.T., and Braun, R.E. (2008). Cre recombinase activity specific to postnatal, premeiotic male germ cells in transgenic mice. Genesis *46*, 738-742.

Safran, M., Kim, W.Y., Kung, A.L., Horner, J.W., DePinho, R.A., and Kaelin, W.G., Jr. (2003). Mouse reporter strain for noninvasive bioluminescent imaging of cells that have undergone Cre-mediated recombination. Mol Imaging *2*, 297-302.

Sansom, O.J., Griffiths, D.F., Reed, K.R., Winton, D.J., and Clarke, A.R. (2005). Apc deficiency predisposes to renal carcinoma in the mouse. Oncogene *24*, 8205-8210.

Sansom, O.J., Meniel, V., Wilkins, J.A., Cole, A.M., Oien, K.A., Marsh, V., Jamieson, T.J., Guerra, C., Ashton, G.H., Barbacid, M.*, et al.* (2006). Loss of Apc allows phenotypic manifestation of the transforming properties of an endogenous K-ras oncogene in vivo. Proc Natl Acad Sci U S A *103*, 14122-14127.

Santoni-Rugiu, E., Nagy, P., Jensen, M.R., Factor, V.M., and Thorgeirsson, S.S. (1996). Evolution of neoplastic development in the liver of transgenic mice co-expressing c-myc and transforming growth factor-alpha. Am J Pathol *149*, 407-428.

Sauer, B., and Henderson, N. (1989). Cre-stimulated recombination at loxP-containing DNA sequences placed into the mammalian genome. Nucleic Acids Res *17*, 147-161.

Schmidt, E.V., Pattengale, P.K., Weir, L., and Leder, P. (1988). Transgenic mice bearing the human c-myc gene activated by an immunoglobulin enhancer: a pre-B-cell lymphoma model. Proc Natl Acad Sci U S A *85*, 6047-6051.

Schmitt, C.A., Fridman, J.S., Yang, M., Baranov, E., Hoffman, R.M., and Lowe, S.W. (2002). Dissecting p53 tumor suppressor functions in vivo. Cancer Cell *1*, 289-298.

Schuster-Gossler, K., Lee, A.W., Lerner, C.P., Parker, H.J., Dyer, V.W., Scott, V.E., Gossler, A., and Conover, J.C. (2001). Use of coisogenic host blastocysts for efficient establishment of germline chimeras with C57BL/6J ES cell lines. Biotechniques *31*, 1022-1024, 1026.

Seibler, J., Kleinridders, A., Kuter-Luks, B., Niehaves, S., Bruning, J.C., and Schwenk, F. (2007). Reversible gene knockdown in mice using a tight, inducible shRNA expression system. Nucleic Acids Res *35*, e54.

Seibler, J., Kuter-Luks, B., Kern, H., Streu, S., Plum, L., Mauer, J., Kuhn, R., Bruning, J.C., and Schwenk, F. (2005). Single copy shRNA configuration for ubiquitous gene knockdown in mice. Nucleic Acids Res *33*, e67.

Seidler, B., Schmidt, A., Mayr, U., Nakhai, H., Schmid, R.M., Schneider, G., and Saur, D. (2008). A Cre-loxP-based mouse model for conditional somatic gene expression and knockdown in vivo by using avian retroviral vectors. Proc Natl Acad Sci U S A *105*, 10137-10142.

Sharpless, N.E., and Depinho, R.A. (2006). The mighty mouse: genetically engineered mouse models in cancer drug development. Nat Rev Drug Discov *5*, 741-754.

Shepherd, F.A. (2005). A targeted approach to reducing lung cancer mortality. J Clin Oncol *23*, 3173-3174.

Shepherd, F.A., Rodrigues Pereira, J., Ciuleanu, T., Tan, E.H., Hirsh, V., Thongprasert, S., Campos, D., Maoleekoonpiroj, S., Smylie, M., Martins, R.*, et al.* (2005). Erlotinib in previously treated non-small-cell lung cancer. N Engl J Med *353*, 123-132.

Shinagawa, T., and Ishii, S. (2003). Generation of Ski-knockdown mice by expressing a long double-strand RNA from an RNA polymerase II promoter. Genes Dev *17*, 1340-1345.

Silva, J.M., Li, M.Z., Chang, K., Ge, W., Golding, M.C., Rickles, R.J., Siolas, D., Hu, G., Paddison, P.J., Schlabach, M.R.*, et al.* (2005). Second-generation shRNA libraries covering the mouse and human genomes. Nat Genet *37*, 1281-1288.

Sinn, E., Muller, W., Pattengale, P., Tepler, I., Wallace, R., and Leder, P. (1987). Coexpression of MMTV/v-Ha-ras and MMTV/c-myc genes in transgenic mice: synergistic action of oncogenes in vivo. Cell *49*, 465-475.

Smith, D.J., Stevens, M.E., Sudanagunta, S.P., Bronson, R.T., Makhinson, M., Watabe, A.M., O'Dell, T.J., Fung, J., Weier, H.U., Cheng, J.F.*, et al.* (1997). Functional screening of 2 Mb of human chromosome 21q22.2 in transgenic mice implicates minibrain in learning defects associated with Down syndrome. Nat Genet *16*, 28-36.

Snove, O., Jr., and Rossi, J.J. (2006). Toxicity in mice expressing short hairpin RNAs gives new insight into RNAi. Genome Biol *7*, 231.

Soriano, P. (1999). Generalized lacZ expression with the ROSA26 Cre reporter strain. Nat Genet *21*, 70-71.

Sotillo, R., Hernando, E., Diaz-Rodriguez, E., Teruya-Feldstein, J., Cordon-Cardo, C., Lowe, S.W., and Benezra, R. (2007). Mad2 overexpression promotes aneuploidy and tumorigenesis in mice. Cancer Cell *11*, 9-23.

Soucek, L., Whitfield, J., Martins, C.P., Finch, A.J., Murphy, D.J., Sodir, N.M., Karnezis, A.N., Swigart, L.B., Nasi, S., and Evan, G.I. (2008). Modelling Myc inhibition as a cancer therapy. Nature *455*, 679-683.

Srinivas, S., Watanabe, T., Lin, C.S., William, C.M., Tanabe, Y., Jessell, T.M., and Costantini, F. (2001). Cre reporter strains produced by targeted insertion of EYFP and ECFP into the ROSA26 locus. BMC Dev Biol *1*, 4.

Stegmeier, F., Hu, G., Rickles, R.J., Hannon, G.J., and Elledge, S.J. (2005). A lentiviral microRNA-based system for single-copy polymerase II-regulated RNA interference in mammalian cells. Proc Natl Acad Sci U S A *102*, 13212-13217.

Stein, P., Svoboda, P., and Schultz, R.M. (2003). Transgenic RNAi in mouse oocytes: a simple and fast approach to study gene function. Dev Biol *256*, 187-193.

Stewart, T.A., Pattengale, P.K., and Leder, P. (1984). Spontaneous mammary adenocarcinomas in transgenic mice that carry and express MTV/myc fusion genes. Cell *38*, 627-637.

Stripp, B.R., Sawaya, P.L., Luse, D.S., Wikenheiser, K.A., Wert, S.E., Huffman, J.A., Lattier, D.L., Singh, G., Katyal, S.L., and Whitsett, J.A. (1992). cis-acting elements that confer lung epithelial cell expression of the CC10 gene. J Biol Chem *267*, 14703-14712.

Tam, R.C., Lin, C.J., Lim, C., Pai, B., and Stoisavljevic, V. (1999). Inhibition of CD28 expression by oligonucleotide decoys to the regulatory element in exon 1 of the CD28 gene. J Immunol *163*, 4292-4299.

Teng, Y., Sun, A.N., Pan, X.C., Yang, G., Yang, L.L., Wang, M.R., and Yang, X. (2006). Synergistic function of Smad4 and PTEN in suppressing forestomach squamous cell carcinoma in the mouse. Cancer Res *66*, 6972-6981.

Thomas, K.R., and Capecchi, M.R. (1987). Site-directed mutagenesis by gene targeting in mouse embryo-derived stem cells. Cell *51*, 503-512.

Thomas, K.R., Folger, K.R., and Capecchi, M.R. (1986). High frequency targeting of genes to specific sites in the mammalian genome. Cell *44*, 419-428.

Tichelaar, J.W., Lu, W., and Whitsett, J.A. (2000). Conditional expression of fibroblast growth factor-7 in the developing and mature lung. J Biol Chem *275*, 11858-11864.

Tiscornia, G., Singer, O., Ikawa, M., and Verma, I.M. (2003). A general method for gene knockdown in mice by using lentiviral vectors expressing small interfering RNA. Proc Natl Acad Sci U S A *100*, 1844-1848.

Tucker, K.L., Wang, Y., Dausman, J., and Jaenisch, R. (1997). A transgenic mouse strain expressing four drug-selectable marker genes. Nucleic Acids Res *25*, 3745-3746.

Tuveson, D.A., and Jacks, T. (1999). Modeling human lung cancer in mice: similarities and shortcomings. Oncogene *18*, 5318-5324.

Tuveson, D.A., and Jacks, T. (2002). Technologically advanced cancer modeling in mice. Curr Opin Genet Dev *12*, 105-110.

Van Dyke, T., and Jacks, T. (2002). Cancer modeling in the modern era: progress and challenges. Cell *108*, 135-144.

Van Mater, D., Kolligs, F.T., Dlugosz, A.A., and Fearon, E.R. (2003). Transient activation of beta -catenin signaling in cutaneous keratinocytes is sufficient to trigger the active growth phase of the hair cycle in mice. Genes Dev *17*, 1219-1224.

Vanderhyden, B.C. (2005). Loss of ovarian function and the risk of ovarian cancer. Cell Tissue Res *322*, 117-124.

Vasquez, K.M., Marburger, K., Intody, Z., and Wilson, J.H. (2001). Manipulating the mammalian genome by homologous recombination. Proc Natl Acad Sci U S A *98*, 8403-8410.

Ventura, A., Meissner, A., Dillon, C.P., McManus, M., Sharp, P.A., Van Parijs, L., Jaenisch, R., and Jacks, T. (2004). Cre-lox-regulated conditional RNA interference from transgenes. Proc Natl Acad Sci U S A *101*, 10380-10385.

Voinnet, O., Vain, P., Angell, S., and Baulcombe, D.C. (1998). Systemic spread of sequence-specific transgene RNA degradation in plants is initiated by localized introduction of ectopic promoterless DNA. Cell *95*, 177-187.

Wang, J., Theunissen, T.W., and Orkin, S.H. (2007). Site-directed, virus-free, and inducible RNAi in embryonic stem cells. Proc Natl Acad Sci U S A *104*, 20850-20855.

Wang, S., Gao, J., Lei, Q., Rozengurt, N., Pritchard, C., Jiao, J., Thomas, G.V., Li, G., Roy-Burman, P., Nelson, P.S.*, et al.* (2003). Prostate-specific deletion of the murine Pten tumor suppressor gene leads to metastatic prostate cancer. Cancer Cell *4*, 209-221.

Weinstein, I.B. (2000). Disorders in cell circuitry during multistage carcinogenesis: the role of homeostasis. Carcinogenesis *21*, 857-864.

Weinstein, I.B. (2002). Cancer. Addiction to oncogenes--the Achilles heal of cancer. Science *297*, 63-64.

West, A.G., and Fraser, P. (2005). Remote control of gene transcription. Hum Mol Genet *14 Spec No 1*, R101-111.

Westra, W.H. (2000). Early glandular neoplasia of the lung. Respir Res *1*, 163-169.

Wiekowski, M.T., Chen, S.C., Zalamea, P., Wilburn, B.P., Kinsley, D.J., Sharif, W.W., Jensen, K.K., Hedrick, J.A., Manfra, D., and Lira, S.A. (2001). Disruption of neutrophil migration in a conditional transgenic model: evidence for CXCR2 desensitization in vivo. J Immunol *167*, 7102-7110.

Williams, R.L., Courtneidge, S.A., and Wagner, E.F. (1988). Embryonic lethalities and endothelial tumors in chimeric mice expressing polyoma virus middle T oncogene. Cell *52*, 121-131.

Wilson, C., Bellen, H.J., and Gehring, W.J. (1990). Position effects on eukaryotic gene expression. Annu Rev Cell Biol *6*, 679-714.

Woo, S.K., Lee, T.S., Kim, K.M., Kim, J.Y., Jung, J.H., Kang, J.H., Cheon, G.J., Choi, C.W., and Lim, S.M. (2008). Anesthesia condition for (18)F-FDG imaging of lung metastasis tumors using small animal PET. Nucl Med Biol *35*, 143-150.

Wu, C.H., van Riggelen, J., Yetil, A., Fan, A.C., Bachireddy, P., and Felsher, D.W. (2007a). Cellular senescence is an important mechanism of tumor regression upon c-Myc inactivation. Proc Natl Acad Sci U S A *104*, 13028-13033.

Wu, R., Hendrix-Lucas, N., Kuick, R., Zhai, Y., Schwartz, D.R., Akyol, A., Hanash, S., Misek, D.E., Katabuchi, H., Williams, B.O.*, et al.* (2007b). Mouse model of human ovarian endometrioid adenocarcinoma based on somatic defects in the Wnt/beta-catenin and PI3K/Pten signaling pathways. Cancer Cell *11*, 321-333.

Xiao, A., Yin, C., Yang, C., Di Cristofano, A., Pandolfi, P.P., and Van Dyke, T. (2005). Somatic induction of Pten loss in a preclinical astrocytoma model reveals major roles in disease progression and avenues for target discovery and validation. Cancer Res *65*, 5172-5180.

Xue, W., Zender, L., Miething, C., Dickins, R.A., Hernando, E., Krizhanovsky, V., Cordon-Cardo, C., and Lowe, S.W. (2007). Senescence and tumour clearance is triggered by p53 restoration in murine liver carcinomas. Nature *445*, 656-660.

Zamore, P.D., Tuschl, T., Sharp, P.A., and Bartel, D.P. (2000). RNAi: double-stranded RNA directs the ATP-dependent cleavage of mRNA at 21 to 23 nucleotide intervals. Cell *101*, 25-33.

Zender, L., Spector, M.S., Xue, W., Flemming, P., Cordon-Cardo, C., Silke, J., Fan, S.T., Luk, J.M., Wigler, M., Hannon, G.J.*, et al.* (2006). Identification and validation of oncogenes in liver cancer using an integrative oncogenomic approach. Cell *125*, 1253-1267.

Zender, L., Xue, W., Cordon-Cardo, C., Hannon, G.J., Lucito, R., Powers, S., Flemming, P., Spector, M.S., and Lowe, S.W. (2005). Generation and analysis of genetically defined liver carcinomas derived from bipotential liver progenitors. Cold Spring Harb Symp Quant Biol *70*, 251-261.

Zhao, X., Li, C., Paez, J.G., Chin, K., Janne, P.A., Chen, T.H., Girard, L., Minna, J., Christiani, D., Leo, C.*, et al.* (2004). An integrated view of copy number and allelic alterations in the cancer genome using single nucleotide polymorphism arrays. Cancer Res *64*, 3060-3071.

Zhou, Z., Flesken-Nikitin, A., Corney, D.C., Wang, W., Goodrich, D.W., Roy-Burman, P., and Nikitin, A.Y. (2006). Synergy of p53 and Rb deficiency in a conditional mouse model for metastatic prostate cancer. Cancer Res *66*, 7889-7898.

Zhu, X.D., Pan, G., Luetke, K., and Sadowski, P.D. (1995). Homology requirements for ligation and strand exchange by the FLP recombinase. J Biol Chem *270*, 11646-11653.

Zhu, X.D., and Sadowski, P.D. (1995). Cleavage-dependent ligation by the FLP recombinase. Characterization of a mutant FLP protein with an alteration in a catalytic amino acid. J Biol Chem *270*, 23044-23054.

Zilfou, J.T., and Lowe, S.W. (2009). Tumor Suppressive Functions of p53. Cold Spring Harb Perspect Biol *1*, a001883.

Zuber, J., Radtke, I., Pardee, T.S., Zhao, Z., Rappaport, A.R., Luo, W., McCurrach, M.E., Yang, M.M., Dolan, M.E., Kogan, S.C.*, et al.* (2009). Mouse models of human AML accurately predict chemotherapy response. Genes Dev *23*, 877-889.

Zundelevich, A., Elad-Sfadia, G., Haklai, R., and Kloog, Y. (2007). Suppression of lung cancer tumor growth in a nude mouse model by the Ras inhibitor salirasib (farnesylthiosalicylic acid). Mol Cancer Ther *6*, 1765-1773.